ฤทธิ์ยับยั้งไลเพสและองค์ประกอบทางเคมีของผลมะเขือขื่น *Solanum aculeatissimum* Jacq.

นายวีระศักดิ์ เมฆวี

วิทยานิพนธ์นี้เป็นส่วนหนึ่งของการศึกษาตามหลักสูตรปริญญาวิทยาศาสตรมหาบัณฑิต
สาขาวิชาเทคโนโลยีชีวภาพ
คณะวิทยาศาสตร์ จุฬาลงกรณ์มหาวิทยาลัย
ปีการศึกษา 2559

ANTILIPASE ACTIVITY AND CHEMICAL CONSTITUENTS OF *Solanum aculeatissimum* Jacq. FRUITS

Mr. Weerasak Megwee

A Thesis Submitted in Partial Fulfillment of the Requirements
for the Degree of Master of Science Program in Biotechnology
Faculty of Science
Chulalongkorn University
Academic Year 2016

Thesis Title	ANTILIPASE ACTIVITY AND CHEMICAL CONSTITUENTS OF*Solanum aculeatissimum* Jacq. FRUITS
By	Mr. Weerasak Megwee
Field of Study	Biotechnology
Thesis Advisor	Assistant Professor Chanya Chaicharoenpong, Ph.D.
Thesis Co-Advisor	Associate Professor Surachai Pornpakakul, Ph.D.

Accepted by the Faculty of Science, Chulalongkorn University in Partial Fulfillment of the Requirements for the Master's Degree

.....Dean of the Faculty of Science
(Associate Professor Polkit Sangvanich, Ph.D.)

THESIS COMMITTEE

.....Chairman
(Associate Professor Nattaya Ngamrojanavanich, Ph.D.)

.....Thesis Advisor
(Assistant Professor Chanya Chaicharoenpong, Ph.D.)

.....Thesis Co-Advisor
(Associate Professor Surachai Pornpakakul, Ph.D.)

.....Examiner
(Yupyn Chintapakorn, Ph.D.)

.....External Examiner
(Damrong Sommit, Ph.D.)

วีระศักดิ์ เมฆวี : ฤทธิ์ยับยั้งไลเพสและองค์ประกอบทางเคมีของผลมะเขือขื่น *Solanum aculeatissimum* Jacq. (ANTILIPASE ACTIVITY AND CHEMICAL CONSTITUENTS OF*Solanum aculeatissimum* Jacq. FRUITS) อ.ที่ปรึกษาวิทยานิพนธ์หลัก: ผศ. ดร.จรรยา ชัยเจริญพงศ์, อ.ที่ปรึกษาวิทยานิพนธ์ร่วม: รศ. ดร.สุรชัย พรภคกุล, 155 หน้า.

พืชสมุนไพรไทยจำนวน 19 ชนิด ถูกตรวจสอบฤทธิ์ยับยั้งไลเพส พืชสมุนไพรไทยเหล่านี้ถูกสกัดด้วยเมทานอลและน้ำที่กำจัดไอออนแล้ว นำสารสกัดเมทานอลและน้ำที่ได้มาทดสอบฤทธิ์ยับยั้งไลเพส พบว่าสารสกัดเมทานอลของผลมะเขือขื่นแสดงฤทธิ์ยับยั้งไลเพสดีที่สุด ดังนั้นสารสกัดเมทานอลของผลมะเขือขื่นจึงถูกนำมาสกัดด้วยวิธีการสกัดของเหลวด้วยของเหลวได้สารสกัดหยาบเฮกเซน, เอทิลแอซิเทต, บิวทานอล และน้ำ สารสกัดหยาบเฮกเซนและบิวทานอลของผลมะเขือขื่นแสดงฤทธิ์ยับยั้งไลเพสที่ระดับดีที่ความเข้มข้น 25 mg/mL ด้วยเปอร์เซ็นต์การยับยั้ง 81.88 ± 0.98% และ 80.74 ± 1.39% ตามลำดับ สารสกัดหยาบเอทิลแอซิเทตของผลมะเขือขื่นแสดงฤทธิ์ยับยั้งไลเพสที่ระดับปานกลางที่ความเข้มข้น 25 mg/mL ด้วยเปอร์เซ็นต์การยับยั้ง 60.41 ± 7.36% สารสกัดหยาบน้ำแสดงฤทธิ์ยับยั้งไลเพสที่ระดับต่ำที่ความเข้มข้น 25 mg/mL ด้วยเปอร์เซ็นต์การยับยั้ง 22.12 ± 1.29% สารสกัดหยาบเฮกเซนและบิวทานอลถูกแยกต่อได้สาร 6 ชนิด สารสกัดหยาบเฮกเซนถูกแยกได้ของผสมกรดไขมัน (สาร 209) และของผสมสเตียรอยด์ (สาร 210) สารสกัดหยาบบิวทานอลถูกแยกได้ของผสมของ steroidal glycosides (สาร 211), solasodine (สาร 212), solasonine (สาร 213) และ alpha-solanine (สาร 214) สาร 209 - 212 แสดงฤทธิ์ยับยั้งไลเพสระดับต่ำที่ IC_{50} เท่ากับ 523.30 ± 0.91, 675.58 ± 1.29, 565.06 ± 1.27 µg/mLและ 404.26 ± 1.39 µM, ตามลำดับ สาร 213 และ 214 แสดงฤทธิ์ยับยั้งไลเพสระดับกลางด้วยค่า IC_{50} เท่ากับ 198.75 ± 0.96 และ 223.43 ± 0.16 µM, ตามลำดับ ออร์ลิสแทตแสดงฤทธิ์ยับยั้งไลเพสระดับดีที่ IC_{50} เท่ากับ 0.27 ± 0.07 µg/mL สาร 209 - 214 แสดงช่วงฤทธิ์ยับยั้งไลเพสในระดับต่ำถึงปานกลาง แต่ว่าสารสกัดหยาบเฮกเซนและบิวทานอลแสดงฤทธิ์ยับยั้งไลเพสที่ระดับดี ผลการทดลองเหล่านี้เสนอแนะว่าองค์ประกอบทางเคมีของผลมะเขือขื่นควรสืบค้นหาส่วนประกอบที่ออกฤทธิ์ยับยั้งไลเพสต่อไป

สาขาวิชา เทคโนโลยีชีวภาพ ลายมือชื่อนิสิต .....

ปีการศึกษา 2559 ลายมือชื่อ อ.ที่ปรึกษาหลัก .....

ลายมือชื่อ อ.ที่ปรึกษาร่วม .....

5672212523 : MAJOR BIOTECHNOLOGY
KEYWORDS: ANTILIAPSE ACTIVITY / LIPASE INHIBITION / SOLANUM ACULEATISSIMUM

WEERASAK MEGWEE: ANTILIPASE ACTIVITY AND CHEMICAL CONSTITUENTS OF*Solanum aculeatissimum* Jacq. FRUITS. ADVISOR: ASST. PROF. CHANYA CHAICHAROENPONG, Ph.D., CO-ADVISOR: ASSOC. PROF. SURACHAI PORNPAKAKUL, Ph.D., 155 pp.

The nineteen Thai medicinal plants were investigated for anti-lipase activity. These plants were extracted with methanol and DI water. The methanolic and aqueous crude extracts of these plants were evaluated on anti-lipase activity. It was found that the methanolic extract of fruits of *Solanum aculeatissimum* showed the strongest inhibition of lipase activity. Thus, methanolic crude extract of *S. aculeatissimum* fruits were extracted by liquid-liquid extraction to obtain hexane, ethyl acetate, *n*-butanol and aqueous crude extracts. The hexane and *n*-butanol crude extracts of *S. aculeatissimum* fruits showed strong lipase inhibitory activity at a concentration of 25 mg/mL with percent inhibition as 81.88 ± 0.98% and 80.74 ± 1.39%, respectively. The ethyl acetate crude extract of *S. aculeatissimum* fruits showed moderate lipase inhibitory activity at a concentration of 25 mg/mL with percent inhibition as 60.41 ± 7.36%. Aqueous crude extract showed weak activity at a concentration of 25 mg/mL with percent inhibition as 22.12 ± 1.29%. The hexane and *n*-butanol crude extracts were further isolated to obtain six compounds. The hexane crude extract was isolated to give a mixture of fatty acids (compound 209) and steroidal mixture (compound 210). The *n*-butanol crude extract was isolated to give a mixture of steroidal glycosides (compound 211), solasodine (compound 212), solasonine (compound 213) and alpha-solanine (compound 214). Compounds 209 - 212 showed weak lipase inhibitory activity with IC_{50} values of 523.30 ± 0.91, 675.58 ± 1.29, 565.06 ± 1.27 µg/mL and 404.26 ± 1.39 µM, respectively. Compounds 213 and 214 exhibited moderate lipase inhibitory activity with IC_{50} values of 198.75 ± 0.96 and 223.43 ± 0.16 µM, respectively. Orlistat showed lipase inhibitory activity with IC_{50} value of 0.27 ± 0.07 µM. Compounds 209 - 214 exhibited in ranging of weak to moderate lipase inhibitory activity whereas hexane and *n*-butanol crude extracts showed strong lipase inhibitory. These results suggested that the chemical constituents of *S. aculeatissimum* fruits should be further investigated for the active components responsible for anti-lipase activity.

Field of Study: Biotechnology
Academic Year: 2016

Student's Signature .....
Advisor's Signature .....
Co-Advisor's Signature .....

ACKNOWLEDGEMENTS

I would like to express my sincere gratitude and deep appreciation to my advisor and co-advisor, Assistant Professor Dr. Chanya Chaicharoenpong and Associate Professor Dr. Surachai Pornpakakul, respectively, for their guidance, valuable suggestions and special supports in correcting and criticizing all of this study.

I would like to express sincere thanks to examination committees, Associate Professor Dr. Nattaya Ngamrojanavanich, Dr. Yupyn Chintapakorn and Dr. Damrong Sommit for useful advice and carefully reviewing of my thesis.

In addition, I would like to thank National Research Council of Thailand (NRCT) in 2016 for the financial support on my research.

Moreover, I would like to thank the Institute of Biotechnology and Genetic Engineering (IBGE) for supporting, encouragement and remarkable experiences during my thesis work. And I also extend my sincere thanks to all of wonderful staff members room no. 604 who always provide me valuable advice and assistance when need. Finally, I would like to express my appreciation to my parent and my family for their love, support useful guidance and wonderful inspiration. They are the most important persons in my life forever.

CONTENTS

Page
THAI ABSTRACT iv
ENGLISH ABSTRACT v
ACKNOWLEDGEMENTS vi
CONTENTS vii
LIST OF TABLES ix
LIST OF FIGURES xii
LIST OF ABBREVIATIONS xv
CHAPTER I INTRODUCTION 1
CHAPTER II THEORETICAL 3
2.1 Obesity 3
2.2 Lipase enzyme 5
2.3 Assays and detection of lipase enzyme 5
2.4 Obesity treatment 7
2.5 Orlistat 9
2.6 Literature reviews 10
2.7 Chemical constituents of *Solanum* spp. in family of Solanaceae 34
2.8 *Solanum aculeatissimum* 45
CHAPTER III MATERIALS AND METHODS 50
3.1 Plants materials 50
3.2 Chemicals and reagents 52
3.3 General experimental procedures 52
3.4 Methods 54
CHAPTER IV RESULTS AND DISSCUSSION 63
4.1 Plants materials 63
4.2 Lipase inhibitory activity of Thai medicinal plants 63
4.3 Extraction of *S. aculeatissimum* fruits 66
4.4 Separation of the crude extracts of *S. aculeatissimum* fruits 66
4.5 Identification of compound 209 85

Page

4.6 Identification of compound 210....86
4.7 Identification of compound 211....87
4.8 Identification of compound 212....87
4.9 Identification of compound 213....91
4.10 Identification of compound 214....96
4.11 Lipase inhibitory activity and IC_{50} values of compounds 209 - 214 and orlistat....102
CHAPTER V CONCLUSION....107
REFERENCES....109
APPENDIX....120
VITA....155

LIST OF TABLES

Page

Table 1 Appropriate BMI for Asian and Thai adults 4

Table 2 Classification of overweight and obesity by BMI, waist circumference and associated disease risks 4

Table 3 Summary of pancreatic lipase inhibitors from plants ..... 10 - 16

Table 4 Chemical constituents of *Solanum* spp. in family of Solanaceae..... 34 - 37

Table 5 Chemical constituents of *S. aculeatissimum* 47

Table 6 The list of Thai medicinal plants for preliminary screening 51

Table 7 Yield of dried weight of Thai medicinal plants for preliminary screening....64

Table 8 Yield of extraction and lipase inhibitory activity of Thai medicinal plants...65

Table 9 Lipase inhibitory activity of crude extracts of *S. aculeatissimum* fruits 66

Table 10 Lipase inhibitory activity of fractions Hx-A - Hx-D 67

Table 11 Separation of fraction Hx-A.....67

Table 12 Separation of fraction Hx-AF.....68

Table 13 Separation of fraction Hx-AFE 68

Table 14 Separation of fraction Hx-AFE3 69

Table 15 Separation of fraction Hx-AH.....69

Table 16 Separation of fraction Hx-AHE 70

Table 17 Lipase inhibitory activity of fractions Hx-DA - Hx-DE 70

Table 18 Lipase inhibitory activity of fractions Hx-DAA - Hx-DAE 70

Table 19 Separation of fraction Hx-DAB 71

Table 20 Separation of fraction Hx-DAB2 71

Table 21 Separation of fraction Hx-DAB24 72

Table 22 Separation of fraction Hx-DAB243 72

Table 23 Separation of fraction Hx-DAD 72

Table 24 Separation of fraction Hx-DB 73

Table 25 Separation of fraction Hx-DBC 73

Page

Table 26 Separation of fraction Hx-DBC2 74
Table 27 Separation of fraction Hx-DBC24 74
Table 28 Separation of fraction Hx-DBC4 75
Table 29 Separation of fraction Hx-DBD 75
Table 30 Separation of fraction Hx-DBD5 75
Table 31 Separation of fraction Hx-DBD52 76
Table 32 Separation of fraction Hx-DBD52C.....76
Table 33 Separation of fraction Hx-DBD52CE 77
Table 34 Separation of fraction Hx-DC 77
Table 35 Lipase inhibitory activity of subfractions Bu-A - Bu-E.....78
Table 36 Separation of fraction Bu-B 78
Table 37 Separation of fraction Bu-BD 78
Table 38 Separation of fraction Bu-BD2 79
Table 39 Separation of fraction Bu-BD2A 79
Table 40 Separation of fraction Bu-C 80
Table 41 Separation of fraction Bu-CG 80
Table 42 Separation of fraction Bu-CGB.....80
Table 43 Separation of fraction Bu-D 81
Table 44 Separation of fraction Bu-DA 81
Table 45 Separation of fraction Bu-DB 82
Table 46 Separation of fraction Bu-DB3 82
Table 47 Re-separation of fraction Bu 82
Table 48 Separation of fraction Bu-C 83
Table 49 Separation of fraction Bu-C2 83
Table 50 Separation of fraction Bu-C21 83
Table 51 Separation of fraction Bu-C22 83
Table 52 Separation of fraction Bu-D 84
Table 53 Separation of fraction Bu-DA 84

Page

Table 54 Separation of fraction Bu-DA1 84

Table 55 Separation of fraction Bu-DC 85

Table 56 Integration peak list of compound **209**.....86

Table 57 Integration peak list of compound **210**.....87

Table 58 ^{1}H (300 MHz) and ^{13}C (75 MHz) NMR data of compound **212** in $CDCl_3$ .90

Table 59 ^{1}H (500 MHz) and ^{13}C (125 MHz) NMR data of compound **213** in pyridine-d_5.....95 - 96

Table 60 *^{1}H (500 MHz) and ^{13}C (125 MHz) NMR data of compound **214** in pyridine-d_5*.....100 - 101

Table 61 Lipase inhibitory activity *in vitro* of compounds **209 - 214** and orlistat....103

Table 62 IC_{50} values of compounds **209 - 214** and orlistat.....103

LIST OF FIGURES

Page

Figure 1 Structure of human pancreatic lipase.....5

Figure 2 (a) Chemical structure of orlistat and (b) Xenical® 9

Figure 3 Chemical structure of pancreatic lipase inhibitors ..... 17 - 33

Figure 4 Chemical structure of chemical constituents of *Solanum* spp. ..... 38 - 44

Figure 5 (a) The ripe fruits (b) the ripe and unripe fruits and (c) whole plant of 46

Figure 6 Chemical structure of chemical constituents of *S. aculeatissimum*.....48

Figure 7 Extraction procedure of plant materials for preliminary screening.....55

Figure 8 Extraction procedure of *S. aculeatissimum* fruits.....56

Figure 9 Chemical structure of compound **209** (mixture of fatty acids).....86

Figure 10 Structure of solasodine (compound **212**).....89

Figure 11 HMBC correlations of compound **212** 89

Figure 12 COSY (bold line) correlations of compound **212**.....90

Figure 13 Structure of solasonine (compound **213**).....93

Figure 14 HMBC correlations of compound **213** 93

Figure 15 COSY (bold line) correlations of compound **213**.....94

Figure 16 NOESY correlations of compound **213**.....94

Figure 17 Structure of α-solanine (compound **214**).....98

Figure 18 HMBC correlation of compound **214**.....99

Figure 19 COSY (bold line) correlation of compound **214** 99

Figure 20 NOESY correlations of compound **214**.....100

Figure 21 Calibration plot of compound **209** on lipase inhibitory assay 104

Figure 22 Calibration plot of compound **210** on lipase inhibitory assay 104

Figure 23 Calibration plot of compound **211** on lipase inhibitory assay 104

Figure 24 Calibration plot of compound **212** on lipase inhibitory assay 105

Figure 25 Calibration plot of compound **213** on lipase inhibitory assay 105

Figure 26 Calibration plot of compound **214** on lipase inhibitory assay 105

Page

Figure 27 Calibration plot of orlistat on lipase inhibitory assay.....106

Figure 28 ^{1}H NMR spectrum ($CDCl_3$) of compound **209**.....122

Figure 29 ^{13}C NMR spectrum ($CDCl_3$) of compound **209**.....123

Figure 30 GC-chromatogram of compound **209**.....124

Figure 31 Mass spectrum of component at retention time 10.716 min of compound **209**.....124

Figure 32 Mass spectrum of component at retention time 12.441 min of compound **209**.....124

Figure 33 Mass spectrum of component at retention time 14.207 min of compound **209**.....125

Figure 34 Mass spectrum of component at retention time 16.747 min of compound **209**.....125

Figure 35 ^{1}H NMR spectrum ($CDCl_3$) of compound **210**.....126

Figure 36 GC-chromatogram of compound **210**.....127

Figure 37 Mass spectrum of component at retention time 15.379 min of compound **210**.....127

Figure 38 Mass spectrum of component at retention time 15.944 min of compound **210**.....127

Figure 39 ^{1}H NMR spectrum (CD_3OD:$CDCl_3$) of compound **211**.....128

Figure 40 ^{13}C NMR spectrum (CD_3OD:$CDCl_3$) of compound **211**.....129

Figure 41 ^{1}H NMR spectrum ($CDCl_3$) of compound **212**.....130

Figure 42 ^{13}C NMR spectrum ($CDCl_3$) of compound **212**.....131

Figure 43 DEPT 90 spectrum ($CDCl_3$) of compound **212**.....132

Figure 44 DEPT 135 spectrum ($CDCl_3$) of compound **212**.....133

Figure 45 HSQC spectrum ($CDCl_3$) of compound **212**.....134

Figure 46 HMBC spectrum ($CDCl_3$) of compound **212**.....135

Figure 47 COSY spectrum ($CDCl_3$) of compound **212**.....136

Figure 48 High resolution mass spectrum of compound **212**.....137

Figure 49 ^{1}H spectrum (pyridine-d_5) of compound **213**.....138

Figure 50 ^{13}C NMR spectrum (pyridine-d_5) of compound **213**.....139

Page

Figure 51 DEPT 90 spectrum (pyridine-d_5) of compound **213**.....140
Figure 52 DEPT 135 spectrum (pyridine-d_5) of compound **213**.....141
Figure 53 HSQC spectrum (pyridine-d_5) of compound **213**.....142
Figure 54 HMBC spectrum (pyridine-d_5) of compound **213**.....143
Figure 55 COSY spectrum (pyridine-d_5) of compound **213**.....144
Figure 56 NOESY spectrum (pyridine-d_5) of compound **213**.....145
Figure 57 High resolution mass spectrum of compound **213**.....146
Figure 58 ^{13}C NMR spectrum (pyridine-d_5) of compound **214**.....147
Figure 59 DEPT 90 spectrum (pyridine-d_5) of compound **214**.....148
Figure 60 DEPT 135 spectrum (pyridine-d_5) of compound **214**.....149
Figure 61 HSQC spectrum (pyridine-d_5) of compound **214**.....150
Figure 62 HMBC spectrum (pyridine-d_5) of compound **214**.....151
Figure 63 COSY spectrum (pyridine-d_5) of compound **214**.....152
Figure 64 NOESY spectrum (pyridine-d_5) of compound **214**.....153
Figure 65 High resolution mass spectrum of compound **214**.....154

LIST OF ABBREVIATIONS

δ	Chemical shift
^{o}C	Degree celsius
%	Percentage
µg	Microgram
µL	Microlitre
µm	Micrometre
µM	Micromolar
Abs	Absorbance
ASTM	American Society for Testing and Materials
bar	A metric unit of pressure (equal to 100,000 Pa)
BDS	Base deactivated silica
BMI	Body mass index
br	Broad signal (for NMR spectra)
$CDCl_3$	Deuterated chloroform
CD_3OD	Deuterated methanol
C_5D_5N	Deuterated pyridine
cm	Centimetre
cm^{-1}	Reciprocal centimetre
^{13}C NMR	Carbon nuclear magnetic resonance spectroscopy
COSY	Correlated spectroscopy
CVD	Cardiovascular disease
d	Doublet (for NMR spectra)
dd	Doublet of doublet (for NMR spectra)
DDI water	Double distilled water
DEPT	Distortionless enhancement by polarization transfer
DI water	Deionized water
DMSO	Dimethyl sulfoxide
DNA	Deoxyribonucleic acid
e.g.	exempli gratia
EC	Enzyme commission
EI^{+}	Electron ionization
et al.	*et alii*
eV	Electron Volt
EtOH	Ethanol
F_{254}	Fluorescent indicator 254 nm
Fast Blue BB	*N*-(4-amino-2,5-diethoxy phenyl) benzamide
FDA	Food and Drug Administration
g	Gram
Gal	Galactose

GC	Gas chromatography
GC-MS	Gas chromatography-mass spectrometry
Glu	Glucose
h	Hours
^{1}H-NMR	Proton nuclear magnetic resonance spectroscopy
HMBC	Heteronuclear multiple bond correlation
HPLC	High performance liquid chromatography
HRESIMS	High-resolution electrospray ionisation mass spectrometry
HSQC	Heteronuclear single quantum correlation
Hz	Hertz
IC_{50}	Half maximal inhibitory concentration
In	Inches
Inches^2	Square of inches
IR	Infrared spectroscopy
J	Coupling constant
kcal	Kilocalorie
kDa	Kilodalton
kg	Kilogram
L	Litre
m	Multiplet (for NMR spectra)
m/z	Mass-to-charge ratio
m^2	Square of metre
mg	Milligram
mHz	Megahertz
min	Minute
mL	Millilitre
mm	Millimetre
NA	No activity
ND	No detection
NHLBI	National heart, lung and blood institute
nm	Nanometre
NMR	Nuclear magnetic resonance spectroscopy
NOESY	Nuclear overhauser enhancement spectroscopy
pH	A logarithmic measure of hydrogen ion concentration
ppm	Part per million
Rha	Rhamnose
Rhodamine B	[9-(2-Carboxyphenyl)-6-(diethylamino) xanthen-3-ylidene]-diethy azanium chloride
rt	Room temperature
s	Singlet (for NMR spectra)
S.D.	Standard deviation

t	Triplet (for NMR spectra)
TLC	Thin layer chromatography
Tris	Tris (hydroxymethyl) aminomethane
Tris-HCL	Tris (hydroxymethyl) aminomethane hydrochloric acid
U.S.	United States
UV	Ultraviolet
UV/VIS	Ultraviolet/Visible
v/v	Volume by volume
w/v	Weight by volume
w/w	Weight by weight
WC	Waist circumference measurement
WHO	World health organization
WHR	Waist-over-hip circumference ratio

CHAPTER I
INTRODUCTION

Overweight and obesity are abnormal or excessive fat accumulation that presents a risk to health [1]. Obesity has been growing of health problems which caused by an imbalance between energy intake from food and the energy spent. It is defined as excessive body fat which is accumulated over-abundance. World Health Organization (WHO) reported that the amount of obese patients increased more than doubled rate since 1980 in worldwide. In 2013, 42 million preschool children in worldwide were represented overweight. In 2014, obese patients were presented more over 600 million and more than 1.9 billion adults, 18 years and older were undergone overweight condition [2]. Classification of obesity is 2 types such as overall obesity and visceral obesity (abdominal obesity). Obesity is considered to be a risk factor for number of chronic diseases such as high blood pressure, cardiovascular disease, diabetes, hyperlipidemia, hypercholesterolemia and cancer. Besides, obesity can be found in anyone regardless of age or gender and it tends to increase continuously in Thai people. According to data of the Thailand National Health Examination Survey (2003-2004), Thai adults who were aged 35 - 59 years, showed significantly increase of overweight and obesity, from 25% in 1991 to 48% in 2004. Thai obese patients were undergone 16 million. It was higher among female than male as 11.3 and 4.7 million of obese patients, respectively in 2009 [3, 4]. Thai male and female were undergone increasingly in obese condition as 36% and 47%, respectively in 2005-2011 [3, 4].

Nowadays, there are many treatments for obesity such as lifestyle therapy, pharmacological interventions and surgical operation especially the change in behavior and lifestyle. The change of behavior and lifestyle are aimed preservation of weight loss and improved health [5]. Presently, medication is a popular choice for obesity treatment especially orlistat (Xenical®), a hydrogenated derivative of lipstatin derived from *Streptomyces toxytricini* [6, 7]. It was known as pancreatic lipase inhibitor and resulted in reduction of fat from the human diet and caloric intake [8]. But some serious side effects were appeared such as oily stool, oily discharge, stomach pain, irregular menstrual periods and headaches [9]. Presently, various studies of natural resources have been investigating and discovering potent agents for newer pancreatic lipase inhibitors with less unpleasant, less toxic and safer adverse effects [10, 11]. Therefore, this study examined the potential effect of natural resource as lipase inhibitors. The nineteen Thai medicinal plants were investigated and screened for anti-lipase activity. These plants were interesting to study anti-lipase activity because they can be found easily at local markets in Thailand and used as folk medicine. The methanolic and aqueous extracts of these medicinal plants were tested for anti-lipase activity including fruits of *Solanum aculeatissimum* Jacq., fruits of *Solanum trilobatum* Linn., fruits of *Capsicum frutescens* Linn., fruits of *Solanum melongena* Linn. (round eggplant), fruits of *Solanum melongena* Linn. (long eggplant), fruits of *Solanum melongena* Linn. (Thai eggplant), fruits of *Solanum melongena* Linn. (round purple eggplant), fruits of *Capsicum annnuum* Linn., fruits of *Momordica charantia* Linn. (bitter cucumber), fruits of *Momordica charantia* Linn.

(Chinese bitter), leaves of *Piper sarmentosum* Roxb., leaves of *Cassia siamea* Lamk., leaves of *Amaranthus lividus* Linn., stems and leaves of *Phyllanthus amarus* Schum. & Thonn., leaves of *Cleome viscose* Linn., leaves of *Sesbania rostrata* Brem. & Oberm., and roots of *Gynandropsis gynandra* (Linn.) Briq. It was found that the methanolic extract of fruits of *S. aculeatissimum* showed the strongest lipase inhibitory activity with percent inhibition as 87.77 ± 4.27% at concentration of 25 mg/mL.

S. aculeatissimum is a Thai folklore medicine which grows on fields and groves of Thailand. *S. aculeatissimum* is locally known as Ma khuea khuen. Nowadays, the scientific research on *S. aculeatissimum* has been reported for several biological activities. However, there is no report on anti-lipase activity. So, this study may shed light on bioactive compounds of *S. aculeatissimum* fruits which can be used as lipase inhibitors.

Objectives

1. To study anti-lipase activity of *S. aculeatissimum* fruits.
2. To isolate and elucidate structure of lipase inhibitors from *S. aculeatissimum* fruits.

CHAPTER II
THEORETICAL

2.1 Obesity

Nowadays, obesity is a worldwide health problem. The new trend of chronic disease as "New World Syndrome" is also defined in this health problem. The most of people are conducing with New World Syndrome. Presently, obesity's trends increase continuously in global [12]. According to the report that one in three of the world's adults were considered overweight condition and one in ten of the world's adults were considered obese condition [13]. World Health Organization (WHO) defines that obesity is a result of abnormal or excessive fat accumulation which may be impaired health. Obesity is considered to be risk factor of chronic diseases and problem health such as hypertension, dyslipidemia, type 2 diabetes, osteoarthritis, coronary artery disease, stroke, gallbladder disease, sleep apnea and respiratory problems [14].

Currently, evaluation of weight and health risk are accepted using three measurements as body mass index (BMI), waist circumference measurement (WC) and waist-over-hip circumference ratio (WHR) [12, 15, 16].

2.1.1 Body mass index (BMI)

Body mass index (BMI) is a statistical measurement for screening condition of overweight or obesity. BMI is the most commonly evaluation to use a simple calculation. BMI can be calculated to define as a person's weight in kilograms (kg) divided by the square of height in metre (kg/m^2). If pounds and inches are recorded for determine BMI, can be calculated to define as a person's weight (pounds) which multiple with 703 divided by the square of height in inches ($inches^2$) to meters (kg/m^2). WHO defined, BMI greater than or equal to 25.0 kg/m^2 is generally considered overweight and BMI greater than or equal to 30 kg/m^2 is generally considered obesity. While, BMI for Asian adults is less than BMI for adults who be non-Asian as BMI greater than or equal to 23.0 and 25.0 kg/m^2 are generally considered overweight and obesity, respectively [17, 18].

Appropriate BMI for Thai adults have been applied and correlated with BMI of WHO. The description of appropriate BMI for Thai adults is shown in Table 1 which was adapted from WHO in 1998 [17-19].

Table 1 Appropriate BMI for Asian and Thai adults

Condition	Body mass index (kg/m^2)
Normal	18.5 - 22.99
Overweight	23.0 - 24.99
Obesity	
Level 1	25.00 - 27.49
Level 2	27.50 - 29.99
Level 3	≥ 30.0

2.1.2 Waist circumference measurement (WC)

Waist circumference measurement (WC) is a simple method which can be determined obesity. Determination of WC locates the upper hip bone and the top of the right iliac crest are measured waist circumference. A horizontal plane around the abdomen at the level of the iliac crest is measured with tape. The relative of normal weight and waist circumference including classification of overweight and obesity are shown in Table 2 [19].

Table 2 Classification of overweight and obesity by BMI, waist circumference and associated disease risks

	BMI (kg/m^2)	Obesity class	Disease risk* (Relative to normal weight and waist circumference)	
			Men ≤ 40 In (≤ 102 cm) Women ≤ 35 In (≤ 88 cm)	> 40 In (> 102 cm) > 35 In (> 88 cm)
Underweight	<18.5		-	-
Normal+	18.5 - 24.9		-	-
Overweight	25.0 - 29.9		Increased	High
Obesity	30.0 - 34.9	I	High	Very High
	35.0 - 39.9	II	Very High	Very High
Extreme obesity	≥40	III	Extremely High	Extremely High

*Disease risk for 2 diabetes, hypertension and CVD

The appropriate waist circumference measurement has been adapted and suggested of Thai adults. Male and female adults should be accepted less than 36 inches (or 90 cm) and 32 inches (or 80 cm), respectively [20].

2.1.3 Waist-over-hip circumference ratio (WHR)

Waist-over-hip circumference ratio (WHR) is a method to determine obesity. It uses to measure obesity which comparison between the sizes of hips divided by the sizes of your waist or the ratio of waist circumference to your hip circumference. According to WHO, male WHR more than 1.0 is considered obese condition. Female who has WHR more than 0.85 is considered obese condition. WHR which be considered obese condition for Thai male and female adults are more than 1.0 and 0.80, respectively [21, 22].

2.2 Lipase enzyme

Lipase is well known as a water-soluble enzyme and an important enzyme for human body. A considerable key role of lipase is to catalyze the hydrolysis of ester bonds in lipid substrates at the oil-water interface into free fatty acids and triacylglycerols. Human lipase includes pancreatic, endothelial, hepatic and lipoprotein lipases. Human tissues can be secreted lipase enzyme such as lungs, kidney, skeletal muscles, adipose tissue and placenta [23].

Pancreatic lipase enzyme (triacylglycerol acylhydrolase EC 3.1.1.3) is secreted from pancreas (pancreatic acinar cells). This enzyme is an important enzyme for human which a key role to digest and hydrolyze dietary triglycerols into 1,2-diacylglycerol, 2-acylglycerol and fatty acids in the small intestine with 50 - 70% of total lipid or triglyceride which is intake into body [23]. It is a 50 kDa peptide chain and water soluble. This enzyme contains two structural domains as the catalytically active or 336-amino acid long N-terminal domain and the shorter (113 residues) C-terminal domain. The main role of the shorter (113 residues) C-terminal domain is binding the cofactor colipase [24]. Structure of human pancreatic lipase is shown in Figure 1 [25].

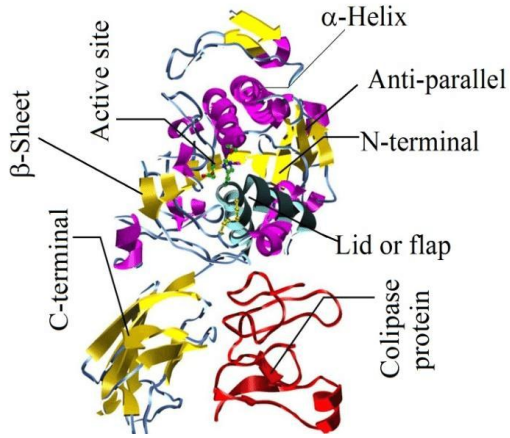

Figure 1 Structure of human pancreatic lipase

2.3 Assays and detection of lipase enzyme

There are several assays and detection of lipase enzyme such as

2.3.1 Titrimetry

Titrimetry is the oldest convenient technique for quantitative assays. Titrimetry is known as pH-stat method which has been widely used to detect of lipase enzyme because it is most reliable, simplicity, accuracy and reproducibility. The pH-stat or pH indicator is used as instruments for detection of neutralization reaction. The reaction based on description using fats and oils/triacylglycerols or methyl esters as substrate of titrimetry to fatty acid as product. However, limited procedure of this method is used time consuming, not rapid for characterizing lipase action and

specificity. And pH values at neutral or alkaline can be determination of this method [26, 27].

2.3.2 Plate assay

Plate assay is a convenient and rapid method for screening short-chain fatty acids product. Tributyrin (tributyrylglycerol) agar plates are cultured lipase-producing strains. The reaction based on description using tributyrin/acylglycerols or esters of long-chain fatty acids as substrate to short-chain fatty acids as product. Lipase activity is detected in a zone of tributyrin hydrolysis. Nile blue sulphate and Victoria blue were used as indicators on tributyrin agar plates. Measurement of fluorescence at 350 nm is used for detection of zone of lipolysis which lipolysis a complex of fatty. The orange color is resulted with fluorescence dye rhodamine B [28-30].

2.3.3 Fluorescence assay

Fluorescence assay is a highly sensitive assay of lipase activity. The quantitative fluorescence lipase assay describes the enzymic hydrolysis of triacylglycerols. The interaction of rhodamine B and fatty acids is used as measurement of the fluorescent fatty acid released. Triacylglycerols having one of the alkyl group substituted with a fluorescent group e.g. conjugated pyrenyl group are substrates and products for analysis are flourescent free prenyl groups. Lipase activity is detected triacylglycerol hydrolysis of a shift in fluorescence wavelength [31, 32]. In addition, a non-fluorescent assay, substrate is 4-methylumbelliferyl oleate and product for analysis is 4-methylumbelliferone. It can be detected in fluorescence assay because 4-methylumbelliferone is highly fluorescent [33, 34]. However, fluorescence assay is very rapid. But, limitation of detection for lipase activity is very expensive method.

2.3.4 Chromatographic techniques

Chromatographic techniques such as TLC, GC and HPLC are one of detection and conclusive method for determination enzyme-catalysed hydrolysis of a lipid substrate. Substrate is triacylglycerols, fats and oils and product for analysis is fatty acids. Fatty acid or residual substrate is analyzed through specific columns. The main limitation of this method depends on instrument such as time consuming in TLC technique, expensive and complication in GC and HPLC techniques [35, 36].

2.3.5 The properties of the interface

2.3.5.1 Monomolecular film technique

Monomolecular film technique is firstly used of lipolysis at the lipid water interface. Substrate is lipid and product for analysis is fatty acid. This method is one of very highly sensitive method for detection amounts of lipase. However, this method is not used widely because pH-stat method is requirement. Accuracy must be necessarily evaluation especially elaborate [37, 38].

2.3.5.2 Oil-drop method

Oil-drop method is known as a monitor of lipase-mediated hydrolysis which is changed in surface tension of a lipid monolayer. Hydrolysis can be effect to result of the shape of the drop changes like as apple to a pear shape. The measurement of lipase assay uses a computer as controlled device. The reaction based on description

using lipid as substrates to fatty acid as product. The limitations of this method are clean materials and equipments. Extension set-ups are important and requirement in this method [39-42].

2.3.6 Fourier transform infrared spectroscopy (FTIR)

Fourier transform infrared spectroscopy (FTIR) is used for measuring lipase-catalysed hydrolysis of triacylglycerol in reverse micelles. Substrate is vegetable oils or trioctanoylglycerol and product for analysis is fatty acid esters and free fatty acids. In this continuous assay, the FTIR spectrum of the entire reaction mixture is recorded lipolysis. Fatty acid esters and free fatty acids (peak maximum at 1751 cm^{-1} and at 1715 cm^{-1}, respectively) were recorded by monitor. The main limitation of Infrared spectroscopy is high cost technique and skill of elucidation in spectrum [43].

2.3.7 Spectrophotometry Assay

2.3.7.1 Tween as substrates

This method is known as a part of spectroscopic assays. Substrate is tween and product for analysis is fatty acid to detect for measurements of turbidity at 500 nm. The reaction can observe precipitation of fatty acid with calcium or copper. Advantage of this method is simple, sensitive and reproducible [44].

2.3.7.2 Assay of β-naphthol

This method is known as a part of spectroscopic assay and colorimetric assay. The reaction is described by hydrolysis of the colourless ester β-naphthyl caprylate (octanoate) as substrate to color of β-naphthol as products by complexation with fast blue BB. The color of β-napthol is measured at 560 nm. The unstable of the ester at extreme pH is a main limitation of this method [45, 46].

2.3.7.3 Assay of *p*-nitrophenol

This method is known as colorimetric assays. The reaction based on description using *p*-nitrophenyl esters as substrate to *p*-nitrophenol as product. The yellow coloured of *p*-nitrophenol at 405 or 410 nm is appeared. The limitation of this assay must not be performed at acidic pH because low pH can be affected with enzyme activity. Moreover, this method is simple and convenient [47].

2.4 Obesity treatment

Obesity can induce the risk factors of many health problems. It has been affected with individual personality [48]. There are many treatments for obesity which are divided into 2 major treatments as follow

2.4.1 Anti-obesity without medication

2.4.1.1 Dietary therapy

Reduction of calories intake from food should be decrease in ranging of 500 to 1,000 calories per day (kcal/day) from currently level which are intake. Long-term nutritional adjustment should be taken for reducing caloric intake. This treatment should be appropriate of calories for diet which should be low calories. However,

very low calories (less than 800 kcal/day) are not appropriate in dietary therapy. Dietary therapy can be decreased with 1 to 2 pounds per week in weight loss.

2.4.1.2 Physical activity

Physical activity is an alternative therapy. This treatment should be combined weight loss management for improvement of efficiency. The suggestion of physical activity is appropriate at least or more than 30 minutes per day in long term for weight loss. Beside, physical activity can reduce the risk of heart disease in comparison with weight loss alone including reduction of body fat.

2.4.1.3 Behavior therapy

Behavior therapy is modification or changing in behavior of food intake and increasing physical activity. Behavior therapy is included behaviors such as self-monitoring, stress management, problem-solving, contingency management, cognitive restructuring and social support.

2.4.1.4 Weight loss surgery

Nowadays, surgery is not only treatment for beauty, but it can also be treatment for obesity. Weight loss surgery for patients who be considered extreme obesity are alternative treatment with taking care of doctor. This qualification of surgery is appropriate treatment for patients who undergo BMI greater than or equal to 40.0 kg/m^2 or more than 100 pounds overweight.

2.4.2 Anti-obesity medication or pharmacotherapy [49]

Medication is a popular choice for using as treatment of obesity. Anti-obesity medication is divided into two groups. First group acts on mode of action as centrally and peripherally acting drugs. Second group is medication of peripherally acting in gastrointestinal tract. First group of centrally acting drugs consists of fenfluramine, dexfenfluramine, phentermine, diethylpropion (or amfepramone), mazindol and sibutramine. These drugs can be leaded reducing the desire of eating which is acted of improvement of neurotransmitter containing serotonin or catecholamine. They lead to control of eating behavior and mood states in human. Phentermine, diethylpropion and mazindol are interacted and stimulated via catecholaminergic pathway. Phentermine, diethylpropion and mazindol have many serious side effects such as dry mouth, constipation, dizziness, headache, diarrhea, itching, trouble breathing, fainting, chest pain and decreasing ability to exercise. Fenfluramine and dexfenfluramine are interacted via serotoninergic pathways. In 2000, fenfluramine and dexfenfluramine have been withdrawn from market by Thai Food and Drug Administration (Thai FDA) because they are leading to primary pulmonary hypertension and valvular heart disease and it can lead to die. Sibutramine is a drug which be acted of noradrenergic and serotoninergic pathways. Sibutramine has many serious side effects such as headache, dry mouth, anorexia, constipation, insomnia, rhinitis, pharyngitis, increased appetite, back pain, asthenia, nausea, arthralgia, nervousness and dyspepsia. Nowadays, sibutramine has been removed from the market because sibutramine concerns of the risk of heart attack and stroke effect and it can lead to die.

The second group, medication of peripherally acting in gastrointestinal tract consists of bulk forming agents and lipase inhibitor as orlistat. Bulk forming agents can be hold water in stomach and decreased of eating behavior. Moreover, calories

are not received from bulk forming agents such as glucomannan, methylcellulose and lemon basil seed.

2.5 Orlistat

In 1998, Roche pharmaceutical company in United Kingdom has been discovered and produced orlistat as a new pharmacological class to be an obesity treatment [50]. Orlistat is a well-known trade name as Xenical®. Orlistat or tetrahydrolipstatin (Chemical formula: $C_{29}H_{53}NO_5$, Molecular weight: 495.74) is a commercial lipase inhibitor which produced from a semisynthetic hydrogenated derivative of lipstatin derived from Streptomyces toxitricini [6, 7]. It has been proven to be effective treatment for obesity [50]. In 1999, orlistat was approved by the U.S. Food and Drug Administration (FDA) for long term weight management including critical obese patients when are used combination with reducing calories diet and lifestyle modification [51]. It inactivates pancreatic lipase and results in reduction of fat from the human diet and caloric intake. Orlistat is a safe novel anti-obesity medication. It inhibits hydrolysis of dietary fat. Moreover, orlistat can be only 30% decrease in fat absorption. Chemical structure of orlistat and Xenical® drug are shown in Figure 2.

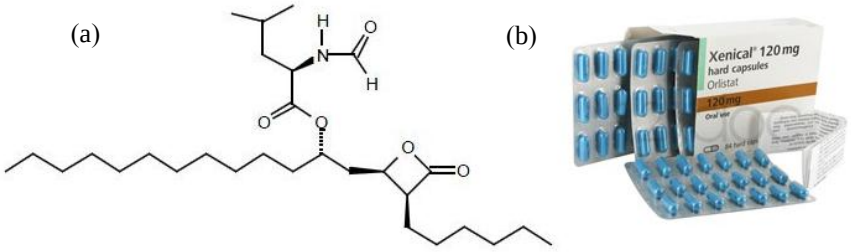

Figure 2 (a) Chemical structure of orlistat and (b) Xenical®

The mechanism of orlistat leads to acylation of a hydroxyl group on serine residue burden on the active site of the enzyme which is reformed to inactive enzyme as lipase. The inactivated lipase excretes passage with faeces. Fatty acids and monoglycerides could not absorb at the human intestine because inactive lipase was inhibited breakdown of dietary triglcerides which hydrolysed fats into fatty acids and monoglycerides. The half-life of orlistat is 14 - 19 h. The 360 mg radioactive orlistat was ingested and orlistat was found only 1% in urine [52]. It was found more than 96% which was recovered in stool over the following 48 h of administration. M1 (4 members lactone ring hydrolyzed) and M3 (M1 with N-formylleucine moiety cleaved) are two main metabolites which are excreted via the bile and show no pharmacological activity in comparison to parent compound. M1 results from the opening of β-lactone moiety in orlistat and the M3 metabolite results from both the hydrolysis of β-lactone and estergroup at the N-formyl leucine side chain. Approximately 2 h and 3 h are the half-life of M1 and M3, respectively [52].

2.6 Literature reviews

The biologically active pancreatic lipase inhibitors investigated from various plants extracts. Presently, various studies of natural resources have been investigated and discovered potent agents for newer pancreatic lipase inhibitors with less unpleasant, less toxic and safer adverse effects [10, 23, 53]. The summary of plants with lipase inhibitory activity was presented in Table 3 and chemical structure of pancreatic lipase inhibitors were shown in Figure 3.

Table 3 Summary of pancreatic lipase inhibitors from plants

Botaniacl name	Plant part	Lipase inhibitor (IC_{50})	Reference
Actinidia arguta	Roots	3-*O*-*trans*-*p*-coumaroyl actinidic acid (**1**) (IC_{50} = 14.95 ± 0.21 μM)	[54]
		ursolic acid (**2**) (IC_{50} = 15.83 ± 1.10 μM)	
		23-hydroxyursolic acid (**3**) (IC_{50} = 41.67 ± 0.66 μM)	
		corosolic acid (**4**) (IC_{50} = 20.42 ± 0.95 μM)	
		asiatic acid (**5**) (IC_{50} = 76.45 ± 0.51 μM)	
		betulinic acid (**6**) (IC_{50} = 21.10 ± 0.55 μM)	
Acanthopanax senticosus	Fruits	silphioside F (**7**) (IC_{50} = 0.22 μM)	[55]
		copteroside B (**8**) (IC_{50} = 0.25 μM)	
		hederagenin 3-*O*-*β*-D glucuronopyranoside 6′-*O*-methyl ester (**9**) (IC_{50} = 0.26 μM)	
		gypsogenin 3-*O*-*β*-D-glucuronopyranoside (**10**) (IC_{50} = 0.29 μM)	
Acanthopanax sessiliflorus	Leaves	sessiloside (**11**) (IC_{50} = 0.36 mg/mL)	[56]
		chiisanoside (**12**) (IC_{50} = 0.75 mg/mL)	
Aesculus turbinata	Seeds	escins Ia (**13**) (IC_{50} = 48 μg/mL)	[57]
		escins IIa (**14**) (IC_{50} = 61 μg/mL)	
		escins Ib (**15**) (IC_{50} = 24 μg/mL)	
		escins IIb (**16**) (IC_{50} = 14 μg/mL)	
Adiantum capillus-veneris	Aerial parts	ferulic acid (**17**) (IC_{50} = 0.48 ± 0.06 μg/mL) ellagic acid (**18**) (IC_{50} = 13.53 ± 1.83 μg/mL) chlorogenic acid (**19**) (IC_{50} = 38.40 ± 2.8 μg/mL)	[58]
Alpinia galanga	Rhizomes	galangin (**20**) (IC_{50} = 48.20 mg/mL)	[59]

Table 3 Summary of pancreatic lipase inhibitors from plants (continue)

Botanical name	Plant part	Lipase inhibitor (IC_{50})	Reference
Alpinia officinarum	Rhizomes	3-methyletherglangin (**21**) (IC_{50} = 1.30 mg/mL)	[60]
Aronia melanocarpa	Fruits	cyanidin-3-glucoside (**22**) (IC_{50} = 1.17 ± 0.05 mg/mL)	[61]
Broussonetia kanzinoki	Stem barks	broussonone A (**23**) (IC_{50} = 28.40 μM)	[62]
		broussonin A (**24**) (IC_{50} = 98.70 μM)	
		broussonin B (**25**) (IC_{50} = 75.40 μM)	
		7,4′-dihydroxyflavan (**26**) (IC_{50} = 85.10 μM)	
		3′,7-dihydroxy-4′-methoxyflavan (**27**) (IC_{50} = > 100 μM)	
		3,7-dihydroxy-4′-methoxyflavone (**28**) (IC_{50} = > 100 μM)	
		3,7,3′-trihydroxy-4′-methoxyflavone (**29**) (IC_{50} = > 100 μM)	
Camellia sinensis	Flower buds	chakasaponins I (**30**) (IC_{50} = 0.17 mM)	[63-65]
		chakasaponins II (**31**) (IC_{50} = 0.18 mM)	
		chakasaponins III (**32**) (IC_{50} = 0.53 mM)	
Camellia sinensis	Leaves	(-)-epigallocatechin-3-*O*-gallate (**33**) (IC_{50} = 0.349 μM)	[66]
		(-)-epigallocatechin-3,5-digallate (**34**) (IC_{50} = 0.098 μM)	
		(+)-catechin (**35**) (IC_{50} = > 20 μM)	
		(-)-epicatechin (**36**) (IC_{50} = >20 μM)	
		(+)-gallocatechin (**37**) (IC_{50} = >20 μM)	
		(-)-epigallocatechin (**38**) (IC_{50} = >20 μM)	
		oolonghomobisflavan A (**39**) (IC_{50} = 0.048 μM)	
		oolonghomobisflavan B (**40**) (IC_{50} = 0.11 μM)	
		oolongtheanin 3′-*O*-gallate (**41**) (IC_{50} = 0.07 μM)	
		monodesgalloyl (**42**) (IC_{50} = 0.27 μM)	
		didesgalloyl (**43**) (IC_{50} = 2.08 μM)	
		prodelphinidin B-2,3,3′-di-*O*-gallate (**44**) IC_{50} = 0.11 μM)	

Table 3 Summary of pancreatic lipase inhibitors from plants (continue)

Botanical name	Plant part	Lipase inhibitor (IC_{50})	Reference
		assamicain A (**45**) IC_{50} = 0.12 μM)	
		theasinensin D (**46**) IC_{50} = 0.05 μM)	
		oolongtheanin-3′-*O*-gallate (**47**)	
		theaflavin (**48**) (IC_{50} = 0.11 μM)	
		theaflavin-3,3′-*O*-gallate (**49**) (IC_{50} = 0.09 μM)	
Cassia auriculata	Aerial parts	kaempferol-3-*O*-rutinoside (**50**) (IC_{50} = 2.90 μM)	[67]
		rutin (**51**) (IC_{50} = > 100.00 μM)	
		kaempferol (**52**) (IC_{50} = > 100.00 μM)	
		quercetin (**53**) (IC_{50} = > 100.00 μM)	
		luteolin (**54**) (IC_{50} = > 100.00 μM)	
Cassia nomame	Fruits	(2S)-3,4,7-trihydroxyflavan-(4α→8)-catechin (**55**) (IC_{50} = 5.50 μM)	[68]
Citrus unshiu	Peels	hesperidin (**56**) (IC_{50} = 32 μg/ml) neohesperidin (**57**) (IC_{50} = 46 μg/ml)	[69]
Chrysanthemum morifolium	Flowers	10α-hydroxy-1α,4α-endoperoxy-guaia-2-en-12,6α -olide (**58**) (IC_{50} = 161.00 μM)	[70]
Cudrania tricuspidata	Root barks	5,7-dihydroxychromone (**59**) (IC_{50} = > 100 μM)	[71]
		5-hydroxy-2,2-dimethyl-2*H*,6*H*-benzodipyran-6-one (**60**) (IC_{50} = > 100 μM)	
		genistein (**61**) (IC_{50} = > 100 μM)	
		biochanin A (**62**) (IC_{50} = > 100 μM)	
		3′-*o*-methylorobol (**63**) (IC_{50} = > 100 μM)	
		wighteone (**64**) (IC_{50} = > 100 μM)	
		kaempferol (**52**) (IC_{50} = > 100 μM)	
		morin (**65**) (IC_{50} = > 100 μM)	
		aromadendrine (**66**) (IC_{50} = > 100 μM)	
		(2*R*,3*R*)-2,3-dihydro-3,5,6,7-tetrahydroxy-2-(4-hydroxyphenyl)-4*H*-1-benzopyran-4-one (**67**) (IC_{50} = > 100 μM)	
		naringenin (**68**) (IC_{50} = > 100 μM)	
		5,7,3′,5′-tetrahydroxyflavanone (**69**) (IC_{50} = 81.80 μM)	
		8-prenylnaringenin (**70**) (IC_{50} = 76.9 μM)	

Table 3 Summary of pancreatic lipase inhibitors from plants (continue)

Botanical name	Plant part	Lipase inhibitor (IC_{50})	Reference
		cudraflavanone D (**71**) (IC_{50} = 9.0 μM)	
		cudraflavanone A (**72**) (IC_{50} = 6.50 μM)	
		2′,5,7-trihydroxy-4,5′-(2,2-dimethylchromeno)-8-(3-hydroxy-3-methylbuthyl)flavanone (**73**) (IC_{50} = 84.60 μM)	
		cudracuspiflavanone A (**74**) (IC_{50} = 54.80 μM)	
Dioscorea nipponica	Roots	dioscin (**75**) (IC_{50} = 20 μg/mL)	[72]
		gracillin (**76**) (IC_{50} = 28.90 μg/mL)	
		diosgenin (**77**) (IC_{50} = 28 μg/mL)	
		prosapogenin A (**78**) (IC_{50} = 1.80 μg/mL)	
		prosapogenin C (**79**) (IC_{50} = 42.20 μg/mL)	
Eisenia bicyclis	Brown seaweed	7-phloroeckol (**80**) (IC_{50} = 12.70 ± 1.0 μM)	[73]
Eremochloa ophiuroides	Leaves	luteolin-6-*C*-*β*-D-boivinopyranoside (**81**) (IC_{50} = 50.50 ± 3.9 μM)	[74]
		orientin (**82**) (IC_{50} = 31.60 ± 2.7 μM)	
		isoorientin (**83**) (IC_{50} = 44.60 ± 1.3 μM)	
		derhamnosylmaysin (**84**) (IC_{50} = 25.90 ± 3.7 μM)	
		isoorientin-2-*O*-α-Lrhamnoside (**85**) (IC_{50} = 18.50 ± 2.6 μM)	
Erythrina abyssinica	Bark	eriodictyol (**86**) (IC_{50} = 134.00 ± 19.39 μM)	[75]
		sigmoidin A (**87**) (IC_{50} = 4.50 ± 0.87 μM)	
Filipendula kamtschatica	Aerial part	3-*O*-caffeoyl-4-*O*-galloyl-L-threonic acid (**88**) (IC_{50} = 26 μM)	[76]
Garcinia cowa	Leaves	vitexin (**89**)	[77]
		orietin (**90**)	
Gardenia jasminoides	Fructus	crocin (**91**) (IC_{50} = 2.10 mg/ml)	[78]
		crocetin (**92**) (IC_{50} = 2.60 mg/ml)	
Ginkgo biloba	Leaves	ginkgolides A (**93**) (IC_{50} = 22.90 μg/mL) ginkgolides B (**94**) (IC_{50} = 60.10 μg/mL) bilobalide (**95**) (IC_{50} = 90 μg/mL)	[79]

Table 3 Summary of pancreatic lipase inhibitors from plants (continue)

Botanical name	Plant part	Lipase inhibitor (IC_{50})	Reference
Glycyrrhiza glabra	Roots	licuroside (**96**) (IC_{50} = 14.90 μM)	[80]
		isoliquiritoside (**97**) (IC_{50} = 37.60 μM)	
		isoliquiritigenin (**98**) (IC_{50} = 7.30 μM)	
		3,3′,4,4′-tetrahydroxy-2 methoxy-chalcone (**99**) (IC_{50} = 35.50 μM)	
Glycyrrhiza uralensis	Roots	licochalcone A (**100**) (IC_{50} = 35 μg/mL)	[81]
Gnetum gnemon	Seeds	gnetin L (**101**) (IC_{50} = 7.2 ± 1.8 μM)	[82]
		gnetin C (**102**) (IC_{50} = 12.2 ± 2.2 μM)	
		gnemonosides A (**103**) (IC_{50} = 125.7 ± 6.4 μM)	
		gnemonosides C (**104**) (IC_{50} = 19.6 ± 3.0 μM)	
		gnemonosides D (**105**) (IC_{50} = 41.4 ± 2.5 μM)	
		resveratrol (**106**) (IC_{50} = >200 μM)	
Monarda punctata	Whole plants	carvacrol (**107**) (IC_{50} = 4.07 mM)	[83]
Morus bombycis	Roots	methanolic extract	[84]
Nelumbo nucifera	Leaves	leaves extract (IC_{50} = 0.46 mg/mL)	[85]
Panax ginseng	Roots	ginseng saponin (IC_{50} = 500 μg/ml)	[86]
Salacia reticulata	Roots	mangiferin (**108**)	[87]
		(-)-4′-*O*-methylepigallocatechin (**109**)	
		(-)-epiafzelechin-(4β→8)-(-)-4′-*O*-methylepigallocatechin (**110**) (IC_{50} = 270 mg/L)	
		(-)-epicatechin-(4β→8)-(–)-4′-*O*-methylepigallocatechin (**111**) (IC_{50} = 68 mg/L)	
		19-hydroxyferruginol (**112**)	
		lambertic acid (**113**) (IC_{50} = 225 mg/L)	
		kotalagenin 16-acetate (**114**)	
		26-hydroxy-1,3-friedelanedione (**115**)	
		maytenfolic acid (**116**)	
		3β,22β-Dihydroxyolean-12-en-29-oic acid (**117**)	

Table 3 Summary of pancreatic lipase inhibitors from plants (continue)

Botanical name	Plant part	Lipase inhibitor (IC_{50})	Reference
		salacino (**118**)	
		carnosic acid (**119**)	
		tannin fraction (IC_{50} = 188 mg/L)	
Salvia officinalis	Leaves	carnosic acid (**113**) (IC_{50} = 12 µg/mL)	[88]
		carnosol (**120**) (IC_{50} = 4.40 µg/mL)	
		roylenoic acid (**121**) (IC_{50} = 35 µg/mL)	
		7-methoxyrosmanol (**122**) (IC_{50} = 32 µg/mL)	
		oleanolic acid (**123**) (IC_{50} = 83 µg/mL)	
Sapindus rarak	Pericarps	rarasaponins I (**124**) (IC_{50} = 131 µM)	[89]
		rarasaponins II (**125**) (IC_{50} = 172 µM)	
		raraoside A (**126**) (IC_{50} = 151 µM)	
Smilax china	Stems	protocatechuic acid (**127**) (IC_{50} = 22.9 ± 0.8 µM)	[90]
		3-*O*-caffeoylquinic acid (**128**) (IC_{50} = > 1000 µM)	
		4-*O*-caffeoylquinic acid (**129**) (IC_{50} = > 1000 µM)	
		5-*O*-caffeoylquinic acid (**130**) (IC_{50} = 474 ± 35 µM)	
		kaempferol 3-*O*-*β*-D-glucopyranosyl-7-*O*-*β*-L-rhamnopyranoside (**131**) (IC_{50} = > 1000 µM)	
		quercitrin (**132**) (IC_{50} = 96.70 ± 7.0 µM)	
		afzelin (**133**) (IC_{50} = 572 ± 102 µM)	
		trans-resveratrol (**134**) (IC_{50} = 61.2 ± 11.70 µM)	
		helonioside A (**135**) (IC_{50} = > 1000 µM)	
		isoscutellarein-8-*O*-rhamnoside (**136**) (IC_{50} = 101 ± 18 µM)	

Table 3 Summary of pancreatic lipase inhibitors from plants (continue)

Botanical name	Plant part	Lipase inhibitor (IC_{50})	Reference
Vitis vinifera	Roots	wilsonol C (**137**) (IC_{50} = 6.70 ± 0.7 μM) heyneanol A (**138**) (IC_{50} = > 200 μM) ampelopsin A (**139**) (IC_{50} = 143.6 ± 3.8 μM) pallidol A (**140**) (IC_{50} = 144.2 ± 3.9 μM) *cis*-piceid (**141**) (IC_{50} = 76.1 ± 3.0 μM) *trans*-piceid (**142**) (IC_{50} = 121.5 ± 3.7 μM) *trans*-resveratrol (**143**) (IC_{50} = > 200 μM)	[91]

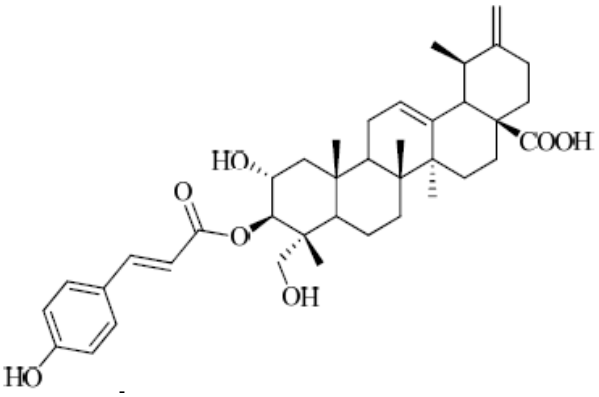

3-*O*-*trans*-*p*-coumaroyl actinidic acid (**1**)

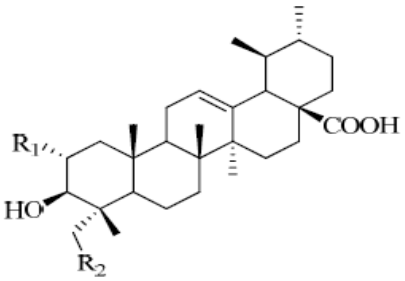

ursolic acid (**2**) $R_1 = R_2 = H$
23-hydroxyursolic acid (**3**) $R_1 = H$, $R_2 = OH$
corosolic acid (**4**) $R_1 = OH$, $R_2 = H$
asiatic acid (**5**) $R_1 = R_2 = OH$

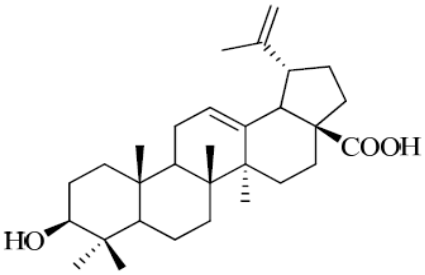

betulinic acid (**6**)

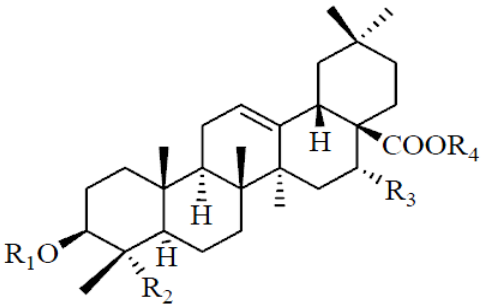

silphioside F (**7**) R_1 = GlcA, $R_2 = CH_3$, $R_3 = R_4 = H$
copteroside B (**8**) R_1= GlcA, $R_2 = CH_2OH$, $R_3 = R_4 = H$
hederagenin 3-*O*-*β*-D-glucuronopyranoside 6′-*O*-methyl ester (**9**) R_1 = 6-*O*-methyl-GlcA, $R_2 = CH_2OH$, $R_3 = R_4 = H$
gypsogenin 3-*O*-*β*-D-glucuronopyranoside (**10**) R_1=GlcA, R_2 = CHO, $R_3 = R_4 = H$

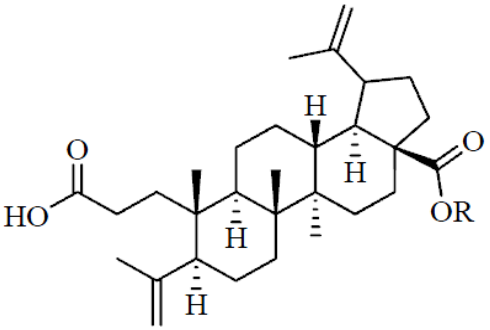

sessiloside (**11**) R = α-L-Rha(1→4)-*β*-D-Glc(1→6)-*β*-D-Glc

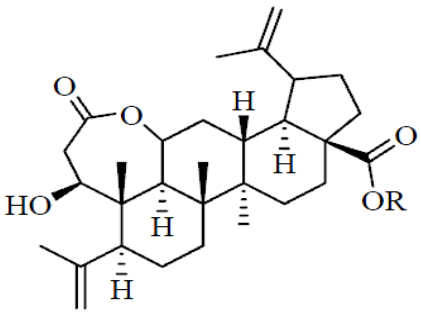

chiisanoside (**12**) R = α-L-Rha(1→4)-*β*-D-Glc(1→6)-*β*-D-Glc

Figure 3 Chemical structure of pancreatic lipase inhibitors

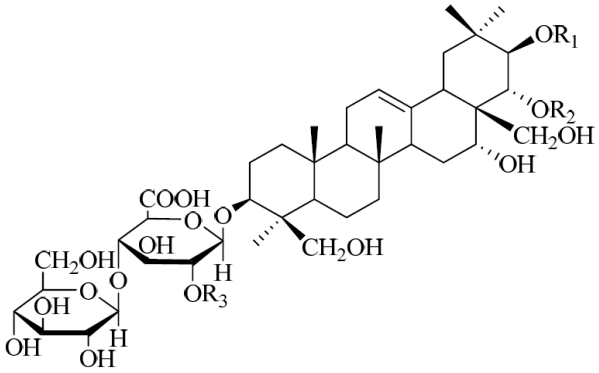

escins Ia (**13**) R_1 = Trigloyl, R_2 = Acetyl, R_3 = D-glucopyranosly
escins IIa (**14**) R_1 = Trigloyl, R_2 = Acetyl, R_3 = D-xylopyranosly
escins Ib (**15**) R_1 = Angeloyl, R_2 = Acetyl, R_3 = D-glucopyranosly
escins IIb (**16**) R_1 = Angeloyl, R_2 = Acetyl, R_3 = D-xylopyranosly

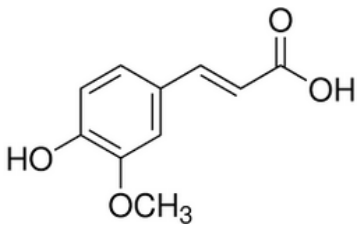

ferulic acid (**17**)

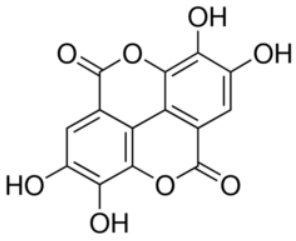

ellagic acid (**18**)

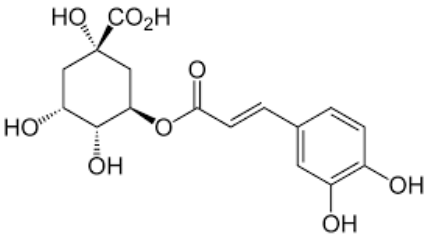

chlorogenic acid (**19**)

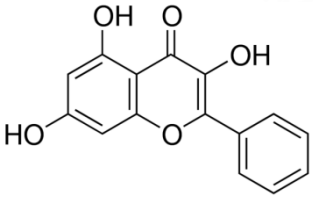

galangin (**20**)

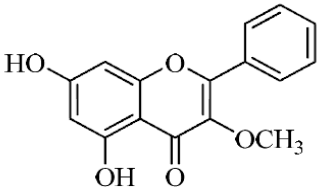

3-methyletherglangin (**21**)

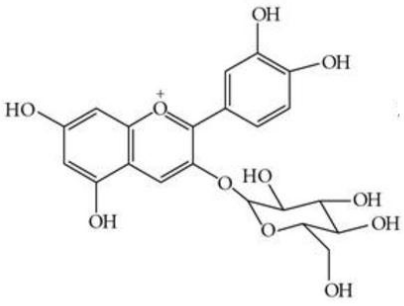

cyanidin-3-glucoside (**22**)

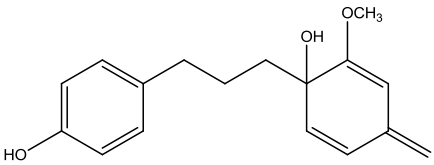

broussonone A (**23**)

Figure 3 Chemical structure of pancreatic lipase inhibitors (continue)

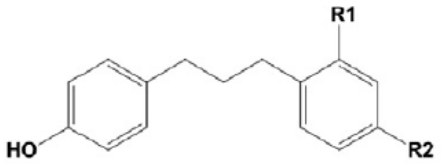

broussonin A (**24**) R_1 = OH, R_2 = OCH_3

broussonin B (**25**) R_1 = OCH_3, R_2 = OH

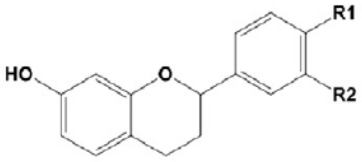

7,4′-dihydroxyflavan (**26**) R= H

3′,7-dihydroxy-4′-methoxyflavan (**27**) R= OCH_3

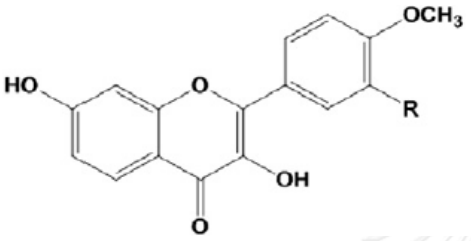

3,7-dihydroxy-4′-methoxyflavone (**28**)

R= H

3,7,3′-trihydroxy-4′-methoxyflavone (**29**)
R= OH

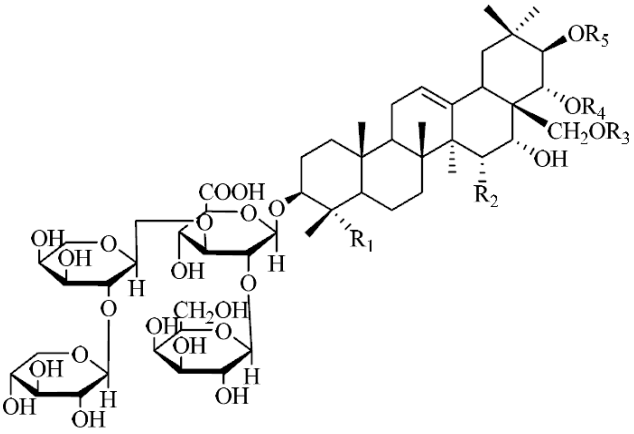

chakasaponins I (**30**) R_1 = CH_3, R_2 = R_3 = H,

R_4 = Acetyl, R_5 = Tigloyl

chakasaponins II (**31**) R_1 = CH_3, R_2 = OH, R_3 = H,

R_4 = Tigloyl, R_5 = Tigloyl

chakasaponins III (**32**) R_1 = CH_3, R_2 = OH, R_3 = H,

R_4 = Acetyl, R_5 = Tigloyl

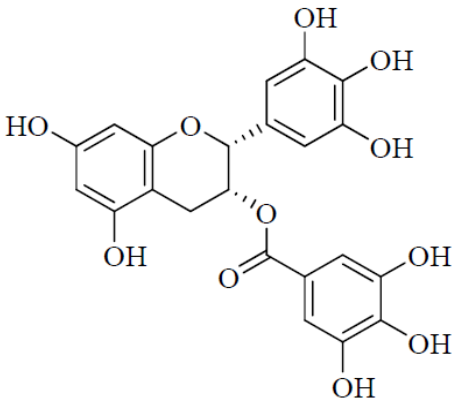

(-)-epigallocatechin-3-*O*-gallate (**33**)

Figure 3 Chemical structure of pancreatic lipase inhibitors (continue)

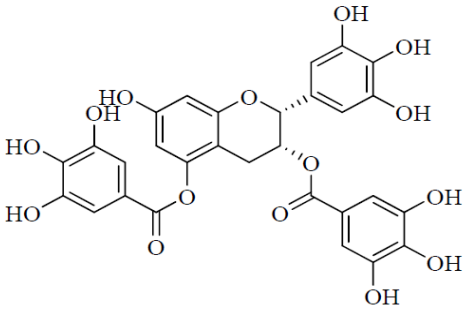

(-)-epigallocatechin-3,5-digallate (**34**)

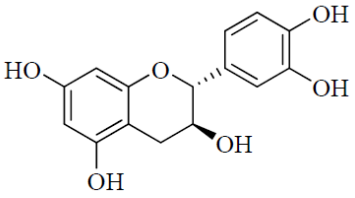

(+)-catechin (**35**)

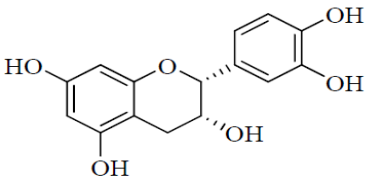

(-)-epicatechin (**36**)

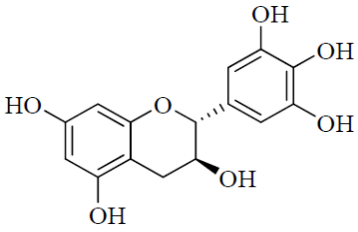

(+)-gallocatechin (**37**)

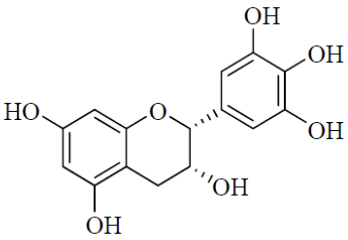

(-)-epigallocatechin (**38**)

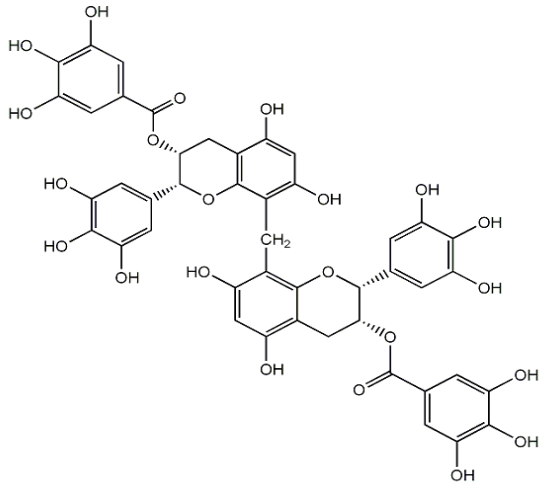

oolonghomobisflavan A (**39**)

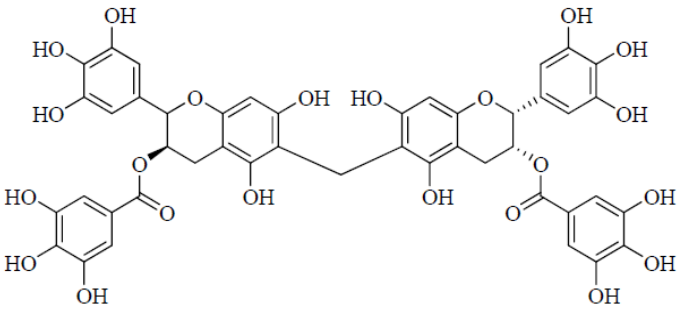

oolonghomobisflavan B (**40**)

Figure 3 Chemical structure of pancreatic lipase inhibitors (continue)

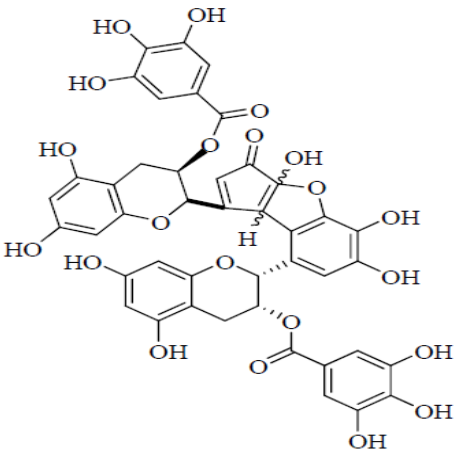

oolongtheanin 3′-*O*-gallate (**41**)

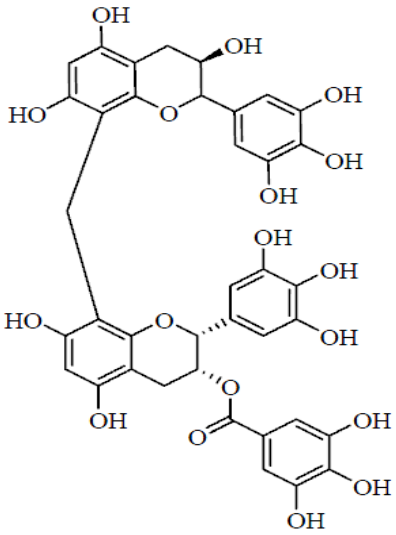

monodesgalloyl (**42**)

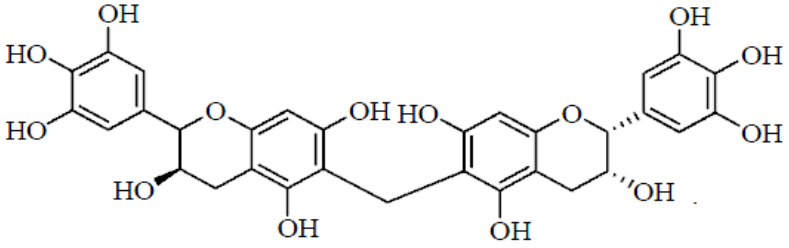

didesgalloyl (**43**)

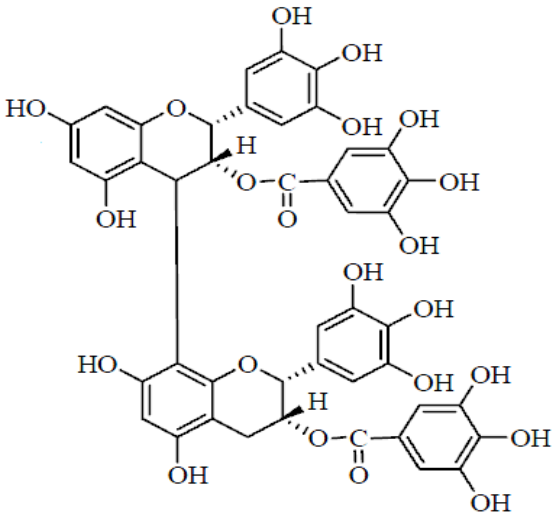

prodelphinidin B-2,3,3′-di-*O*-gallate (**44**)

Figure 3 Chemical structure of pancreatic lipase inhibitors (continue)

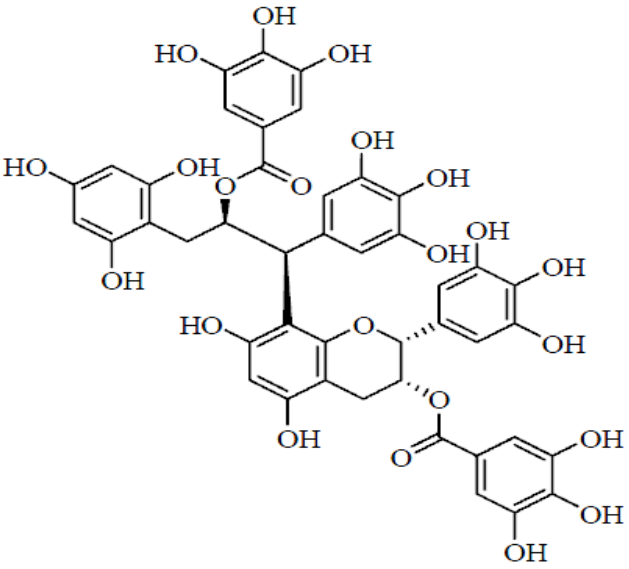

assamicain A (**45**)

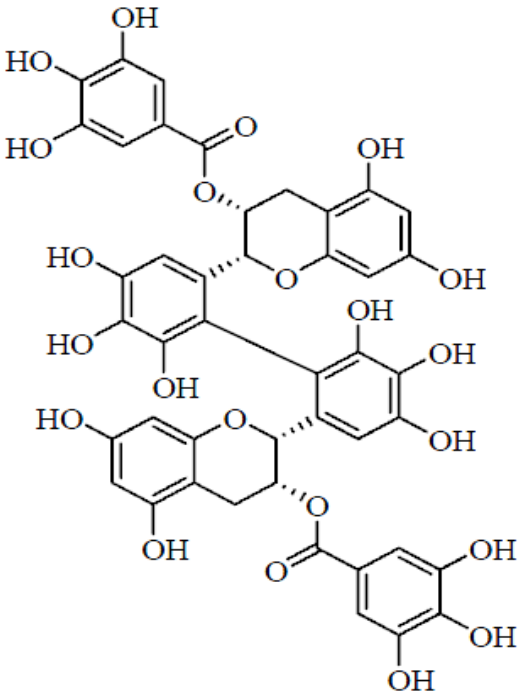

theasinensin D (**46**)

Figure 3 Chemical structure of pancreatic lipase inhibitors (continue)

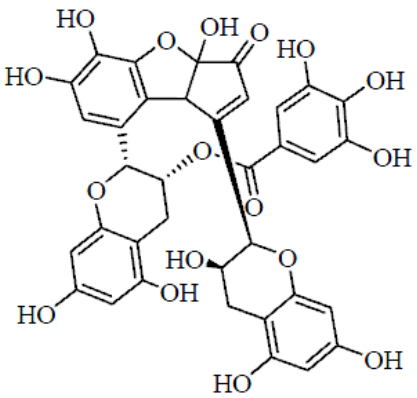

oolongtheanin-3′-*O*-gallate (**47**)

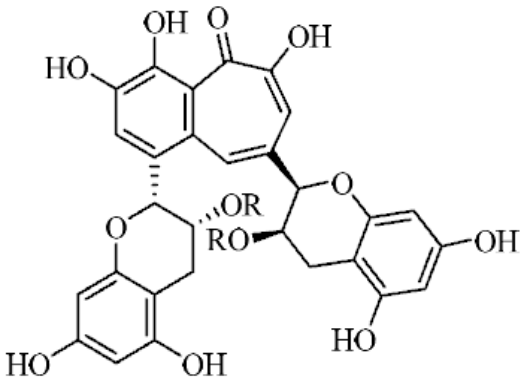

theaflavin (**48**) R = H
theaflavin-3,3′-*O*-gallate (**49**) R = Galloyl

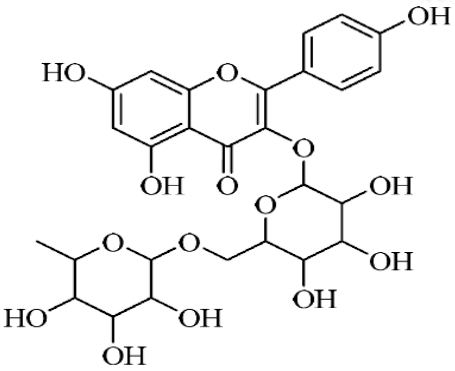

kaempferol-3-*O*-rutinoside (**50**)

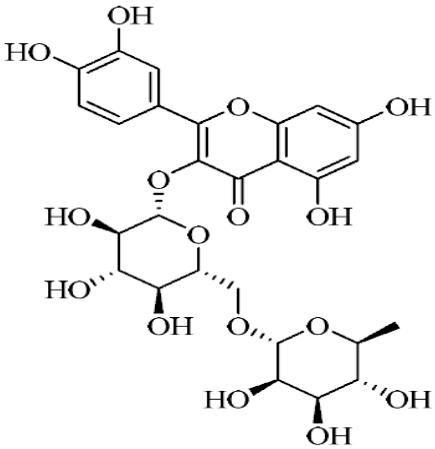

rutin (**51**)

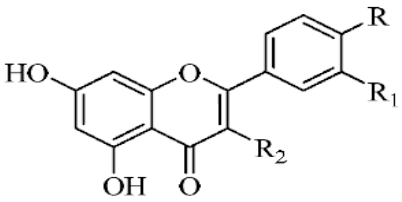

kaempferol (**52**) R = OH, R_1 = H, R_2 = OH
quercetin (**53**) R = OH, R_1 = OH, R_2 = OH
luteolin (**54**) R = OH, R_1 = OH, R_2 = H

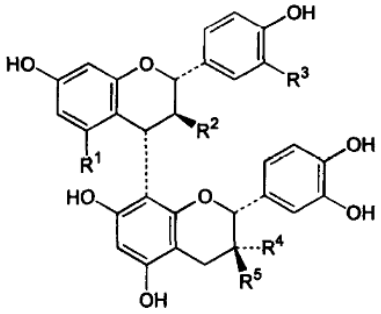

(2S)-3,4,7-trihydroxyflavan-(4α→8)-catechin
(**55**) R_1 = R_2 = R_4 = H, R_3 = R_5 = OH

Figure 3 Chemical structure of pancreatic lipase inhibitors (continue)

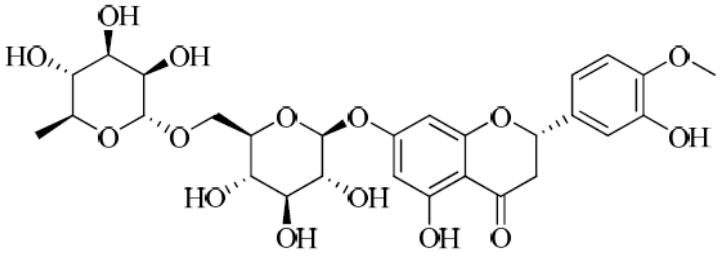

hesperidin (**56**)

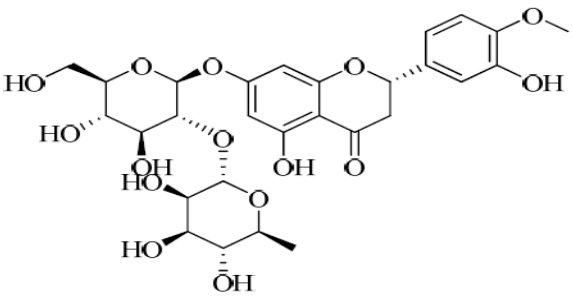

neohesperidin (**57**)

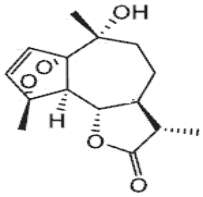

10α-hydroxy-1α,4α-endoperoxy-guaia-2-en-12,6α-olide (**58**)

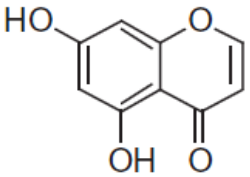

5,7-dihydroxychromone (**59**)

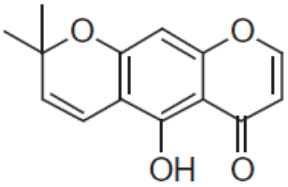

5-hydroxy-2,2-dimethyl-2*H*,6*H*-benzodipyran-6-one (**60**)

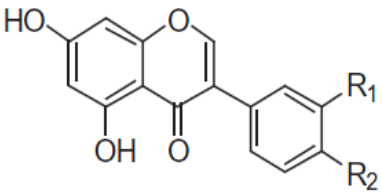

genistein (**61**) R_1 = H, R_2 = OH
biochanin A (**62**) R_1 = H, R_2 = OCH_3
3′-*O*-methylorobol (**63**) R_2 = OCH_3, R_1= OH

Figure 3 Chemical structure of pancreatic lipase inhibitors (continue)

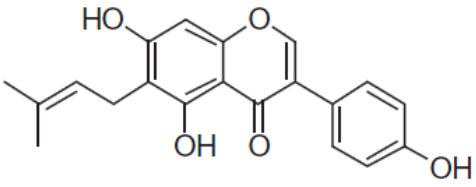

wighteone (**64**)

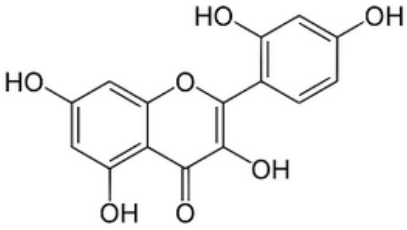

morin (**65**)

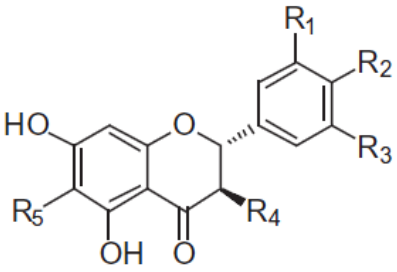

aromadendrine (**66**) R_1= R_3 = R_5= H, R_2 = R_4 = OH

2*R*,3*R*)-2,3-dihydro-3,5,6,7-tetrahydroxy-2-(4-hydroxyphenyl)-4*H*-1-benzopyran-4-one (**67**) R_1 = R_3 = H, R_2 = R_4= R_5 = OH

naringenin (**68**) R_1 = R_3 = R_4 = R_5 = H, R_2 = OH

5,7,3′,5′-tetrahydroxyflavanone (**69**) R_1 = R_3= OH, R_2 = R_4= R_5 = H

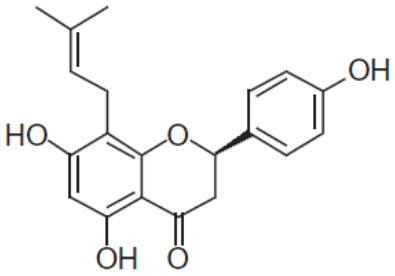

8-prenylnaringenin (**70**)

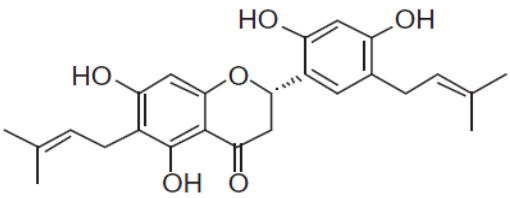

cudraflavanone D (**71**)

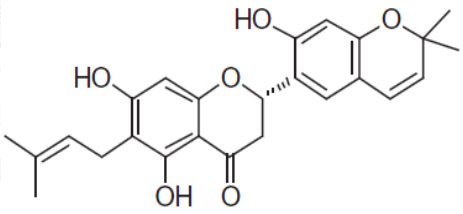

cudraflavanone A (**72**)

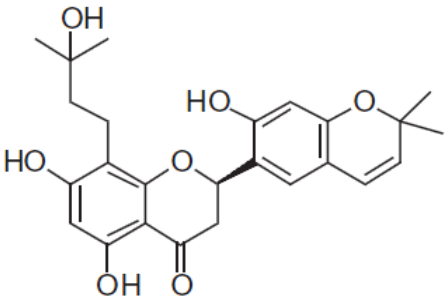

2′,5,7-trihydroxy-4,5′-(2,2-dimethylchromeno)-8-(3-hydroxy-3-methylbuthyl)flavanone (**73**)

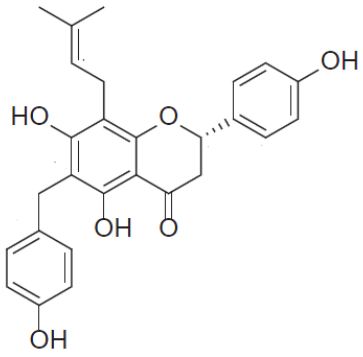

cudracuspiflavanone A (**74**)

Figure 3 Chemical structure of pancreatic lipase inhibitors (continue)

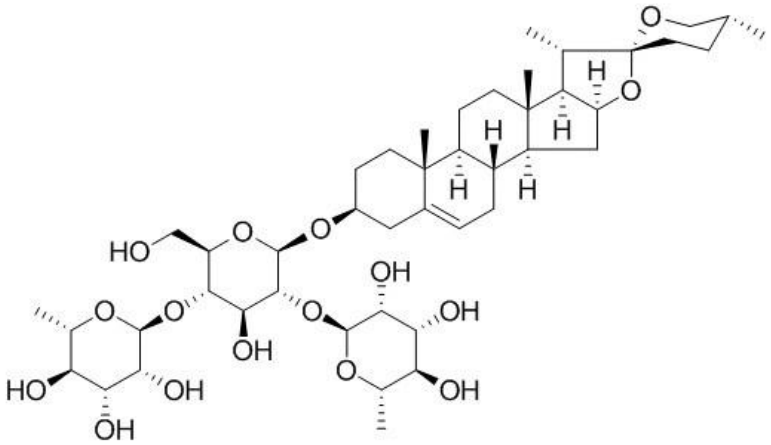

dioscin (**75**)

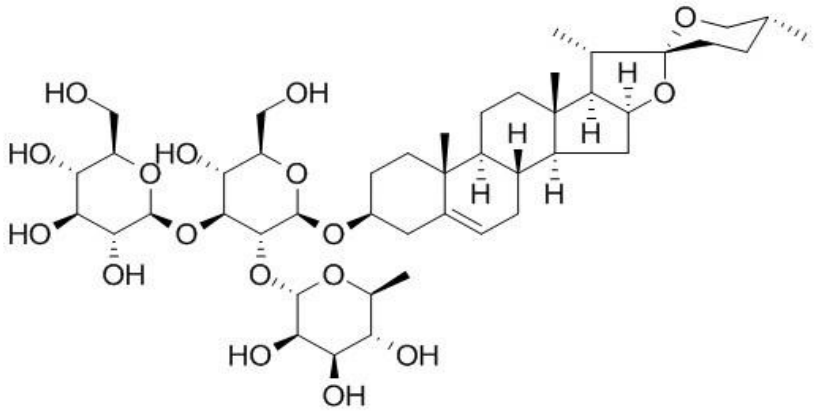

gracillin (**76**)

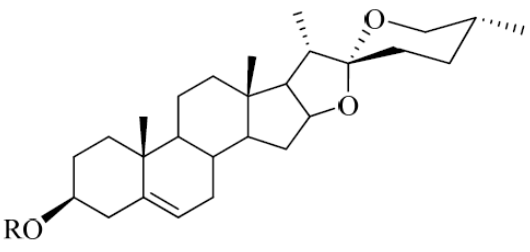

diosgenin (**77**) R = H
prosapogenin A (**78**) R = -Glc^2-Rha
prosapogenin C (**79**) R = -Glc

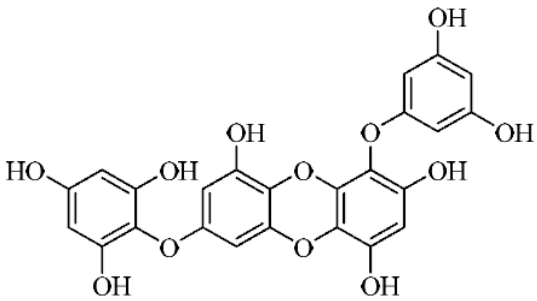

7-phloroeckol (**80**)

Figure 3 Chemical structure of pancreatic lipase inhibitors (continue)

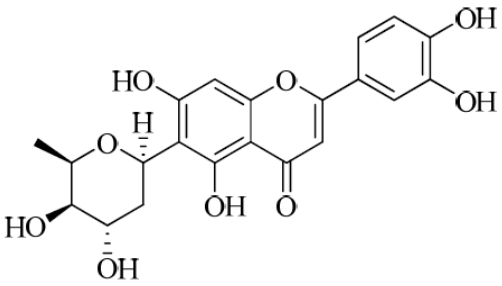

luteolin-6-*C*-ß-D-boivinopyranoside (**81**)

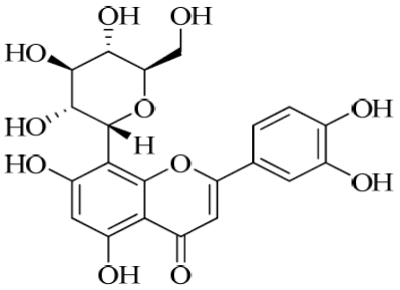

orientin (**82**)

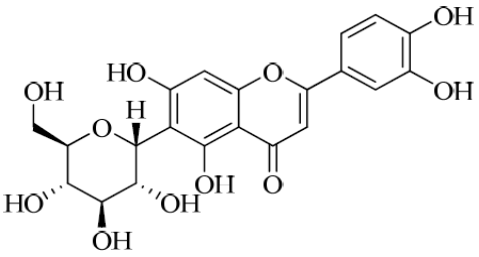

isoorientin (**83**)

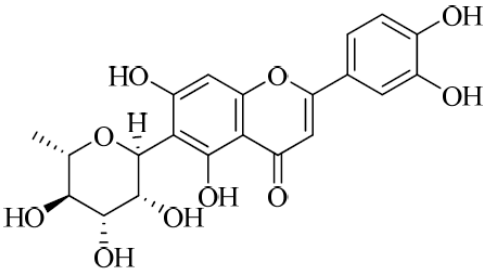

derhamnosylmaysin (**84**)

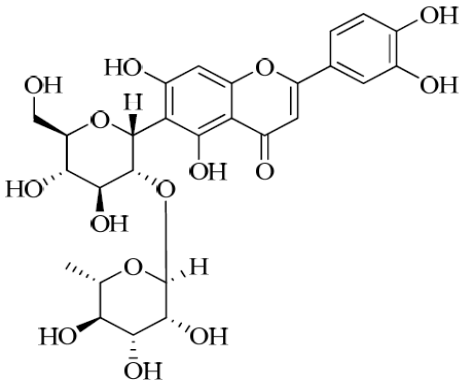

isoorientin-2-*O*-α-L-rhamnoside (**85**)

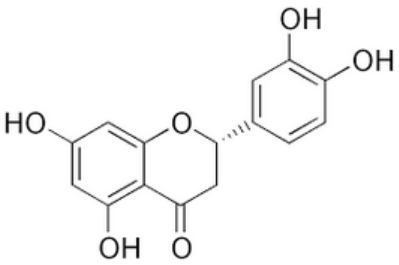

eriodictyol (**86**)

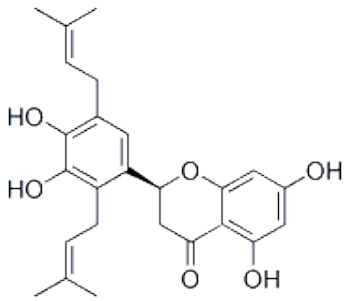

sigmoidin A (**87**)

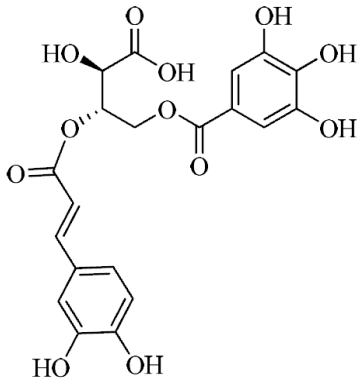

3-*O*-caffeoyl-4-*O*-galloyl-L-threonic acid **(88**)

Figure 3 Chemical structure of pancreatic lipase inhibitors (continue)

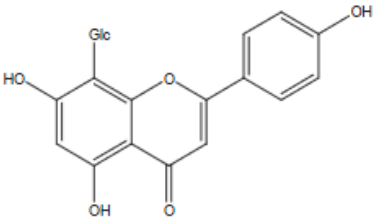

vitexin (**89**)

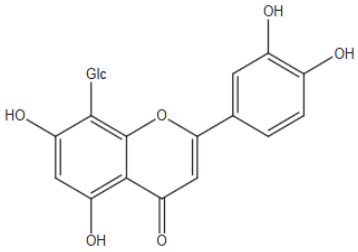

orietin (**90**)

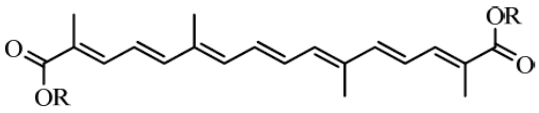

crocin (**91**) R = β-gentiobiosy

crocetin (**92**) R = H

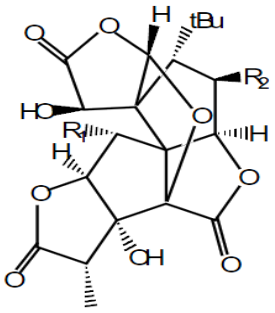

ginkgolides A (**93**) $R_1 = R_2 = H$

ginkgolides B (**94**) R_1 = OH, R_2 = H

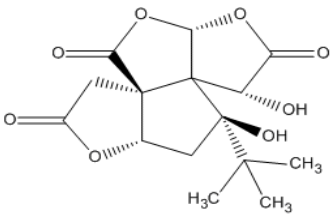

bilobalide (**95**)

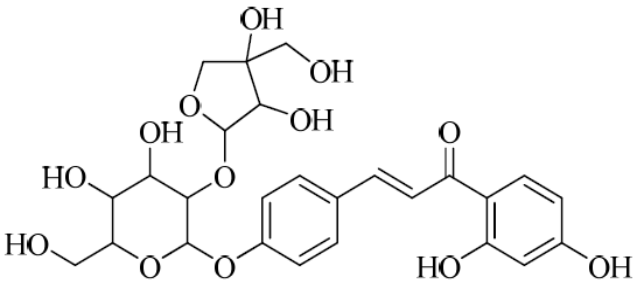

licuroside (**96**)

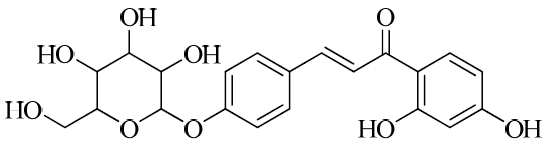

isoliquiritoside (**97**)

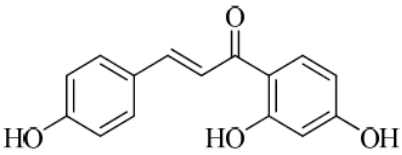

isoliquiritigenin (**98**)

Figure 3 Chemical structure of pancreatic lipase inhibitors (continue)

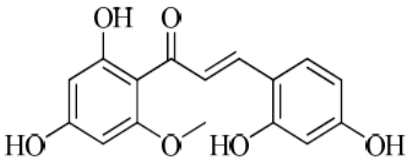

3,3′,4,4′-tetrahydroxy-2-methoxychalcone (**99**)

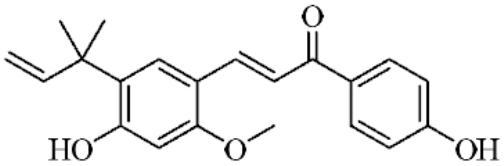

licochalcone A (**100**)

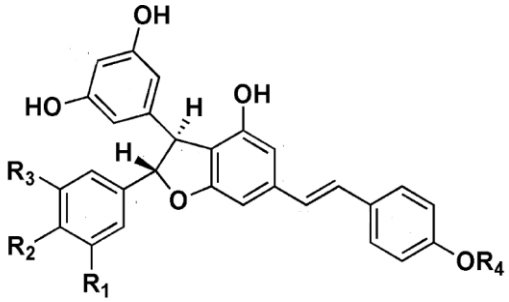

gnetin L (**101**) $R_1 = OCH_3$, $R_2 = R_4 = H$, $R_4 = R_3 = OH$
gnetin C (**102**) $R_1 = R_3 = R_4 = H$, $R_2 = OH$
gnemonosides A (**103**) $R_1 = R_3 = H$, $R_2 = OGlc$, $R_4 = Glc$
gnemonosides C (**104**) $R_1 = R_3 = R_4 = H$, $R_2 = OGlc$
gnemonosides D (**105**) $R_1 = R_3 = H$, $R_2 = OH$, $R_4 = Glc$

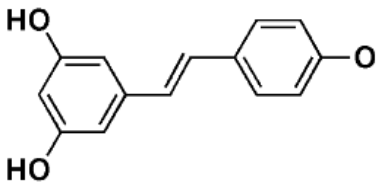

resveratrol (**106**)

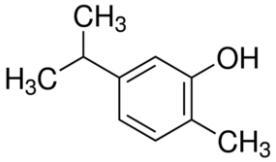

carvacrol (**107**)

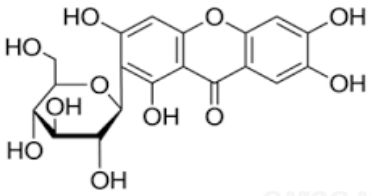

mangiferin (**108**)

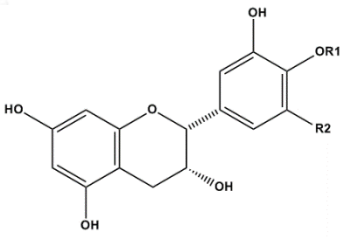

(-)-4′-*O*-methylepigallocatechin (**109**)
$R_1 = CH_3$, $R_2 = OH$

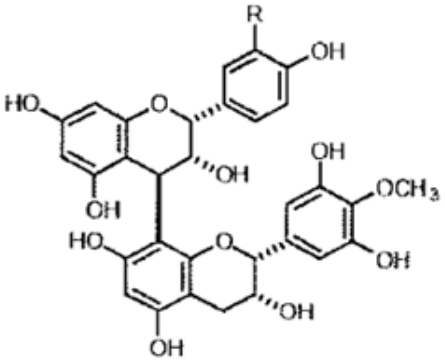

(-)-epiafzelechin-(4β→8)-(-)-4′-*O*-methylepigallocatechin (**110**) R= H
(-)-epicatechin-(4β→8)-(–)-4′-*O*-methylepigallocatechin (**111**) R= OH

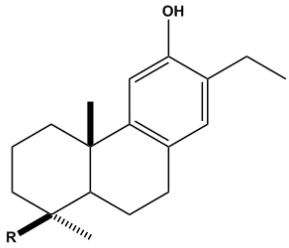

19-hydroxyferruginol (**112**) R = CH_2OH
lambertic acid (**113**) R= COOH

Figure 3 Chemical structure of pancreatic lipase inhibitors (continue)

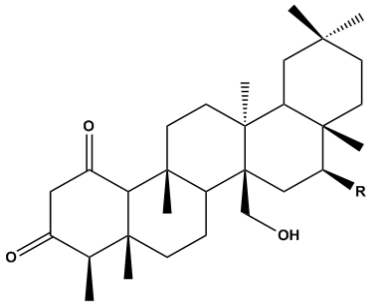

kotalagenin 16-acetate (**114**) R= $OCOCH_3$

26-hydroxy-1,3-friedelanedione (**115**) R= H

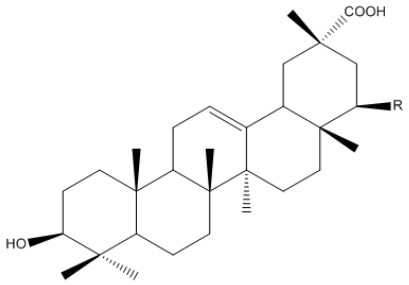

maytenfolic acid (**116**) R= α-OH

3*β*,22*β*-dihydroxyolean-12-en-29-oic acid (**117**)

R = *β*-OH

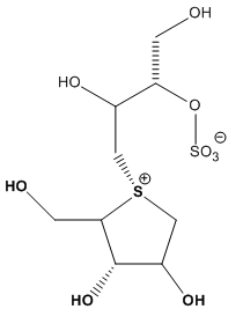

salacino (**118**)

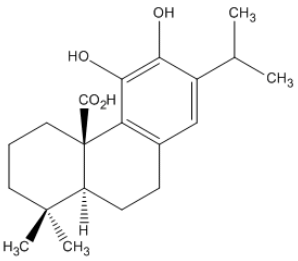

carnosic acid (**119**)

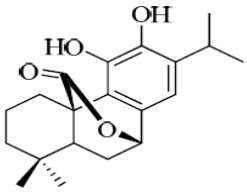

carnosol (**120**)

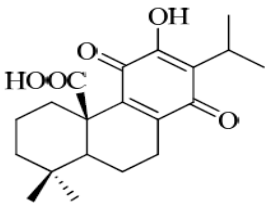

roylenoic acid (**121**)

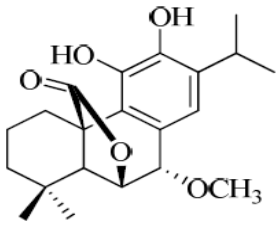

7-methoxyrosmanol (**122**)

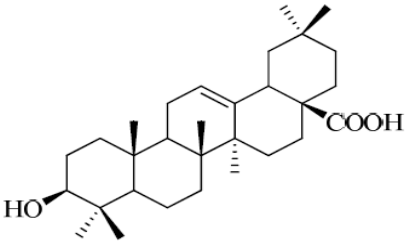

oleanolic acid (**123**)

Figure 3 Chemical structure of pancreatic lipase inhibitors (continue)

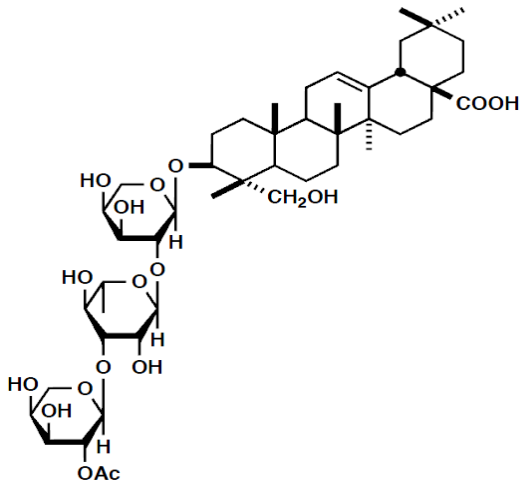

rarasaponins I (**124**)

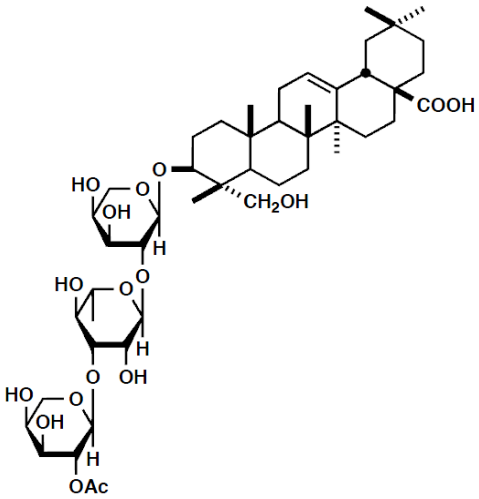

rarasaponins II (**125**)

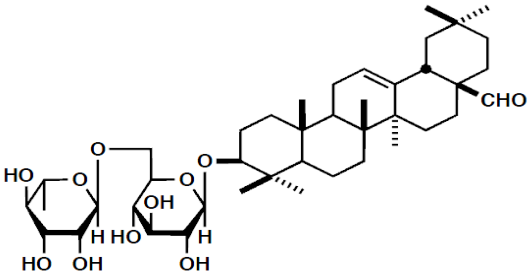

raraoside A (**126**)

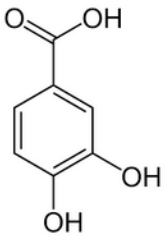

protocatechuic acid (**127**)

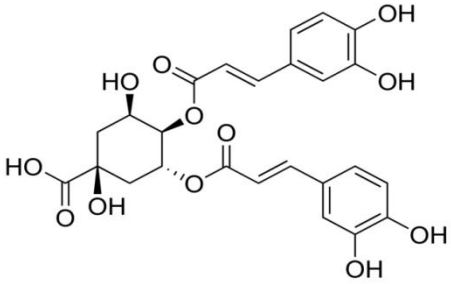

3-*O*-caffeoylquinic acid (**128**)

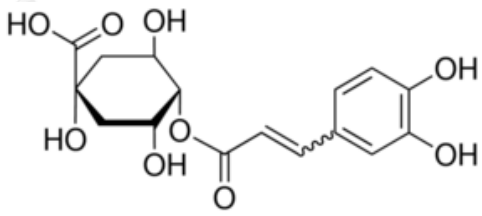

4-*O*-caffeoylquinic acid (**129**)

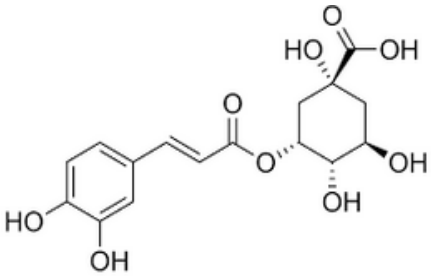

5-*O*-caffeoylquinic acid (**130**)

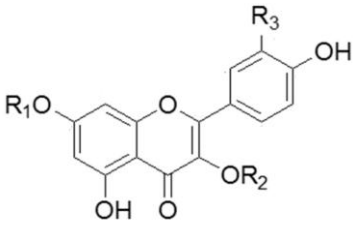

kaempferol 3-*O*-*β*-D-glucopyranosyl-7-*O*-*β*-L-rhamnopyranoside (**131**) R_1 = Rhamnose, R_2 = Glucose, R_3 = H

quercitrin (**132**) R_1 = H, R_2 = Rhamnose, R_3 = OH

hafzelin (**133**) R_1 = H, R_2 = Rhamnose, R_3 = H

Figure 3 Chemical structure of pancreatic lipase inhibitors (continue)

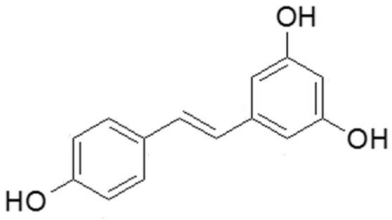

trans-resveratrol (**134**)

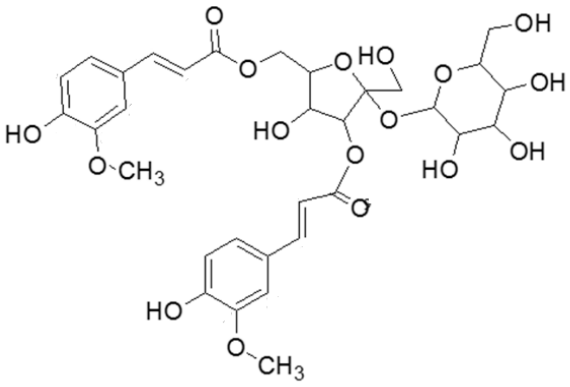

helonioside A (**135**)

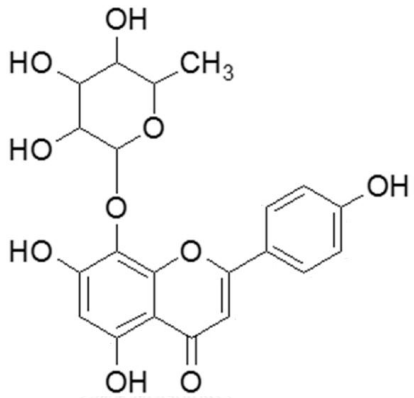

isoscutellarein-8-*O*-rhamnoside (**136**)

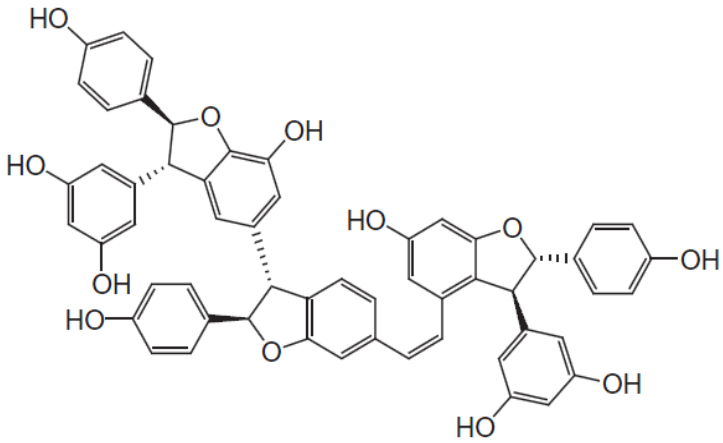

wilsonol C (**137**)

Figure 3 Chemical structure of pancreatic lipase inhibitors (continue)

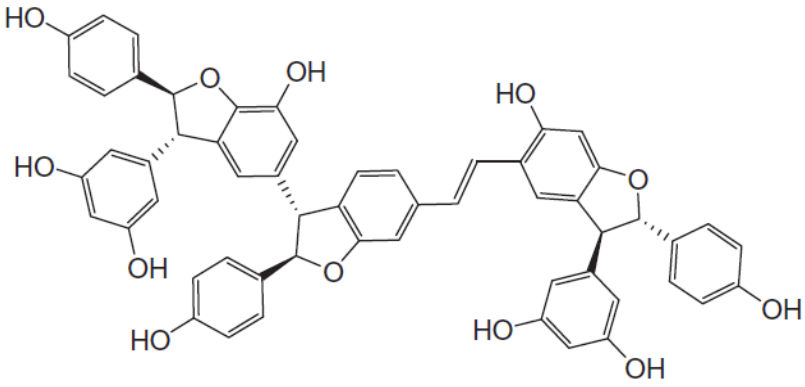

heyneanol A (**138**)

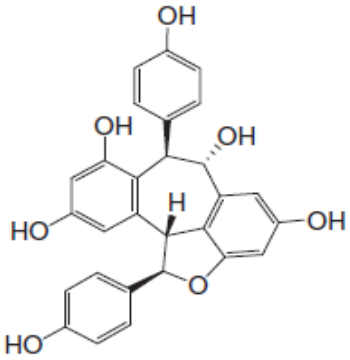

ampelopsin A (**139**)

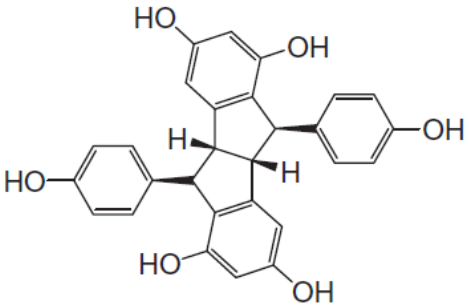

pallidol A (**140**)

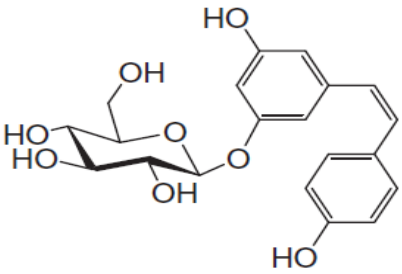

cis-piceid (**141**)

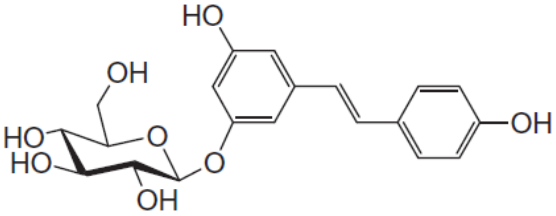

trans-piceid (**142**)

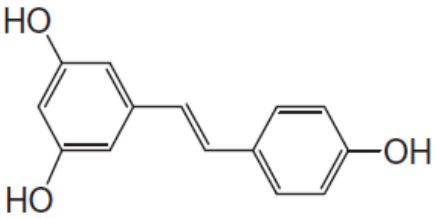

trans-resveratrol (**143**)

Figure 3 Chemical structure of pancreatic lipase inhibitors (continue)

2.7 Chemical constituents of *Solanum* spp. in family of Solanaceae

The genus *Solanum* in member of Solanaceae family commonly grows in the fields of temperate climate zones to the tropics. Previous investigation, plants in the genus *Solanum* are rich of phytochemical compounds such as steroidal glycosides and steroidal alkaloid glycosides [92]. Genus *Solanum* has investigated and reported biological activities such as against herbivores, against pathogenic microorganism, molluscicidal activity, anabolic, anti-fertility, anti-inflammatory and anti-allergic drugs [93, 94]. The trichomes of young branches of *S. crinitum* were isolated to obtain flavonoids and reported biological activity as cytotoxic and antitumoral activities. The green fruits of *S. crinitum* contain glycoalkaloids and reported biological activity as allelopathic activity [94]. The leaves of *S. spirale* reported as anaestheti, killing intestinal worms, against beriberi and swollen stomach [95]. The whole plant of *S. nigrum* contains alkaloids, glycoproteins, flavonoids, polyphenols and triterpenoids. They reported biological activities as anti-inflammatory, anti-oxidant, anti-nociceptive, anti-pyretic, anti-tumor, anti-ulcerogenic, cancer chemopreventive and hepatoprotective [96-100]. The leaves of *S. corymbiflorum* have been used for treatment of inflamed legs, low back pain, otitis, scabies, tick bite, mastitis and inflammatory disorders [101]. The methanolic extract of aerial parts of *S. schimperianum* extract showed antitrypanosomal activity against *Trypanosoma brucei* [102]. While, the hexane crude extract showed activity against *Bacillus subtilis* and *Staphylococcus aureus* [103]. Chemical constituents of the genus *Solanum* were summarized in Table 4. Chemical structure of chemical constituents of *Solanum* spp. was shown in Figure 4.

Table 4 Chemical constituents of *Solanum* spp. in family of Solanaceae

Botanical name	Plant part	Chemical constituents	Reference
Solanum aculeastrum	Berries	tomatidine (**144**) solasodine (**145**)	[104]
Solanum coagulans	Aerial parts	methyl salicylate 2-*O*-*β*-D-glucopyranosyl-(1→2)-*β*-D- gucopyranoside (**146**)	[105]
		isorhamnetin 3-*O*-*β*-D-glucopyranoside (**147)**	
		quercetin 3-*O*-*β*-D-galactopyranoside (**148**)	
		N-*p*-coumaroyltyramine (**149**)	
		syringaresinol (**150**)	
		radulignan (**151**)	
		neochlorogenin 6-*O*-*β*-D-xylopyranosyl (1→3)-*β*-D-quinovopyranoside (**152**)	
		neochlorogein 6-*O*-α-L-rhamnpyranosyl(1→3)-*β*-D-quinovopyranoside (**153**)	

Table 4 Chemical constituents of *Solanum* spp. in family of Solanaceae (continue)

Botanical name	Plant part	Chemical constituents	Reference
		(22*R*,23*S*,25*R*)-3*β*,6α,23-trihydroxy-5α-spirostane 6-*O*-*β*-D-xylopyranosyl (1→3)-*β*-D-quinovopyranoside (**154**)	
		torvoside K (**155**)	
		(22*R*,23*R*,25*S*)-3 *β*,6*α*,23-trihydroxy-5*α*-spirostane 6-*O*-*β*-D-xylopyranosyl (1→3)-*O*-*β*-D-quinovopyranoside (**156**)	
		torvoside L (**157**)	
		torvoside M (**158**)	
Solanum corymbiflorum	Leaves	chlorogenic acid (**19**)	[101]
		rutin (**51**)	
		rosmarinic acid (**159**)	
		caffeic acid (**160**)	
		gallic acid (**161**)	
Solanum crinitum	Fruits	tiliroside (**162**)	[106]
		astragalin (**163**)	
		kaempferol (**52**)	
		biochanin A-7-O-*β*-D-apiofuranosyl-(1→5)-*β*-D-apiofuranosyl-(1→6)-*β*-D-glucopyranoside (**164**)	
		cis-cumaric acids (**165**)	
		trans-cumaric acids (**166**)	
		cis-ethyl cumarate esters (**167**)	
		trans-ethyl coumarate (**168**)	
		4-hydroxybenzoic acid (**169**)	
Solanum lycocarpum	Fruits	solasonine (**170**)	[107]
		β-solamargine (**171**)	
Solanum nigrum	Leaves	gentisic acid (**172**)	[108, 109]
		luteolin (**173**)	
		apigenin (**174**)	
		kaempferol (**52**)	
		m-coumaric acid (**175**)	

Table 4 Chemical constituents of *Solanum* spp. in family of Solanaceae (continue)

Botanical name	Plant parts	Chemical constituents	Reference
	Fruits	anthocyanidin	
		spirost-5-ene-3*β*,12*β*-diol (**176**)	
		N-*trans*-feruloyltyramine (**177**)	
		(*R*)-3-(4-hydroxy-3-methoxyphenyl)-*N*-[2-(4-hydroxyphenyl)-2-methoxyethyl]acrylamide (**178**)	
		(*E*)-ethyl caffeate (**179**)	
		Ethyl 4-hydroxy-3-methoxycinnamate (**180**)	
		methylsinapate (**181**)	
		chlorogenic acid (**19**)	
		caffeic acid (**160**)	
		β-sitosterol (**182**)	
		tryptophol acetate (**183**)	
		4-amino-3-methoxyphenol (**184**)	
Solanum spirale	Leaves	lupeol (**185**)	[110]
		protocatechuic acid (**186**)	
		trans-cinnamic acid (**187**)	
Solanum stramonifolium	Fruits	carpesterol (**188**)	[111]
Solanum torvum	Aerial parts	neochlorogenin 6-*O*-*β*-D-quinovopyranoside (**189**)	[112]
		neochlorogenin 6-*O*-*β*-D-xylopyranosyl-(1→3)-*β*-D-quinovopyranoside (**190**)	
		solagenin 6-*O*-*β*-D-quinovopyranoside (**191**)	
		solagenin 6-*O*-α-L-rhamnopyranosyl-(1→3)-*β*-D-quinovopyranoside (**192**)	
		isoquercetin (**193**)	
		rutin (**51**)	
		kaempferol (**52**)	
		quercetin (**53**)	
	Fruits	scopoletin (**194**)	[112]

Table 4 Chemical constituents of *Solanum* spp. in family of Solanaceae (continue)

Botanical name	Plant parts	Chemical constituents	Reference
Solanum trilobatum	Leaves, stems	sobatum (**195**) *β*-solamagine (**171**) tomatidine (**144**) solasodine (**145**) solanine (**196**) diosogenin (**197**)	[113]
Solanum xanthocarpum	Fruits	apigenin (**174**) scopoletin (**195)** esculetin (**198**) courmarin (**199**) methyl caffeate (**200**) caffeic acid (**160**) carpesterol (**188**) campesterol (**201**) *β*-sitosterol (**182**) lupeol (**185**) cycloartenol (**202**) stigmasterol (**203**) solasodine (**145**) diosgenin (**77**) tomatidenol (**204**) α-solamargine (**205**)	[114]

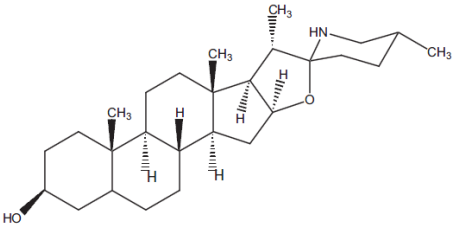

tomatidine (**144**)

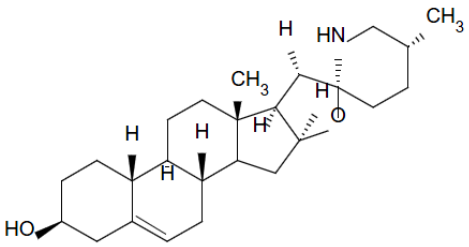

solasodine (**145**)

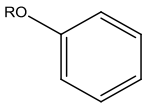

methyl salicylate 2-*O*-β-Dglucopyranosyl-(1→2)-β-D-gucopyranoside (**146**) R = β-D-Glc-(1→2)-β-D-Glc-

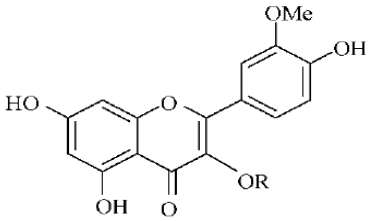

isorhamnetin 3-*O*-β-D-glucopyranoside (**147**) R = β-D-Glc

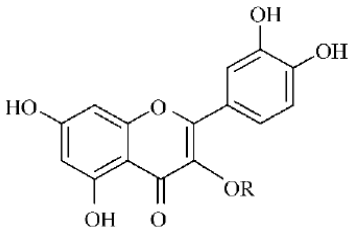

quercetin 3-*O*-β-D-galactopyranoside (**148**) R = β-D-Gal

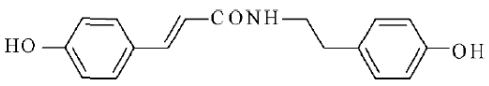

N-*p*-coumaroyltyramine (**149**)

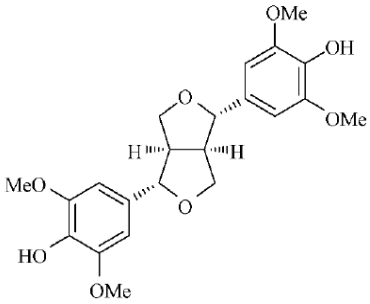

Syringaresinol (**150**)

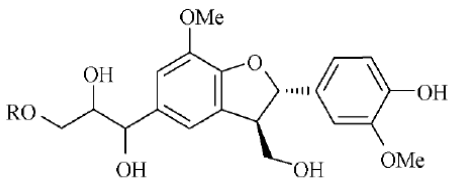

radulignan (**151**) R = β-D-Glc

Figure 4 Chemical structure of chemical constituents of *Solanum* spp.

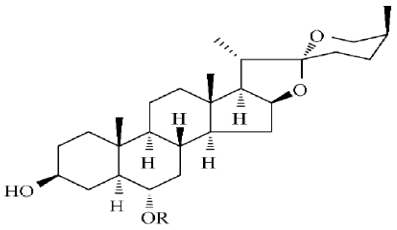

neochlorogenin 6-*O*-*β*-D-xylopyranosyl (1→3)-*β*-D-quinovopyranoside (**152**)
R = *β*-D-Xyl-(1→3)-*β*-D-Qui-
neochlorogenin 6-*O*-α-L-rhamnpyranosyl (1→3)-*β*-D-quinovopyranoside (**153**) R = α-L-Rha-(1→3)-*β*-D-Qui-

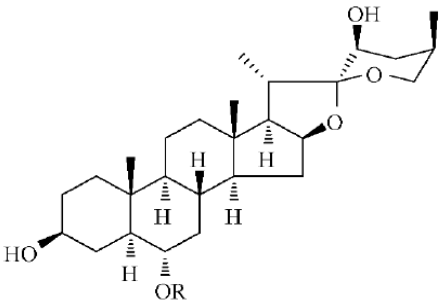

(22*R*, 23*S*, 25*R*)-3*β*,6α,23-trihydroxy-5α-spirostane 6-*O*-*β*-D-xylopyranosyl (1→3)-*β*-D-quinovopyranoside (**154**) R = *β*-D-Xyl-(1→3)-*β*-D-Qui-
torvoside K (**155**) R = α-L-Rha-(1→3)-*β*-D-Qui-

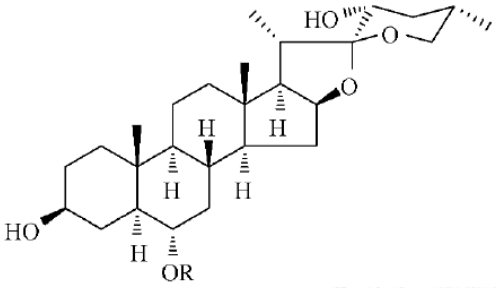

(22*R*, 23*R*, 25*S*)-3*β*,6*α*,23-trihydroxy-5*α*-spirostane 6-*O*-*β*-D-xylopyranosyl (1→3)-*O*-*β*-D-quinovopyranoside (**156**)
R = *β*-D-Xyl-(1→3)-*β*-D-Qui-
torvoside L (**157**) R = α-L-Rha-(1→3)-*β*-D-Qui-

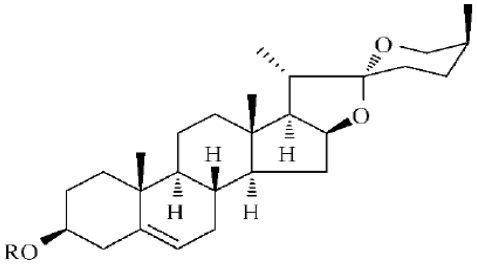

torvoside M (**158**) = *β*-D-Glc-(1→6)-*β*-D-Glc-

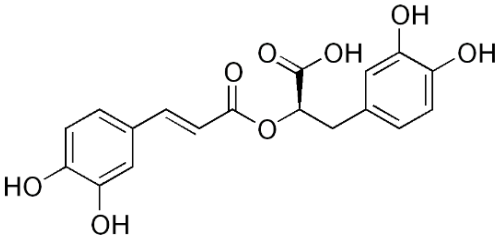

rosmarinic acid (**159**)

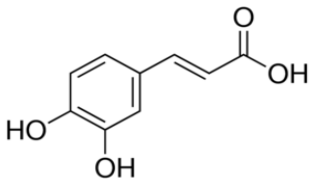

caffeic acid (**160**)

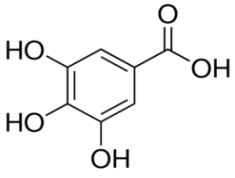

gallic acid (**161**)

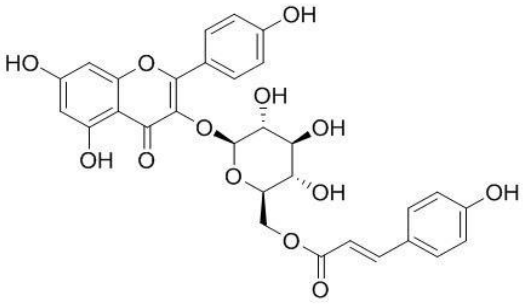

tiliroside (**162**)

Figure 4 Chemical structure of chemical constituents of *Solanum* spp. (continue)

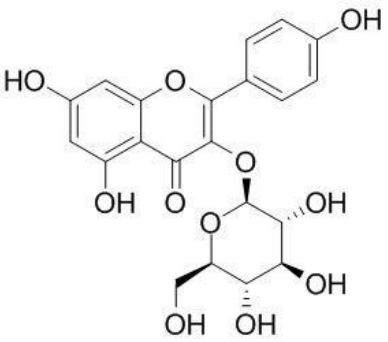

astragalin (**163**)

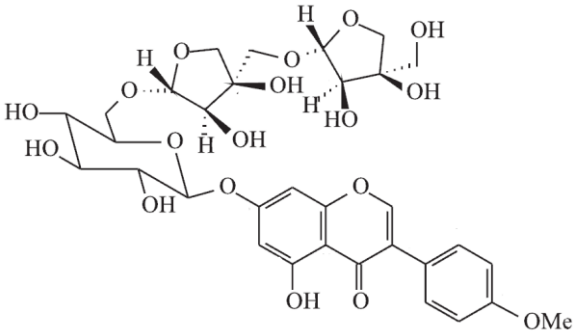

biochanin A-7-*O*-*β*-D-apiofuranosyl-(1→5)-*β*-D-apiofuranosyl-(1→6)-*β*-D-glucopyranoside (**164**)

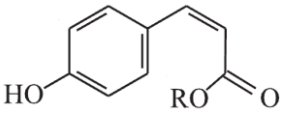

cis-cumaric acids (**165**) R = H
ethyl *cis*-cumarate esters (**167**) R = CH_2CH_3

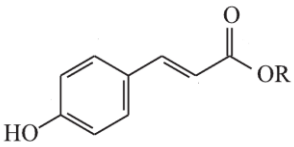

trans-cumaric acids (**166**) R = H
ethyl *trans*-coumarate (**168**) R = CH_2CH_3

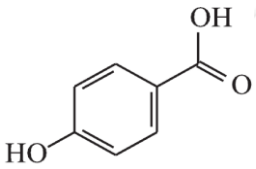

4-hydroxybenzoic acid (**169**)

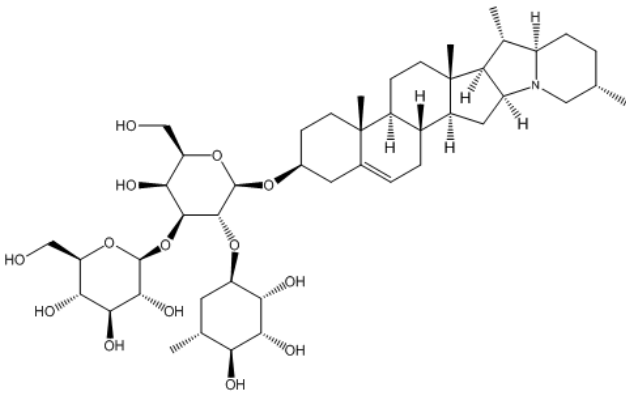

solasonine (**170**)

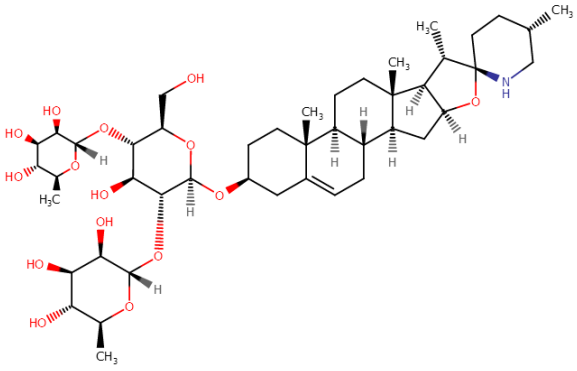

β-solamargine (**171**)

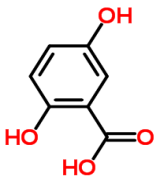

gentisic acid (**172**)

Figure 4 Chemical structure of chemical constituents of *Solanum* spp. (continue)

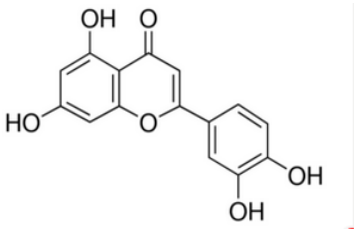

luteolin (**173**)

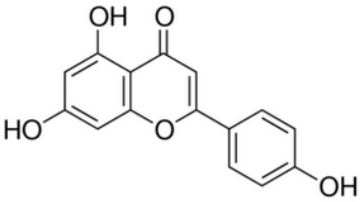

apigenin (**174**)

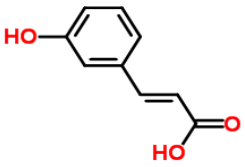

m-coumaric acid (**175**)

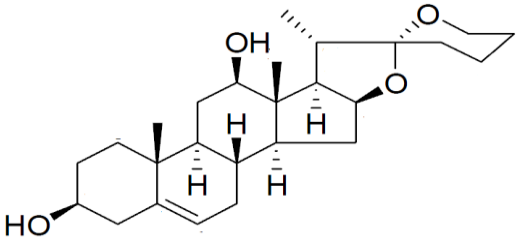

spirost-5-ene-3*β*,12*β*-diol (**176**)

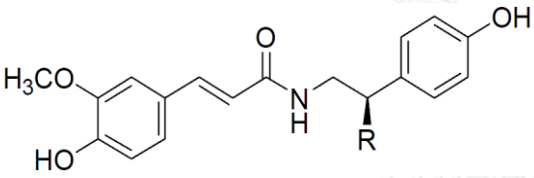

N-*trans*-feruloyltyramine (**177**) R = H
(*R*)-3-(4-hydroxy-3-methoxyphenyl)-*N*-[2-(4-hydroxyphenyl)-2-methoxyethyl]acrylamide (**178**) R = OCH_3

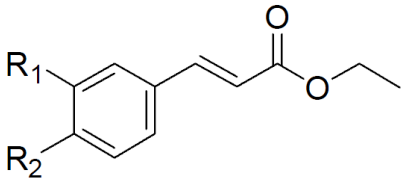

(*E*)-ethyl caffeate (**179**) $R_1 = R_2 = OH$

ethyl 4-hydroxy-3-methoxycinnamate (**180**) $R_1 = OCH_3$, $R_2 = OH$

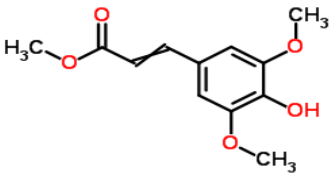

methylsinapate (**181**)

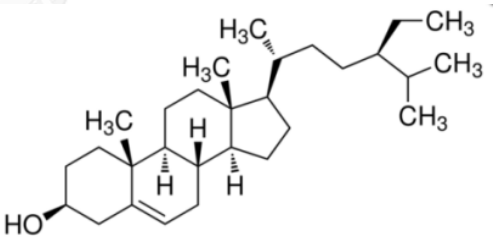

β-sitosterol (**182**)

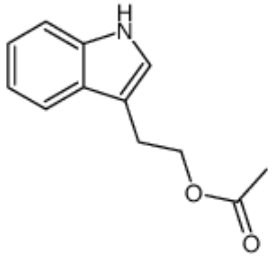

tryptophol acetate (**183**)

Figure 4 Chemical structure of chemical constituents of *Solanum* spp. (continue)

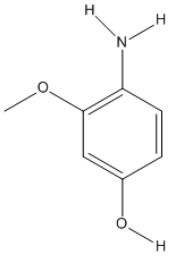

4-amino-3-methoxyphenol (**184**)

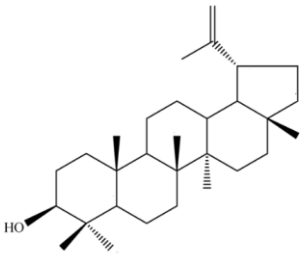

lupeol (**185**)

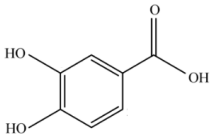

protocatechuic acid (**186**)

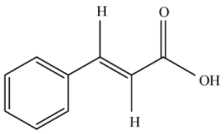

trans-cinnamic acid (**187**)

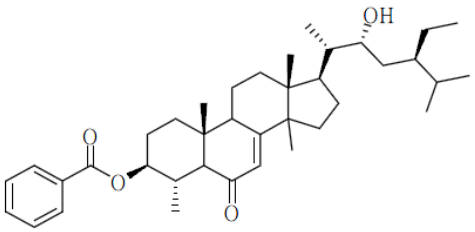

carpesterol (**188**)

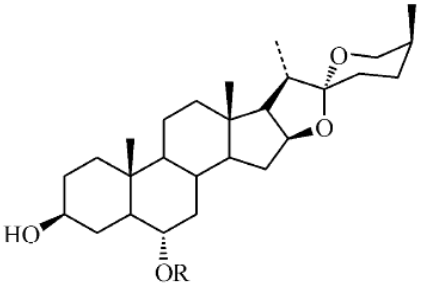

neochlorogenin 6-*O*-*β*-D-quinovopyranoside (**189**)

R = 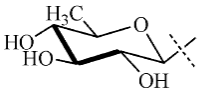

neochlorogenin 6-*O*-α-L-rhamnopyranosyl-(1→3)-*β*-D-quinovopyranoside (**190**)

R = 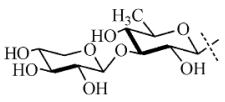

Figure 4 Chemical structure of chemical constituents of *Solanum* spp. (continue)

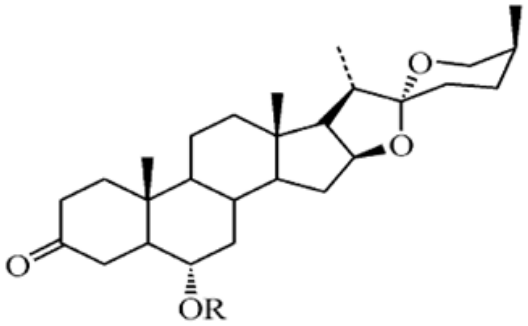

solagenin 6-*O*-*β*-D-quinovopyranoside (**191**) R =

solagenin 6-*O*-α-L-rhamnopyranosyl-(1→3)-*β*-D-quinovopyranoside (**192**) R =

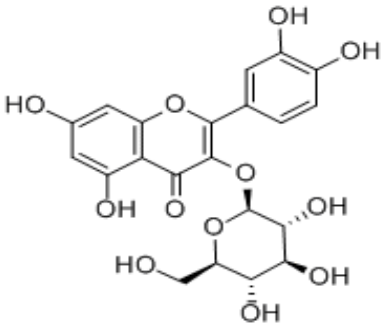

isoquercetin (**193**)

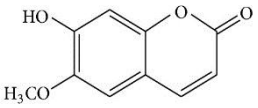

scopletin (**194**)

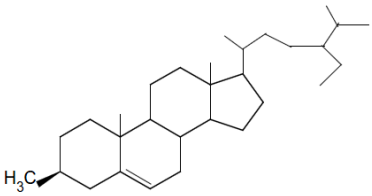

sobatum (**195**)

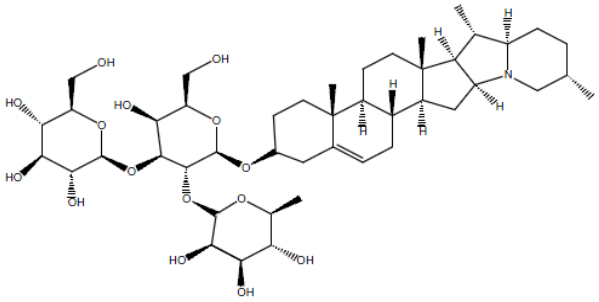

solanine (**196**)

Figure 4 Chemical structure of chemical constituents of *Solanum* spp. (continue)

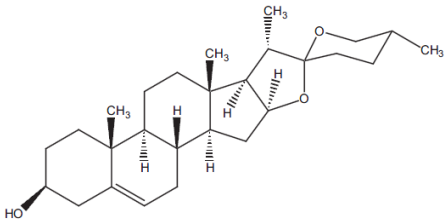

diosogenin (**197**)

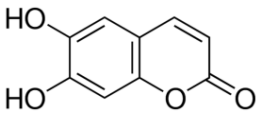

esculetin (**198**)

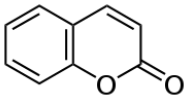

courmarin (**199**)

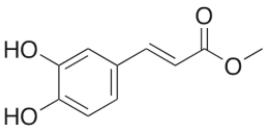

methyl caffeate (**200**)

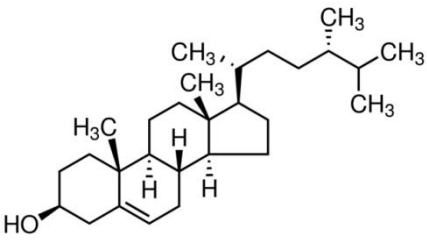

campesterol (**201**)

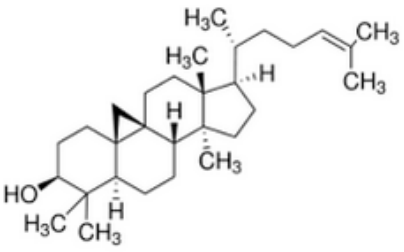

cycloartenol (**202**)

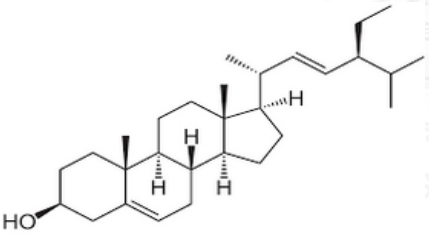

stigmasterol (**203**)

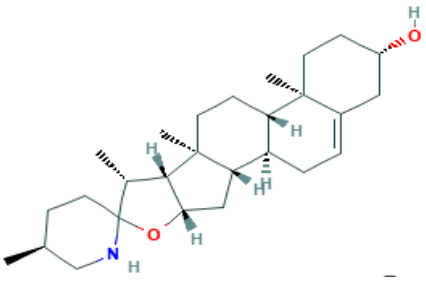

tomatidenol (**204**)

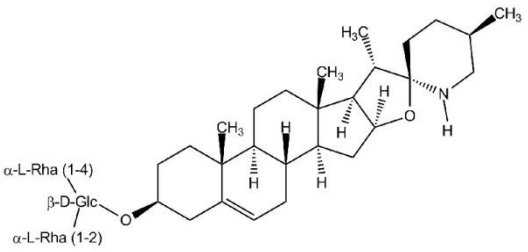

α-solamargine **(205)**

Figure 4 Chemical structure of chemical constituents of *Solanum* spp. (continue)

2.8 *Solanum aculeatissimum*

2.8.1 Description

S. aculeatissimum is belongs to the genus *Solanum* of family Solanaceae. It is also known as cockroach berry or Ma khuea khuen (Thailand). This plant is a perennial shrub widely. The tropical America zone is an originally place. It can be grown throughout worldwide which are found various tropical zones especially Asia and Africa. This shrubby perennial can grow up to 1-3 m height, its trunk can be found short spines. Diameter of spherical fruit is 2-3 cm, striped green and creamy-white are showed in unripe fruits while fresh yellow is showed in ripe fruits. The characteristic of fruit is bitter flavor. *S. aculeatissimum* is known as Thai folklore medicines which grow on fields and groves. Its name is called upon part of Thailand as Ma khuea khuen (Central and Northeastern), Ma khuea chae (Northern) and Khuea hin (Southern). Fruits and whole plant of *S. aculeatissimum* are shown in Figure 5 [115].

2.8.2 Medicinal properties

The fruits of *S. aculeatissimum* have been using as medicine and an ingredient in cosmetics such as treatment of headache, toothache, scabies, tooth decay, constipation, purgative, back pain, male impotence, snakebites, skin infections, flatulence, cough and dysmenorrhea [116, 117]. In India and Nepal, fruits of *S. aculeatissimum* have been used as traditional medicine for a long time [118]. In China, it was used for the treatment of bronchitis and rheumatism [116, 117]. Besides, fruits of *S. aculeatissimum* have been used as folklore medicine for Akgsannibat and cure of phlegm [117].

2.8.3 Chemical constituents and biological compounds

S. aculeatissimum contains steroidal alkaloids and saponins which be found and isolated from leaves, stems, roots, seeds and fruits [119, 120]. Previously studies, the methanolic extract of leaves of *S. aculeatissimum* was reported biological activity with antibacterial properties [121]. The ethanolic extract of leaves of *S. aculeatissimum* showed allelopathic substances with phytotoxic activity. While, the fruits of *S. aculeatissimum* were isolated to obtain as double-headed protease inhibitor which used to inhibit endogenous proteases [122]. The total phenolic content of *S. aculeatissimum* fruits was 3.52 ± 0.01 g/100 g of crude extract as gallic acid and 0.37 g/100 g of dry herb powder as gallic acid. IC_{50} value of antioxidant activity was 852.0 µg/mL [123]. Biological activities and chemical constituents of *S. aculeatissimum* have been investigated and reported as summarized in Table 5. Chemical structure of chemical constituents of *S. aculeatissimum* were shown in Figure 6.

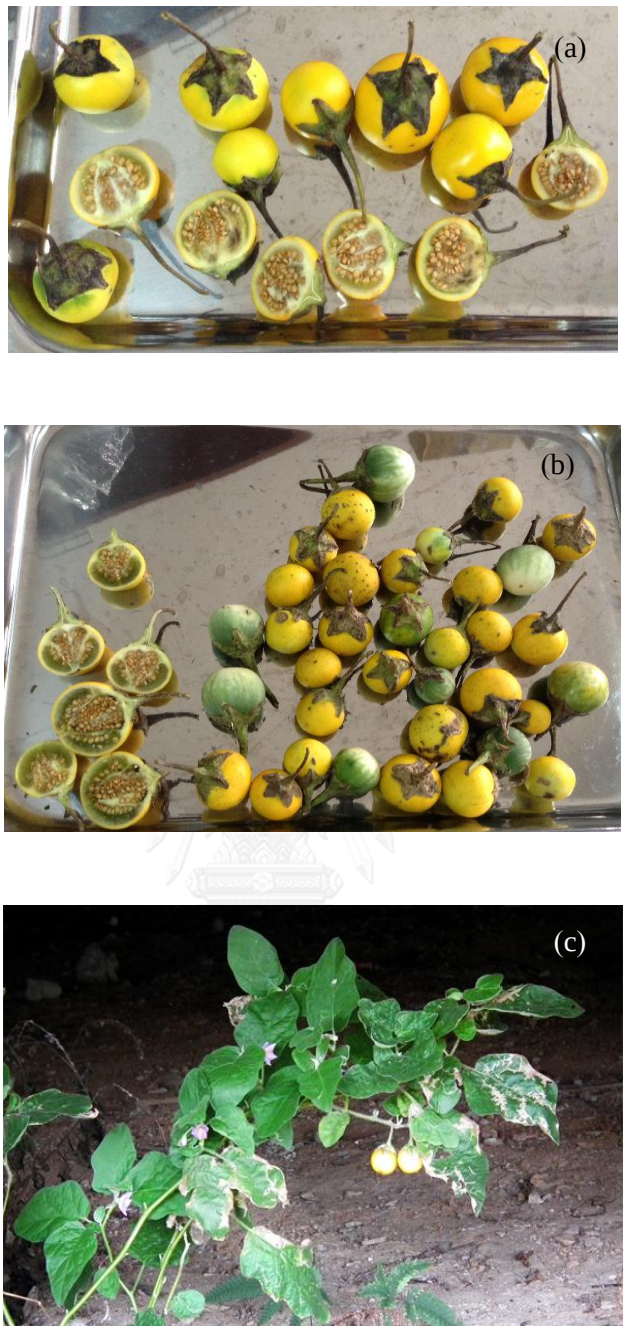

Figure 5 (a) The ripe fruits (b) the ripe and unripe fruits and (c) whole plant of *S. aculeatissimum*

Table 5 Chemical constituents of *S. aculeatissimum*

Plant parts	Chemical constituents	Bioactivity	Reference
Fruits	solanine (**196**)	acetylcholinesterase inhibitor,	[120, 124]
	solasonine (**170**)	antifeedant, fungicide and pesticide activities	
		cytotoxicity against several human cancer cell lines and skin tumours	
	β-solamargine (**171**)	anti-cancer	
	Protease inhibitor	Antihaemolytic and anti-lipid peroxidative potential	[125]
Roots	aculeatiside A (**206**)	production of steroid hormones	[119, 126]
	aculeatiside B (**207**)		
Cell and tissue cultures	solasodine (**145**)	anti-cancer, antifungal, antiandrogenic and antispermatogenetic	[119]
	solasonine (**170**)		
	β-solamargine (**171**)		
	nuatigenin (**208**)	precursors for the manufacture of steroidal hormones and pharmaceuticals	
Aerial parts	genomic DNA	A glucosyltransferase involved in steroid saponin biosynthesis	[127]
Leaves	ethanolic extract	phytotoxic potential activity	[128]
	methanolic extract	antibacterial properties	[121]

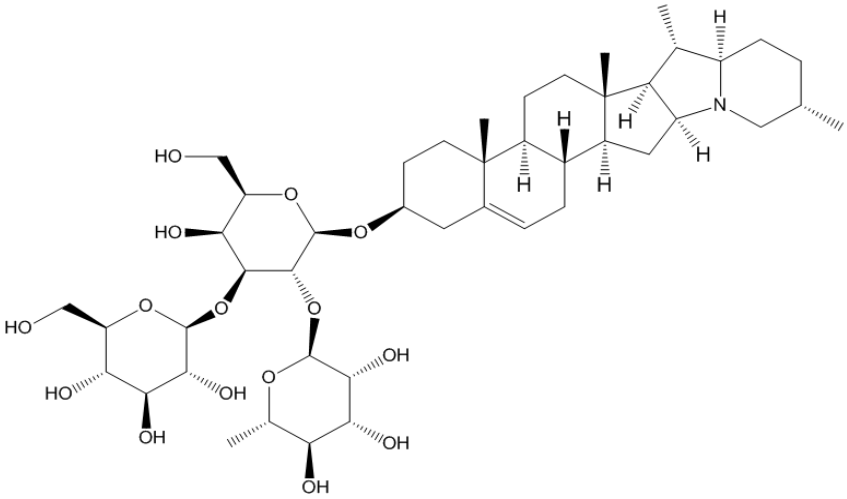

solanine (**196**)

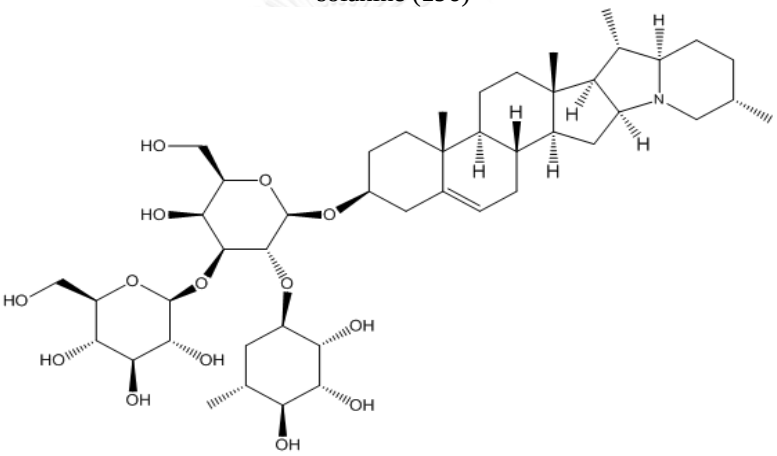

solasonine (**170**)

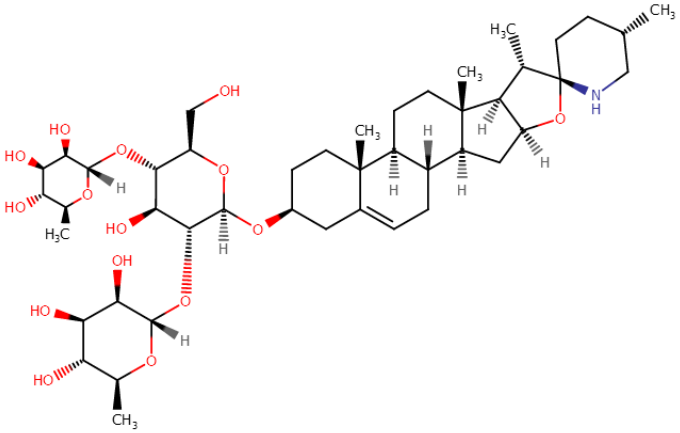

β-solamargine (**171**)

Figure 6 Chemical structure of chemical constituents of *S. aculeatissimum*

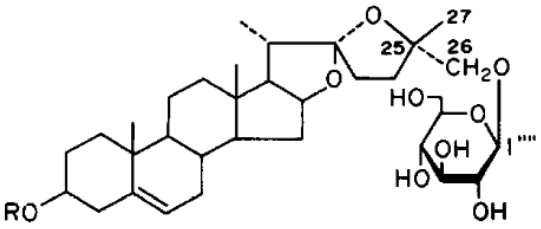

aculeatisides A (**206**)

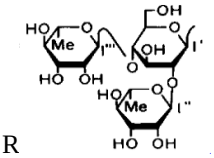

R =

aculeatisides B (**207**)

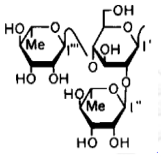

R =

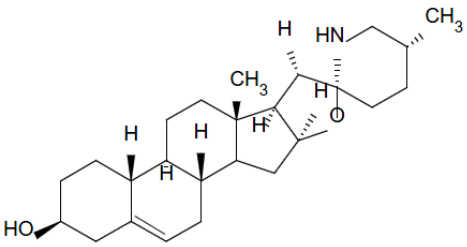

solasodine (**145**)

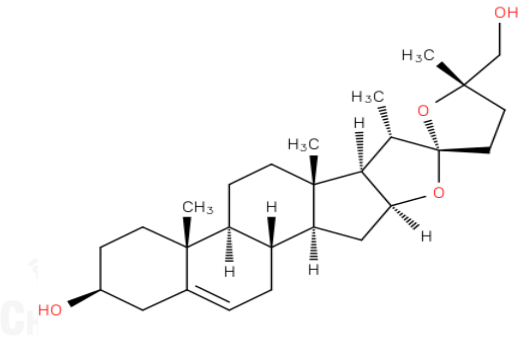

nuatigenin (**208**)

Figure 6 Chemical structure of chemical constituents of *S. aculeatissimum* (continue)

CHAPTER III
MATERIALS AND METHODS

3.1 Plants materials

3.1.1 Plants for preliminary screening

Nineteen Thai medicinal plants were purchased from Phrakhanong market, Bangkok, Thailand. The list of Thai medicinal plants for preliminary screening of anti-lipase activity including scientific name, common name, family and part used are shown in Table 6.

3.1.2 Plant materials of *S. aculeatissimum*

The fresh ripe fruits of *S. aculeatissimum* were collected from Amphoe Atsamart, Roi Et Province, Thailand, in December 2014. A voucher specimen (BCU No. A 015372) was deposited at the Professor Kasin Suvatabhandhu Herbarium, Department of Botany, Faculty of Science, Chulalongkorn University, Bangkok, Thailand.

Table 6 The list of Thai medicinal plants for preliminary screening

No.	Family	Scientific name	Common name (Thai name)	Part used
1	Amaranthaceae	*A. lividus*	Amaranth green (โขมไทย)	Leaves
2	Capparidaceae	*C. viscose*	Stinking cleome (ผักเสี้ยนผี)	Stems, leaves
3	Capparidaceae	*G. gynandra*	Wild spider flower (ผักเสี้ยน)	Roots
4	Cucurbitaceae	*M. charantia*	Bitter cucumber (มะระขี้นก)	Fruits
5	Cucurbitaceae	*M. charantia*	Chinese bitter (มะระจีน)	Fruits
6	Cucurbitaceae	*M. cochinchinensis*	Baby jackfruit, gac (ฟักข้าว)	Fruits
7	Euphorbiaceae	*P. amarus*	Tamalaki, hazardana (ใต้ใบ)	Stems, leaves
8	Fabaceae	*C. siamea*	Siamese cassia (ขี้เหล็ก)	Leaves
9	Leguminosae	*S. rostrata*	Sesbania (โสนผี)	Stems, leaves
10	Menispermaceae	*T. triandra*	Ya-Nang (ย่านาง)	Leaves
11	Piperaceae	*P. sarmentosum*	Wild betal leaf (ชะพลู)	Leaves
12	Solanaceae	*C. annnuum*	Chili spur pepper (พริกชี้ฟ้า)	Fruits
13	Solanaceae	*C. frutescens*	Bird pepper (พริกขี้หนู)	Fruits
14	Solanaceae	*S. aculeatissimum*	Cockroach berry (มะเขือขื่น)	Fruits
15	Solanaceae	*S. melongena*	Long eggplant (มะเขือยาว)	Fruits
16	Solanaceae	*S. melongena*	Round eggplant (มะเขือเสวย)	Fruits
17	Solanaceae	*S. melongena*	Thai eggplant (มะเขือเปราะ)	Fruits
18	Solanaceae	*S. melongena*	Round purple eggplant (มะเขือม่วง)	Fruits
19	Solanaceae	*S. trilobatum*	Purple-fruited pea eggplant (มะแว้งเครือ)	Fruits

3.2 Chemicals and reagents

3.2.1 All commercial grade organic solvents were distrilled prior to use such as hexane, dichloromethane, ethyl acetate, acetone and methanol
3.2.2 All organic solvents for HPLC grade such as acetonitrile, methanol and DDI water were filtrated prior to use, Sigma, Germany
3.2.3 Dimethy sulfoxide (DMSO), ACS reagent, Fluka, Switzerland
3.2.4 Ethanol, Merck, Germany
3.2.5 Acetonitrile, J.T. Baker, USA
3.2.6 Hydrochloric acid, Merck, Germany
3.2.7 Vanillin reagent (powder), Merck, Germany
3.2.8 Tris (hydroxymethyl) aminomethane (Tris-base), MB grade, USB, USA
3.2.9 *p*-Nitrophenylpalmitate, Sigma, Germany
3.2.10 Lipase (porcine pancreas Type II, crude), Promega, USA
3.2.11 Chloroform-d 99.8 atom % D ($CDCl_3$), Merck, Germany
3.2.12 Methanol-d 99.8 atom % D (CD_3OD), Cambridge Isotope Laboratories, USA
3.2.13 Pyridine-d 99.8 atom % D (C_5D_5N), Merck, Germany

3.3 General experimental procedures

3.3.1 Chromatographic techniques

3.3.1.1 Thin layer chromatography (TLC)
Technique: One dimension, ascending
Stationary phase: Silica gel 60 F_{254} pre-coated plates (Merck), layer thickness 0.2 mm
Developing distance: 4.0 cm
Mobile phase: Various solvent systems
Temperature: Room temperature (30 - 35 °C)
Detection: a. Observe under UV light 254 nm
b. Dip 10% sulfuric acid in aqueous ethanol and heat on hot plate
c. Dip 1% vanillin reagent (powder) in sulfuric acid and heat on hot plate

3.3.1.2 Column chromatography

Column: Flat bottom glass column
Stationary phase: a. Diaion HP20 (Mitsubishi, Japan) particle sizes > 250 µm
b. Sephadex LH-20 (GE Healthcare Life Sciences, GE Healthcare Bio-Sciences, USA) particle sizes 18 - 111 µm (Hydroxypropylated, cross-linked dextran matrix)
c. Silica gel 60 (Merck) particle sizes 0.063 - 0.200 nm. (70 - 230 mesh ASTM)
Mobile phase: Various solvent systems
Packing method: Wet packing
Detection: All fractions were detected and examined by TLC

3.3.1.3 Flash chromatography

The samples were analysis and purified using PuriFlash®system (Interchim, France) which consisted of pump, UV Detector (200 - 600 nm), integrated column holders and sample loading (Flash - dry load and liquid load), fraction collector and chromatographic data processing software (Interchim® software). Fractions which were separated from hexane crude extract using PuriFlash column 15 Silica HP - 4.0 g (22 bar). The flow rate was 5 mL/min. The mobile phase was adjusted and used linear gradient at analytical level which composed various organic solvents by increasing polarities. Fractions which were separated from *n*-butanol crude extract using PuriFlash column 15 C18 HP - 6.0 g (22 bar). The flow rate was 5 mL/min. The mobile phase was adjusted and applied with methanol - DI water depending on characteristic of isolated fractions.

3.3.1.4 High performance liquid chromatography (HPLC)

The samples were analyzed using HPLC system (Thermo Separation Products, USA), which consisted of an auto-sampler (AS3000), a manual injection with 20 µL loop (RESTEK SGE syringe), a quaternary pump system (spectra system P4000), vacuum degasser (spectra system SN400), an UV variable-wavelength detector (spectra system UV6000LP) and a chromatographic data processing software (ChromQuest 4.2.34®). Fractions which separated from *n*-butanol crude extract were operated on a Hypersil BDS Cyano column (ø 4.6 mm x 25 cm, 5 µm, Thermo Hypersil-Keystone, Germany). The mobile phase was adjusted and applied with methanol - DDI water depending on characteristic of isolated fractions.

3.3.2 pH meter

The Mettler Toledo (SevenCompactTM) pH meter model S220 was used for adjustment pH of Tris-HCL buffer to 8.50.

3.3.3 Melting point apparatus

The Electrothermal (Mel-Temp®) was used for determination melting points.

3.3.4 Rotary evaporator

The Eyela rotary evaporator model N-1 (EYELA, Japan) was used for evaporating organic solvents under vacuum.

3.3.5 Hot air oven

The WiseVen hot air oven (Witeg, Germany) was used for drying the plants materials.

3.3.6 Water bath

The Memmert (Memmert GmbH, Germany) water bath was used for extraction aqueous extract of plants and incubation of samples reaction for anti-lipase assay.

3.3.7 UV/VIS Spectrophotometer

Instrument name: Microplate reader Multiscan GO (Thermo Fisher Scientific, USA), SkanIT 3.2 (software)
Temperature of incubation: 31.2 °C
Wavelength: 405 nm

3.3.8 Gas chromatography-mass spectrometer (GC-MS)

Instrument name: Triple Quadrupole GC/MS (GC-QQQ), Agilent Technologies
GC Model: Agilent 7890B GC system
MSD model: Agilent 7000C GC/MS triple Quad
GC column: HP-5ms part no. 19091S-433 (5% phenyl methyl siloxane, 30 m x 0.25 mm, 0.25 µm) and HP-INNOWax column (30 m x 0.25 mm, 0.25 µm)

3.3.9 Nuclear magnetic resonance spectrometer (NMR)

The ^{1}H and ^{13}C NMR spectra were obtained either at 300 MHz and 75.5 MHz, respectively on Bruker model Fourier 300 spectrometer (Bruker, USA) and 500 MHz and 125.5 MHz, respectively on Bruker model Fourier 500 spectrometer (Bruker, USA). NMR solvents were used as deuterated chloroform ($CDCl_3$), deuterated methanol (CD_3OD) and deuterated pyridine (C_5D_5N).

3.3.10 High resolution mass spectrometer

The high resolution mass spectra were recorded by Bruker model MICROTOF (Bruker Daltonics, USA). The coupled mass spectrometer was operated in electrospray ionization (ESI) mode. Scan range of beginning and end were 50 - 3000 m/z.

3.4 Methods

3.4.1 Extraction of plant materials for preliminary screening

Plant materials were washed with water and dried in hot air oven at 60 ^{o}C. Then, the dry samples were ground into small pieces. The dried-ground plant was extracted three times with methanol at room temperature for three days. Then, the extract was filtrated with Whatman no. 1 filter paper. The methanolic crude extract was obtained by removal of solvent *in vacuo*. For aqueous extraction, the dried-ground plant was extracted three times with DI water at 60 ^{o}C for 30 minutes. Then, the extract was filtrated with Whatman no. 1 filter paper and removed solvent *in vacuo* to give aqueous crude extract as shown in Figure 7.

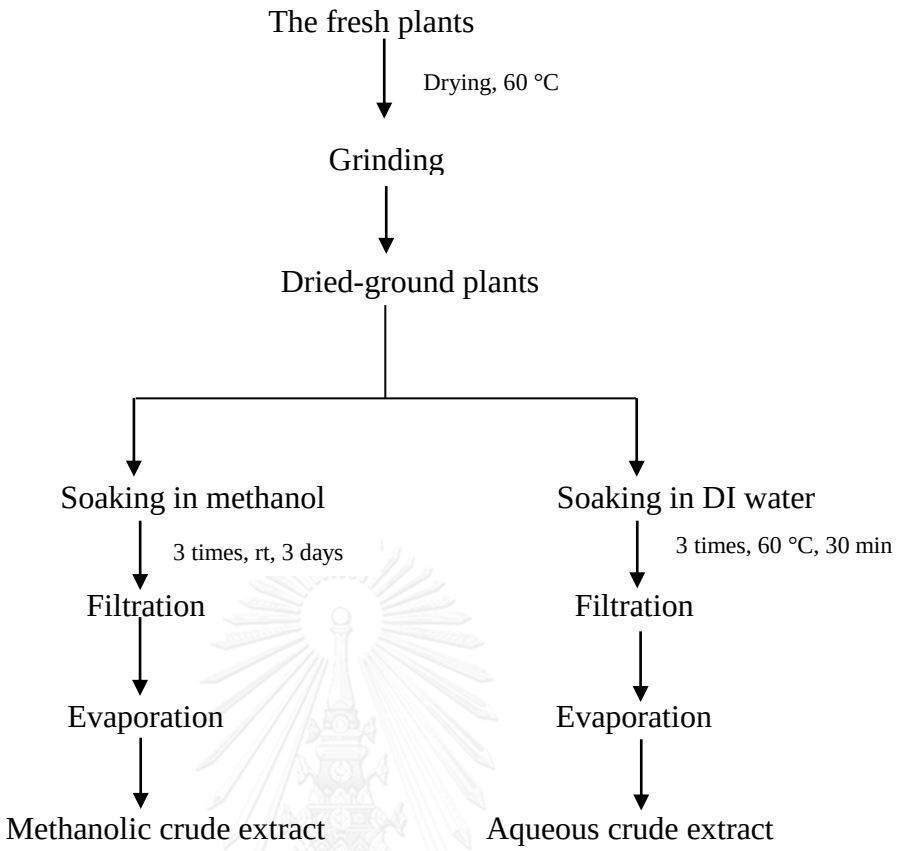

Figure 7 Extraction procedure of plant materials for preliminary screening

3.4.2 Extraction of *S. aculeatissimum* fruits

The fresh ripe fruits of *S. aculeatissimum* (37.83 kg) were washed with water and dried in hot air oven at 60 °C. Then, the dried samples were ground into small pieces. The dried-ground fruits (6.56 kg) were extracted with methanol (16 L) for 48 h at room temperature for 4 times. Then, the extract was filtrated with Whatman no. 1 filter paper and was evaporated *in vacuo* to obtain methanolic crude extract (1.01 kg). The methanolic crude extract was partitioned with various solvents by increasing polarities to obtain four subfractions as hexane crude extract, ethyl acetate crude extract, *n*-butanol crude extract and aqueous crude extract as shown in Figure 8. All crude extracts were evaluated for lipase inhibitory activity.

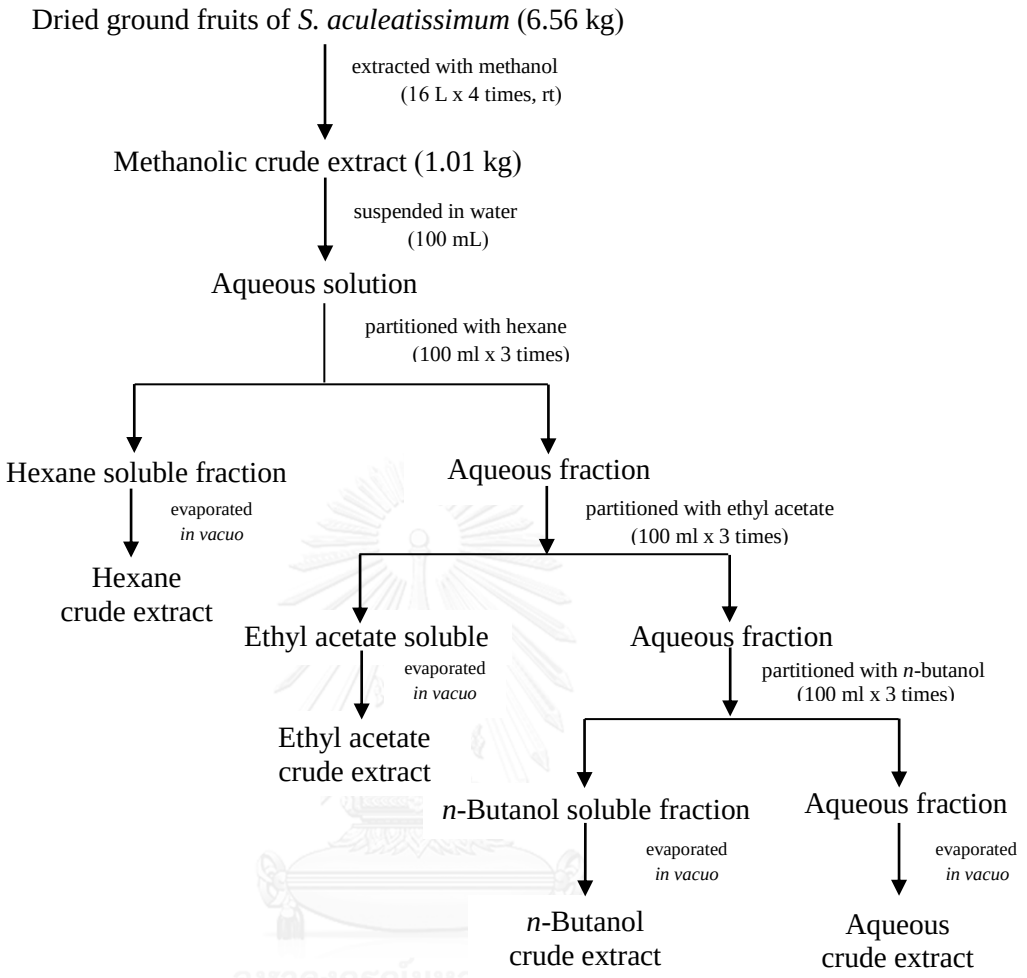

Figure 8 Extraction procedure of *S. aculeatissimum* fruits

3.4.2.1 Separation of hexane crude extract of *S. aculeatissimum* fruits

The hexane crude extract (fraction Hx, 130.00 g) was subjected to quick column chromatography on silica gel (300 g) using hexane (7 L), hexane:ethyl acetate (1:1 v/v) (4 L), ethyl acetate (6 L) and ethyl acetate:methanol (9:1 v/v) (4 L) as the eluent to afford four subfractions (Hx-A - Hx-D). Each subfraction was evaluated for lipase inhibitory activity *in vitro*. The active fractions were further separated to obtain pure compounds.

The fraction Hx-A (8.62 g) was separated by silica gel column chromatography eluting with hexane, hexane:ethyl acetate (9.5:0.5 v/v), hexane:ethyl acetate (9:1 v/v), hexane:ethyl acetate (1:1 v/v) and ethyl acetate to give nine subfractions (Hx-AA - Hx-AI). The fraction Hx-AF (2.95 g) was separated by silica gel column chromatography eluting with heptane:hexane (1:1 v/v), hexane, hexane:dichloromethane (1:1 v/v) and ethyl acetate to give nine subfractions (Hx-AFA - Hx-AFI). Fraction Hx-AFE (290.0 mg) was separated by column

chromatography using silica gel and eluting with petroleum ether, petroleum ether:ethyl acetate (8:2 v/v), petroleum ether:ethyl acetate (6:4 v/v), petroleum ether:ethyl acetate (4:6 v/v), petroleum ether:ethyl acetate (2:8 v/v) and ethyl acetate to give eight subfractions (Hx-AFE1 - Hx-AFE8). Fraction Hx-AFE3 (270.0 mg) was further separated by column chromatography using silica gel and eluting with petroleum ether, petroleum ether:dichloromethane (8:2 v/v), petroleum ether:dichloromethane (6:4 v/v), petroleum ether:dichloromethane (4:6 v/v) and dichloromethane to give twelve subfractions (Hx-AFE3A - Hx-AFE3L). The fraction Hx-AH (280.1 mg) was separated by silica gel column chromatography eluting with hexane, hexane:acetone (9.5:0.5 v/v), hexane:acetone (9:1 v/v), hexane:acetone (8.5:1.5 v/v), hexane:acetone (8:2 v/v), hexane:acetone (1:1 v/v) and acetone to give seven subfractions (Hx-AHA - Hx-AHG). Fraction Hx-AHE (58.0 mg) was separated by column chromatography using silica gel and eluting with hexane, hexane:ethyl acetate (9:1 v/v), hexane:ethyl acetate (8:2 v/v), hexane:ethyl acetate (7:3 v/v), hexane:ethyl acetate (1:1 v/v) and ethyl acetate to give eight subfractions (Hx-AHE1 - Hx-AHE8). Fraction Hx-AHE4 (compound **209**) was obtained as white solid (8.2 mg, 0.0063% w/w of hexane crude extract).

The fraction Hx-D (5.01 g) was separated by column chromatography using Diaion HP20 with ethyl acetate, ethyl acetate:methanol (1:1 v/v), methanol and DI water as eluents to give five subfractions (Hx-DA - Hx-DE). All fractions were tested for lipase inhibitory activity. The fraction Hx-DA (1.95 g) was separated by column chromatography on silica gel eluting with ethyl acetate, ethyl acetate:methanol (9:1 v/v), ethyl acetate:methanol (8:2 v/v) and ethyl acetate:methanol (7:3 v/v) to give five subfractions (Hx-DAA - Hx-DAE). Fraction Hx-DAB (230.9 mg) was subjected to flash chromatography using PuriFlash column 15 Silica HP - 4.0 g (22 bar) eluting with gradient mobile phase as hexane, hexane:ethyl acetate (1:1 v/v), ethyl acetate, ethyl acetate:methanol (9:1 v/v) and ethyl acetate:methanol (6:4 v/v) to give four subfractions (Hx-DAB1 - Hx-DAB4). Fraction Hx-DAB2 (162.1 mg) was further separated by flash chromatography using PuriFlash column 15 Silica HP - 4.0 g (22 bar) eluting with gradient mobile phase as hexane, hexane:dichloromethane (1:1 v/v) and dichloromethane to give five subfractions (Hx-DAB21 - Hx-DAB25). The fraction Hx-DAB24 (115.1 mg) was separated by flash chromatography using PuriFlash column 15 Silica HP - 4.0 g (22 bar) eluting with hexane, hexane:dichloromethane (1:1 v/v) and dichloromethane to give four subfractions (Hx-DAB241 - Hx-DAB244). Fraction Hx-DAB243 (45.2 mg) was separated by flash chromatography eluting using PuriFlash column 15 Silica HP - 4.0 g (22 bar) with hexane, hexane:dichloromethane (1:1 v/v), dichloromethane, dichloromethane:methanol (9:1 v/v) and dichloromethane:methanol (8:2 v/v) to give five subfractions (Hx-DAB2431 - Hx-DAB2435). Fraction Hx-DAD was subjected to flash chromatography eluting with hexane, hexane:ethyl acetate (1:1 v/v), ethyl acetate, ethyl acetate:methanol (9:1 v/v), ethyl acetate:methanol (8:2 v/v), ethyl acetate:methanol (7:3 v/v) and ethyl acetate:methanol (6:4 v/v) to give four subfractions (Hx-DAD1 - Hx-DAD4).

The fraction Hx-DB showed strong anti-lipase activity. Thus, it was separated by column chromatography on silica gel eluting with ethyl acetate, ethyl acetate:methanol (9:1 v/v), ethyl acetate:methanol (8:2 v/v) and ethyl acetate:methanol (7:3 v/v) to give six subfractions (Hx-DBA - Hx-DBF). Fraction Hx-

DBC (160.5 mg) was subjected to silica gel column chromatography eluting with hexane, hexane:acetone (9:1 v/v), hexane:acetone (7:3 v/v), hexane:acetone (1:1 v/v), hexane:acetone (3:7 v/v), acetone and ethyl acetate:methanol (7:3 v/v) to give six subfractions (Hx-DBC1 - Hx-DBC6). Fraction Hx-DBC2 (62.2 mg) was further separated by column chromatography using silica gel with hexane, hexane:ethyl acetate (9.5:0.5 v/v), hexane:ethyl acetate (9:1 v/v), hexane:ethyl acetate (8:2 v/v), hexane:ethyl acetate (7:3 v/v), hexane:ethyl acetate (6:4 v/v), hexane:ethyl acetate (1:1 v/v) and ethyl acetate as eluents to give seven subfractions (Hx-DBC21 - Hx-DBC27). The fraction Hx-DBC24 (38.1 mg) was separated by silica gel column chromatography eluting with hexane, hexane:acetone (9.5:0.5 v/v), hexane:acetone (9:1 v/v), hexane:acetone (8.5:1.5 v/v), hexane:acetone (8:2 v/v), hexane:acetone (7.5:2.5 v/v) and hexane:acetone (7:3 v/v) to give eight subfractions (Hx-DBC241 - Hx-DBC248). Fraction Hx-DBC243 (compound **210**) was obtained as white crystal (1.4 mg, 0.0011% w/w of hexane crude extract). It was further analyzed by GC-MS. Fraction Hx-DBC4 (48.2 mg) was separated by flash chromatography using PuriFlash column 15 Silica HP - 4.0 g (22 bar) eluting with gradient mobile phase as hexane:ethyl acetate (1:1 v/v), hexane:ethyl acetate (3:7 v/v), ethyl acetate, ethyl acetate:methanol (9:1 v/v), ethyl acetate:methanol (8:2 v/v), ethyl acetate:methanol (7:3 v/v) and ethyl acetate:methanol (6:4 v/v) to give four subfractions (Hx-DBC41-Hx-DBC44). Fraction Hx-DBD (500.4 mg) was separated by silica gel column chromatography eluting with ethyl acetate, ethyl acetate:methanol (9.5:0.5 v/v), ethyl acetate:methanol (9:1 v/v), ethyl acetate:methanol (8.5:1.5 v/v), ethyl acetate:methanol (8:2 v/v), ethyl acetate:methanol (7.5:2.5 v/v) and ethyl acetate:methanol (7:3 v/v) to give eight subfractions (Hx-DBD1 - Hx-DBD8). Fraction Hx-DBD5 (170.1 mg) was separated by column chromatography using silica gel with ethyl acetate, ethyl acetate:methanol (9.5:1.5 v/v), ethyl acetate:methanol (9:1 v/v), ethyl acetate:methanol (8.5:1.5 v/v), ethyl acetate:methanol (8:2 v/v) and ethyl acetate:methanol (7:3 v/v) as eluents to give four subfractions (Hx-DBD51 - Hx-DBD54). Fraction Hx-DBD52 (142.4 mg) was further separated by silica gel column chromatography eluting with ethyl acetate, ethyl acetate:methanol (9.5:0.5 v/v), ethyl acetate:methanol (9:1 v/v), ethyl acetate:methanol (8.5:1.5 v/v), ethyl acetate:methanol (8:2 v/v) and ethyl acetate:methanol (7.5:2.5 v/v) to afford ten subfractions (Hx-DBD52A - Hx-DBD52J). Fraction Hx-DBD52C (50.9 mg) was separated by column chromatography using silica gel with hexane, hexane:ethyl acetate (9.5:0.5 v/v), dichloromethane, ethyl acetate, ethyl acetate:methanol (9.5:0.5 v/v), ethyl acetate:methanol (9:1 v/v), ethyl acetate:methanol (8:2 v/v) and ethyl acetate:methanol (7:3 v/v) as eluents to afford twelve subfractions (Hx-DBD52CA - Hx-DBD52CL). Fraction Hx-DBD52CE (6.0 mg) was separated by silica gel column chromatography eluting with ethyl acetate, ethyl acetate:methanol (9.5:0.5 v/v), ethyl acetate:methanol (9:1 v/v), ethyl acetate:methanol (8.5:1.5 v/v), ethyl acetate:methanol (8:2 v/v), ethyl acetate:methanol (7.5:2.5 v/v) and ethyl acetate:methanol (7:3 v/v) to give eight subfractions (Hx-DBD52CE1 - Hx-DBD52CE8).

The fraction Hx-DC (1.89 g) was separated by column chromatography on silica gel eluting with ethyl acetate, ethyl acetate:methanol (9:1 v/v), ethyl acetate:methanol (8:2 v/v) and ethyl acetate:methanol (7:3 v/v) to give three subfractions (Hx-DCA - Hx-DCC).

3.4.2.2 Separation of *n*-butanol crude extract of *S. aculeatissimum* fruits

The *n*-butanol crude extract (fraction Bu, 11.52 g) was subjected to column chromatography using Diaion HP20 with ethyl acetate, ethyl acetate:methanol (1:1 v/v), methanol and DI water as eluents and eluates were kept 50 mL per flask to obtain five subfractions (Bu-A - Bu-E). Each subfraction was evaluated for lipase inhibitory activity. The active fractions were further separated to obtain pure compounds.

Fraction Bu-B (5.72 g) was separated by column chromatography on silica gel eluting with dichloromethane:methanol (9:1 v/v), dichloromethane:methanol (7:3 v/v), dichloromethane:methanol (1:1 v/v) and dichloromethane:methanol (3:7 v/v) to afford five subfractions (Bu-BA - BU-BE). Then, fraction Bu-BD (1.38 g) was further subjected to Sephadex LH-20 column chromatography with methanol to yield two subfractions (Bu-BD1 - Bu-BD2). Fraction Bu-BD2 (897.8 mg) was further subjected to Sephadex LH-20 column chromatography with dichloromethane:methanol (1:1 v/v) and methanol as eluents to yield five subfractions (Bu-BD2A - Bu-BD2E). Fraction Bu-BD2A (176.2 mg) was separated by column chromatography on silica gel with dichloromethane:methanol (9:1 v/v), dichloromethane:methanol (7:3 v/v), dichloromethane:methanol (1:1 v/v) and dichloromethane:methanol (3:7 v/v) as eluents to yield twelve subfractions (Bu-BD2AA - Bu-BD2AL). Fraction of Bu-BD2AC (compound **211**) was obtained as white solid (3.8 mg, 0.0330% w/w of *n*-butanol crude extract).

Fraction Bu-C (4.10 g) was separated by column chromatography on silica gel with ethyl acetate, ethyl acetate:methanol (9.5:0.5 v/v), ethyl acetate:methanol (9:1 v/v), ethyl acetate:methanol (8.5:1.5 v/v), ethyl acetate:methanol (8:2 v/v), ethyl acetate:methanol (7.5:2.5 v/v), ethyl acetate:methanol (7:3 v/v), ethyl acetate:methanol (6:4 v/v) and ethyl acetate:methanol (5.5:4.5 v/v) as eluents to afford twelve subfractions (Bu-CA - Bu-CL). Then, fraction Bu-CG (132.8 mg) was subjected to Sephadex LH-20 column chromatography with methanol to yield four subfractions (Bu-CGA - Bu-CGD). Fraction Bu-CGB (38.9 mg) was further subjected to Sephadex LH-20 column chromatography with methanol as eluent to yield four subfractions (Bu-CGBA - Bu-CGBD).

Fraction Bu-D (0.56 g) was separate by column chromatography using Sephadex LH-20 with methanol as eluent to yield five subfractions (Bu-DA - Bu-DE). The active fractions were further separated to obtain pure compounds. Fraction Bu-DA (33.0 mg) was further fractionated by HPLC and was operated on a Hypersil BDS Cyano column (ø 4.6 mm ×25 cm, 5 µm, Thermo Hypersil-Keystone, Germany). The gradient elution system consisted of methanol (A) and DDI water (B) as the mobile phase using the following gradient: 70-90% A at 0-40 min, 90-100% A at 40-50 min, 100% A at 50-60 min. The injection volume was 20 µL. Flow rate was 1.0 mL/min, and UV absorption was measured at wavelengths of 220 nm to yield four subfractions (Bu-DA1 - Bu-DA4). Subfraction Bu-DA2 was obtained as compound **212** as white crystals (4.5 mg, 0.0391% w/w of *n*-butanol crude extract). Fraction Bu-DB (90.2 mg) was further fractionated by HPLC and was operated on a Hypersil BDS Cyano column (ø 4.6 mm ×25 cm, 5 µm, Thermo Hypersil-Keystone, Germany). The gradient elution system consisted of methanol (A) and DDI water (B) as the mobile phase using the following gradient: 50-80% A at 0-40 min, 80-100% A at 40-50 min, 100% A at 50-60 min. The injection volume was 20 µL. Flow rate was 1.0 mL/min,

and UV absorption was measured at wavelengths of 220 nm to yield four subfractions (Bu-DB1 - Bu-DB4). Subfraction Bu-DB2 was re-crystallized with a mixture of dichloromethane and methanol to obtain compound **213** as white crystals (3.0 mg, 0.0260% w/w of *n*-butanol crude extract). Subfraction Bu-DB3 (22.0 mg) was further isolated by HPLC and was operated on a Hypersil BDS Cyano column (ø 4.6 mm ×25 cm, 5 µm, Thermo Hypersil-Keystone, Germany). The gradient elution system consisted of methanol (A) and DDI water (B) as the mobile phase using the following gradient: 80-80% A at 0-40 min, 80-100% A at 40-50 min, 100% A at 50-60 min. The injection volume was 20 µL. Flow rate was 1.0 mL/min, and UV absorption was measured at wavelengths of 220 nm to yield four subfractions (Bu-DB31 - Bu-DB34). Subfraction Bu-DB32 obtained compound **214** as white crystals (4.9 mg, 0.0425% w/w of *n*-butanol crude extract).

The *n*-butanol crude extract (fraction Bu, 30.05 g) was re-separated. It was subjected to column chromatography using Diaion HP20 with ethyl acetate, ethyl acetate:methanol (1:1 v/v), methanol and DI water as eluents to obtain five subfractions (Bu-A - Bu-E).

Fraction Bu-C (0.50 g) was re-separated by flash chromatography using PuriFlash column 15 C18 HP - 6.0 g (22 bar) eluting with methanol:DI water (1:1 v/v), methanol:DI water (6:4 v/v), methanol:DI water (7:3 v/v), methanol:DI water (8:2 v/v), methanol:DI water (9:1 v/v) and methanol to give five subfractions (Bu-C1 - Bu-C5). Fraction Bu-C2 (120.1 mg) was further subjected to flash chromatography using PuriFlash column 15 C18 HP - 6.0 g (22 bar) eluting with methanol:DI water (1:1 v/v), methanol:DI water (6:4 v/v), methanol:DI water (7:3 v/v), methanol:DI water (8:2 v/v), methanol:DI water (9:1 v/v) and methanol to give three subfractions (Bu-C21 - Bu-C23). Fraction C21 (60.0 mg) was subjected to flash chromatography using PuriFlash column 15 C18 HP - 6.0 g (22 bar) eluting with methanol:DI water (1:1 v/v), methanol:DI water (6:4 v/v), methanol:DI water (7:3 v/v), methanol:DI water (8:2 v/v), methanol:DI water (9:1 v/v) and methanol to give four subfractions (Bu-C211 - Bu-C214). The fraction Bu-C22 (22.5 mg) was subjected to flash chromatography using PuriFlash column 15 C18 HP - 6.0 g (22 bar) eluting with methanol:DI water (1:1 v/v), methanol:DI water (6:4 v/v), methanol:DI water (7:3 v/v), methanol:DI water (8:2 v/v), methanol:DI water (9:1 v/v) and methanol to give four subfractions (Bu-C221 - Bu-C224).

Fraction Bu-D (1.19 mg) was re-separated by column chromatography using Sephadex LH-20 with methanol as eluent to yield five subfractions (Bu-DA - Bu-DE). Fraction Bu-DA (272.1 mg) was re-separated by flash chromatography using PuriFlash column 15 C18 HP - 6.0 g (22 bar) eluting with methanol:DI water (1:1 v/v), methanol:DI water (6:4 v/v), methanol:DI water (7:3 v/v), methanol:DI water (8:2 v/v), methanol:DI water (9:1 v/v) and methanol to give four subfractions (Bu-DA1 - Bu-DA4). Fraction Bu-DA1 (42.0 mg) was further subjected to flash chromatography using PuriFlash column 15 C18 HP - 6.0 g (22 bar) eluting with methanol:DI water (1:1 v/v), methanol:DI water (6:4 v/v), methanol:DI water (7:3 v/v), methanol:DI water (8:2 v/v), methanol:DI water (9:1 v/v) and methanol to give three subfractions (Bu-DA11 - Bu-DA13). Fraction Bu-DC (38.5 mg) was subjected to flash chromatography using PuriFlash column 15 C18 HP - 6.0 g (22 bar) eluting with methanol:DI water (1:1 v/v), methanol:DI water (6:4 v/v), methanol:DI water

(7:3 v/v), methanol:DI water (8:2 v/v), methanol:DI water (9:1 v/v) and methanol to give four subfractions (Bu-DC1 - Bu-DC4).

3.4.3 Gas chromatography-mass spectrometry (GC-MS) analysis of compounds **209** and **210**

GC-MS is an analytical method which combines the features of gas-liquid chromatography and mass spectrometry to provide the identification of compounds which be separated, identified and quantified the complex mixtures of chemicals. GC-MS was used to analyze and identify compounds **209** and **210**.

The condition for GC of compound **209** was analyzed using HP-INNOWax column (30 m x 0.25 mm, 0.25 µm). Injector volume was 1.50 µL and split ratio was 20:1. Helium was used as carrier gas with flow rate at 1.50 mL/min. Temperature programming of the initial column temperature was 250 ^{o}C, the programmed for heating of 20 ^{o}C/min and remained at 220 ^{o}C for 2 minutes. Next, column temperatures were programmed for heating of 10 ^{o}C/min and remained at 250 ^{o}C for 15 minutes. The coupled mass spectrometer was operated in electron impact (EI) ionization mode with electron energy of 70 eV. Interface temperature and ion source temperature were 230 ^{o}C with scan range of 33 - 400 m/z.

The condition for GC of compound **210** was analyzed using HP-5 MS column (5% phenyl methyl siloxane, 30 m x 0.25 mm, 0.25 µm). Injector volume was 1.50 µL and split ratio was 5:1. Helium was used as carrier gas with flow rate at 1.50 mL/min. Temperature programming of the initial column temperature was 120 ^{o}C, then programmed for heating of 15 ^{o}C/min and remained at 300 ^{o}C for 10 minutes. The coupled mass spectrometer was operated in EI ionization mode with electron energy of 70 eV. Interface temperature and ion source temperature were 280 ^{o}C with scan range of 45 - 450 m/z.

3.4.4 Assay for lipase inhibitory activity *in vitro*

Method for measuring pancreatic lipase activity was employed with some modifications from that of Slanc *et al*. [129] Briefly, reaction based on determination by measuring hydrolysis reaction of *p*-nitrophenylpalmitate (*p*-NPP) as a substrate to *p*-nitrophenol as product. The samples were dissolved in dimethyl sulfoxide (DMSO) at a concentration of 25 mg/mL. An enzyme buffer was prepared by addition porcine pancreatic lipase (type II, crude, Promega) in Tris-HCL buffer (pH 8.5). The mixture of reaction contained crude extract, enzyme buffer and Tris-HCL. Reaction solution was incubated and shaked at 37 °C for 25 minutes. Then, ethanol was added to stop reaction. For negative control reaction, ethanol was added to stop reaction before addition of enzyme buffer. Pancreatic lipase inhibitory activity was determined by measuring hydrolysis reaction of *p*-nitrophenyl palmitate to *p*-nitrophenol in microplate reader at 405 nm. Positive control as orlistat was dissolved in DMSO at a concentration of 25 µg/mL. Pancreatic lipase inhibitory activity was tested in triplicate. The results were averaged and expressed with standard deviations. Lipase inhibition (%) was calculated according the following formula:

$$\text{Inhibition activity (\%)} = \frac{(A-a)-(B-b)}{(A-a)} \times 100$$

Where A is an absorbance without sample

a is an absorbance of negative control (ethanol was added before enzyme) without sample
B is an absorbance with sample
b is an absorbance negative control (ethanol was added before enzyme) with sample

3.4.5 Determination of IC_{50} of isolated compounds

The half maximal inhibitory concentration (IC_{50}) is a concentration of measurement of inhibitor on anti-lipase activity *in vitro* which is reduced by half or 50% inhibition. The isolated compounds were evaluated by dissolving in DMSO. Concentrations were prepared for evaluation anti-lipase activity when comparing with orlistat as positive control. Briefly, compound **209** was prepared for five dilutions as 100, 200, 500, 700 and 1000 µg/mL. Compound **210** was prepared for five dilutions as 50, 100, 200, 400 and 800 ug/mL. Compound **211** was prepared for five dilutions as 125, 250, 500, 750 and 1000 µg/mL. Compound **212** was prepared for four dilutions as 25, 50, 100 and 400 µg/mL. Compounds **213** and **214** were prepared for four dilutions as 25, 50, 100 and 200 µg/mL. While, orlistat was prepared for six dilutions as 0.00625, 0.0125, 0.025, 0.05, 0.1 and 0.2 µg/mL.

CHAPTER IV
RESULTS AND DISSCUSSION

4.1 Plants materials

Fresh nineteen of Thai medicinal plants were dried in hot air oven at 60 ^{o}C. These plants gave percent yield of dried plant was 5.24 - 36.46% w/w of fresh plant. The fruits of *S. trilobatum* gave the highest percent yield with 36.46% w/w of fresh plant. While, the roots of *G. gynandra* gave the lowest percent yield with 5.24% w/w of fresh plant. The percent yield of dried plant is shown in Table 7. After that, they were extracted with methanol and DI water, respectively. The percent yield of methanolic and aqueous crude extracts was ranging of 1.98 - 28.54% and 1.39 - 44.87% w/w of dried plant, respectively. The highest percent yield of methanolic and aqueous extracts were leaves *P. sarmentosum* and fruits of *C. annnuum* with 28.54 and 44.87% w/w of dried plants, respectively. The lowest percent yield of methanolic and aqueous extracts were fruits of *S. trilobatum* and stems and leaves *P. amarus* with 1.98 and 1.39% w/w of dried plants, respectively as shown in Table 8.

4.2 Lipase inhibitory activity of Thai medicinal plants

The results of preliminary screening were enlisted and showed the list of percent inhibition of methanolic and aqueous extracts at concentration of 25 mg/mL (Table 8). Methanolic extract of fruits of *S. aculeatissimum*, methanolic extract of fruits of *S. trilobatum* and methanolic extract of stems and leaves of *P. amarus* showed strong inhibition with percent inhibition as 87.77 ± 4.27%, 83.69 ± 4.27% and 83.57 ± 1.48%, respectively. Methanolic extract of fruits of *C. frutescens*, methanolic extract of fruits of *S. melongena* (round eggplant), aqueous extract of fruits of *S. trilobatum*, aqueous extract of fruits of *S. melongena* (Thai eggplant) and methanolic extract of fruits of *S. melongena* (long eggplant) showed moderate anti-lipase activity with percent inhibition as 69.28 ± 2.79%, 51.58 ± 9.50%, 67.43 ± 4.89%, 53.02 ± 15.60% and 47.76 ± 8.44%, respectively. Methanolic extract of stems and leaves of *C. viscose*, methanolic extract of fruits of *S. melongena* (Thai eggplant), methanolic extract of leaves of *P. sarmentosum*, methanolic extract of stems and leaves of *S. rostrata*, methanolic extract of leaves of *T. triandra*, methanolic extract of fruits of *C. annnuum*, aqueous extract of fruits of *S. melongena* (round eggplant) and aqueous extract of fruits of *S. melongena* (long eggplant) showed weak anti-lipase activity with percent inhibition as 37.74 ± 1.71%, 37.03 ± 0.66%, 34.09 ± 19.55%, 31.31 ± 1.93%, 28.56 ± 10.48%, 16.78 ± 1.40%, 40.46 ± 23.19% and 5.02 ± 18.10%, respectively. Aqueous extract of fruits of *S. aculeatissimum*, aqueous extract of stems and leaves of *S. rostrata*, aqueous extract of fruits of *C. frutescens*, aqueous extract of stems and leaves of *C. viscose*, aqueous extract of leaves of *P. sarmentosum*, aqueous extract of leaves of *T. triandra*, aqueous extract of fruits of *C. annnuum*, methanolic and aqueous extracts of leaves of *C. siamea*, methanolic and aqueous extracts of roots of *G. gynandra*, methanolic and aqueous extract of fruits of *M. cochinchinensis*, methanolic and aqueous extracts of fruits of *S. melongena* (round purple eggplant),

methanolic and aqueous extracts of leaves of *A. lividus* and methanolic and aqueous extracts of fruits of *M. charantia* (bitter cucumber and Chinese bitter) showed no activity of anti-lipase. Orlistat as positive control showed percent inhibition as 96.37 ± 1.48% at concentration of 25 µg/mL. These results are shown in Table 8. Methanolic extract of fruits of *S. aculeatissimum* exhibited the strongest anti-lipase activity when comparison with other crude extracts. It is interesting to isolate lipase inhibitors from *S. aculeatissimum* fruits. In Thailand, this plant has been used as Thai folklore medicines. Presently, there is no report of biological activity as anti-lipase activity. This natural source from *S. aculeatissimum* fruits will be promoted biological activity, especially as lipase inhibitors.

Table 7 Yield of dried weight of Thai medicinal plants for preliminary screening

No.	Family	Scientific name	Common name (Thai name)	Part used[a]	Percent yield (%)[b]
1	Amaranthaceae	*A. lividus*	Amaranth green (โขมไทย)	L	10.66
2	Capparidaceae	*C. viscose*	Stinking cleome (ผักเสี้ยนผี)	S, L	17.17
3	Capparidaceae	*G. gynandra*	Wild spider flower (ผักเสี้ยน)	R	5.24
4	Cucurbitaceae	*M. charantia*	Bitter cucumber (มะระขี้นก)	F	10.60
5	Cucurbitaceae	*M. charantia*	Chinese bitter (มะระจีน)	F	5.99
6	Cucurbitaceae	*M. cochinchinensis*	Baby jackfruit, gac (ฟักข้าว)	F	18.64
7	Euphorbiaceae	*P. amarus*	Tamalaki, hazardana (ใต้ใบ)	S, L	11.53
8	Fabaceae	*C. siamea*	Siamese cassia (ขี้เหล็ก)	L	28.81
9	Leguminosae	*S. rostrata*	Sesbania (โสนผี)	S, L	15.71
10	Menispermaceae	*T. triandra*	Ya-Nang (ย่านาง)	L	32.89
11	Piperaceae	*P. sarmentosum*	Wild betal leaf (ชะพลู)	L	18.69
12	Solanaceae	*C. annnuum*	Chili spur pepper (พริกขี้ฟ้า)	F	13.45
13	Solanaceae	*C. frutescens*	Bird pepper (พริกขี้หนู)	F	27.34
14	Solanaceae	*S. aculeatissimum*	Cockroach berry (มะเขือขื่น)	F	21.24
15	Solanaceae	*S. melongena*	Long eggplant (มะเขือยาว)	F	6.68
16	Solanaceae	*S. melongena*	Round eggplant (มะเขือเสวย)	F	9.50
17	Solanaceae	*S. melongena*	Thai eggplant (มะเขือเปราะ)	F	7.14
18	Solanaceae	*S. melongena*	Round purple eggplant (มะเขือม่วง)	F	10.08
19	Solanaceae	*S. trilobatum*	Purple-fruited pea eggplant (มะแว้งเครือ)	F	36.46

[a]Plant parts: F = fruits; L = leaves; S = stems; R = roots

[b]Percent yield of dried plant (compare with fresh weight, % w/w)

Table 8 Yield of extraction and lipase inhibitory activity of Thai medicinal plants

No.	Scientific name	Common name (Thai name)	Yield of extract (%)		Inhibitory activity (%)	
			Me[a]	Aq[b]	Me[a]	Aq[b]
1	*S. aculeatissimum*	Cockroach berry (มะเขือขื่น)	16.14	13.21	87.77 ± 4.27*	NA*
2	*S. trilobatum*	Purple-fruited pea eggplant (มะแว้งเครือ)	1.98	2.18	83.69 ± 4.27*	67.43 ± 4.89*
3	*P. amarus*	Tamalaki, hazardana (ใต้ใบ)	11.54	1.39	83.57 ± 1.48*	NA*
4	*C. frutescens*	Bird pepper (พริกขี้หนู)	9.36	42.72	69.28 ± 2.79*	NA*
5	*S. melongena*	Round eggplant (มะเขือเสวย)	20.31	19.75	51.58 ± 9.50*	40.46 ± 23.19*
6	*S. melongena*	Long eggplant (มะเขือยาว)	27.85	12.16	47.76 ± 8.44*	5.02 ± 18.10*
7	*C. viscose*	Stinking cleome (ผักเสี้ยนผี)	17.17	14.03	37.74 ± 1.71*	NA*
8	*S. melongena*	Thai eggplant (มะเขือเปราะ)	25.12	24.33	37.03 ± 0.66*	53.02 ± 15.60*
9	*P. sarmentosum*	Wild betal leaf (ชะพลู)	28.54	16.93	34.09 ± 19.55*	NA*
10	*S. rostrata*	Sesbania (โสนผี)	15.71	8.30	31.31 ± 1.93*	NA*
11	*T. triandra*	Ya-Nang (ย่านาง)	16.46	7.32	28.56 ± 10.48*	NA*
12	*C. annnuum*	Chili spur pepper (พริกขี้ฟ้า)	13.82	44.87	16.78 ± 1.40*	NA*
13	*C. siamea*	Siamese cassia (ขี้เหล็ก)	25.48	16.93	NA*	NA*
14	*G. gynandra*	Wild spider flower (ผักเสี้ยน)	5.23	9.76	NA*	NA*
15	*M. cochinchinensis*	Baby jackfruit, gac (฿ักข้าว)	7.90	27.93	NA*	NA*
16	*S. melongena*	Round purple eggplant (มะเขือม่วง)	13.30	16.71	NA*	NA*
17	*A. lividus*	Amaranth green (โขมไทย)	19.39	11.47	NA*	NA*
18	*M. charantia*	Bitter cucumber (มะระขี้นก)	7.60	24.96	NA*	NA*
19	*M. charantia*	Chinese bitter (มะระจีน)	9.19	44.02	NA*	NA*
	Orlistat (positive control)				96.37 ± 1.48**	

* at a concentration of 25 mg/mL

** at a concentration of 25 µg/mL

[a] Me = Methanolic crude extract

[b] Aq = Aqueous crude extract

NA = No activity

Yield (%) = Percent yield of crude extract (compare with dried fruits, % w/w)

4.3 Extraction of *S. aculeatissimum* fruits

The fresh ripe fruits of *S. aculeatissimum* (37.83 kg) were washed with water and dried in hot air oven at 60 °C. Then, the dried sample was ground into small pieces. The dried-ground fruits of *S. aculeatissimum* (6.56 kg) were extracted with methanol and then evaporated in vacuo to obtain methanolic crude extract (1.01 kg, 15.40% w/w). The methanolic crude extract was partitioned with various solvents by increasing polarities to obtain four subfractions as hexane crude extract (fraction Hx, dark green gum, 132.04 g, 13.07% w/w), ethyl acetate crude extract (fraction Ea, brown gum, 44.82 g, 4.44% w/w), *n*-butanol crude extract (fraction Bu, brown solid, 77.46 g, 7.66% w/w) and aqueous crude extract (fraction Aq, dark brown gum, 649.73 g, 64.33% w/w). All crude extracts were evaluated for anti-lipase activity. The hexane and *n*-butanol crude extracts of *S. aculeatissimum* fruits showed strong lipase inhibitory activity with percent inhibition as 81.88 ± 0.98% and 80.74 ± 1.39%, respectively. The ethyl acetate crude extract of *S. aculeatissimum* fruits showed moderate lipase inhibitory activity with percent inhibition as 60.41 ± 7.36%. Whereas, aqueous crude extract showed weak activity with 22.12 ± 1.29% inhibition as shown in Table 9.

Table 9 Lipase inhibitory activity of crude extracts of *S. aculeatissimum* fruits

Crude extract/sample	Appearance	Weight (g)	% w/w of crude extract	Inhibitory activity (%)
Hexane	Dark green gum	132.04	13.07	81.88 ± 0.98*
Ethyl acetate	Brown gum	44.82	4.44	60.41 ± 7.36*
n-Butanol	Brown solid	77.46	7.67	80.74 ± 1.39*
Aqueous	Dark brown gum	649.73	64.33	22.12 ± 1.29*
Orlistat				96.37 ± 1.48**

* at a concentration of 25 mg/mL

** at a concentration of 25 µg/mL

4.4 Separation of the crude extracts of *S. aculeatissimum* fruits

4.4.1 Separation of hexane crude extract

The hexane crude extract (fraction Hx, 130.00 g) was subjected to quick column chromatography on silica gel (300 g) using hexane (7 L), hexane:ethyl acetate (1:1 v/v) (4 L), ethyl acetate (6 L) and ethyl acetate:methanol (9:1 v/v) (4 L) as eluents to give four subfractions (Hx-A - Hx-D). Each subfraction was evaluated for lipase inhibitory activity. Fractions Hx-A, Hx-B and Hx-D showed strong activity with percent inhibition as 82.35 ± 3.03%, 81.88 ± 0.98% and 80.74 ± 1.39%, respectively. While, fraction Hx-C showed moderate activity with percent inhibition as 60.41 ± 7.36%. These results are shown in Table 10.

Table 10 Lipase inhibitory activity of fractions Hx-A - Hx-D

Fraction	Weight (g)	Characteristic of fraction	Inhibitory activity (%)
Hx-A	11.52	Dark green gum	82.35 ± 3.03*
Hx-B	49.78	Dark green gum	81.88 ± 0.98*
Hx-C	17.78	Brown gum	60.41 ± 7.36*
Hx-D	5.98	Light brown solid	80.74 ± 1.39*

* at a concentration of 25 mg/mL

The fraction Hx-A showed the strongest anti-lipase activity. It (8.62 g) was separated by silica gel column chromatography eluting with hexane, hexane:ethyl acetate (9.5:0.5 v/v), hexane:ethyl acetate (9:1 v/v), hexane:ethyl acetate (1:1 v/v) and ethyl acetate to give nine subfractions (Hx-AA - Hx-AI). These results are shown in Table 11.

Table 11 Separation of fraction Hx-A

Fraction	Weight (mg)	Characteristic of fraction
Hx-AA	4,675.0	Dark brown solid
Hx-AB	14.0	White solid
Hx-AC	94.0	Brown solid
Hx-AD	27.0	White solid
Hx-AE	14.2	White solid
Hx-AF	2,959.0	Yellow oil
Hx-AG	788.0	Green solid
Hx-AH	290.0	Light yellow solid
Hx-AI	238.0	Light yellow solid

The fraction Hx-AF (2.95 g) was a major fraction. So, it was separated by silica gel column chromatography eluting with heptane:hexane (1:1 v/v), hexane, hexane:dichloromethane (1:1 v/v) and ethyl acetate to give nine subfractions (Hx-AFA - Hx-AFI) as shown in Table 12. Fraction Hx-AFE (290.0 mg) was separated by column chromatography using silica gel and eluting with petroleum ether, petroleum ether:ethyl acetate (8:2 v/v), petroleum ether:ethyl acetate (6:4 v/v), petroleum ether:ethyl acetate (4:6 v/v), petroleum ether:ethyl acetate (2:8 v/v) and ethyl acetate to give eight subfractions (Hx-AFE1 - Hx-AFE8). These results are shown in Table 13.

Table 12 Separation of fraction Hx-AF

Fraction	Weight (mg)	Characteristic of fraction
Hx-AFA	10.9	White solid
Hx-AFB	0.9	White solid
Hx-AFC	8.5	White solid
Hx-AFD	5.3	White solid
Hx-AFE	301.5	Light yellow solid
Hx-AFF	405.4	White solid
Hx-AFG	37.4	White solid
Hx-AFH	1,953.5	White solid
Hx-AFI	221.3	White solid

Table 13 Separation of fraction Hx-AFE

Fraction	Weight (mg)	Characteristic of fraction
Hx-AFE1	1.8	White solid
Hx-AFE2	1.0	White solid
Hx-AFE3	272.2	Yellow oil
Hx-AFE4	10.6	White solid
Hx-AFE5	5.4	White solid
Hx-AFE6	3.2	White solid
Hx-AFE7	2.4	White solid
Hx-AFE8	8.7	White solid

Fraction Hx-AFE3 (270.0 mg) was a major component. It was further separated by column chromatography using silica gel and eluting with petroleum ether, petroleum ether:dichloromethane (8:2 v/v), petroleum ether:dichloromethane (6:4 v/v), petroleum ether:dichloromethane (4:6 v/v) and dichloromethane to give twelve subfractions (Hx-AFE3A - Hx-AFE3L). Unfortunately, isolation of fraction Hx-AFE3 did not succeed to obtain pure compound. These results are shown in Table 14.

Table 14 Separation of fraction Hx-AFE3

Fraction	Weight (mg)	Characteristic of fraction
Hx-AFE3A	15.5	White solid
Hx-AFE3B	10.4	White solid
Hx-AFE3C	0.4	Colorless
Hx-AFE3D	94.8	White solid
Hx-AFE3E	30.9	White solid
Hx-AFE3F	22.5	White solid
Hx-AFE3G	4.2	White solid
Hx-AFE3H	6.8	White solid
Hx-AFE3I	19.2	White solid
Hx-AFE3J	28.6	White solid
Hx-AFE3K	2.4	White solid
Hx-AFE3L	0.3	Colorless

The fraction Hx-AH (280.1 mg) showed a major component on TLC. It was separated by silica gel column chromatography eluting with hexane, hexane:acetone (9.5:0.5 v/v), hexane:acetone (9:1 v/v), hexane:acetone (8.5:1.5 v/v), hexane:acetone (8:2 v/v), hexane:acetone (1:1 v/v) and acetone to give seven subfractions (Hx-AHA - Hx-AHG). These results are shown in Table 15.

Table 15 Separation of fraction Hx-AH

Fraction	Weight (mg)	Characteristic of fraction
Hx-AHA	23.5	Light yellow solid
Hx-AHB	21.0	White solid
Hx-AHC	64.5	White solid
Hx-AHD	36.2	Light yellow solid
Hx-AHE	58.1	Light yellow solid
Hx-AHF	50.6	White solid
Hx-AHG	10.6	White solid

Fraction Hx-AHE (58.0 mg) was separated by silica gel column chromatography using silica gel eluting with hexane, hexane:ethyl acetate (9:1 v/v), hexane:ethyl acetate (8:2 v/v), hexane:ethyl acetate (7:3 v/v), hexane:ethyl acetate (1:1 v/v) and ethyl acetate to give eight subfractions (Hx-AHE1 - Hx-AHE8). Fraction Hx-AHE4 (compound **209**) was obtained as white solid (8.2 mg, 0.0063% w/w of hexane crude extract). These results are shown in Table 16.

Table 16 Separation of fraction Hx-AHE

Fraction	Weight (mg)	Characteristic of fraction
Hx-AHE1	0.6	Light white solid
Hx-AHE2	1.5	White solid
Hx-AHE3	0.3	White solid
Hx-AHE4	8.2	White solid
Hx-AHE5	19.9	White solid
Hx-AHE6	5.9	White solid
Hx-AHE7	1.2	White solid
Hx-AHE8	19.6	White solid

Then, fraction Hx-D (5.01 g) which showed strong activity and was further separated by column chromatography using Diaion HP20 with ethyl acetate, ethyl acetate:methanol (1:1 v/v), methanol and DI water as eluents to give five subfractions (Hx-DA - Hx-DE). They were tested for lipase inhibitory activity (Table 17). Fractions Hx-DA - Hx-DC showed strong anti-lipase activity.

Table 17 Lipase inhibitory activity of fractions Hx-DA - Hx-DE

Fraction	Weight (g)	Characteristic of fraction	Inhibitory activity (%)
Hx-DA	2.03	Brown gum	79.87 ± 1.31*
Hx-DB	0.76	Yellow solid	93.86 ± 1.31*
Hx-DC	1.89	Light yellow solid	86.01 ± 1.97*
Hx-DD	0.18	Brown solid	NA*
Hx-DE	0.15	Light brown solid	NA*

* at a concentration of 25 mg/mL

NA = No activity

The fraction Hx-DA (1.95 g) gave a major component on TLC. Fraction Hx-DA was separated by column chromatography on silica gel eluting with ethyl acetate, ethyl acetate:methanol (9:1 v/v), ethyl acetate:methanol (8:2 v/v) and ethyl acetate:methanol (7:3 v/v) to give five subfractions (Hx-DAA - Hx-DAE). These results are shown in Table 18.

Table 18 Lipase inhibitory activity of fractions Hx-DAA - Hx-DAE

Fraction	Weight (mg)	Characteristic of fraction	Inhibitory activity (%)
Hx-DAA	68.3	Light yellow solid	55.09 ± 3.97*
Hx-DAB	279.7	Light yellow solid	21.61 ± 2.78*
Hx-DAC	46.1	Light brown solid	36.63 ± 1.99*
Hx-DAD	23.2	Brown solid	52.82 ± 3.88*
Hx-DAE	1,510.8	Brown solid	63.44 ± 1.89*

* at a concentration of 25 mg/mL

Fraction Hx-DAB (230.9 mg) showed a major component on TLC. It was subjected to flash chromatography using PuriFlash column 15 Silica HP - 4.0 g (22 bar) eluting with gradient mobile phase as hexane, hexane:ethyl acetate (1:1 v/v), ethyl acetate, ethyl acetate:methanol (9:1 v/v) and ethyl acetate:methanol (6:4 v/v) to give four subfractions (Hx-DAB1 - Hx-DAB4) (as shown in Table 19). Fraction Hx-DAB2 (162.1 mg) was further separated by flash chromatography using PuriFlash column 15 Silica HP - 4.0 g (22 bar) eluting with gradient mobile phase as hexane, hexane:dichloromethane (1:1 v/v) and dichloromethane to give five subfractions (Hx-DAB21 - Hx-DAB25). These results are shown in Table 20.

Table 19 Separation of fraction Hx-DAB

Fraction	Weight (mg)	Characteristic of fraction	Inhibitory activity (%)
Hx-DAB1	15.3	White solid	ND
Hx-DAB2	164.4	Light yellow solid	ND
Hx-DAB3	20.3	Light yellow solid	ND
Hx-DAB4	33.4	Light yellow solid	ND

ND = No detection

Table 20 Separation of fraction Hx-DAB2

Fraction	Weight (mg)	Characteristic of fraction	Inhibitory activity (%)
Hx-DAB21	25.0	White solid	ND
Hx-DAB22	3.1	White solid	ND
Hx-DAB23	1.3	White solid	ND
Hx-DAB24	118.7	White solid	ND
Hx-DAB25	1.8	White solid	ND

ND = No detection

The fraction Hx-DAB24 (115.1 mg) showed a major component on TLC. Fraction Hx-DAB24 was separated by flash chromatography using PuriFlash column 15 Silica HP - 4.0 g (22 bar) eluting with hexane, hexane:dichloromethane (1:1 v/v) and dichloromethane to give four subfractions (Hx-DAB241 - Hx-DAB244) (Table 21). Fraction Hx-DAB243 (45.2 mg) was a major component and further separated by flash chromatography using PuriFlash column 15 Silica HP - 4.0 g (22 bar) eluting with hexane, hexane:dichloromethane (1:1 v/v), dichloromethane, dichloromethane:methanol (9:1 v/v) and dichloromethane:methanol (8:2 v/v) to give five subfractions (Hx-DAB2431 - Hx-DAB2435). These results are shown in Table 22.

Table 21 Separation of fraction Hx-DAB24

Fraction	Weight (mg)	Characteristic of fraction	Inhibitory activity (%)
Hx-DAB241	1.3	White solid	ND
Hx-DAB242	34.9	White solid	ND
Hx-DAB243	52.5	White solid	ND
Hx-DAB244	2.5	White solid	ND

ND = No detection

Table 22 Separation of fraction Hx-DAB243

Fraction	Weight (mg)	Characteristic of fraction	Inhibitory activity (%)
Hx-DAB2431	2.0	White solid	ND
Hx-DAB2432	4.0	White solid	ND
Hx-DAB2433	35.1	White solid	ND
Hx-DAB2434	5.2	White solid	ND
Hx-DAB2435	1.2	White solid	ND

ND = No detection

Fraction Hx-DAD (19.6 mg) was subjected to flash chromatography using PuriFlash column 15 Silica HP - 4.0 g (22 bar) eluting with hexane, hexane:ethyl acetate (1:1 v/v), ethyl acetate, ethyl acetate:methanol (9:1 v/v), ethyl acetate:methanol (8:2 v/v), ethy acetate:methanol (7:3 v/v) and ethyl acetate:methanol (6:4 v/v) to give four subfractions (Hx-DAD1 - Hx-DAD4) as shown in Table 23. Unfortunately, isolation of fraction Hx-DAD was not successful to get pure compound.

Table 23 Separation of fraction Hx-DAD

Fraction	Weight (mg)	Characteristic of fraction	Inhibitory activity (%)
Hx-DAD1	5.1	White solid	ND
Hx-DAD2	8.2	White solid	ND
Hx-DAD3	16.5	White solid	ND
Hx-DAD4	25.0	White solid	ND

ND = No detection

Fraction Hx-DB (750.1 mg) was a major fraction. It was separated by column chromatography using silica gel with ethyl acetate, ethyl acetate:methanol (9:1 v/v), ethyl acetate:methanol (8:2 v/v) and ethyl acetate:methanol (7:3 v/v) as eluents to give six subfractions (Hx-DBA - Hx-DBF). These results are shown in Table 24.

Table 24 Separation of fraction Hx-DB

Fraction	Weight (mg)	Characteristic of fraction	Inhibitory activity (%)
Hx-DBA	5.0	White solid	ND
Hx-DBB	1.2	White solid	ND
Hx-DBC	164	Light yellow solid	ND
Hx-DBD	502	Yellow gum	ND
Hx-DBE	17.0	Yellow solid	ND
Hx-DBF	59.0	Yellow solid	20.15 ± 1.8*

* at a concentration of 100 µg/mL

ND = No detection

Fraction Hx-DBC (160.5 mg) was separated by silica gel column chromatography eluting with hexane, hexane:acetone (9:1 v/v), hexane:acetone (7:3 v/v), hexane:acetone (1:1 v/v), hexane:acetone (3:7 v/v), acetone and ethyl acetate:methanol (7:3 v/v) to give six subfractions (Hx-DBC1 - Hx-DBC6). The results are shown in Table 25. Fraction Hx-DBC2 (62.2 mg) was a major fraction and was separated by column chromatography using silica gel with hexane, hexane:ethyl acetate (9.5:0.5 v/v), hexane:ethyl acetate (9:1 v/v), hexane:ethyl acetate (8:2 v/v), hexane:ethyl acetate (7:3 v/v), hexane:ethyl acetate (6:4 v/v), hexane:ethyl acetate (1:1 v/v) and ethyl acetate as eluents to give seven subfractions (Hx-DBC21 - Hx-DBC27). The results are shown in Table 26.

Table 25 Separation of fraction Hx-DBC

Fraction	Weight (mg)	Characteristic of fraction	Inhibitory activity (%)
Hx-DBC1	1.5	White solid	34.52 ± 4.68*
Hx-DBC2	64.2	Light yellow solid	ND
Hx-DBC3	32.9	White solid	NA*
Hx-DBC4	50.2	White solid	23.63 ± 3.19*
Hx-DBC5	3.7	White solid	33.18 ± 2.54*
Hx-DBC6	1.5	White solid	21.52 ± 3.25*

* at a concentration of 100 µg/mL

NA = No activity

ND = No detection

Table 26 Separation of fraction Hx-DBC2

Fraction	Weight (mg)	Characteristic of fraction	Inhibitory activity (%)
Hx-DBC21	2.3	White solid	55.44 ± 7.01*
Hx-DBC22	0.9	White solid	ND
Hx-DBC23	0.6	White solid	ND
Hx-DBC24	40.7	White solid	ND
Hx-DBC25	1.0	White solid	44.70 ± 4.18*
Hx-DBC26	0.7	White solid	ND
Hx-DBC27	13.4	White solid	41.93 3.94*

* at a concentration of 100 µg/mL

ND = No detection

The fraction Hx-DBC24 (38.1 mg) showed a major component on TLC. So, it was separated by silica gel column chromatography eluting with hexane, hexane:acetone (9.5:0.5 v/v), hexane:acetone (9:1 v/v), hexane:acetone (8.5:1.5 v/v), hexane:acetone (8:2 v/v), hexane:acetone (7.5:2.5 v/v) and hexane:acetone (7:3 v/v) to give eight subfractions (Hx-DBC241 - Hx-DBC248). The results are shown in Table 27. Fraction Hx-DBC243 (compound **210**) was obtained as white crystal (1.4 mg, 0.0011% w/w of hexane crude extract). It was further analyzed by GC-MS.

Table 27 Separation of fraction Hx-DBC24

Fraction	Weight (mg)	Characteristic of fraction	Inhibitory activity (%)
Hx-DBC241	1.5	White solid	ND
Hx-DBC242	8.6	White solid	ND
Hx-DBC243	1.8	White crystal	26.74 ± 3.20*
Hx-DBC244	0.9	White solid	ND
Hx-DBC245	3.3	White solid	44.70 ± 4.18*
Hx-DBC246	3.8	White solid	ND
Hx-DBC247	2.8	White solid	ND
Hx-DBC248	7.8	White solid	60.60 ± 6.47*

* at a concentration of 100 µg/mL

ND = No detection

Fraction Hx-DBC4 (48.2 mg) was separated by flash chromatography eluting with gradient mobile phase as hexane:ethyl acetate (1:1 v/v), hexane:ethyl acetate (3:7 v/v), ethyl acetate, ethyl acetate:methanol (9:1 v/v), ethyl acetate:methanol (8:2 v/v), ethyl acetate:methanol (7:3 v/v) and ethyl acetate:methanol (6:4 v/v) to give four subfractions (Hx-DBC41 - Hx-DBC44) as shown in Table 28. Unfortunately, isolation of fraction Hx-DBC4 did not succeed to obtain pure compound.

Table 28 Separation of fraction Hx-DBC4

Fraction	Weight (mg)	Characteristic of fraction	Inhibitory activity (%)
Hx-DBC41	5.0	White solid	ND
Hx-DBC42	8.2	White solid	ND
Hx-DBC43	16.5	White solid	ND
Hx-DBC44	25.0	White solid	ND

ND = No detection

Fraction Hx-DBD (500.4 mg) was separated by silica gel column chromatography eluting with ethyl acetate, ethyl acetate:methanol (9.5:0.5 v/v), ethyl acetate:methanol (9:1 v/v), ethyl acetate:methanol (8.5:1.5 v/v), ethyl acetate:methanol (8:2 v/v), ethyl acetate:methanol (7.5:2.5 v/v) and ethyl acetate:methanol (7:3 v/v) to give eight subfractions (Hx-DBD1 - Hx-DBD8). The results are shown in Table 29.

Table 29 Separation of fraction Hx-DBD

Fraction	Weight (mg)	Characteristic of fraction	Inhibitory activity (%)
Hx-DBD1	10.3	White - yellow solid	70.92 ± 3.97*
Hx-DBD2	0.4	White solid	ND
Hx-DBD3	105.7	White solid	58.02 ± 2.53*
Hx-DBD4	36.4	White solid	NA
Hx-DBD5	178.1	White solid	ND
Hx-DBD6	23.5	White solid	ND
Hx-DBD7	51.8	White solid	NA*
Hx-DBD8	42.1	White solid	NA*

* at a concentration of 100 µg/mL

NA = No activity

ND = No detection

Fraction Hx-DBD5 (170.1 mg) was separated by silica gel column chromatography with ethyl acetate, ethyl acetate:methanol (9.5:1.5 v/v), ethyl acetate:methanol (9:1 v/v), ethyl acetate:methanol (8.5:1.5 v/v), ethyl acetate:methanol (8:2 v/v) and ethyl acetate:methanol (7:3 v/v) as eluents to give four subfractions (Hx-DBD51 - Hx-DBD54). The results are shown in Table 30.

Table 30 Separation of fraction Hx-DBD5

Fraction	Weight (mg)	Characteristic of fraction	Inhibitory activity (%)
Hx-DBD51	1.9	White solid	ND
Hx-DBD52	143.4	White solid	ND
Hx-DBD53	3.1	White solid	ND
Hx-DBD54	12.3	White solid	ND

ND = No detection

Fraction Hx-DBD52 (142.4 mg) showed a major component on TLC. It was further separated on silica gel column chromatography with ethyl acetate, ethyl acetate:methanol (9.5:0.5 v/v), ethyl acetate:methanol (9:1 v/v), ethyl acetate:methanol (8.5:1.5 v/v), ethyl acetate:methanol (8:2 v/v) and ethyl acetate:methanol (7.5:2.5 v/v) as eluents to afford ten subfractions (Hx-DBD52A - Hx-DBD52J) as shown in Table 31. Fraction Hx-DBD52C (50.9 mg) was separated by column chromatography using silica gel with hexane, hexane:ethyl acetate (9.5:0.5 v/v), dichloromethane, ethyl acetate, ethyl acetate:methanol (9.5:0.5 v/v), ethyl acetate:methanol (9:1 v/v), ethyl acetate:methanol (8:2 v/v) and ethyl acetate:methanol (7:3 v/v) as eluents to afford twelve subfractions (Hx-DBD52CA - Hx-DBD52CL). The results are shown in Table 32.

Table 31 Separation of fraction Hx-DBD52

Fraction	Weight (mg)	Characteristic of fraction	Inhibitory activity (%)
Hx-DBD52A	2.9	White solid	4.99 ± 1.69*
Hx-DBD52B	1.4	White solid	4.23 ± 1.28*
Hx-DBD52C	53.6	White solid	ND
Hx-DBD52D	4.0	White solid	66.97 ± 2.98*
Hx-DBD52E	10.7	White solid	34.53 ± 4.26*
Hx-DBD52F	8.2	White solid	76.77 ± 3.13*
Hx-DBD52G	6.9	White solid	63.75 ± 4.23*
Hx-DBD52H	18.2	White solid	72.42 ± 1.62*
Hx-DBD52I	4.0	White solid	63.75 ± 3.45*
Hx-DBD52J	13.3	White solid	63.86 ± 2.99*

* at a concentration of 100 µg/mL

ND = No detection

Table 32 Separation of fraction Hx-DBD52C

Fraction	Weight (mg)	Characteristic of fraction	Inhibitory activity (%)
Hx-DBD52CA	0.1	White solid	ND
Hx-DBD52CB	0.6	White solid	ND
Hx-DBD52CC	1.5	White solid	ND
Hx-DBD52CD	3.8	White solid	NA*
Hx-DBD52CE	6.7	White solid	ND
Hx-DBD52CF	15.1	White solid	NA*
Hx-DBD52CG	13.7	White solid	13.67 ± 3.06*
Hx-DBD52CH	4.0	White solid	38.57 ± 2.83*
Hx-DBD52CI	0.8	White solid	ND
Hx-DBD52CJ	14.7	White solid	23.19 ± 1.83*
Hx-DBD52CK	13.8	White solid	40.63 ± 3.77*
Hx-DBD52CL	15.2	White solid	45.02 ± 5.58*

* at a concentration of 100 µg/mL
NA = No activity
ND = No detection

Fraction Hx-DBD52CE (6.0 mg) was a major fraction. It was further separated by silica gel column chromatography eluting with ethyl acetate, ethyl acetate:methanol (9.5:0.5 v/v), ethyl acetate:methanol (9:1 v/v), ethyl acetate:methanol (8.5:1.5 v/v), ethyl acetate:methanol (8:2 v/v), ethyl acetate:methanol (7.5:2.5 v/v) and ethyl acetate:methanol (7:3 v/v) to give eight subfractions (Hx-DBD52CE1 - Hx-DBD52CE8). The results are shown in Table 33. Unfortunately, isolation of fraction Hx-DBD52CE was not successful to obtain pure compound.

Table 33 Separation of fraction Hx-DBD52CE

Fraction	Weight (mg)	Characteristic of fraction	Inhibitory activity (%)
Hx-DBD52CE1	0.4	White solid	ND
Hx-DBD52CE2	6.4	White solid	16.47 ± 0.43*
Hx-DBD52CE3	5.7	White solid	NA*
Hx-DBD52CE4	5.9	White solid	50.63 ± 3.37*
Hx-DBD52CE5	4.6	White solid	56.84 ± 1.41*
Hx-DBD52CE6	0.2	White solid	ND
Hx-DBD52CE7	1.3	White solid	ND
Hx-DBD52CE8	1.2	White solid	ND

* at a concentration of 100 µg/mL
NA = No activity
ND = No detection

The fraction Hx-DC (1.89 g) showed strong anti-lipase activity. It was separated by column chromatography on silica gel eluting with ethyl acetate, ethyl acetate:methanol (9:1 v/v), ethyl acetate:methanol (8:2 v/v) and ethyl acetate:methanol (7:3 v/v) to give three subfractions (Hx-DCA - Hx-DCC). The results are shown in Table 34. Unfortunately, isolation of fraction Hx-DC was not successful to obtain pure compound.

Table 34 Separation of fraction Hx-DC

Fraction	Weight (mg)	Characteristic of fraction	Inhibitory activity (%)
Hx-DCA	289.3	Light yellow solid	60.59 ± 2.95*
Hx-DCB	712.7	Light yellow solid	62.05 ± 2.45*
Hx-DCC	698.5	Light yellow solid	55.53 ± 4.50*

* at a concentration of 25 mg/mL

4.4.2 Separation of *n*-butanol crude extract

The *n*-butanol crude extract (fraction Bu, 11.52 g) was subjected to column chromatography using Diaion HP20 with ethyl acetate, ethyl acetate:methanol,

methanol and DI water as eluents to give five subfractions (Bu-A - Bu-E). All subfractions were evaluated for lipase inhibitory activity. Fractions Bu-C, Bu-D and Bu-B showed strong activity with percent inhibition as 91.07 ± 0.09%, 82.56 ± 4.81% and 80.44 ± 1.95%, respectively. While, fraction Bu-A showed moderate activity with percent inhibition as 51.31 ± 3.06%. These results are shown in Table 35.

Table 35 Lipase inhibitory activity of subfractions Bu-A - Bu-E

Fraction	Weight (g)	Characteristic of fraction	Inhibitory activity (%)
Bu-A	0.09	Yellow solid	51.31 ± 3.06*
Bu-B	5.83	Brown gum	80.44 ± 1.95*
Bu-C	4.26	Brown gum	91.07 ± 0.09*
Bu-D	0.57	Brown solid	82.56 ± 4.81*
Bu-E	0.25	Brown solid	NA*

* at a concentration of 25 mg/mL

NA = No activity

Fraction Bu-B (5.72 g) was separated by column chromatography on silica gel eluting with dichloromethane:methanol (9:1 v/v), dichloromethane:methanol (7:3 v/v), dichloromethane:methanol (1:1 v/v) and dichloromethane:methanol (3:7 v/v) to afford five subfractions (Bu-BA - Bu-BE) as shown in Table 36. Then, fraction Bu-BD showed stronger anti-lipase activity than other fractions. So, fraction Bu-BD (1.38 g) was subjected to Sephadex LH-20 column chromatography with methanol to yield two subfractions (Bu-BD1 - Bu-BD2) in Table 37. Fraction Bu-BD2 (897.8 mg) was subjected to Sephadex LH-20 column chromatography with dichloromethane:methanol (1:1 v/v) as eluent to yield five subfractions (Bu-BD2A - Bu-BD2E). The results are shown in Table 38.

Table 36 Separation of fraction Bu-B

Fraction	Weight (g)	Characteristic of fraction	Inhibitory activity (%)
Bu-BA	1.33	Brown solid	30.11 ± 2.86*
Bu-BB	1.24	Brown solid	25.29 ± 1.00*
Bu-BC	1.41	Brown solid	54.76 ± 1.44*
Bu-BD	1.59	Brown solid	62.13 ± 1.33*
Bu-BE	0.16	Brown solid	44.85 ± 3.08*

* at a concentration of 100 µg/mL

Table 37 Separation of fraction Bu-BD

Fraction	Weight (g)	Characteristic of fraction	Inhibitory activity (%)
Bu-BD1	0.49	Brown solid	37.49 ± 2.80*
Bu-BD2	0.90	Brown solid	47.83 ± 0.90*

* at a concentration of 100 µg/mL

Table 38 Separation of fraction Bu-BD2

Fraction	Weight (mg)	Characteristic of fraction	Inhibitory activity (%)
Bu-BD2A	186.5	Light brown solid	46.82 ± 1.80*
Bu-BD2B	175.3	Light brown solid	47.98 ± 3.25*
Bu-BD2C	132.6	Light brown solid	21.24 ± 3.24*
Bu-BD2D	178.3	Light brown solid	35.84 ± 4.13*
Bu-BD2E	163.5	Light brown solid	24.13 ± 1.41*

* at a concentration of 100 µg/mL

Fraction Bu-BD2A (176.2 mg) was separated by column chromatography on silica gel eluting with dichloromethane:methanol (9:1 v/v), dichloromethane:methanol (7:3 v/v), dichloromethane:methanol (1:1 v/v) and dichloromethane:methanol (3:7 v/v) to yield twelve subfractions (Bu-BD2AA - Bu-BD2AL). Fraction Bu-BD2AC (compound **211**) was obtained as white solid (3.8 mg, 0.0330% of *n*-butanol crude extract). The results are shown in Table 39.

Table 39 Separation of fraction Bu-BD2A

Fraction	Weight (mg)	Characteristic of fraction	Inhibitory activity (%)
Bu-BD2AA	5.0	White solid	ND
Bu-BD2AB	3.9	White solid	ND
Bu-BD2AC	3.8	White solid	ND
Bu-BD2AD	5.2	White solid	ND
Bu-BD2AE	3.4	Light yellow solid	ND
Bu-BD2AF	30.2	Light yellow solid	ND
Bu-BD2AG	20.8	Light yellow solid	ND
Bu-BD2AH	7.3	Light yellow solid	ND
Bu-BD2AI	30.8	Light yellow solid	ND
Bu-BD2AJ	0.2	Light yellow solid	ND
Bu-BD2AK	25.3	Light yellow solid	ND
Bu-BD2AL	34.2	Light yellow solid	ND

* at a concentration of 100 µg/mL

ND = No detection

Fraction Bu-C (4.10 g) showed strong activity and was separated by column chromatography on silica gel eluting with ethyl acetate, ethyl acetate:methanol (9.5:0.5 v/v), ethyl acetate:methanol (9:1 v/v), ethyl acetate:methanol (8.5:1.5 v/v), ethyl acetate:methanol (8:2 v/v), ethyl acetate:methanol (7.5:2.5 v/v), ethyl acetate:methanol (7:3 v/v), ethyl acetate:methanol (6:4 v/v) and ethyl acetate:methanol (5.5:4.5 v/v) to afford twelve subfractions (Bu-CA - Bu-CL) as shown in Table 40. Then, fraction Bu-CG (132.8 mg) was a major fraction and it was subjected to Sephadex LH-20 column chromatography with methanol as eluent to yield four subfractions (Bu-CGA - Bu-CGD). The results are shown in Table 41. Fraction Bu-CGB (38.9 mg) was a major fraction. It was subjected to Sephadex LH-20 column chromatography with methanol as eluent to yield four subfractions (Bu-

CGB1 - Bu-CGB4). The results are shown in Table 42. Unfortunately, isolation of fraction Bu-CGB was not successful to obtain pure compound.

Table 40 Separation of fraction Bu-C

Fraction	Weight (mg)	Characteristic of fraction	Inhibitory activity (%)
Bu-CA	10.8	Yellow solid	72.20 ± 1.75*
Bu-CB	2.6	Yellow solid	80.91 ± 0.79*
Bu-CC	13.5	Yellow solid	68.48 ± 3.02*
Bu-CD	5.5	Yellow solid	82.88 ± 1.40*
Bu-CE	59.1	Light brown solid	59.63 ± 2.52*
Bu-CF	62.3	Light brown solid	54.83 ± 2.32*
Bu-CG	135	Light brown solid	ND
Bu-CH	793.6	Light brown solid	62.76 ± 2.01*
Bu-CI	333.5	Light brown solid	46.63 ± 3.98*
Bu-CJ	1,062.2	Light brown solid	65.62 ± 1.99*
Bu-CK	364.2	Dark brown solid	23.95 ± 0.46*
Bu-CL	193.0	Dark brown solid	35.14 ± 4.29*

* at a concentration of 100 µg/mL
ND = No detection

Table 41 Separation of fraction Bu-CG

Fraction	Weight (mg)	Characteristic of fraction	Inhibitory activity (%)
Bu-CGA	23.6	Light brown solid	35.31 ± 1.51*
Bu-CGB	39.7	Light brown solid	44.06 ± 3.61*
Bu-CGC	27.7	Brown solid	41.18 ± 1.97*
Bu-CGD	19.7	Brown solid	42.92 ± 1.18*

* at a concentration of 100 µg/mL
ND = No detection

Table 42 Separation of fraction Bu-CGB

Fraction	Weight (mg)	Characteristic of fraction	Inhibitory activity (%)
Bu-CGB1	18.9	Brown solid	ND
Bu-CGB2	14.3	Brown solid	ND
Bu-CGB3	1.5	Brown solid	ND
Bu-CGB4	2.4	Brown solid	ND

ND = No detection

Fraction Bu-D (0.56 g) showed strong anti-lipase activity. It was separated by column chromatography on Sephadex LH-20 with methanol as eluent to yield five subfractions (Bu-DA - Bu-DE) (Table 43). Fraction Bu-DA (33.0 mg) was further fractionated by HPLC. The gradient elution system consisted of methanol (A) and DDI water (B) as the mobile phase using the following gradient: 70-90% A at 0-40

min, 90-100% A at 40-50 min, 100% A at 50-60 min. The injection volume was 20 µL. Flow rate was 1.0 mL/min, and UV absorption was measured at wavelengths of 220 nm to yield four subfractions (Bu-DA1 - Bu-DA4) (Table 44). Subfraction Bu-DA2 was obtained as compound **212** as white crystals (4.5 mg, 0.0391% w/w of *n*-butanol crude extracts). Fraction Bu-DB (92.2 mg) was further fractionated by HPLC. The gradient elution system consisted of methanol (A) and DDI water (B) as the mobile phase using the following gradient: 50-80% A at 0-40 min, 80-100% A at 40-50 min, 100% A at 50-60 min. The injection volume was 20 µL. Flow rate was 1.0 mL/min, and UV absorption was measured at wavelengths of 220 nm to yield four subfractions (Bu-DB1 - Bu-DB4) (Table 45). Subfraction Bu-DB2 was re-crystallized with a mixture of dichloromethane and methanol to obtain compound **213** as white crystals (3.0 mg, 0.0260% w/w of *n*-butanol crude extract). Fraction Bu-DB3 was (22.0 mg) further fractionated by HPLC. The gradient elution system consisted of methanol (A) and DDI water (B) as the mobile phase using the following gradient: 80-80% A at 0-40 min, 80-100% A at 40-50 min, 100% A at 50-60 min. The injection volume was 20 µL. Flow rate was 1.0 mL/min, and UV absorption was measured at wavelengths of 220 nm to yield four subfractions (Bu-DB31 - Bu-DB34) (Table 46). Subfraction Bu-DB32 obtained compound **214** as white crystals (4.9 mg, 0.0425% w/w of *n*-butanol crude extract).

Table 43 Separation of fraction Bu-D

Fraction	Weight (mg)	Characteristic of fraction	Inhibitory activity (%)
Bu-DA	33.6	Brown solid	80.43 ± 2.73*
Bu-DB	94.6	Brown solid	76.92 ± 1.71*
Bu-DC	15.0	Brown solid	ND
Bu-DD	19.7	Brown solid	ND
Bu-DE	11.4	Brown solid	91.46 ± 1.72*

* at a concentration of 100 µg/mL

ND = No detection

Table 44 Separation of fraction Bu-DA

Fraction	Weight (mg)	Characteristic of fraction	Inhibitory activity (%)
Bu-DA1	3.9	White solid	ND
Bu-DA2	4.5	White solid	ND
Bu-DA3	9.7	White solid	ND
Bu-DA4	13.6	Colorless	ND

ND = No detection

Table 45 Separation of fraction Bu-DB

Fraction	Weight (mg)	Characteristic of fraction	Inhibitory activity (%)
Bu-DB1	13.9	White solid	ND
Bu-DB2	15.5	White solid	ND
Bu-DB3	22.6	White solid	ND
Bu-DB4	12.8	Colorless	ND

ND = No detection

Table 46 Separation of fraction Bu-DB3

Fraction	Weight (mg)	Characteristic of fraction	Inhibitory activity (%)
Bu-DB31	2.1	White solid	ND
Bu-DB32	4.7	White solid	ND
Bu-DB33	5.8	White solid	ND
Bu-DB34	10.9	White solid	ND

ND = No detection

The *n*-butanol crude extract (fraction Bu, 30.05 g) was re-separated. So, it was subjected to column chromatography using Diaion HP20 with ethyl acetate, ethyl acetate:methanol (1:1 v/v), methanol and DI water as eluents to obtain five subfractions (Bu-A - Bu-E). The results are shown in Table 47.

Table 47 Re-separation of fraction Bu

Fraction	Weight (g)	Characteristic of fraction	Inhibitory activity (%)
Bu-A	7.70	Yellow solid	ND
Bu-B	13.29	Brown gum	ND
Bu-C	6.11	Brown gum	ND
Bu-D	1.25	Brown solid	ND
Bu-E	0.32	Brown solid	ND

ND = No detection

Fraction Bu-C (0.50 g) was re-separated by flash chromatography eluting using PuriFlash column 15 C18 HP - 6.0 g (22 bar) with methanol:DI water (1:1 v/v), methanol:DI water (6:4 v/v), methanol:DI water (7:3 v/v), methanol:DI water (8:2 v/v), methanol:DI water (9:1 v/v) and methanol to give five subfractions (Bu-C1 - Bu-C5). The results are shown in Table 48. Fraction Bu-C2 (120.1 mg) was further subjected to flash chromatography using PuriFlash column 15 C18 HP - 6.0 g (22 bar) eluting with methanol:DI water (1:1 v/v), methanol:DI water (6:4 v/v), methanol:DI water (7:3 v/v), methanol:DI water (8:2 v/v), methanol:DI water (9:1 v/v) and methanol to give three subfractions (Bu-C21 - Bu-C23). The results are shown in Table 49. Fraction Bu-C21 (60.0 mg) was subjected to flash chromatography using PuriFlash column 15 C18 HP - 6.0 g (22 bar) eluting with methanol:DI water (1:1 v/v), methanol:DI water (6:4 v/v), methanol:DI water (7:3 v/v), methanol:DI water

(8:2 v/v), methanol:DI water (9:1 v/v) and methanol to give four subfractions (Bu-C211 - Bu-C214). The results are shown in Table 50.

Table 48 Separation of fraction Bu-C

Fraction	Weight (mg)	Characteristic of fraction	Inhibitory activity (%)
Bu-C1	10.2	Light brown solid	ND
Bu-C2	125.0	Light brown solid	ND
Bu-C3	50.5	Light brown solid	ND
Bu-C4	152.0	Light brown solid	ND
Bu-C5	120.2	Light brown solid	ND

ND = No detection

Table 49 Separation of fraction Bu-C2

Fraction	Weight (mg)	Characteristic of fraction	Inhibitory activity (%)
Bu-C21	60.1	Light brown solid	ND
Bu-C22	22.5	Light brown solid	ND
Bu-C23	14.0	Light brown solid	ND

ND = No detection

Table 50 Separation of fraction Bu-C21

Fraction	Weight (mg)	Characteristic of fraction	Inhibitory activity (%)
Bu-C211	13.3	Light brown solid	ND
Bu-C212	2.4	Light brown solid	ND
Bu-C213	15.8	Light brown solid	ND
Bu-C214	14.4	Light brown solid	ND

ND = No detection

The fraction Bu-C22 (22.5 mg) was a major fraction. It was subjected to flash chromatography using PuriFlash column 15 C18 HP - 6.0 g (22 bar) eluting with methanol:DI water (1:1 v/v), methanol:DI water (6:4 v/v), methanol:DI water (7:3 v/v), methanol:DI water (8:2 v/v), methanol:DI water (9:1 v/v) and methanol to give four subfractions (Bu-C221 - Bu-C224). The results are shown in Table 51. Unfortunately, isolation of fraction Bu-C22 was not successful to obtain pure compound.

Table 51 Separation of fraction Bu-C22

Fraction	Weight (mg)	Characteristic of fraction	Inhibitory activity (%)
Bu-C221	9.4	Light brown solid	ND
Bu-C222	3.6	Light brown solid	ND
Bu-C223	2.5	White solid	ND
Bu-C224	4.1	White solid	ND

ND = No detection

Fraction Bu-D (1.19 g) was re-separated by column chromatography using Sephadex LH-20 with methanol as eluent to yield five subfractions (Bu-DA - Bu-DE). The results are shown in Table 52.

Table 52 Separation of fraction Bu-D

Fraction	Weight (mg)	Characteristic of fraction	Inhibitory activity (%)
Bu-DA	276.2	Brown solid	ND
Bu-DB	160.2	Brown solid	ND
Bu-DC	40.4	Brown solid	ND
Bu-DD	50.1	Brown solid	ND
Bu-DE	609.8	Brown solid	ND

ND = No detection

Fraction Bu-DA (272.1 mg) was re-separated by flash chromatography using PuriFlash column 15 C18 HP - 6.0 g (22 bar) eluting with methanol:DI water (1:1 v/v), methanol:DI water (6:4 v/v), methanol:DI water (7:3 v/v), methanol:DI water (8:2 v/v), methanol:DI water (9:1 v/v) and methanol to give four subfractions (Bu-DA1 - Bu-DA4). The results are shown in Table 53. Fraction Bu-DA1 (42.0 mg) was a major fraction and it was further subjected to flash chromatography using PuriFlash column 15 C18 HP - 6.0 g (22 bar) eluting with methanol:DI water (1:1 v/v), methanol:DI water (6:4 v/v), methanol:DI water (7:3 v/v), methanol:DI water (8:2 v/v), methanol:DI water (9:1 v/v) and methanol to give three fractions (Bu-DA11 - Bu-DA13). The results are shown in Table 54. Unfortunately, all of fractions were not successful to obtain pure compound.

Table 53 Separation of fraction Bu-DA

Fraction	Weight (mg)	Characteristic of fraction	Inhibitory activity (%)
Bu-DA1	42.0	Light brown solid	ND
Bu-DA2	30.8	Light brown solid	ND
Bu-DA3	32.2	Light brown solid	ND
Bu-DA4	112.0	Light brown solid	ND

ND = No detection

Table 54 Separation of fraction Bu-DA1

Fraction	Weight (mg)	Characteristic of fraction	Inhibitory activity (%)
Bu-DA11	8.0	Light brown solid	ND
Bu-DA12	10.5	Light brown solid	ND
Bu-DA13	20.5	Light brown solid	ND

ND = No detection

Fraction Bu-DC (38.5 mg) was subjected to flash chromatography using PuriFlash column 15 C18 HP - 6.0 g (22 bar) eluting with methanol:DI water (1:1 v/v), methanol:DI water (6:4 v/v), methanol:DI water (7:3 v/v), methanol:DI water (8:2 v/v), methanol:DI water (9:1 v/v) and methanol to give four subfractions (Bu-DC1 - Bu-DC4). The results are shown in Table 55. Unfortunately, all of them were not successful to obtain pure compound.

Table 55 Separation of fraction Bu-DC

Fraction	Weight (mg)	Characteristic of fraction	Inhibitory activity (%)
Bu-DC1	4.0	Light brown solid	ND
Bu-DC2	10.2	Light brown solid	ND
Bu-DC3	15.3	Light brown solid	ND
Bu-DC4	4.1	Light brown solid	ND

ND = No detection

4.5 Identification of compound 209

Compound **209** was obtained as white solid (8.2 mg, 0.0063% w/w of haexane crude extract) with melting point of 70 - 75 °C. The ^{1}H NMR of compound **209** showed the presence of a terminal methyl groups at δ 0.88 (t) ppm. ^{1}H NMR spectrum also showed protons at δ 1.25 (s) ppm which indicated the methylene (CH_2) protons of saturated alkyl chain. ^{1}H NMR spectrum of compound **209** indicated a $COCH_2$ group at δ 2.34 (t) ppm. These spectrums presence the CH_2 α to COOH which linked methylene carbon at C-2 was indicated 2.34 (t) ppm. The proton of methylene carbon at C-3 was indicated δ 1.63 (m) ppm (Figure 28). The ^{13}C NMR spectrum (Figure 29) displayed signals for carbonyl group of carboxylic acid at δ 180.3 ppm. The methyl carbon showed signal at δ 14.1 ppm. The methylene carbon showed signal appearing at δ 22.7 - 34.1 ppm. These structure components contain methyl carbon, methylene carbons (more than 12 carbons) and carbonyl carbon of carboxylic acid. The combinations of ^{1}H NMR and ^{13}C NMR spectra were observation and identify as saturated fatty acid. Thus, compound **209** was further analyzed using GC-MS and compared their mass fragmentation pattern of each component with a Wiley and Nist standard chart library as shown in Figure 9. Compound **209** consisted of four components with retention times as 10.716, 12.441, 14.207 and 16.747 min, respectively as shown in Figure 30. Their Mass spectra were presented in Figures 31 - 34. Compound **209** was identified as a mixture of fatty acids including tetradecanoic acid (0.21%), hexadecanoic acid (45.86%), octadecanoic acid (43.29%) and eicosanoic acid (5.03%), respectively as shown in Table 56.

Table 56 Integration peak list of compound **209**

Peak	Name	Chemical formula	Molecular weight	Acquisition time (min)	% Composition
1	Tetradecanoic acid	$C_{14}H_{28}O_2$	228.31	10.716	0.22
2	Hexadecanoic acid	$C_{16}H_{32}O_2$	256.42	12.441	48.59
3	Octadecanoic acid	$C_{18}H_{36}O_2$	284.48	14.207	45.86
4	Eicosanoic acid	$C_{20}H_{40}O_2$	312.58	16.747	5.33

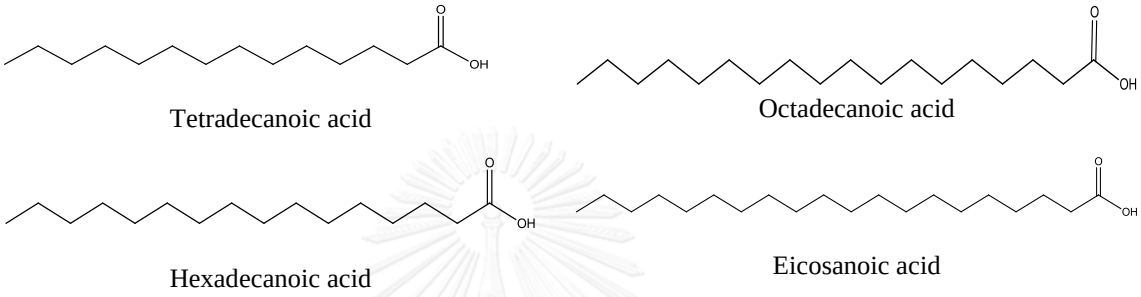

Figure 9 Chemical structure of compound **209** (mixture of fatty acids)

Fatty acids were reported biological activities as antibacterial and antifungal properties [130]. However, fatty acids can be used as active ingredients in cosmetic such as hexadecanoic acid, octadecanoic acid and tetradecanoic acid. They can be reduced inflammation of the skin and improved moisture into face and body [131]. In Solanaceae family, tetradecanoic acid, hexadecanoic acid and octadecanoic acid were previously isolated from *S. torvum* fruits which exhibited antifungal activity especially *Trichophytonton surans* and *Aspergillus niger* [132]. Octadecanoic acid was isolated from fruits of *S. xanthocarpum* [114].

4.6 Identification of compound 210

Compound **210** was obtained as white crystal (1.4 mg, 0.0011% w/w of hexane crude extract). The ^{1}H NMR of compound **210** (Figure 35) showed the presence of six methyl groups at δ 0.69 (d), 0.80 (s), 0.82 (s), 1.01 (s) and 1.03 (s) ppm and the endocyclic double bond proton at δ 5.35 (d) ppm. Moreover, ^{1}H NMR spectrum of compound **210** indicated a proton on oxygenated carbons at δ 3.53 (m) ppm. The proton resonances at δ 5.01 (dd), 5.15 (dd) and 5.35 (d) ppm suggested the presence of three olefinic protons bond. The protons resonance at δ 3.51 (m) ppm was corresponded to the hydroxymethine proton H-3. The ^{1}H NMR spectral data of compound **210** suggested that it was a mixture of steriods (Figure 35). Thus, compound **210** was further analyzed using GC-MS and the resulted mass fragmentations of each component were with a Wiley and Nist standard chart library (Figure 36). The GC-MS results showed that, compound **210** consisted of two components with retention times as 15.397 (69.82%) min and 15.944 (30.18%) min, respectively (Figures 37 and 38, Table 57). Unfortunately, they could not identify their structures.

Table 57 Integration peak list of compound **210**

Peak	Name	Acquisition time (min)	% Composition
1	Component I	15.397	69.82
2	Component II	15.944	30.18

Phytosterols are usually found in plants and found in a form of either free sterol or esterified sterol. Phytosterol are an ingredient in foods and dietary supplements. They have several biological activities and health benefits [133-136]. Steroidal compound such as stigmasterol was reported as thyroid inhibiting property, hypoglycemic inhibiting property, antibacterial activity and antioxidant activity [137]

4.7 Identification of compound 211

Compound **211** was obtained as white solid (3.8 mg, 0.0330% w/w of *n*-butanol crude extract). The ^{1}H NMR spectrum (Figure 40) of compound **211** indicated two protons with substituted olefinic at δ 5.36 (m) and 5.15 (m) ppm. The ^{1}H NMR spectrum of compound **211** showed six methyl groups (-CH_3) at δ 0.71 (s), 0.73 (s), 0.86 (d), 0.88 (d), 0.94 (d), 1.02 (s) ppm and sugar moiety at δ 4.39 - 3.21 ppm. The different methylene and methine protons indicated from δ 1.45 - 1.93 (m) ppm which did not show double bond in structure. One anomeric proton displayed at δ 4.39 (d) ppm. The ^{13}C NMR spectrum of compound **211** (Figure 40) showed more than 35 carbon atoms. The ^{13}C carbon signal at δ 102.33 ppm indicated as an anomeric carbon which showed a single monosaccharide moiety. The olefinic resonances at δ 122.7, 130.46 and 139.6 ppm indicated methine carbons. Compound **211** was identified as a mixture of steroidal glycosides. But, the combination of spectroscopic data could not identify the chemical structure of compound **211**.

4.8 Identification of compound 212

Compound **212** was obtained as white solid (4.5 mg, 0.0391% w/w of *n*-butanol crude extract) with melting point of 199 - 202 °C. The molecular formula of compound **212** was suggested as $C_{27}H_{43}NO_2$ by HRESIMS (*m*/*z* 414.3368 $[M + H]^+$, calcd 413.0007) (Figure 48). The ^{1}H NMR spectrum of compound **212** (Figure 41) displayed signals for four methyl groups at δ 0.81 (s), 0.84 (d), 0.95 (d) and 1.02 (s) ppm. The signal revealed characteristic of steroids at δ 0.81-1.25 ppm, 3α-H which displayed for hydroxyl group at δ 3.51 (m) ppm and C=C-H proton signal at δ 5.34 (dt) ppm. A signal at 4.28 (dt) ppm was assigned for one proton present in structure at C-16 position as δ 78.8 ppm. Two protons was attacted nitrogen in hexacylic ring at position C-26 which observed at δ 2.60 (t) and 2.65 (dd) ppm. The combination of ^{13}C NMR (Figure 42), DEPT 90 (Figure 43) and 135 spectra (Figure 44) showed the presence of 27 signals, including four methyl, ten methylene, nine methine and four quaternary carbons. The displayed signals for four methyl carbon groups at C-21, C-18, C-27 and C-19 which displayed signal appearing at δ 15.3, 16.4, 19.3 and 19.4 ppm, respectively. The displayed signals for ten methylene carbon groups at C-11, C-

24, C-15, C-7, C-2, C-23, C-1, C-12, C-4 and C-26 which displayed signal appearing at δ 20.9, 30.3, 31.6, 32.1, 32.7, 34.0, 39.9, 42.3 and 47.6 ppm. The displayed signals for nine methine carbon groups appeared at C-8, C-25, C-20, C-9, C-14, C-17, C-3, C-16 and C-6 which displayed signal appearing at 31.4, 31.4, 41.2, 50.1, 56.5, 62.8, 71.7, 78.8 and 121.4 ppm. The displayed signals for four quaternary carbons appeared at C-10, C-13, C-22 and C-5 which displayed signal appearing δ 36.6, 40.5, 98.3 and 140.8 ppm. Olefinic carbon atoms were displayed at 140.8 and 121.4 ppm which were assigned to C-5 and C-6 carbon atoms, respectively. The HSQC NMR spectrum is correlation between H and C which was resulted observation including H-1a (1.85, m) and H-1b (1.07, m)/C-1 (37.2), H-2a (1.98, m) and H-2b (1.28, m)/C-2 (32.2), H-3 (3.51, m)/C-3 (71.7), H-4a (2.23, dd) and H-4b (2.28, dd)/C-4 (42.3), H- 6 (5.34, dt)/C-6 (121.4), H-7(1.99, m)/C-7 (32.1), H-8 (1.68, m)/C-8 (31.4), H-9 (0.94, m)/C-9 (50.1), H-11 (1.46, m)/C-11 (20.9), H-12a (1.73, m) and H-12b (1.15, m)/C-12 (39.9), H-14 (1.09, m)/C-14 (56.5), H-15a (1.68, m) and H-15b (1.51, m)/C-15 (31.6), H-16 (4.28, dt)/C-16 (78.8), H-17 (1.70, m)/C-17 (62.8), H-18 (0.81, s)/C-18 (16.4), H-19 (1.02, s)/C-19 (19.4), H-20 (1.88, t)/C-20 (41.2), H-21 (0.95, d)/C-21 (15.3), H-23 (1.61, m)/C-23 (34.0), H-24 (1.62 m)/C-24 (30.3), H-25 (1.69, m)/C-25 (31.4), H-26a (2.60, t), H-26b (2.65, dd)/C-26 (47.6) and H-27 (0.84, t)/C-27 (19.3) (Figure 45). The HMBC NMR showed correlations between H-1/C-3and 5; H-4/C-2, 3, 5, 6, 8 and 10; H-6/C-4, 7, 8 and 10; H-7/C-8, 13 and 14; H-9/C-10 and 19; H-11/C-8 and 9; H-12/C-18 and 21; H-14/C-13 and 18; H-15/C-21; H-16/C-13; H-17/C-12, 16 and 21; H-18/C-13, 14, 17 and 20; H-19/C-1, 5, 9 and 10; H-20/C-13, 16, 17 and 22; H-21/C-17, 20, and 22; H-23/C-26; H-24/C-26; H-25/C-24 and 26; H-26/C-22, 24 and 25 and H-27/C-24 and 26 (Figures 11 and 46). The COSY spectrum exhibited correlation of H and H between H1/H-2; H2/H-1 and H-3; H-3/H-2 and H-4; H-4/H-3; H-6/H-7; H-7/ H-6 and H-8; H-8/H-7 and H-9; H-9/H-8 and H-11; H-11/H-9; H-11; H-14/H-8 and H-15; H-15/H-14 and H-16; H-16/H-15 and H-17; H-17/H-16 and H-20; H-20/H-17 and H-21; H-21/H-20; H-22/H-23; H-23/H-22 and H-24; H-24/H-23 and H-25; H-25/H-26 and H-27; H-26/H-25 and H-27/H-26 (Figures 12 and 47). ^{1}H (300 MHz) and ^{13}C (75 MHz) NMR data of compound **212** in $CDCl_3$ are shown in Table 58. On the basis of above observations, compound **212** was identified as solasodine and chemical structure of solasodine is shown in Figure 10.

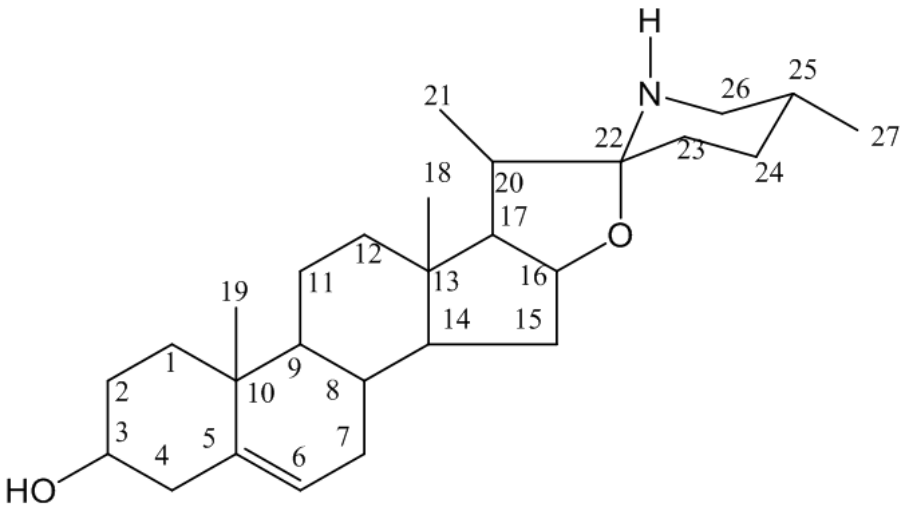

Figure 10 Structure of solasodine (compound **212**)

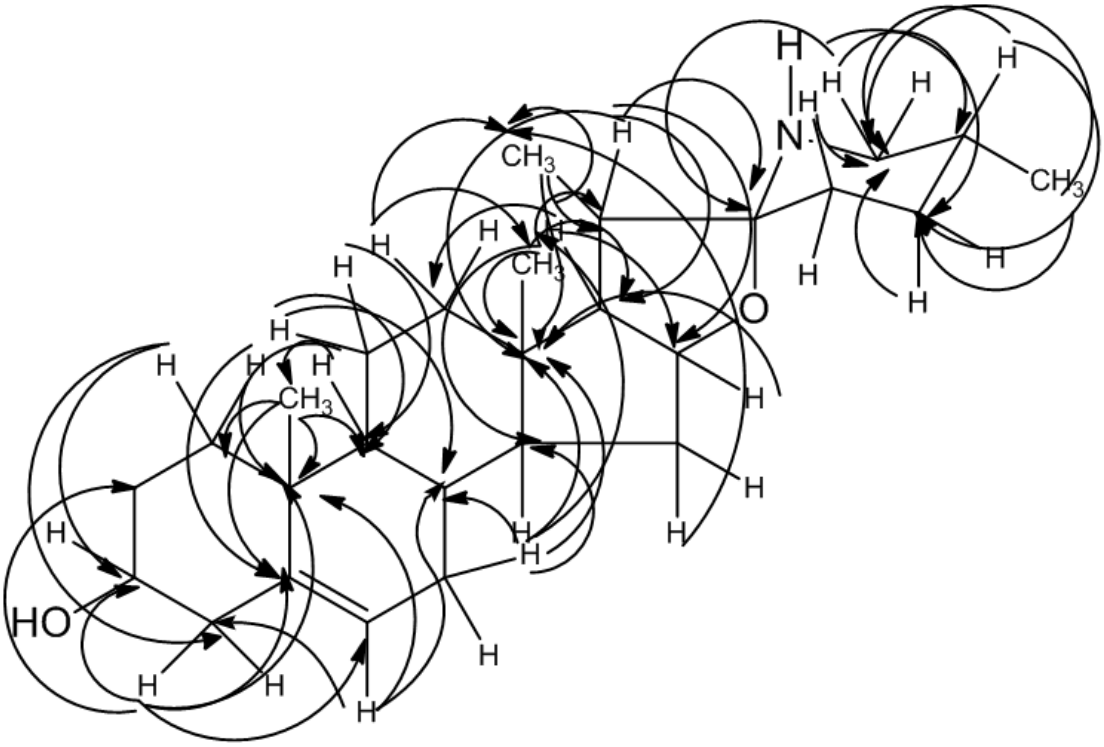

Figure 11 HMBC correlations of compound **212**

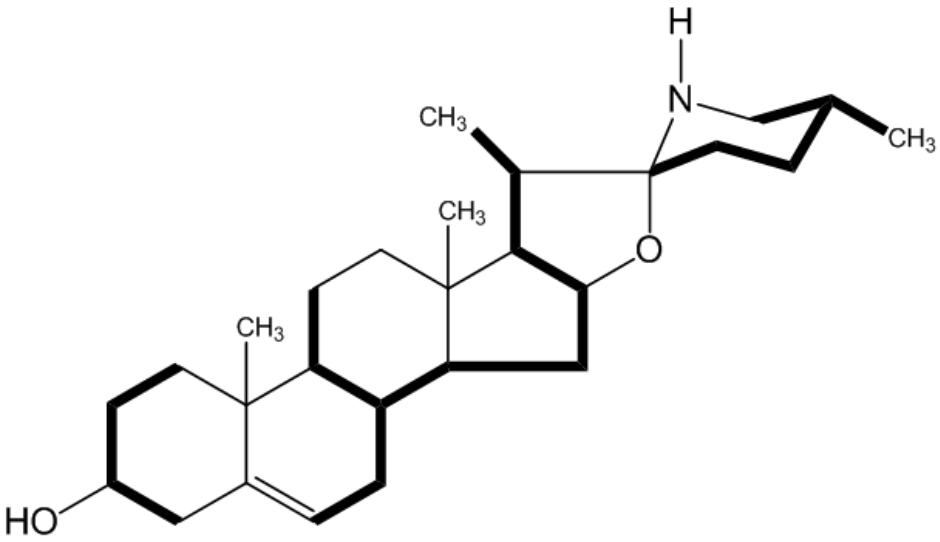

Figure 12 COSY (bold line) correlations of compound **212**

In Solanaceae family, solasodine was previously isolated from roots bark and berries of *S. aculeastrum*, fruits of *S. platanifolium*, roots of *S.trilobatum* and berries of *S. xanthocarpum.* It is used for diuretic, anticancer, antifungal, antispermatogenetic, antiandrogenic, immunomodulatory and antipyretic activity [138-140].

Table 58 ^{1}H (300 MHz) and ^{13}C (75 MHz) NMR data of compound **212** in $CDCl_3$

	Compound **212** in $CDCl_3$			Solasodine in $CDCl_3$ [140]	
Position	δ_H (multiplicity, J_{HH})	δc	HMBC correlations	δ_H	δc
1	1.85 (m), 1.07 (m)	37.2	C-3, 5	0.91, 1.90	37.2
2	1.98 (m), 1.28 (m)	32.2		1.79, 1.42	32.1
3	3.51 (m)	71.7		3.65	71.7
4	2.23 (dd, *J* = 5.1, 8.8 Hz), 2.28 (dd, *J* = 8.4, 17.1 Hz)	42.3	C-2, 3, 5, 6, 8,10	2.50, 2.31	42.2
5	-	140.8		-	140.8
6	5.34 (dt, *J* = 8.7, 3.3 Hz)	121.4	C-4, 7, 8, 10	5.36	121.3
7	1.99 (m)	32.1	C-8, 13, 14	1.59, 2.03	32.1
8	1.68 (m)	31.4		1.59	30.2
9	0.94 (m)	50.1	C-10, 19	0.91	50.1
10	-	36.6		-	37.6
11	1.46 (m)	20.9	C-8, 9	1.37, 1.49	20.9
12	1.73 (m), 1.15 (m)	39.9	C-18, 21	1.70, 1.15	39.9
13	-	40.5		-	40.5
14	1.09 (m)	56.5	C-13, 18	1.01	56.5
15	1.68 (m), 1.51 (m)	31.6	C-21	1.83, 1.30	31.2
16	4.28 (dt, *J* = 13.1, 12.0 Hz)	78.8	C-13	4.40	78.9
17	1.70 (m)	62.8	C-12, 16, 21	1.64-1.69	62.7
18	0.81 (s)	16.4	C-13, 14, 17, 20	0.85	16.4
19	1.02 (s)	19.4	C-1, 5, 9, 10	1.05	19.4
20	1.88 (t, *J* = 11.9 Hz)	41.2	C-13, 16, 17, 22	1.79-1.84	41.3

Table 58 ^{1}H (300 MHz) and ^{13}C (75 MHz) NMR data of compound **212** in $CDCl_3$ (continue)

Position	Compound **212** in $CDCl_3$ δ_H (multiplicity, J_{HH})	δc	HMBC correlations	Solasodine in $CDCl_3$ [140] δ_H	δc
21	0.95 (d, *J* = 11.9 Hz)	15.3	C-17, 20, 22	1.18	14.8
22	-	98.3		-	98.3
23	1.61 (m)	34.0	C-26	1.59	34.0
24	1.62 (m)	30.3	C-26	1.36-1.54	31.6
25	1.69 (m)	31.4	C-24, 26	1.52	31.4
26	2.60 (t, *J* = 18.6 Hz), 2.65 (dd, *J* = 5.9, 17.1 Hz)	47.6	C-22, 24, 25	2.25-2.23	47.6
27	0.84 ((t, *J* = 10.3 Hz)	19.3	C-24, 26	0.98	19.3

4.9 Identification of compound 213

The compound **213** was isolated as white crystal (3.0 mg, 0.0260% w/w of *n*-butanol crude extract) with melting point of 295 - 300 °C. The molecular formula of compound **213** was suggested as $C_{45}H_{73}NO_{16}$ by HRESIMS (*m/z* 884.5006 $[M + H]^+$, calcd 884.5007) (Figure 57). The ^{1}H NMR signals of five methyl groups indicated at H-27, H-18, H-19, H-21 and H-6‴ displayed at δ 0.83 (d), 0.88 (s), 1.08 (s), 1.10 (d) and 1.71 (d) ppm, respectively. The signals of anomeric signals appeared at H-1′, H-1″ and H-1‴ shown at δ 4.94 (m), 5.22 (m) and 6.31 (m) ppm, respectively. Signals of olefinic proton at H-6 appeared at δ 5.34 (d) ppm. The signal of H-16 which was neighbor to oxygen at 4.41 (m) ppm obtained at the lower field. The signal H-26 which was neighbour to nitrogen at δ 2.80 (m) ppm and its signal was obtained at the lower field. The sugar moiety showed at δ 5.0 - 1.71 ppm. The sugar moieties of galactose, glucose and rhamnose showed at δ 4.94 - 4.03, 5.22 - 3.99 and 6.31 - 1.71 ppm, respectively.The ^{1}H NMR spectrum is shown in Figure 49. The ^{13}C NMR spectrum (Figure 50) exhibited signals for anomeric ether linked carbons at C-1′, C-1‴ and C-1″ as δ 100.9, 102.7 and 106.4 ppm, respectively. The combination of ^{13}C NMR, DEPT 90 (Figure 51), DEPT 135 (Figure 52) and HSQC (Figure 53) spectra showed the presence of 45 carbon signals including five methyl, twelve methylene, twenty-four methine and four quaternary carbons. The signals of five methyl carbon groups at C-21, C-18, C-6‴, C-19 and C-27 displayed signal appearing at δ 16.4, 16.9,19.0, 19.8 and 20.1 ppm. The signals for twelve methylene carbon groups at C-11, C-2, C-24, C-7, C-15, C-23, C-1, C-4, C-12, C-26, C-6″ and C-6′ displayed at δ 21.6, 30.6, 31.6, 32.9, 33.1, 35.2, 38.0, 39.3, 40.6, 48.5, 63.0 and 63.1 ppm, respectively. The signals for twenty-four methine carbon groups at C-8, C-25, C-20, C-9, C-14, C-17, C-5‴, C-4′, C-5″, C-2‴, C-4‴, C-3‴, C-2″, C-2′, C-5′, C-3, C-3″, C-4″, C-16, C-3′, C-1′, C-1‴, C-1″ and C-6 appeared at δ 32.1, 32.2, 42.1, 50.8, 57.2, 64.0, 69.9,7 0.9, 72.1, 73.1, 73.3, 74.7, 75.4, 75.6, 77.0, 78.0, 78.8, 79.0, 79.3, 85.3, 100.9, 102.7, 106.4 and 122.2 ppm, respectively. The signals for four quaternary carbons groups at C-10, C-13, C-22 and C-5 which displayed at δ 37.7, 41.1, 98.8 and 141.4 ppm, respectively. These anomeric signals were confirmed from HSQC

correlations. The HSQC NMR (Figure 53) spectrum is correlation between H and C which was resulted observation including H-1a (0.95, m) and H-1b (0.95, m)/C-1 (38.0), H-2a (2.12, m) and H-2b (1.90, m)/C-2 (30.6), H-3 (3.99, m)/C-3 (78.0), H-4 (2.80, m)/C-5 (39.3), H-6 (5.34, m)/C-6 (122.2), H-7a (1.50, m) and H-7b (1.90, d)/C-7 (32.9), H-8 (1.50, m)/C-8 (32.4), H-9 (0.94, m)/C- 9 (50.8), H-11 (1.50, m)/C-11 (21.6), H-12a (1.11, m) and H-12b (1.75, m)/C-12 (40.6), H-14 (1.11, m)/C-14 (57.2), H-15a (2.09, m) and H-15b (1.50, m)/C-15 (33.1), H-16 (4.41, m)/C-16 (79.3), H-17 (1.75, m)/C-17 (64.0), H-18 (0.88, s)/C-18 (17.0), H-19 (1.07, s)/C-19 (19.9), H-20 (1.98, m)/C-20(42.1), H-21 (1.10, d)/C-21 (16.2), H-23a (1.77, m) and H-23b (1.73, m)/C-23 (35.2), H-24 (1.64, m)/C-24 (31.6), H-25 (1.64, t)/C- (32.2), H-26 (2.80, m)/C-26 (48.5) and H-27 (0.83, d)/C-27 (20.2). While, the HSQC NMR spectrum of the sugar moiety is correlation including, H-1′ (4.94, m)/C-1′ (100.9), H-2′ (4.72, dd)/C-2′ (75.6), H-3′ (4.33, m)/C-3′ (85.3), H-4′ (4.83, m)/C-4′ (70.9), H-5′ (4.03, m)/C-5′ (77.0), H-6a′ (4.49, m) and H-6b′ (4.33, m)/C-6′ (63.1), H-1′′ (5.22, d)/C-1′′(106.4), H-2′′(3.97, m)/C-2′′ (75.4), H-3′′ (3.99, m)/C-3′′ (78.8), H-4′′ (4.23, m)/C-4′′ (79.0), H-5′′ (4.23, m)/C-5′′ (72.1), H-6a′′ (4.39, dd) and H-6b′′ (4.26, m)/C-6′′ (63.0), H-1′′′ (6.31, m)/C-1′′′ (102.7), H-2′′′ (4.94, m)/C-2′′′ (73.1), H-3′′′ (4.30, m)/C-3′′′ (74.7), H-4′′′ (4.62, m)/C-4′′′ (73.3), H-5′′′ (4.94, m)/C-5′′′ (69.9) and H-6′′′ (1.75, m)/C-6′′′ (19.1) (Figure 53). The HMBC NMR spectrum is correlations between H-1/C-5, H-3/C-1′, H-4/C-2, 3, 5, 6 and 10; H-6/C-4, 8 and 10; H-7/C-5 and 6; H-8/C-6; H-12/C-9 and 14; H-15/C-14 and 20; H-16/C-13; H-17/C-13 and 21; H-18/C-12, 13, 14 and 17; H-19/C-1, 5, 9 and 10; H-20/C-13, 21, 22 and 23; H-23/C-22; H-24/C-22 and 26; H-27/C-26; H-1′/C-3 and 5′; H-2′/C-1′, 3′ and 1′′′; H-3′/C-1′′; H-4′/C-2′ and 3′; H-5′/C-1′ and 6′; H-1′′/C-3′ and 3′′; H-2′′/C-1′′; H-1′′′/C-2′, 3′′′, 4′′′; and 5′′′; H-2′′′/C-3′′′; H-4′′′/C-6′′′, H-5′′′/C-6′′′ and H-6′′′/C-3′′′ and 5′′′ (Figure 54). The HMBC spectrum exhibited correlation peaks of GalH-1 with C-3 and H-3 with GalC-1 which suggesting D-galactose unit was linked to solasodine as aglycone unit. The correlations between GluC-1 and GalH-3 and GalH-3 and GluH-1 indicated D-glucose unit was linked to C-3 of D-galactose unit. The correlations between RhaC-1 and GalH-2 and GalH-2 and RhaH-1 indicated L-rhamnose unit was linked to C-2 of D-galactose unit. The COSY spectrum (Figure 55) exhibited correlation of H and H between H1/H-2; H2/H-1 and H-3; H-3/H-2 and H-4; H-4/H-3and H-5; H-6/H-7; H-7/H-6 and H-8; H-8/H-7 and H-9; H-9/H-8 and H-11; H-11/H-9; H-11/H-9 and H-12; H-14/H-8 and H-15; H-15/H-14 and H-16; H-16/H-15 and H-17; H-17/H-16 and H-20; H-20/H-17 and H-21; H-21/H-20; H-22/H-23; H-23/H-24; H-24/H-23 and H-25; H-25/H-26 and H-27; H-26/H-25; H-27/H-26; H-25; H-27/H-25. The COSY spectrum of sugar moiety is correlation including, H-1′/H-2′; H-2′/H-1′ and H-3′; H-3′/H-2′ and H-4′; H-4′/H-3′ and H-5′; H-5′/H-4′ and H-6′; H-6′/H-5′; H-1′′/H-2′′; H-2′′/H-1′′ and H-3′′; H-3′′/H-2′′ and H-4′′; H-4′′/H-3′′ and H-5′′; H-5′′/H-4′′ and H-6′′; H-6′′/H-5′′; H-1′′′/H-2′′′; H-2′′′/H-1′′′ and H-3′′′; H-3′′′/H-2′′′ and H-4′′′; H-4′′′/H-3′′′and H-5′′′; H-5′′′/H-4′′′ and H-6′′′; H-6′′′/H-5′′′ (Figures 15 and 55). The NOESY spectrum, the relative stereochemistry of **213** and it was observed from NOESY spectrum between H-1/H_3-19, H-6/H-14, H-14/H-16, H-16/H-18, H-17/H_3-21, H_3-18/H-20 and H_3-18/H_3-21, H_3-27/H-23, H-1′/H-3′, H-3′/ H-4′, H-3′/H-5′, H-3′/H-1′′, H-3′′/H-5′′, H-2′′′/H-3′′′ and H-3′′′/H_3-6′′′(Figures 16 and 56). ^{1}H (500 MHz) and ^{13}C (125 MHz) NMR data of compound **213** in pyridine-d_5 are shown in Table 59. On the basic of the

above evidence and all siganals including the 2D NMR (HSQC, HMBC, COSY and NOESY) analysis suggested that compound **213** is alkaloid glycoside which contains solasodine as aglycone. Saccharides as L-rhamnose, D-galactose and D-glucose moieties bind to the 3-hydroxy position of solasodine. All of the above arguments allowed the complete assignment of all signals and identified of compound **213** as solasonine (Figures 13). Compound **213** was identified by comparision of spectroscopic data with published in the literature [141, 142].

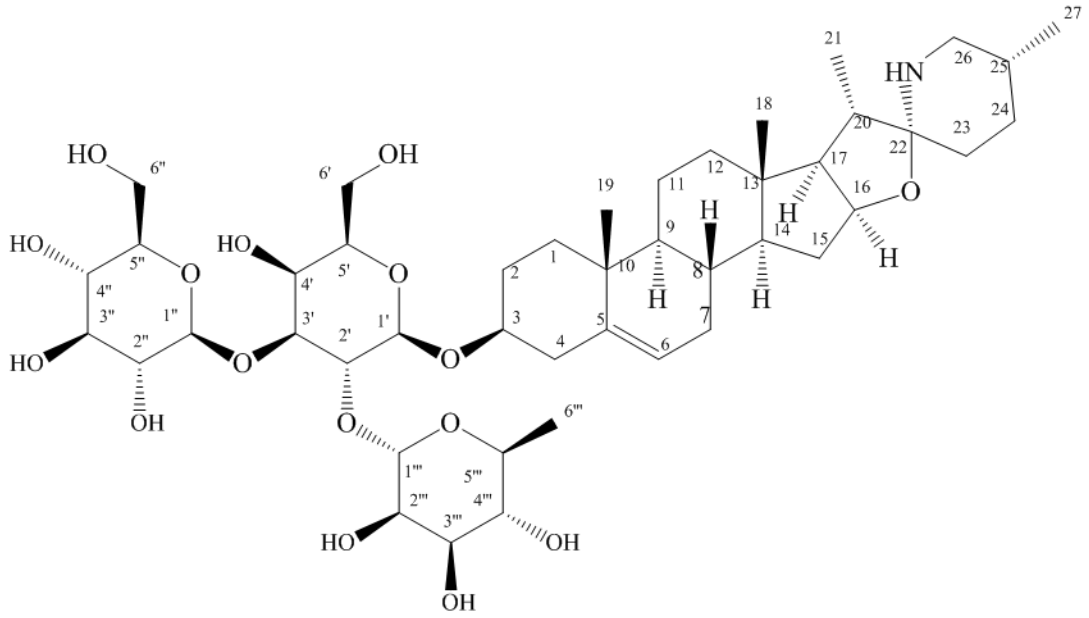

Figure 13 Structure of solasonine (compound **213**)

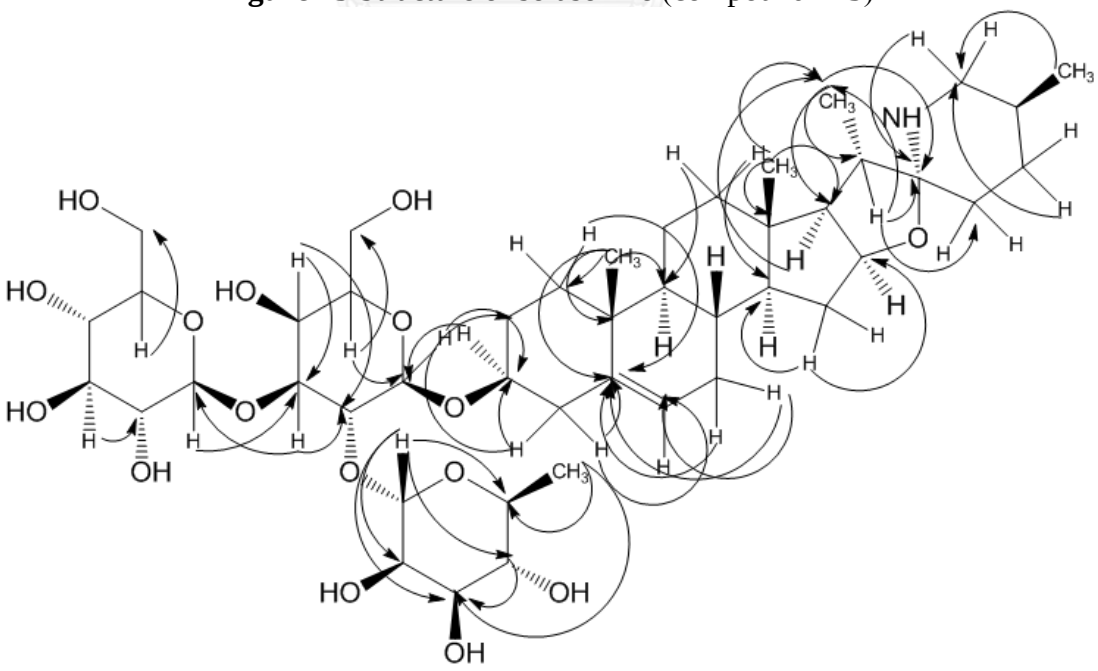

Figure 14 HMBC correlations of compound **213**

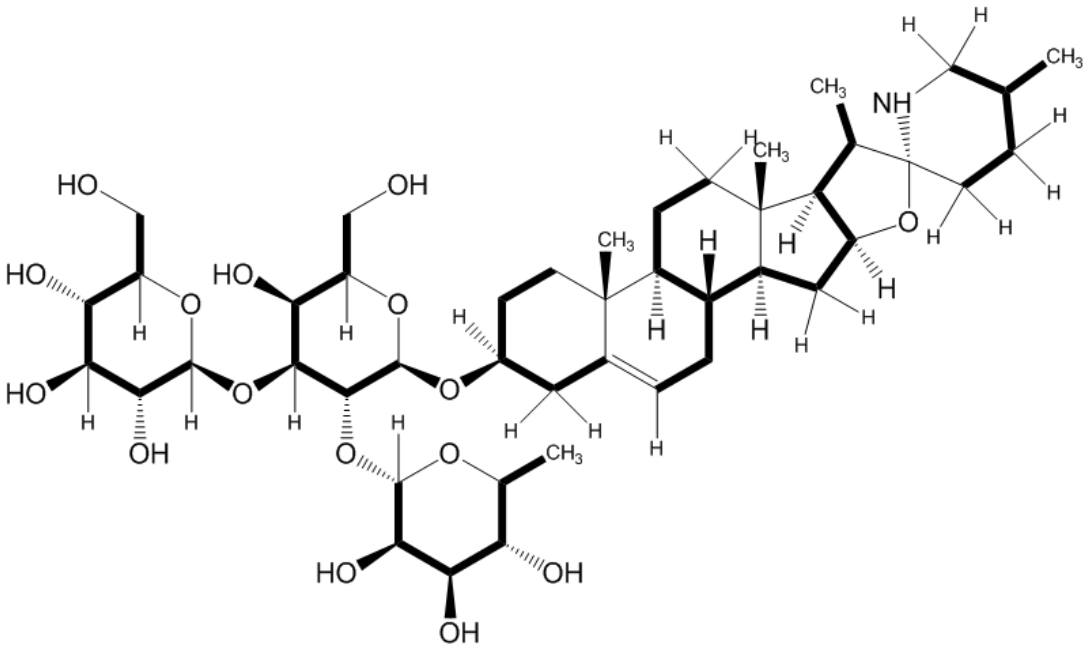

Figure 15 COSY (bold line) correlations of compound **213**

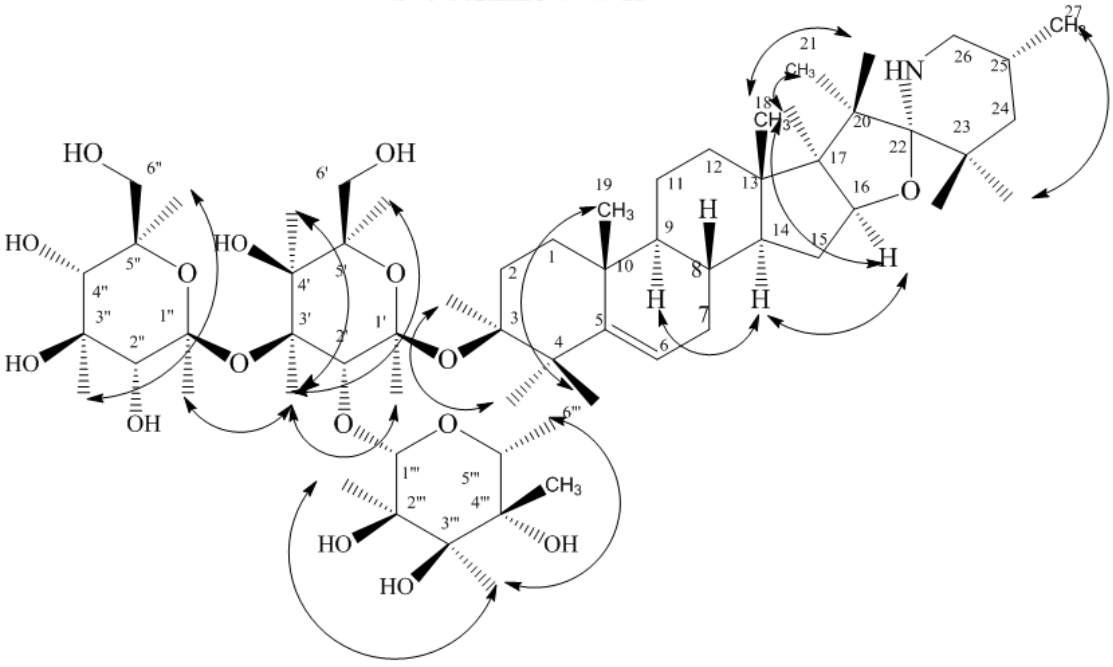

Figure 16 NOESY correlations of compound **213**

In Solanaceae family, solasonine was isolated from fruits of *S. aculeatissimum*, fruits of *S. asperum*, branches and fruits of *S. crinitum*, fruits of *S. khasianum*, fruits of *S. lycocarpum*, fruits of *S. platanifolium* and fruits of *S. tuberosum* [142-144]. It is used for antineoplastic biological, therapeutic agents and exhibited molluscicidal activity, cytotoxicity against several human cancer cell lines and skin tumours [124, 143-145].

Table 59 ^{1}H (500 MHz) and ^{13}C (125 MHz) NMR data of compound **213** in pyridine-d_5

Compound **213** in pyridine-d_5				Solasonine in pyridine-d_5 [141]	
Position	δ_H (multiplicity, J_{HH})	δc	HMBC correlations	δ_H (multiplicity, J_{HH})	δc
1	0.95 (m)	38.0	C-5	0.98	37.4
	1.75 (m)			1.80	
2	2.12 (m)	30.6		1.78	30.1
	1.90 (m)			1.48	
3	3.99 (dd, *J* = 6.6, 11.5 Hz)	78.0	C-1′	3.50	78.3
4	2.80 (m)	39.3	C-2, 3, 5, 6, 10	2.41	38.8
				2.18	
5	-	141.4		-	140.7
6	5.34 (d, *J* = 5.0 Hz)	122.2	C-4, 8, 10	5.33	121.6
7	1.50 (m)	32.9	C-5, 6	1.50	32.5
	1.90 (d, *J* = 14.0 Hz)			1.95	
8	1.50 (m)	32.1	C-6	1.53	32.5
9	0.94 (m)	50.8		0.90	50.3
10	-	37.7		-	37.1
11	1.50 (m)	21.6		1.50	21.1
12	1.11 (m)	40.6	C-9, 14	1.11	40.1
	1.75 (m)			1.70	
13	-	41.1		-	40.6
14	1.11 (m)	57.2		1.02	56.7
				nd	
15	2.09 (m)	33.1	C-14, 20	1.88	31.7
	1.50 (m)			1.11	
16	4.41 (m)	79.3	C-13	4.19	78.7
17	1.75 (m)	64.0	C-21	1.70	63.5
18	0.88 (s)	17.0	C-12, 13, 14, 17	0.72	16.5
19	1.08 (s)	19.9	C-1, 5, 9, 10	0.98	19.3
20	1.98 (m)	42.1	C-13, 21, 22, 23	1.75	41.5
21	1.10 (d, *J* = 7.1 Hz)	16.2	C-17, 20, 22	0.85	15.6
22	-	98.8		-	98.2
23	1.77 (m)	35.2	C-22	1.50	34.6
	1.73 (m)				
24	1.64 (m)	31.6	C-22, 26	1.57	31.1
				1.40	
25	1.64 (t, *J* = 10.3 Hz)	32.2		1.52	31.7
26	2.80 (m)	48.5	C-22	2.52	47.9
				2.38	
27	0.83 (d, *J* = 5.0 Hz)	20.2	C-26	0.78	19.7

Table 59 ^{1}H (500 MHz) and ^{13}C (125 MHz) NMR data of compound **213** in pyridine-d_5 (continue)

Position	Compound **213** in pyridine-d_5			Solasonine in pyridine-d_5 [141]	
	δ_H (multiplicity, J_{HH})	δc	HMBC correlations	δ_H (multiplicity, J_{HH})	δc
Gal-1′	4.94 (m)	100.9	C-3, 5′,	4.31	100.3
2′	4.72 (dd, *J* = 7.9, 9.5 Hz)	75.6	C-1′, 3′,1 ′′′	3.57	76.3
3′	4.33 (m)	85.3	C-1′′	3.62	84.8
4′	4.83 (s)	70.9	C-2′, 3′	3.88	70.2
5′	4.03 (m)	77.0	C-1′, 6′	3.39	74.9
6′	4.49 (m)	63.1		3.49	62.4
	4.33 (m)			3.47	
Glu-1′′	5.22 (d, *J* = 7.5 Hz)	106.4	. C-3′, 3′′	4.31	105.7
2′′	3.97 (m)	75.4	C-1′′	3.03	74.8
3′′	3.99 (m)	78.8		3.18	78.7
4′′	4.23 (m)	79.0		3.09	71.4
5′′	4.23 (m)	72.1		3.12	78.3
6′′	4.39 (dd, *J* = 5.4, 5.9 Hz)	63.0		3.62, 3.45	61.8
	4.26 (m)				
Rha-1′′′	6.31 (s)	102.7	C-2′, 3′′′, 4′′′, 5′′′	5.03	102.0
2′′′	4.94 (m)	73.1	C-3′′′	3.72	72.4
3′′′	4.30 (m)	74.7		3.40	72.7
4′′′	4.62 (m)	73.3	C-6′′′	3.19	74.0
5′′′	4.94 (m)	69.9	C-6′′′	4.0	69.3
6′′′	1.71 (d, *J* = 6.0 Hz)	19.1	C-3′′′, 5′′′	1.08	18.5

4.10 Identification of compound 214

The compound **214** was isolated as white crystal (4.9 mg, 0.0425% w/w of *n*-butanol crude extract) with melting point of 285 - 288 ^{o}C. Its molecular formula was measured by HRESIMS as $C_{45}H_{73}NO_{15}$ (m/z 868.5063 $[M+H]^+$, calcd. for $C_{45}H_{74}NO_{15}$, 868.5058) (Fugure 66). The ^{1}H NMR signals of five methyl groups at H-27, H-18, H-19, H-21 and H-6′′′ displayed at δ 0.85 (d), 0.94 (s), 0.98 (d), 1.07 (s) and 1.71 (d) ppm, respectively. The signals of anomeric signals displayed at H-1′, H-1′′ and H-1′′′ shown at δ 4.96 (br s), 5.22 (d) and 6.32 (s) ppm, respectively. Signals of olefinic proton at H-6 appeared at δ 5.38 (d) ppm. The signal H-16 which was neighbour to nitrogen at δ 2.65 (td) ppm and its signal was obtained at the lower field. The sugar moiety showed at δ 5.22 - 1.71 ppm. The sugar moieties of galactose, glucose and rhamnose showed at δ 4.96 - 4.04, 5.22 - 3.95 and 6.32 - 1.71 ppm, respectively. The ^{1}H NMR spectrum is shown Figure 58. The ^{13}C NMR spectrum (Figure 59) exhibited signals for anomeric ether linked carbons at C-1′, C-1′′ and C-1′′′ as δ 100.9, 102.3 and 106.3 ppm, respectively. The combination of ^{13}C NMR, DEPT 90 (Figure 60), DEPT 135 (Figure 61) and HSQC spectras (Figure 62) showed the presence of 45 carbon signals including five methyl, thirteen methylene, twenty-four methine and three quaternary carbons. The signals of five methyl carbon groups at C-18, C-21, C-6′′′, C-19 and C-27 displayed signal appeared at δ 17.4, 19.0, 19.1,

19.9 and 20.1 ppm. The signals for thirteen methylene carbon groups appeared at C-11, C-15, C-23, C-24, C-8, C-2, C-7, C-1, C-4, C- 12, C-26, C-6′ and C-6′′ displayed at δ 21.7, 30.1, 30.4, 32.1, 32.4, 32.9, 34.1, 38.1, 39.4, 40.5, 60.8, 63.0 and 63.1 ppm, respectively. The signals for twenty-four methine carbon groups at C-25, C-20, C-9, C-14, C-17, C-16, C-4′′′, C-4′, C-2′′′, C-3′′′, C-4′′′, C-5′′′, C-22, C-4′′, C-2′′, C-5′, C-2′, C-3, C-5′′, C-3′′, C-3′, C-1′, C-1′′′, C-1′′ and C-6 appeared at δ 31.8, 37.4, 51.0, 58.2, 63.9, 69.7, 69.9, 71.0, 72.1, 73.1, 73.4, 74.7, 75.2, 75.4, 75.6, 77.0, 78.1, 78.8, 79.1, 85.3, 100.9, 102.7, 106.3 and 122.4 ppm, respectively. The signals for three quaternary carbon groups at C-10, C-13 and C-5 which displayed at δ 37.6, 41.0 and 141.4 ppm, respectively. The signals for anomeric signals appeared at C-1′, C-1′′′ and C-1′′ shown at δ 100.9, 102.7 and 106.3 ppm, respectively. These anomeric signals were confirm from HSQC correlation. The signals for anomeric signals appeared at C-1′, C-1′′′ and C-1′′ which shown at δ 100.9, 102.7 and 106.3 ppm, respectively. The HSQC NMR (Figure 62) spectrum is correlation between H and C which was resulted observation including, H-1a (1.75, m) and H-1b (0.97, m)/C-1 (38.1), H-2a (2.02, m) and H-2b (1.59, m)/C-2 (32.9), H-3 (4.0, dd)/C-3 (78.1), H-4a (2.83, m) and H-4b (2.77, br t)/C-4 (39.4), H-6 (5.38, d)/C-6 (122.4), H-7a (1.68, m) and H-7b (0.81, m)/C-7 (34.1), H-8 (1.62, m)/C-8 (32.4), H-9 (0.93, m)/C-9 (51.0), H-11 (1.45, m)/C-11 (21.7), H-12a (1.71, m) and H-12b (1.11, m)/C-12 (40.5), H-14 (1.13, m)/C-14 (58.2), H-15a (1.70, m) and H-15b (1.24, m)/C-15 (30.1), H-16 (2.65, td)/C-16 (69.7), H-17 (1.48, dd)/C-17 (63.9), H-18 (0.94, s)/C-18 (17.4), H-19 (1.07, s)/C-19 (19.9), H-20 (1.69, m)/C-20 (37.4), H-21 (0.98, d)/C-21 (19.0), H-22 (4.28, m)/C-22 (74.7), H-23 (1.24 - 1.34, m)/C-23 (30.4), H-24a (1.82, m) and H-24b (1.14, td)/C-24 (32.1), H-25 (1.62, m)/C-25 (31.8), H-26a (2.92, dd) and H-26b (1.39, t)/C-26 (60.8) and H-27 (0.85, d)/C-27 (20.1). While, the HSQC NMR spectrum of the sugar moiety is correlation including, H-1′ (4.96, br s)/C-1′ (100.9), H-2′ (4.04, t)/C-2′ (77.0), H-3′ (4.33, m)/C-3′ (85.3), H-4′ (4.83, d)/C-4′ (71.0), H-5′ (4.73, dd)/C-5′ (75.6), H-6a′ (4.40, m) and H-6b′ (4.27, m)/C-6′ (63.0), H-1′′ (5.22, d)/C-1′′ (106.3), H-2′′(3.97, m)/C-2′′ (75.4), H-3′′ (3.95, m)/C-3′′ (79.1), H-4′′ (1.55, ddd)/C-4′′ (75.2), H-5′′ (3.95, m)/C-5′′ (78.8), H-6a′′ (4.49, dd) and H-6b′′ (4.33, m)/C-6′′ (63.1), H-1′′′ (6.32, m)/C-1′′′ (102.7), H-2′′′ (4.21, m)/C-2′′′ (72.1), H-3′′′ (4.93, dd)/C-3′′′ (73.1), H-4′′′ (4.30, m)/C-4′′′ (69.9), H-5′′′ (4.64, m)/C-5′′′ (73.4) and H-6′′′ (1.71, d)/C-6′′′ (19.1) (Figure 62). The HMBC NMR is correlations between H-4/C-3, 5 and 6; H-6/C-7 and 10; H-8/C-9; H-15/C-16; H-16/C-13 and 17; H-17/C-16; H-18/C-11, 12, 13, 14 and 17; H-19/C-1, 5, 9 and 10; H-21/C-17 and 20; H-22/C-21, 23 and 26; H-24/C-27; H-25/C-26; H-26/C-22, 24 and 25; H-27/C-24 and 26; H-1′/C-3; H-2′/C-1′, 3′ and 1′′′; H-3′/C-2′ and 1′′; H-4′/C-3′; H-5′/C-1′, 3′ and 4′; H-6′/C-5′; H-1′′/C-3′ and 3′′′; H-2′′/C-1′′; H-3′′/C-5′′; H-5′′/C-3′′ and H-1′′′/C-5′′′ (Figures 18 and 63). The HMBC spectrum exhibited correlation peaks of GalH-1 with C-3 and H-3 with GalC-1 which suggesting D-galactose unit was linked to solanidine as aglycone unit. The correlations between GluC-1 and GalH-3 and GalH-3 and GluH-1 indicated D-glucose unit was linked to C-3 of D-galactose unit. The correlations between RhaC-1 and GalH-2 and GalH-2 and RhaH-1 indicated L-rhamnose unit was linked to C-2 of D-galactose unit. The COSY spectrum exhibited correlation of H and H between H1/H-2; H2/H-1 and H-3; H-3/H-2 and H-4; H-4/H-3; H-6/H-7; H-7/H-6 and H-8; H-8/H-7 and H-9; H-9/H-8 and H-11; H-11/H-9 and H-12; H-14/H-8 and H-14; H-15/H-

14 and H-16; H-16/H-15 and H-17; H-17/H-16 and H-20; H-20/H-17 and H-21; H-21/H-20; H-22/H-20 and H-23; H-23/H-22 and H-24; H-24/H-23 and H-25; H-25/H-24 and H-26; H-27/H-25. The COSY spectrum of the sugar moiety is correlation including; H-1′/H-2′; H-2′/H-1′ and H-3′; H-3′/H-2′ and H-4′; H-4′/H-3′ and H-5′; H-5′/H-4′ and H-6′; H-6′/H-5′; H-1′′/H-2′′; H-2′′/H-1′′ and H-3′′; H-3′′/H-2′′ and H-4′′; H-4′′/H-3′′ and H-5′′; H-5′′/H-4′′ and H-6′′; H-6′′/H-5′′; H-1′′′/H-2′′′; H-2′′′/H-1′′′ and H-3′′′; H-3′′′/H-2′′′ and H-4′′′; H-4′′′/H-3′′′and H-5′′′; H-5′′′/H-4′′′ and H-6′′′; H-6′′′/H-5′′′ (Figures 19 and 64). The NOESY spectrum, the relative stereochemistry of **214** and it was observed from NOESY spectrum between H-3/H-4, H-9/H-14, H-12/H-18, H-12/H-19, H-15/H_3-21, H_3-21/H-22, H-24/H_3-27, H-26/H_3-27, H-1′/H-3′, H-3′/H-4′, H-3′/H-6′, H-3′/H-1′′, H-4′′/H-5′′, H-2′′′/H-3′′′ and H-4′′′/H_3-6′′′ (Figures 20 and 65). ^{1}H (500 MHz) and ^{13}C (125 MHz) NMR data of compound **214** in pyridine- d_5 are shown in Table 60. On the basic of the above evidence and all siganals including the 2D NMR (HSQC, HMBC, COSY and NOESY) analysis suggested that compound **214** was a saponin glycoside which contains solanidine as aglycone. Saccharides as L-rhamnose, D-galactose and D-glucose moieties bind to the 3-hydroxy position of solanidine. All of the above arguments allowed the complete assignment of all signals and identified compound **214** as α-solanine comparision of spectroscopic data with published in the literature [146]. Structure of α-solanine is shown in Figure 17.

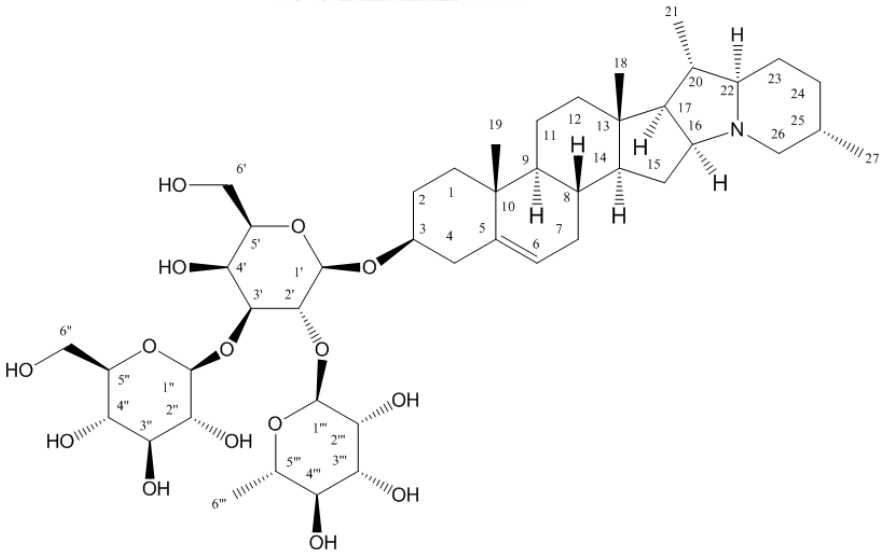

Figure 17 Structure of α-solanine (compound **214**)

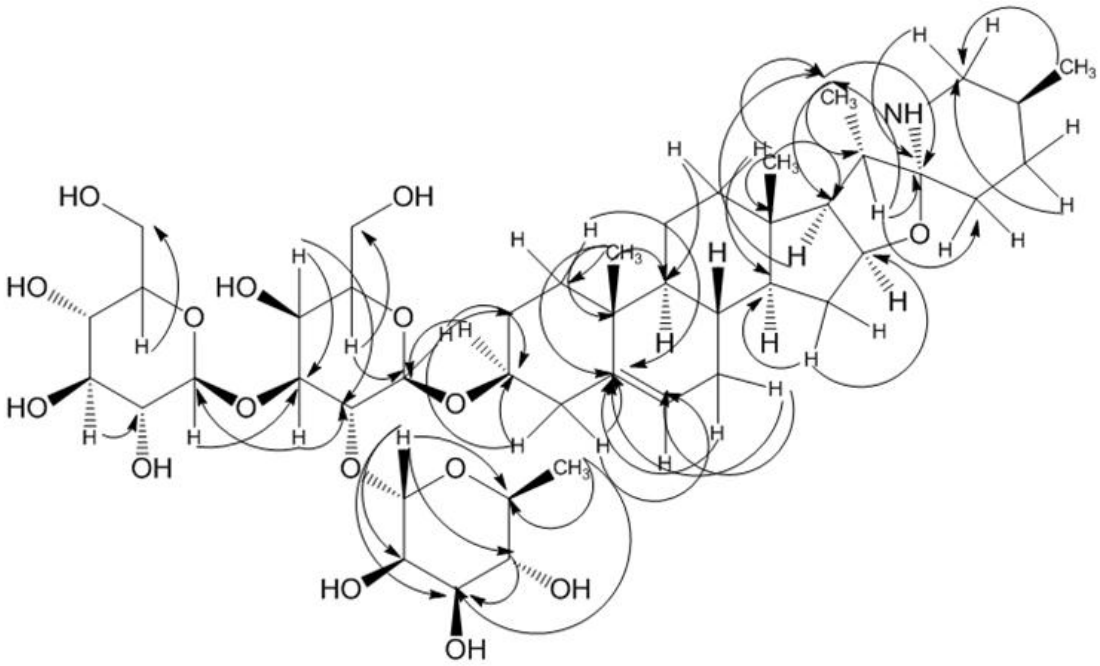

Figure 18 HMBC correlation of compound **214**

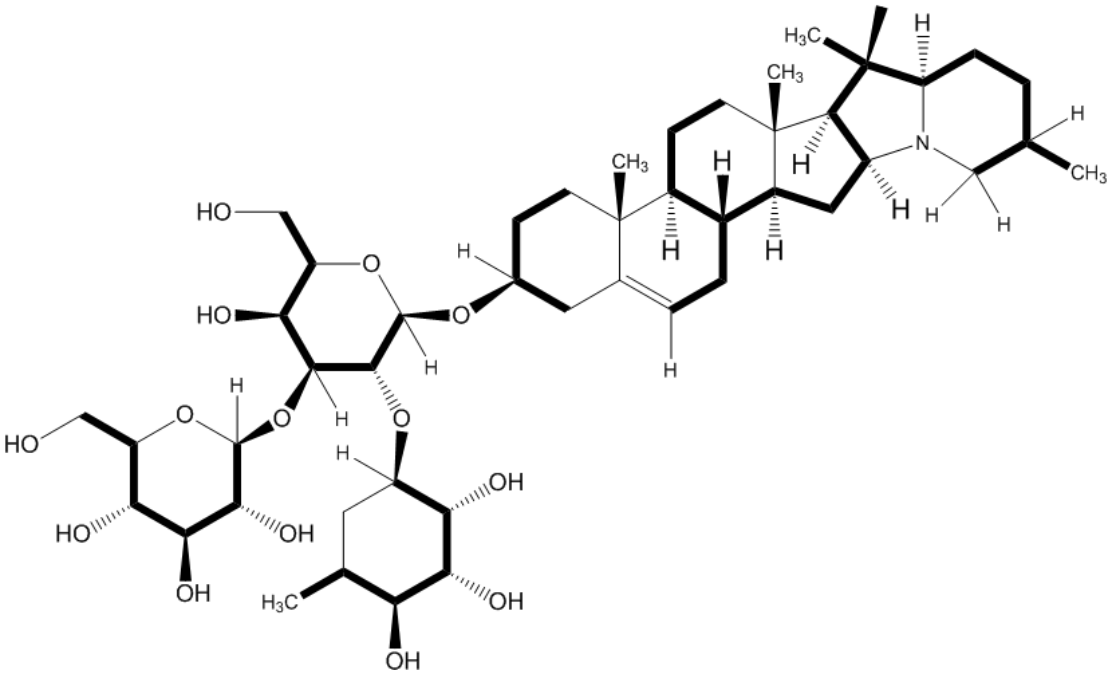

Figure 19 COSY (bold line) correlation of compound **214**

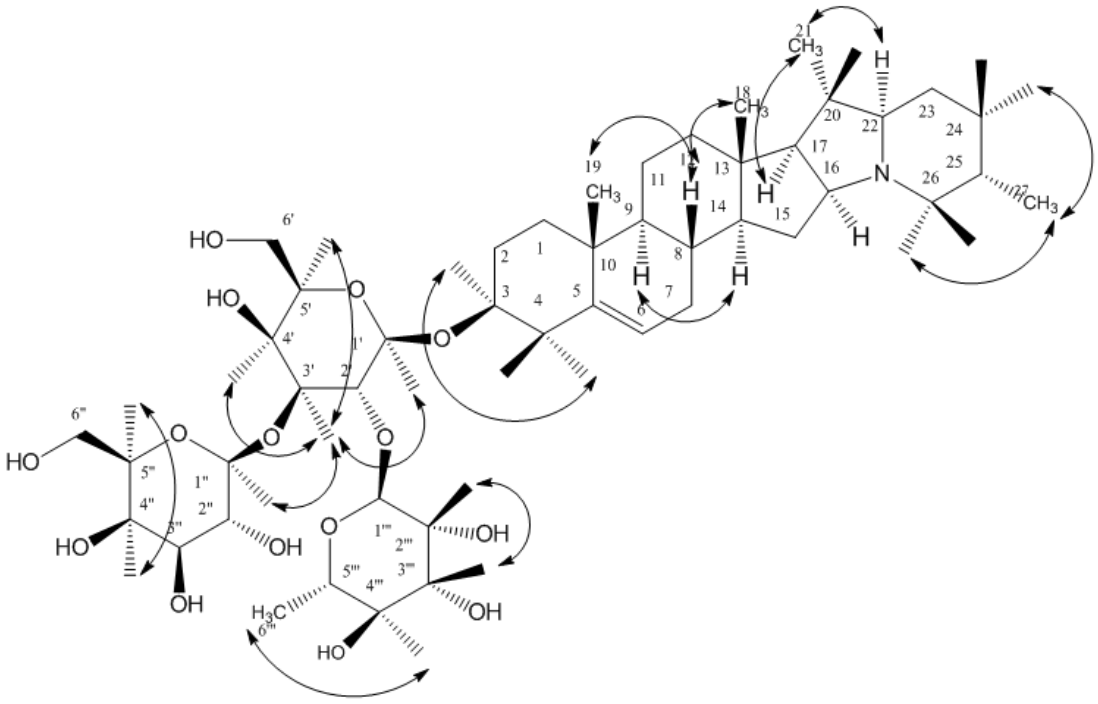

Figure 20 NOESY correlations of compound **214**

In Solanaceae family, α-solanine was isolated from fruits of *S. aculeatissimum*, fruits and leaves of *S. nigrum*, fruits of *S. tuberosum* and *S. xanthocarpum* [124, 144, 146, 147]. It is used for acetylcholinesterase inhibitor, antifeedant, fungicide and pesticide activities [124].

Table 60 ^{1}H (500 MHz) and ^{13}C (125 MHz) NMR data of compound **214** in pyridine-d_5

Position	Compound **214** in pyridine-d_5			α-Solanine in pyridine -d_5 [146]	
	δ_H (multiplicity, J_{HH})	δc	HMBC correlations	δ_H (multiplicity, J_{HH})	δc
1	1.75 (m) 0.97 (m)	38.1			37.4
2	2.02 (m) 1.59 (m)	32.9			32.2
3	4.0 (dd, J = 4.7, 10.5 Hz)	78.1			77.4
4	2.83 (m) 2.77 (br t, J = 11.7 Hz)	39.4	C- 3, 5, 6		40.0
5	-	141.4			140.8
6	5.38 (d, J = 5.0 Hz)	122.4	C-7, 10		121.6
7	1.68 (m) 0.81 (td, J = 11.9, 3.4 Hz)	34.1			32.6
8	1.62 (m)	32.4	C-9		31.5
9	0.93 (m)	51.0			50.2
10	-	37.6			37.0
11	1.45 (m)	21.7			21.0

Table 60 ^{1}H (500 MHz) and ^{13}C (125 MHz) NMR data of compound **214** in Pyridine-d_5 (continue)

Position	compound **214** in Pyridine-d_5			α-solanine in Pyridine-d_5 [146]	
	δ_H (multiplicity, J_{HH})	δc	HMBC correlations	δ_H (multiplicity, J_{HH})	δc
12	1.71 (m)	40.5			38.7
	1.11 (m)				
13	-	41.0			40.4
14	1.13 (m)	58.2			57.5
15	1.70 (m)	30.1	C-16		27.0
	1.24 (m)		C-16		
16	2.65 (td, *J* = 6.4, 8.6 Hz)	69.7	C-13, 17		69.3
17	1.48 (dd, *J* = 6.4, 9.4 Hz)	63.9	C-16		62.3
18	0.94 (s)	17.4	C-11, 12, 13, 14, 17	0.96 (brd)	16.6
19	1.07 (s)	19.9	C-1, 5, 9, 10	1.05 (s)	19.2
20	1.69 (m)	37.4			36.6
21	0.98 (d, *J* = 6.7 Hz)	19.0	C-17, 20	1.06 (s)	19.1
22	4.28 (m)	74.7	C-21, 23, 26		74.9
23	1.24 - 1.34 (m)	30.4			29.5
24	1.82 (m)	32.1	C-27		29.8
	1.14 (m)				
25	1.62 (m)	31.8	C-26		30.0
26	2.92 (dd, *J* = 2.5, 10.0 Hz)	60.8	C-22, 24, 25		59.6
	1.39 (t, *J* = 10.5 Hz)				
27	0.85 (d, *J* = 6.5 Hz)	20.1	C-24, 26	0.83 (d, *J* = 6.6 Hz)	19.2
Gal-1′	4.96 (br s)	100.9	C-3	4.93 (d, *J* = 7.7 Hz)	100.3
2′	4.04 (t, *J* = 6.0 Hz)	77.0	C-1′, 3′, 1‴		76.3
3′	4.33 (m)	85.3	C-2′, 1″		84.8
4′	4.83 (d, *J* = 2.0 Hz)	71.0	C-3′		70.2
5′	4.73 (dd, *J* = 7.8, 9.6 Hz)	75.6	C-1′, 3′, 4′		74.8
6′	4.40 (dd, *J* = 6.5, 10.4 Hz)	63.0	C-5′		62.3
	4.27 (dd, *J* = 6.0, 10.9 Hz)				
Glu-1″	5.22 (d, *J* = 8.0 Hz)	106.3	C-3′, 3‴	5.36 (br s)	105.7
2″	3.97 (m)	75.4	C-1″		74.9
3″	4.22 (m)	79.1	C-5″		78.3
4″	1.55 (ddd, *J* = 5.1, 7.5,	75.2			71.4
5″	3.95 (m)	78.8	C-5″		78.2
6″	4.49 (d, *J* = 10.8 Hz)	63.1			62.4
	4.33 (dd, *J* = 3.2, 9.6 Hz)				
Rha-1‴	6.32 (s)	102.7	C-5‴	6.29 (s)	102.0
2‴	4.21m)	72.1			72.4
3‴	4.93 (m)	73.1		4.92 (m)	72.7
4‴	4.30 (m)	69.9			74.0
5‴	4.64 (m)	73.4		5.19 (d, *J* = 8.1 Hz	69.3
6‴	1.71 (d, *J* = 6.2 Hz)	19.1		1.70 (d, *J* = 6.2 Hz)	18.5

4.11 Lipase inhibitory activity and IC_{50} values of compounds 209 - 214 and orlistat

Compounds **209 - 214** were investigated for lipase inhibitory activity. Concentrations of all isolated compounds were prepared and dissolved in DMSO. Compound **209** was prepared five concentrations as 100, 200, 500, 700 and 1000 µg/mL. Compound **210** was prepared five concentrations as 50, 100, 200, 400 and 800 µg/mL. Compound **211** was prepared five concentrations as 125, 250, 500, 750 and 1000 µg/mL. Compound **212** was prepared four concentrations as 25, 50, 100 and 400 µg/mL. Compounds **213** and **214** were prepared four concentrations as 25, 50, 100 and 200 µg/mL. Orlistat was prepared six concentrations as 0.00625, 0.0125, 0.025, 0.05, 0.1 and 0.2 µg/mL. Lipase inhibitory activity of isolated compounds is shown in Table 61.

IC_{50} is a median concentration of measurement of the effective inhibitor *in vitro* which is reduced by 50% inhibition of anti-lipase activity. IC_{50} was drawn a graph between various concentrations (X-axis) and percentage of inhibition (Y-axis). IC_{50} value was calculated from slope of this graph. Compounds **209 - 211** exhibited weak lipase inhibitory activity with IC_{50} values of 523.30 ± 0.91, 675.58 ± 1.29 and 565.06 ± 1.27 µg/mL, respectively. Compounds **212 - 214** showed lipase inhibition with IC_{50} values of 167.22 ± 0.87, 175.88 ± 0.85 and 193.96 ± 1.04 µg/mL, respectively. Whereas, positive control as orlistat showed strong lipase inhibitory activity with IC_{50} value of 0.13 ± 0.06 µg/mL. IC_{50} values of compounds **212 - 214** and orlistat were 404.26 ± 1.39, 198.75 ± 0.96, 223.43 ± 0.16 and 0.27 ± 0.07 µM (Table 62). Calibration plot of compounds **209 - 214** and orlistat on lipase inhibitory assay were shown in Figures 21 - 27.

Table 61 Lipase inhibitory activity *in vitro* of compounds **209 - 214** and orlistat

Compound	Concentration (µg/mL)	Inhibitory activity (%)
Compound **209**	100	26.74 ± 1.25
	200	35.89 ± 1.11
	500	50.32 ± 0.98
	700	60.25 ± 1.07
	1000	71.25 ± 1.04
Compound **210**	50	6.79 ± 0.86
	100	18.01 ± 1.55
	200	23.24 ± 1.65
	400	34.51 ± 2.02
	800	56.39 ± 1.92
Compound **211**	125	28.14 ± 1.42
	250	41.34 ± 3.17
	500	53.30 ± 1.41
	750	57.94 ± 2.94
	1000	62.06 ± 1.25
Compound **212**	25	34.91 ± 0.98
	50	38.45 ± 1.02
	100	49.32 ± 1.10
	400	67.96 ± 1.25
Compound **213**	25	37.02 ± 1.31
	50	41.08 ± 0.87
	100	45.91 ± 1.69
	200	52.62 ± 1.27
Compound **214**	25	30.14 ± 1.40
	50	35.15 ± 0.96
	100	42.65 ± 1.16
	200	51.20 ± 0.65
Orlistat	0.00625	3.06 ± 0.72
	0.0125	7.49 ± 1.42
	0.025	16.8 ± 0.85
	0.05	27.35 ± 1.49
	0.1	40.34 ± 0.54
	0.2	69.64± 1.19

Table 62 IC_{50} values of compounds **209 - 214** and orlistat

Compound	IC_{50} value	
	in µg/mL	in µM
Compound **209**	523.30± 0.91	-
Compound **210**	675.58 ± 1.29	-
Compound **211**	565.06 ± 1.27	-
Compound **212**	167.22 ± 0.87	404.26 ± 1.39
Compound **213**	175.88 ± 0.85	198.75 ± 0.96
Compound **214**	193.96 ± 1.04	223.43 ± 0.16
Orlistat	0.13 ± 0.06	0.27 ± 0.07

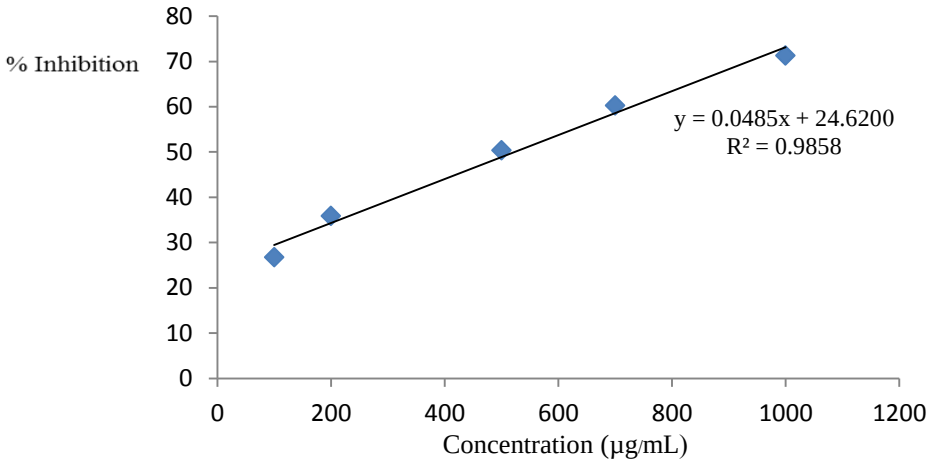

Figure 21 Calibration plot of compound **209** on lipase inhibitory assay

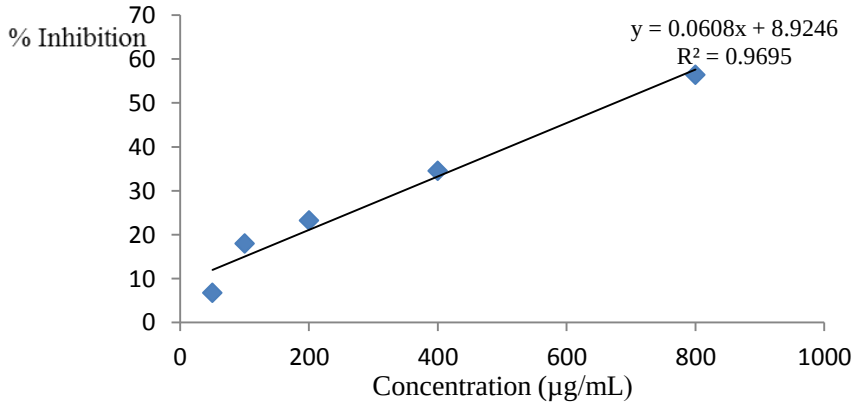

Figure 22 Calibration plot of compound **210** on lipase inhibitory assay

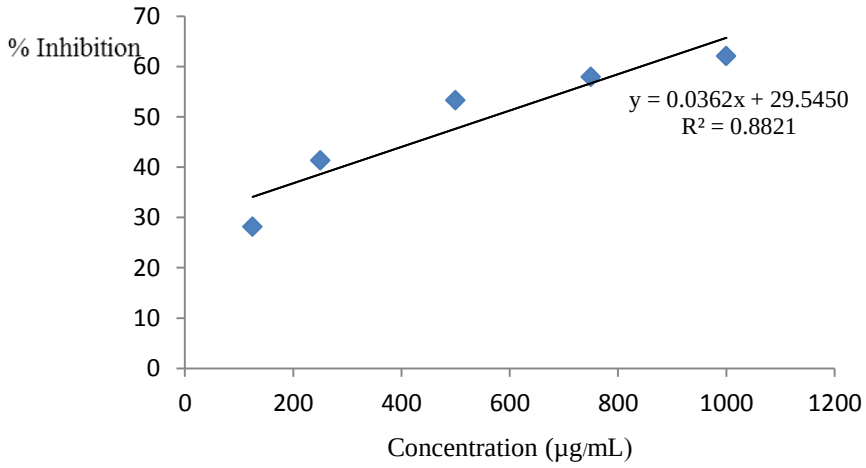

Figure 23 Calibration plot of compound **211** on lipase inhibitory assay

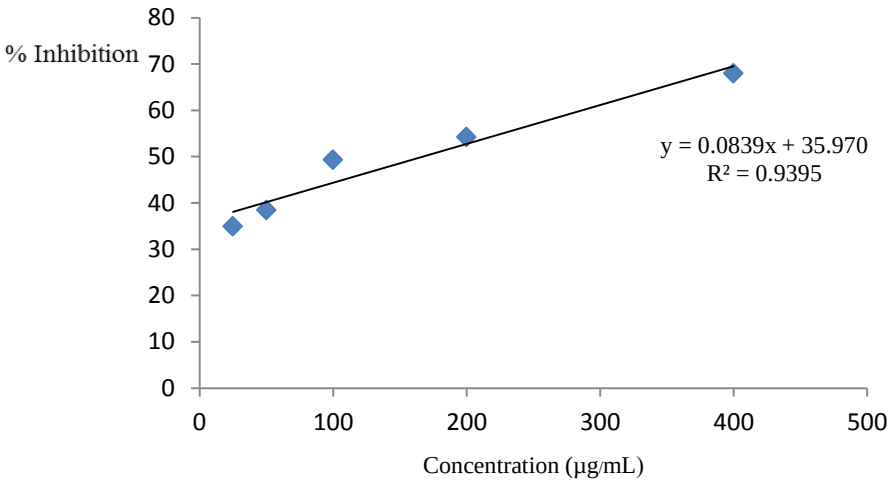

Figure 24 Calibration plot of compound **212** on lipase inhibitory assay

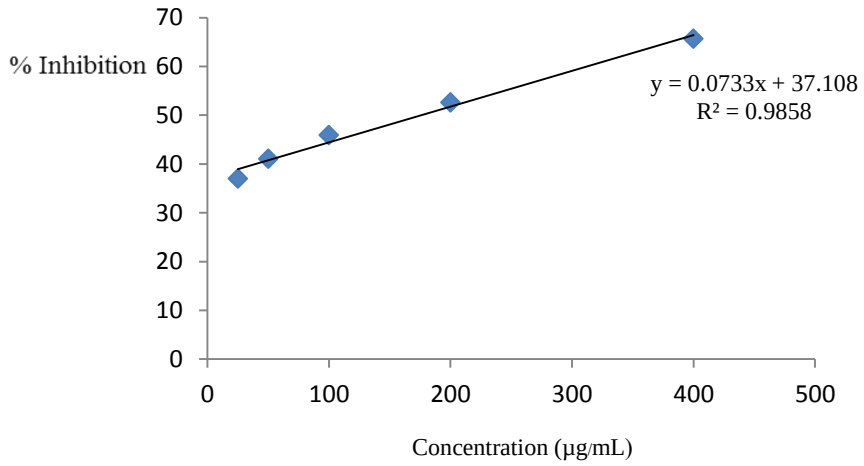

Figure 25 Calibration plot of compound **213** on lipase inhibitory assay

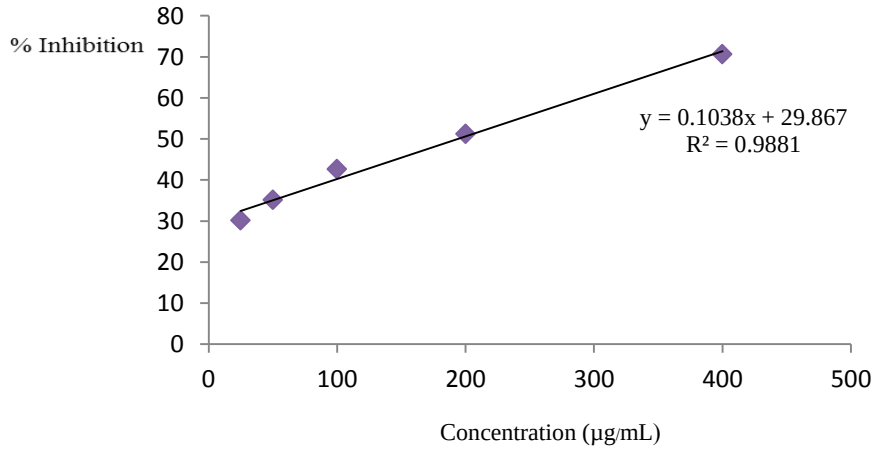

Figure 26 Calibration plot of compound **214** on lipase inhibitory assay

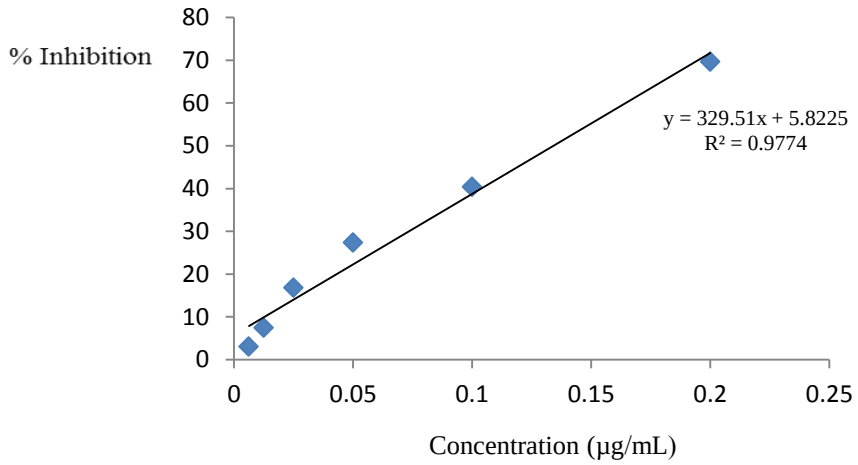

Figure 27 Calibration plot of orlistat on lipase inhibitory assay

Solasodine (**212**), solasonine (**213**) and α-solanine (**214**) exhibited with IC_{50} values of 404.26 ± 1.39, 198.75 ± 0.96 and 223.43 ± 0.16 µM, respectively. In previous studies, oolonghomobisflavan A, oolongtheanin 3′-*O*-gallate, (-)-epigallocatechin-3,5-digallate, oolonghomobisflavan B, silphioside F, copteroside B, hederagenin 3-*O*-*β*-D glucuronopyranoside 6′-*O*-methyl ester, gypsogenin 3-*O*-*β*-D-glucuronopyranoside, kaempferol-3-*O*-rutinoside, 3,3′,4,4′-tetrahydroxy-2 methoxy-chalcone and isoliquiritoside exhibited lipase inhibitory activity with IC_{50} values of 0.048, 0.07, 0.098, 0.11, 0.22, 0.25, 0.26, 0.26, 2.90 35.50 and 37.60 µM, respectively. Solasodine (**212**), solasonine (**213**) and α-solanine (**214**) exhibited lower potent of lipase inhibitory activity when comparision of these compounds on literature reviews [55, 67, 80]. Helonioside A, afzelin, helonioside A, 3-*O*-caffeoylquinic acid and 4-*O*-caffeoylquinic exhibited lipase inhibitory activity with IC_{50} values of more than 200, 572 ± 10, more than 1000 and more than 1000 µM, respectively. Solasodine (**212**), solasonine (**213**) and α-solanine (**214**) shown higher potent of lipase inhibitory activity when comparision of these compounds on literature reviews [90, 91]. 10α-hydroxy-1α,4 α-endoperoxy-guaia-2-en-12,6α-olide exhibited lipase inhibitory activity with IC_{50} value of 161.00 µM [70]. Solasonine (**213**) is gave nearly when comparision of compound were found in flowers of *C. morifolium*. Orlistat exhibited lipase inhibitory activity with IC_{50} value of 0.27 ± 0.07 µM which *p*-nitrophenyl palmitate (*p*-NPP) as a substrate, when comparision of previous studies as 19 µM [148], 294.51 µM [149]. Orlistat exhibited an lipase inhibitory activity of 51% at a concentration of 25 µg/mL [129]. In genus of *solanum* (Solanacea), carpesterol and 7-hydroxy-6-methoxycoumarin exhibited lipase inhibitory activity with IC_{50} values of 99.50 µM and 478.64 mM [150]. The effective factors cause a potential of lipase inhibitor. It may be depended on factors including family of plants, genus of plants, cultivated area, characteristic of plants, characteristic of compound in plants and aglycone in glycoside compound. These suggestion of the results, it may be separation of other major components from fruits of *S. aculeatissimum* which shown strong on anti-lipase activity especially hexane and *n*-butanol crude extracts. Chemical constituents in fruits of *S. aculeatissimum* may be synergist on anti-lipase activity for improving anti-lipase activity as lipase inhibitor.

CHAPTER V
CONCLUSION

The nineteen Thai medicinal plants were screened for anti-lipase activity. These plants were extracted with methanol and DI water to obtain methanolic extract and aqueous extract, respectively. From the results, methanolic extract of fruits of *S. aculeatissimum*, methanolic extract of fruits of *S. trilobatum* and methanolic extract of stems and leaves of *P. amarus* showed strong inhibition with percent inhibition as 87.77 ± 4.27%, 83.69 ± 4.27% and 83.57 ± 1.48%, respectively. Methanolic extract of fruits of *C. frutescens*, aqueous extract of fruits of *S. trilobatum*, aqueous extract of fruits of *S. melongena* (Thai eggplant) and methanolic extract of fruits of *S. melongena* (round eggplant) and methanolic extract of fruits of *S. melongena* (long eggplant) showed moderate anti-lipase activity with percent inhibition as 69.28 ± 2.79%, 67.43 ± 4.89%, 53.02 ± 15.60%, 51.58 ± 9.50% and 47.76 ± 8.44%, respectively. Aqueous extract of fruits of *S. melongena* (round eggplant), methanolic extract of fruits of *S. melongena* (Thai eggplants), methanolic extract of stems and leaves of *C. viscose*, methanolic extract of leaves of *P. sarmentosum*, methanolic extract of stems and leaves of *S. rostrata*, methanolic extract of leaves of *T. triandra*, methanolic extract of fruits of *C. annnuum*, and aqueous extract of fruits of *S. melongena* (long eggplants) showed weak anti-lipase activity with percent inhibition as 40.46 ± 23.19%, 37.74 ± 1.71%, 37.03 ± 0.66%, 34.09 ± 19.55%, 31.31 ± 1.93%, 28.56 ± 10.48%, 16.78 ± 1.40% and 5.02 ± 18.10%, respectively. Aqueous extract of fruits of *S. aculeatissimum*, aqueous extract of stems and leaves of *P. amarus*, aqueous extract of fruits of *C. frutescens*, aqueous extract of stems and leaves of *C. viscose*, aqueous extract of leaves of *P. sarmentosum*, aqueous extract of stems and leaves of *S. rostrata*, aqueous extract of leaves of *T. triandra*, aqueous extract of fruits of *C. annnuum*, methanolic and aqueous extracts of leaves of *C. siamea*, methanolic and aqueous extracts of roots of *G. gynandra*, methanolic and aqueous extracts of fruits of *M. cochinchinensis* (Chinese bitter), methanolic and aqueous extracts of fruits of *S. melongena* (round purple eggplant), methanolic and aqueous extracts of leaves of *A. lividus* and methanolic and aqueous extracts of fruits of *M. charantia* (bitter cucumber) showed no activity of anti-lipase. These results indicated that, plants in families of Solanaceae and Piperaceae showed anti-lipase activity more than other families. So, they have the potential to be excellent source of lipase inhibitors.

The methanolic extract of fruits of *S. aculeatissimum* was further investigated for lipase inhibitors. The dried ripe fruits of *S. aculeatissimum* were extracted with methanol to obtain methanolic crude extract. The methanolic crude extract was partitioned by liquid-liquid extraction with hexane, ethyl acetate, *n*-butanol and DI water to obtain four fractions as hexane crude extract, ethyl acetate crude extract, *n*-butanol crude extract and aqueous crude extract, respectively. The hexane and *n*-butanol crude extracts of *S. aculeatissimum* fruits showed strong lipase inhibitory activity with percent inhibition as 81.88 ± 0.98% and 80.74 ± 1.39%, respectively at a concentration of 25 mg/mL. The ethyl acetate crude extract of *S. aculeatissimum* fruits showed moderated lipase inhibitory activity with percent inhibition as 60.41 ± 7.36%. Whereas, aqueous crude extract showed weak activity with percent inhibition

as 22.12 ± 1.29%. Compound **209** as a mixture of fatty acids (C_{14}, C_{16}, C_{18} and C_{20}) was isolated from hexane crude extract which showed lipase inhibitory activity with IC_{50} value of 523.30 ± 0.91 µg/mL. Compound **210** as steroidal mixture was isolated from hexane crude extract which showed weak lipase inhibition with IC_{50} value of 675.58 ± 1.29 µg/mL. Compounds **211 - 214** were isolated from the *n*-butanol crude extract. Compound **211** was elucidated as steroidal glycoside which showed weak lipase inhibition with IC_{50} value of 565.06 ± 1.27 µg/mL. Compound **212** was elucidated as solasodine ($C_{27}H_{43}NO_2$) which showed weak lipase inhibition with IC_{50} value of 404.26 ± 1.39 µM. Compound **213** was elucidated as solasonine ($C_{45}H_{73}NO_{16}$) which showed moderate lipase inhibition with IC_{50} value of 198.75 ± 0.96 µM. Compound **214** was elucidated as α-solanine ($C_{45}H_{73}NO_{15}$) which showed moderate lipase inhibition with IC_{50} value of 223.43 ± 0.16 µM. Positive control as orlistat showed strong lipase inhibition with IC_{50} value of 0.27 ± 0.07 µM. However, hexane and *n*-butanol crude extracts of fruits of *S. aculeatissimum* exhibited strong lipase inhibitory activity. So, the unpurify fractions from fruits of *S. aculeatissimum* may contain strong lipase inhibitors or compounds from fruits of *S. aculeatissimum* may be synergetic mechanism on anti-lipase activity. However, α-solanine was reported as a toxic glycoalkaloid. Intoxication (2 - 5 mg/kg of body weight) from α-solanine leads toxicity include vomiting, abdominal pain, diarrhea neurological like hallucinations and headache with toxication [151]. The content of α-solanine is usually very low in *S. aculeatissimum* fruits. However, consumption of α-solanine is unsuitable for human. Glycoalkaloid especially α-solanine needs to investigate a possibility for consumption as lipase inhibitor. These results suggested that the chemical constituents of *S. aculeatissimum* fruits should be further investigated for the strong active components responsible for anti-lipase activity which are non-toxic of consumption and potential source for lipase inhibitors.

REFERENCES

[1] World Health Organization (WHO). Health topics: obesity [Online]. 2017. Available from: http://www.who.int/topics/obesity/en/ [2017, July 17]

[2] World Health Organization (WHO). Obesity and overweight [Online]. 2016. Available from: http://www.who.int/mediacentre/factsheets/fs311/en/ [2016, December 13]

[3] Diabassocthai. Statistic of obesity [Online]. 2013. Available from: http://www.diabassocthai.org/statistic/105 [2015, August 2]

[4] Ministry of Public Health (Bureau of Policy and Strateg). Thailand health profile: 2005-2007 [Online]. 2007. Available from: http://www.hiso.or.th/hiso5/report/tph2007eng.php.

[5] Suttisansanee, U., and Kruawan, K. Anti-lipase activities in edible sour leaves of Thai local plants. Thai Journal of Agricultural Science 44(2) (2013): 604-606.

[6] Weibel, E.K., Hadvary, P., Hochuli, E., Kupfer, E., and Lengsfeld, H. Lipstatin, an inhibitor of pancreatic lipase, produced by *Streptomyces toxytricini*. I. Producing organism, fermentation, isolation and biological activity. The Journal of Antibiotics 40(8) (1987): 1081-1085.

[7] Hochuli, E., Kupfer, E., Maurer, R., Meister, W., Mercadal, Y., and Schmidt, K. Lipstatin, an inhibitor of pancreatic lipase, produced by *Streptomyces toxytricini*. II. Chemistry and structure elucidation. The Journal of Antibiotics 40(8) (1987): 1086-1091.

[8] Ballinger, A., and Peikin, S.R. Orlistat: its current status as an anti-obesity drug. European Journal of Pharmacology 440(2-3) (2002): 109-117.

[9] Filippatos, T.D., Derdemezis, C.S., Gazi, I.F., Nakou, E.S., Mikhailidis, D.P., and Elisaf, M.S. Orlistat-associated adverse effects and drug interactions: a critical review. Drug Safety 31(1) (2008): 53-65.

[10] Tsujita, T., Matsuura, Y., and Okuda, H. Studies on the inhibition of pancreatic and carboxylester lipases by protamine. The Journal of Lipid Research 37(7) (1996): 1481-1487.

[11] Singh, G., Suresh, S., Bayineni, K.V., and Kadeppagari, K.R. Lipase inhibitors from plants and their medical applications. International Journal of Pharmacy and Pharmaceutical Sciences 7 (2015): 1-5.

[12] Yun, J.W. Possible anti-obesity therapeutics from nature. Phytochemistry 71(14-15) (2010): 1625-1641.

[13] Roh, C., Jung, U., and Jo, S.K. Screening of anti-obesity agent from herbal mixtures. Molecules 17(4) (2012): 3630-3638.

[14] Padwal, R., Li, S.K., and Lau, D.C. Long-term pharmacotherapy for overweight and obesity: a systematic review and meta-analysis of randomized controlled trials. International Journal of Obesity and Related Metabolic Disorders 27(12) (2003): 1437-1446.

[15] Billington, C.J., Epstein, L.H., Goodwin, N.J., Hill, J.O., Pi-Sunyer, F.X., Rolls, B.J., Stern, J., Wadden, T.A., Weinsier, R., Wilson, G.T., Wing, R.R., Yanovski, S.Z., Hubbard, V.S., Hoofnagle, J.H., Everhart, J., and Harrison, B. Overweight, obesity, and health risk. Archives of Internal Medicine 160(7) (2000): 898-904.

[16] Nawanopparatsakul, S. Obesity and the future of obesity treatment. Thai Journal of Pharmaceutical Sciences 26(1-2) (2002): 1-11.

[17] World Health Organization (WHO). Appropriate body-mass index for Asian populations and its implications for policy and intervention strategies. Lancet 363(9403) (2004): 157-163.

[18] Tse, W.W.Y., and Mak, P.P.Y. Eating: a pleasure, challenge or disorder? HONG KONG Journal of Paediatrics 9(4) (2004): 365-370.

[19] World Health Organization (WHO). Preventing and managing the global epidermis of obesity: report of a WHO consultation on obesity, Geneva, June 1997 [Online]. 1998. Available from: http://apps.who.int/iris/handle/10665/63854 [2017, July 18]

[20] Narksawat, K., Podang, J., Punyarathabundu, P., and Podhipak, A. Waist circumference, body mass index and health risk factors among middle aged Thais. Asia Pacific Journal of Public Health 19(3) (2007): 10-15.

[21] Han, T.S., van Leer, E.M., Seidell, J.C., and Lean, M.E. Waist circumference action levels in the identification of cardiovascular risk factors: prevalence study in a random sample. BMJ:British Medical Journal 311(7017) (1995): 1401-1405.

[22] Tanphaichitr, V., and Leelahagul, P. Clinical needs and opportunities in assessing body composition. Asia Pacific Journal of Clinical Nutrition 4(1) (1995): 23-24.

[23] Lunagariya, N.A., Patel, N.K., Jagtap, S., and Bhutani, K.K. Inhibitors of pancreatic lipase: state of the art and clinical perspectives. Experimental and Clinical Sciences International Online Journal for Advances in Science 13 (2014): 897-921.

[24] Brownlee, I.A., Forster, D.J., Wilcox, M.D., Dettmar, P.W., Seal, C.J., and Pearson, J.P. Physiological parameters governing the action of pancreatic lipase. Nutrition Research Reviews 23(1) (2010): 146-154.

[25] Mukherjee, A.K. Hydrophobic-hydrophilic interaction in lipase catalytic triad and possibility of a cofactor mediated catalysis. International Journal of Agricultural and Food Science 4(3) (2014): 84-89.

[26] Ferrato, F., Carriere, F., Sarda, L., and Verger, R. A critical reevaluation of the phenomenon of interfacial activation. Methods in Enzymology 286 (1997): 327-347.

[27] Ghosh, P.K., Saxena, R.K., Gupta, R., Yadav, R.P., and Davidson, S. Microbial lipases: production and applications. Science Progress 79(2) (1996): 119-157.

[28] Hube, B., Stehr, F., Bossenz, M., Mazur, A., Kretschmar, M., and Schafer, W. Secreted lipases of *Candida albicans*: cloning, characterisation and expression analysis of a new gene family with at least ten members. Archives of Microbiology 174(5) (2000): 362-374.

[29] Kim, E.K., Jang, W.H., Ko, J.H., Kang, J.S., Noh, M.J., and Yoo, O.J. Lipase and its modulator from *Pseudomonas* sp. strain KFCC 10818: proline-to-glutamine substitution at position 112 induces formation of enzymatically active lipase in the absence of the modulator. Journal of Bacteriology 183(20) (2001): 5937-5941.

[30] Martínez, A., and Soberón-Chávez, G. Characterization of the lipA gene encoding the major lipase from *Pseudomonas aeruginosa* strain IGB83. Applied Microbiology and Biotechnology 56(5-6) (2001): 731-735.

[31] Negre-Salvayre, A., Dagan, A., Gatt, S., and Salvayre, R. Use of pyrenemethyl laurate for fluorescence-based determination of lipase activity in intact living lymphoblastoid cells and for the diagnosis of acid lipase deficiency. Biochemical Journal 294 (1993): 885-891.

[32] Thuren, T., Virtanen, J.A., Verger, R., and Kinnunen, P.K. Hydrolysis of 1-palmitoyl-2-[6-(pyren-1-*yl*)]hexanoyl-*sn*-glycero-3-phospholipids by phospholipase A_2: effect of the polar head-group. Biochimica et Biophysica Acta 917(3) (1987): 411-417.

[33] Jacks, T.J., and Kircher, H.W. Fluorometric assay for the hydrolytic activity of lipase using fatty acyl esters of 4-methylumbelliferone. Analytical Biochemistry 21(2) (1967): 279-285.

[34] Roberts, I.M. Hydrolysis of 4-methylumbelliferyl butyrate: a convenient and sensitive fluorescent assay for lipase activity. Lipids 20(4) (1985): 243-247.

[35] Bereuter, T.L., and Lorbeer, E. Monitoring of lipase-catalyzed cleavage of acylglycerols by high-temperature gas chromatography. Journal of Chromatography A 697(1-2) (1995): 469-474.

[36] Gulomova, K., Ziomek, E., Schrag, J.D., Davranov, K., and Cygler, M. Purification and characterization of a *Penicillium* sp. lipase which discriminates against diglycerides. Lipids 31(4) (1996): 379-384.

[37] Jaeger, K.E., Ransac, S., Dijkstra, B.W., Colson, C., van Heuvel, M., and Misset, O. Bacterial lipases. FEMS Microbiology Reviews 15(1) (1994): 29-63.

[38] Verger, R. Enzyme kinetics of lipolysis. Methods in Enzymology 64 (1980): 340-392.

[39] Nury, S., Gaudry-Rolland, N., Riviere, C., Gargouri, Y., Bois, A., Lin, M., Grimaldi, M., Richou, J., and Verger, R. In: Alberghina L,Smith RD, Verger R (ed) Lipases: Structure, Mechanism, and Genetic Engineering, GBF-Monographs. GBF-Monographs 16 (1991): 123-127.

[40] Jaeger, K.E., Ransac, S., Koch, H.B., Ferrato, F., and Dijkstra, B.W. Topological characterization and modeling of the 3D structure of lipase from *Pseudomonas aeruginosa*. Federation of European Biochemical Societies 332(1-2) (1993): 143-149.

[41] Labourdenne, S., Cagna, A., Delorme, B., Esposito, G., Verger, R., and Riviere, C. Oil-drop tensiometer: applications for studying the kinetics of lipase action. Methods in Enzymology 286 (1997): 306-326.

[42] Flipsen, J.A., Kramer, R.A., van Duijnhoven, J.P., van der Hijden, H.T., Egmond, M.R., and Verheij, H.M. Cutinase binding and activity at the triolein-water interface monitored by oil drop tensiometry. Chemistry and Physics of Lipids 95(2) (1998): 169-180.

[43] Walde, P., and Luisi, P.L. A continuous assay for lipases in reverse micelles based on Fourier transform infrared spectroscopy. Biochemistry 28(8) (1989): 3353-3360.

[44] von Tigerstrom, R.G., and Stelmaschuk, S. The use of Tween 20 in a sensitive turbidimetric assay of lipolytic enzymes. Canadian Journal of Microbiology 35(4) (1989): 511-514.

[45] Degrassi, G., Uotila, L., Klima, R., and Venturi, V. Purification and properties of an esterase from the yeast *Saccharomyces cerevisiae* and identification of the encoding gene. Applied and Environmental Microbiology 65(8) (1999): 3470-3472.

[46] Gandolfi, R., Marinelli, F., Lazzarini, A., and Molinari, F. Cell-bound and extracellular carboxylesterases from *Streptomyces*: hydrolytic and synthetic activities. Journal of Applied Microbiology 89(5) (2000): 870-875.

[47] Winkler, U.K., and Stuckmann, M. Glycogen, hyaluronate, and some other polysaccharides greatly enhance the formation of exolipase by *Serratia marcescens.* Journal of Bacteriology 138(3) (1979): 663-670.

[48] Ado, M.A., Abas, F., Mohammed, A.S., and Ghazali, H.M. Anti-and pro-lipase activity of selected medicinal, herbal and aquatic plants, and structure elucidation of an anti-lipase compound. Molecules 18(12) (2013): 14651-14669.

[49] ThaiFDA. Danger of weight loss medicine (in Thai) [Online]. 2012. Available from: http://www.oryor.com/oryor/admin/module/fda_pub_leaflet/file/f_20_1268808996.pdf [2014, December 15]

[50] Malone, M. Orlistat F Hoffmann-La Roche Ltd. The Investigational Drugs Journal 1(2) (1998): 232-241.

[51] Kang, J.G., and Park, C.Y. Anti-obesity drugs: a review about their effects and safety. Diabetes & Metabolism Journal 36(1) (2012): 13-25.

[52] Al-Suwailem, K., Al-Tamimi, A.S., Al-Omar, M.A., and Al-Suhibani, M.S. Safety and mechanism of action of orlistat (Tetrahydrolipstatin) as the first local antiobesity drug. Journal of Applied Sciences Research 2(4) (2006): 205-208.

[53] Seyedan, A., Alshawsh, M.A., Alshagga, M.A., Koosha, S., and Mohamed, Z. Medicinal plants and their inhibitory activities against pancreatic lipase: a review. Evidence-Based Complementary and Alternative Medicine 2015 (2015): 1-13.

[54] Jang, D.S., Lee, G.Y., Kim, J., Lee, Y.M., Kim, J.M., Kim, Y.S., and Kim, J.S. A new pancreatic lipase inhibitor isolated from the roots of *Actinidia arguta.* Archives of Pharmacal Research 31(5) (2008): 666-670.

[55] Li, F., Li, W., Fu, H., Zhang, Q., and Koike, K. Pancreatic lipase-inhibiting triterpenoid saponins from fruits of *Acanthopanax senticosus.* Chemical and Pharmaceutical Bulletin 55(7) (2007): 1087-1089.

[56] Yoshizumi, K., Hirano, K., Ando, H., Hirai, Y., Ida, Y., Tsuji, T., Tanaka, T., Satouchi, K., and Terao, J. Lupane-type saponins from leaves of *Acanthopanax sessiliflorus* and their inhibitory activity on pancreatic lipase. Journal of Agricultural and Food Chemistry 54(2) (2006): 335-341.

[57] Kimura, H., Ogawa, S., Jisaka, M., Kimura, Y., Katsube, T., and Yokota, K. Identification of novel saponins from edible seeds of Japanese horse chestnut (*Aesculus turbinata* Blume) after treatment with wooden ashes and their

nutraceutical activity. Journal of Pharmaceutical and Biomedical Analysis 41(5) (2006): 1657-1665.

[58] Kasabri, V., Al-Hallaq, E.K., Bustanji, Y.K., Abdul-Razzak, K.K., Abaza, I.F., and Afifi, F.U. Antiobesity and antihyperglycaemic effects of *Adiantum capillus-veneris* extracts: *in vitro* and *in vivo* evaluations. Pharmaceutical Biology 55(1) (2017): 164-172.

[59] Kumar, S., and Alagawadi, K.R. Anti-obesity effects of galangin, a pancreatic lipase inhibitor in cafeteria diet fed female rats. Pharmaceutical Biology 51(5) (2013): 607-613.

[60] Shin, J.E., Joo Han, M., and Kim, D.H. 3-Methylethergalangin isolated from *Alpinia officinarum* inhibits pancreatic lipase. Biological and Pharmaceutical Bulletin 26(6) (2003): 854-857.

[61] Worsztynowicz, P., Napierala, M., Bialas, W., Grajek, W., and Olkowicz, M. Pancreatic α-amylase and lipase inhibitory activity of polyphenolic compounds present in the extract of black chokeberry (*Aronia melanocarpa*). Process Biochemistry 49(9) (2014): 1457-1463.

[62] Ahn, J.H., Lui, Q., Chul, L., Ahn, M.J., Yoo, H.S., Hwang, B.Y., and Lee, M.K. A new pancreatic lipase inhibitor from *Broussonetia kanzinoki*. Bioorganic & Medicinal Chemistry Letters 22(8) (2012): 2760-2763.

[63] Yoshikawa, M., Sugimoto, S., Kato, Y., Nakamura, S., Wang, T., Yamashita, C., and Matsuda, H. Acylated oleanane-type triterpene saponins with acceleration of gastrointestinal transit and inhibitory effect on pancreatic lipase from flower buds of chinese tea plant (*Camellia sinensis*). Chemistry & Biodiversity 6(6) (2009): 903-915.

[64] Han, L.K., Takaku, T., Li, J., Kimura, Y., and Okuda, H. Anti-obesity action of oolong tea. International Journal of Obesity and Related Metabolic Disorders 23(1) (1999): 98-105.

[65] Han, L.K., Kimura, Y., Kawashima, M., Takaku, T., Taniyama, T., Hayashi, T., Zheng, Y.N., and Okuda, H. Anti-obesity effects in rodents of dietary teasaponin, a lipase inhibitor. International Journal of Obesity and Related Metabolic Disorders 25(10) (2001): 1459-1464.

[66] Nakai, M., Fukui, Y., Asami, S., Toyoda-Ono, Y., Iwashita, T., Shibata, H., Mitsunaga, T., Hashimoto, F., and Kiso, Y. Inhibitory effects of oolong tea polyphenols on pancreatic lipase *in vitro.* Journal of Agricultural and Food Chemistry 53(11) (2005): 4593-4598.

[67] Habtemariam, S. Antihyperlipidemic components of *Cassia auriculata* aerial parts: identification through *in vitro* studies. Phytotherapy Research 27(1) (2013): 152-155.

[68] Hatano, T., Yamashita, A., Hashimoto, T., Ito, H., Kubo, N., Yoshiyama, M., Shimura, S., Itoh, Y., Okuda, T., and Yoshida, T. Flavan dimers with lipase inhibitory activity from *Cassia nomame.* Phytochemistry 46(5) (1997): 893-900.

[69] Kawaguchi, K., Mizuno, T., Aida, K., and Uchino, K. Hesperidin as an inhibitor of lipases from porcine pancreas and *Pseudomonas.* Bioscience, Biotechnology, and Biochemistry 61(1) (1997): 102-104.

[70] Luyen, N.T., Tram, L.H., Hanh, T.T.H., Binh, P., Dang, N.H., Minh, C.V., and Dat, N.T. Inhibitors of α-glucosidase, α-amylase and lipase from *Chrysanthemum morifolium.* Phytochemistry Letters 6(3) (2013): 322-325.

[71] Jo, Y.H., Kim, S.B., Liu, Q., Lee, J.W., Hwang, B.Y., and Lee, M.K. Benzylated and prenylated flavonoids from the root barks of *Cudrania tricuspidata* with pancreatic lipase inhibitory activity. Bioorganic & Medicinal Chemistry Letters 25(17) (2015): 3455-3457.

[72] Kwon, C.S., Sohn, H.Y., Kim, S.H., Kim, J.H., Son, K.H., Lee, J.S., Lim, J.K., and Kim, J.S. Anti-obesity effect of *Dioscorea nipponica* Makino with lipase-inhibitory activity in rodents. Bioscience, Biotechnology, and Biochemistry 67(7) (2003): 1451-1456.

[73] Eom, S.H., Lee, M.S., Lee, E.W., Kim, Y.M., and Kim, T.H. Pancreatic lipase inhibitory activity of phlorotannins isolated from *Eisenia bicyclis.* Phytotherapy Research 27(1) (2013): 148-151.

[74] Lee, E.M., Lee, S.S., Chung, B.Y., Cho, J.Y., Lee, I.C., Ahn, S.R., Jang, S.J., and Kim, T.H. Pancreatic lipase inhibition by *C*-glycosidic flavones isolated from *Eremochloa ophiuroides.* Molecules 15(11) (2010): 8251-8259.

[75] Habtemariam, S. The anti-obesity potential of sigmoidin A. Pharmaceutical Biology 50(12) (2012): 1519-1522.

[76] Kato, E., Yama, M., Nakagomi, R., Shibata, T., Hosokawa, K., and Kawabata, J. Substrate-like water soluble lipase inhibitors from *Filipendula kamtschatica.* Bioorganic & Medicinal Chemistry Letters 22(20) (2012): 6410-6412.

[77] Pattamadilok, D., Niumsakul, S., Limpeanchob, N., Ingkaninan, K., and Wongsinkongman, P. Chemical constituents and anti-hyperlipidemic activity of *Garcinia cowa* leaves. Journal of Thai Traditional & Alternative Medicine 8 (2010): 152-160.

[78] Lee, I.A., Lee, J.H., Baek, N.I., and Kim, D.H. Antihyperlipidemic effect of crocin isolated from the fructus of *Gardenia jasminoides* and its metabolite Crocetin. Biological and Pharmaceutical Bulletin 28(11) (2005): 2106-2110.

[79] Bustanji, Y., Al-masriI, I.M., Mohammad, M., Hudaib, M., Tawaha, K., Tarazi, H., and Alkhatib, H.S. Pancreatic lipase inhibition activity of trilactone terpenes of *Ginkgo biloba.* Journal of Enzyme Inhibition and Medicinal Chemistry 26(4) (2011): 453-459.

[80] Birari, R.B., Gupta, S., Gopi, C.G., and Bhutani, K.K. Antiobesity and lipid lowering effects of *Glycyrrhiza* chalcones: experimental and computational studies. Phytomedicine 18(8-9) (2011): 795-801.

[81] Won, S.R., Kim, S.K., Kim, Y.M., Lee, P.H., Ryu, J.H., Kim, J.W., and Rhee, H.L. Licochalcone A: a lipase inhibitor from the roots of *Glycyrrhiza uralensis.* Food Research International 40(8) (2007): 1046-1050.

[82] Kato, E., Tokunaga, Y., and Sakan, F. Stilbenoids isolated from the seeds of Melinjo (*Gnetum gnemon* L.) and their biological activity. Journal of Agricultural and Food Chemistry 57(6) (2009): 2544-2549.

[83] Yamada, K., Murata, T., Kobayashi, K., Miyase, T., and Yoshizaki, F. A lipase inhibitor monoterpene and monoterpene glycosides from *Monarda punctata.* Phytochemistry 71(16) (2010): 1884-1891.

[84] Kim, Y.S., Lee, Y.M., Kim, J.H., Kim, H., Kim, J., Jang, D.S., Kim, J.H., and Kim, J.S. Anti-obesity effect of *Morus bombycis* root extract: anti-lipase

activity and lipolytic effect. Journal of Ethnopharmacology 130(3) (2010): 621-624.

[85] Ono, Y., Hattori, E., Fukaya, Y., Imai, S., and Ohizumi, Y. Anti-obesity effect of *Nelumbo nucifera* leaves extract in mice and rats. Journal of Ethnopharmacology 106(2) (2006): 238-244.

[86] Karu, N., Reifen, R., and Kerem, Z. Weight gain reduction in mice fed *Panax ginseng* saponin, a pancreatic lipase inhibitor. Journal of Agricultural and Food Chemistry 55(8) (2007): 2824-2828.

[87] Yoshikawa, M., Shimoda, H., Nishida, N., Takada, M., and Matsuda, H. *Salacia reticulata* and its polyphenolic constituents with lipase inhibitory and lipolytic activities have mild antiobesity effects in rats. The Journal of Nutrition 132(7) (2002): 1819-1824.

[88] Ninomiya, K., Matsuda, H., Shimoda, H., Nishida, N., Kasajima, N., Yoshino, T., Morikawa, T., and Yoshikawa, M. Carnosic acid, a new class of lipid absorption inhibitor from sage. Bioorganic & Medicinal Chemistry Letters 14(8) (2004): 1943-1946.

[89] Morikawa, T., Xie, Y., Asao, Y., Okamoto, M., Yamashita, C., and Muraoka, O. Oleanane-type triterpene oligoglycosides with pancreatic lipase inhibitory activity from the pericarps of *Sapindus rarak.* Phytochemistry 70(9) (2009): 1166-1172.

[90] Lee, H.E., Jin Ah Kim, J.A., and Whang, W.K. Chemical constituents of *Smilax china* L. stems and their inhibitory activities against glycation, aldose reductase, α-glucosidase, and lipase. Molecules 22(3) (2017): 451-468.

[91] Kim, Y.M., Lee, E.W., Eom, S.H., and Kim, T.H. Pancreatic lipase inhibitory stilbenoids from the roots of *Vitis vinifera.* International Journal of Food Sciences and Nutrition 65(1) (2014): 97-100.

[92] Yoshimitsu, H., Nishida, M., and Nohara, T. Steroidal glycosides from the fruits of *Solanum abutiloides.* Phytochemistry 64(8) (2003): 1361-1366.

[93] Silva, T.M.S., Câmara, C.A., Agra, M.F., Carvalho, M.G., Frana, M.T., Brandoline, S.V.P.B., Paschoal, L.S., and Braz-Filho, R. Molluscicidal activity of *Solanum* species from the Northeast of Brazil (Solanaceae) against *Biomphalaria glabrata.* Fitoterapia 77(6) (2006): 449-452.

[94] Alves, C.C.F., Alves, J.M., Silva, T.M.S., Carvalho, M.G., and Neto, J.J. Allelopathic activity by glycoalkaloids from *Solanum crinitum* Lam. Brazilian Journal of Forestry and Environment 10(1) (2003): 93-97.

[95] Hu, K., Dong, A., Sun, Q., and Yao, X. Bioactivity of 247 traditional Chinese medicines against *Pyricularia oryzae.* Pharmaceutical Biology 39(1) (2001): 47-53.

[96] Zakaria, Z.A., Sulaiman, M.R., Morsid, N.A., Aris, A., Zainal, H., Pojan, N.H., and Kumar, G.H. Antinociceptive, anti-inflammatory and antipyretic effects of *Solanum nigrum* aqueous extract in animal models. Methods and Findings in Experimental and Clinical Pharmacology 31(2) (2009): 81-88.

[97] Heo, K.S., and Lim, K.T. Antioxidative effects of glycoprotein isolated from *Solanum nigrum* L. Journal of Medicinal Food 7(3) (2004): 349-357.

[98] Li, J., Li, Q.W., Gao, D.W., Han, Z.S., and Li, K. Antitumor effects of total alkaloids isolated from *Solanum nigrum in vitr*o and *in vivo*. Die Pharmazie 63(7) (2008): 534-538.

[99] Jeong, J.B., Jeong, H.J., Park, J.H., Lee, S.H., Lee, J.R., Lee, H.K., Chung, G.Y., Choi, J.D., and de Lumen, B.O. Cancer-preventive peptide lunasin from *Solanum nigrum* L. inhibits acetylation of core histones H3 and H4 and phosphorylation of retinoblastoma protein (Rb). Journal of Agricultural and Food Chemistry 55(26) (2006): 10707-10713.

[100] Li, J., Li, Q.W., Gao, D.W., Han, Z.S., and Lu, W.Z. Antitumor and immunomodulating effects of polysaccharides isolated from *Solanum nigrum* Linne. Phytotherapy Research 23(11) (2009): 1524-1530.

[101] Piana, M., Camponogara, C., Boligon, A.A., Machado, M.M., de Brum, T.F., Oliveira, S.M., and de Freitas Bauermann, L. Topical anti-inflammatory activity of *Solanum corymbiflorum* leaves. Journal of Ethnopharmacology 179 (2016): 16-21.

[102] Abdel-Sattar, E., Harraz, F.M., Al-Ansari, S.M., El-Mekkawy, S., Ichino, C., Kiyohara, H., Otoguro, K., Omura, S., and Yamada, H. Antiplasmodial and antitrypanosomal activity of plants from the Kingdom of Saudi Arabia. Journal of Natural Medicines 63(2) (2009): 232-239.

[103] Al-Oqail, M., Hassan, W.H.B., Ahmad, M.S., and Al-Rehaily, A.J. Phytochemical and biological studies of *Solanum schimperianum* Hochst. Saudi Pharmaceutical Journal 20(4) (2012): 371-379.

[104] Koduru, S., Jimoh, F.O., Grierson, D.S., and Afolayan, A.J. Antioxidant activity of two steroid alkaloids extracted from *Solanum aculeastrum.* Journal of Pharmacology and Toxicology 2(2) (2007): 160-167.

[105] Qin, X.J., Lunga, P.K., Zhao, Y.L., Liu, Y.P., and Luo, X.D. Chemical constituents of *Solanum coagulans* and their antimicrobial activities. Chinese Journal of Natural Medicines 14(4) (2016): 308-312.

[106] Cornelius, M.T., Carvalho, M.G., Silva, T., Alves, C.C., Siston, A.P., Alves, K.Z., Sant'Anna, C.M., Neto, M.B., Eberlin, M.N., and Braz-Filho, R. Other chemical constituents isolated from *Solanum crinitum* Lam. (Solanaceae). Journal of the Brazilian Chemical Society 21(12) (2010): 2211-2219.

[107] Tiossi, R.F., Miranda, M.A., de Sousa, J.P., Praça, F.S., Bentley, M.V., McChesney, J.D., and Bastos, J.K. A validated reverse phase HPLC analytical method for quantitation of glycoalkaloids in *Solanum lycocarpum* and its extracts. Journal of Analytical Methods in Chemistry 2012 (2012): 1-8.

[108] Huang, H.C., Syu, K.Y., and Lin, J.K. Chemical composition of *Solanum nigrum* Linn extract and induction of autophagy by leaf water extract and its major flavonoids in AU565 breast cancer cells. Journal of Agricultural and Food Chemistry 58(15) (2010): 8699-8708.

[109] Cai, X.F., Chin, Y.W., Oh, S.R., Kwon, O.K., Ahn, K.S., and Le, H.K. Anti-inflammatory constituents from *Solanum nigrum.* Bulletin of the Korean Chemical Society 31(1) (2010): 199-201.

[110] Keawsa-ard, S., Natakankitkul, S., Liawruangrath, S., Teerawutgulrag, A., Trisuwan, K., Charoenying, P., Pyne, S.G., and Liawruangrath, B. Anticancer and antibacterial activities of the isolated compounds from *Solanum spirale* Roxb. leaves. Chiang Mai Journal of Science 39(3) (2012): 445-454.

[111] Chanmee, W., Chaicharoenpong, C., and Petsom, A. Lipase inhibitor from fruits of *Solanum stramonifolium* Jacq. Food and Nutrition Sciences 4 (2013): 554-558.

[112] Lu, Y.Y., Luo, J.G., and Kong, L. Chemical constituents from *Solanum torvum.* Chinese Journal of Natural Medicines 9(1) (2011): 30-32.
[113] Sahu, J., Rathi, B., Koul, S., and Khosa, R. *Solanum trilobatum* (Solanaceae) – an overview. Journal of Natural Remedies 13(2) (2013): 76-80.
[114] Reddy, N.M., and Reddy N, R. *Solanum xanthocarpum* chemical constituents and medicinal properties: a review. Scholars Academic Journal of Pharmacy 3(2) (2014): 146-149.
[115] Homhual, S. *Solanum aculeatissimum* Jacq. [Online]. 2010. Available from: http://www.phargarden.com/main.php?action=viewpage&pid=259 [2014, December 5]
[116] Acharya, E., and Pokhrel, B. Ethano-medicinal plants used by bantar of bhaudaha, morang, Nepal. Our Nature 4(1) (2006): 96-103.
[117] Pl@ntUse. *Solanum aculeatissimum* (PROTA) [Online]. 2015. Available from: http://uses.plantnetproject.org/e/index.php?title=Solanum_aculeatissimum_(PROTA)&oldid=173983 [2017, March 15]
[118] Nabeta, K. XXIII *Solanum aculeatissimum* Jacq.:*in vitro* culture and production of secondary metabolites. in Bajaj, Y.P.S. (ed.)Medicinal and Aromatic Plant V, pp. 329-341. New York: Springer, Berlin Heidelberge, 1993.
[119] Saijo, R., Fuke, C., Murakami, K., Nohara, T., and Tomimastu, T. Two steroidal glycoside, aculeatiside A and B, from *Solanum aculeatissimum.* Phytochemistry 22(3) (1983): 733-736.
[120] Kadkade, P.G., Recinos, J.A., and Madrid, T.R. Studies on the distribution of glycoalkaloids in *Solanum aculeatissimum.* Planta Medica 37(1) (1979): 70-72.
[121] Pereira, A.C., Carvalho, H.W.P., Prado, N.R.T., Oliveira, D.F., Figueiredo, H.C.P., Carvalho, D.A., and Cavalheiro, A.J. Identification of a substance responsible by antibacterial activity of *Solanum aculeatissimum* Jacq. Annals of the Brazilian Academy of Sciences 80(3) (2008): 427-432.
[122] Krishnan, V.G.M., and Murugan, K. Purification, characterization and kinetics of protease inhibitor from fruits of *Solanum aculeatissimum* Jacq. Food Science and Human Wellness 4(3) (2015): 97-107.
[123] Wetwitayaklung, P., and Phaechamud, T. Antioxidant activities and phenolic content of *Solamun* and *Capsicum* sp. Research Journal of Pharmaceutical, Biological and Chemical Sciences 2(2) (2011): 146-154.
[124] Maurya, A., Gupta, S., Negi, S., and Srivastava, S.K. pH-Zone-refining centrifugal partition chromatography for preparative isolation and purification of steroidal glycoalkaloids from *Solanum Xanthocarpum.* Journal of Separation Science 32(18) (2009): 3126-3132.
[125] Meenu Krishnan, V.G., Manoj, G.S., and Murugan, K. Antihaemolytic, anti-lipid peroxidative potential by purified protease inhibitors from the fruits of *Solanum aculeatissimum* Jacq. in human erythrocytes against hydrogen peroxide. Journal of Pharmacognosy and Phytochemistry 4(3) (2015): 203-208.

[126] Putalun, W., Tanaka, H., Muranaka, T., and Shoyama, Y. Determination of aculeatisides based on immunoassay using a polyclonal antibody against aculeatiside A. The Analyst 127(10) (2002): 1328-1332.
[127] Kohara, A., Nakajima, C., Hashimoto, K., Ikenaga, T., Tanaka, H., Shoyama, Y., Yoshida, S., and Muranaka, T. A novel glucosyltransferase involved in steroid saponin biosynthesis in *Solanum aculeatissimum.* Plant Molecular Biology 57(2) (2005): 225-239.
[128] Gonçalves da Silva, R.M., Merle, P.J.R., Martins, G.R., Mecina, G.F., Marinho dos Santos, V.H., Lima, G.P.P., Santos, P.C., Toledo de Mello Peixoto, E.C., and Pereira da Silva, L. Phytotoxicity of *Solanum aculeatissimum* Jacq. leaves extract. African Journal of Agricultural Research 10(12) (2015): 1442-1449.
[129] Slanc, P., Doljak, B., Mlinaric, A., and Strukelj, B. Screening of wood damaging fungi and macrofungi for inhibitors of pancreatic lipase. Phytotherapy Research 18(9) (2004): 758-762.
[130] Agoramoorthy, G., Chandrasekaran, M., Venkatesalu, V., and Hsu, M. Antibacterial and antifungal activities of fatty acid methyl esters of the blind-your-eye mangrove from India. Brazilian Journal of Microbiology 38(4) (2007): 739-742.
[131] Zielinska, A., and Nowak, I. Fatty acids in vegetable oils and their importance in cosmetic industry. CHEMIK 68(2) (2014): 103-110.
[132] Muthezhilan, R., Yogananth, N., Priyanka, and Hussain, A. Fatty acid composition and antimicrobial activity of *Solanum torvum* SW. Journal of Modern Biotechnology 1(2) (2012): 75-78.
[133] Berges, R.R., Windeler, J., Trampisch, H.J., and Senge, T. Randomised, placebo-controlled, double-blind clinical trial of beta-sitosterol in patients with benign prostatic hyperplasia. beta-sitosterol study group. Lancet 345(8964) (1995): 1529-1532.
[134] Ogbe, R.J., Ochalefu, D.O., Mafulul, S.G., and Olaniru, O.B. A review on dietary phytosterols: their occurrence, metabolism and health benefits. Asian Journal of Plant Science and Research 5(4) (2015): 10-21.
[135] Rawal, G., Yadav, S., and Nagayach, S. Phytosterols and the health. Medico Research Chronicles 2(3) (2015): 441-444.
[136] Vuorio, A., and Gylling, H. Benefits of dietary phytosterols. Clinical Lipidology 7(4) (2012): 375-378.
[137] Panda, S., Jafri, M., Kar, A., and Meheta, B.K. Thyroid inhibitory, antiperoxidative and hypoglycemic effects of stigmasterol isolated from *Butea monosperma.* Fitoterapia 80(2) (2009): 123-126.
[138] Patel, K., Singh, R.B., and Patel, D.K. Medicinal significance, pharmacological activities, and analytical aspects of solasodine: a concise report of current scientific literature. Journal of Acute Disease 2(2) (2013): 92-98.
[139] Koduru, S., Grierson, D.S., van de Venter, M., and Afolayan, A.J. Anticancer activity of steroid alkaloids isolated from *Solanum aculeastrum.* Pharmaceutical Biology 45(8) (2007): 613-618.

[140] Wanyonyi, A.W., Tarus, P.K., and Chhabra, S.C. A novel glycosidic steroidal alkaloid from *Solanum aculeastrum.* Bulletin of the Chemical Society of Ethiopia 17(1) (2003): 61-66.

[141] Mahato, S.B., Sahu, N.P., Ganguly, A.N., Kasai, R., and Tanaka, O. Steroidal alkaloids from *Solanum khasianum*: application of ^{13}C NMR spectroscopy to their structural elucidation. Phytochemistry 19(9) (1980): 2017-2020.

[142] Puri, R., Wong, T.C., and Puri, R.K. ^{1}H- and ^{13}C-NMR assigments and structural determination of a novel glycoalkaloid from *Solanum platanifolium.* Journal of Natural Products 57(5) (1994): 587-596.

[143] Silva, T.M.S., Camara, C.A., Freire, K.R.L., Silva, T.G., Agra, M.F., and Bhattacharyya, J. Steroidal glycoalkaloids and molluscicidal activity of *Solanum asperum* Rich. fruits. Journal of the Brazilian Chemical Society 19(5) (2008): 1048-1052.

[144] Jayakumar, K., and Murugan, K. *Solanum* alkaloids and their pharmaceutical roles: a review. Journal of Analytical & Pharmaceutical Research 3(6) (2016): 1-14.

[145] Esteves-Souza, A., Silva, T.M.S., Alves, C.C.F., Carvalho, M.G., Braz-Filho, R., and Echevarria, A. Cytotoxic activities against ehrlich carcinoma and human K562 leukaemia of alkaloids and flavonoid from two *Solanum* species. Journal of the Brazilian Chemical Society 13(6) (2002): 838-842.

[146] Devkota, H., Joshi, K., Ozasa, T., Fukunaga, S., Yoshida, N., and Yahara, S. Steroidal glycosides from the fruits, aerial parts and tubers of potato (*Solanum tuberosum*). Journal of Pharmacognosy and Phytochemistry 3(6) (2015): 252-255.

[147] Parmar, S., Gangwal, A., and Navin, S. *Solanum xanthocarpum* (yellow berried night shade): a review. Der Pharmacia Lettre 2(4) (2010): 373-383.

[148] Singh, S., Gupta, J., and Kanwar, S.S. Antilipase, antiproliferatic and antiradical activities of methanolic extracts of *Vinca major*. Journal of Pharmacognosy and Phytochemistry 3(3) (2014): 54-63.

[149] Maqsood, M., Ahmed, D., Atique, I., and Malik, W. Lipase inhibitory activity of *Lagenaria siceraria* fruit as a strategy to treat obesity. Asian Pacific Journal of Tropical Medicine 10(3) (2017): 305-310.

[150] Likitdacharote, P., and Chaicharoenpong, C. Chemical constituents and lipase inhibitory activity of *Solanum torvum* fruit. Proceeding of the 6th Burapha University International Conference 2015, pp. ST-P-049. Chonburi, Thailand, 2015.

[151] Cantwell, M. A review of important facts about potato glycoalkaloids. Perishables Handling Newsletter 87 (1996): 26-27.

APPENDIX

Quantitative calculation for reagents of anti-lipase activity assay

1. Preparation of *p*-NPP solution (6.66 mM)

0.3775 g of *p*-Nitrophenylpalmitate (*p*-NPP) was dissolved in 100 mL of acetonitrile to give a stock sultution with a concentration of 10 mM of *p*-NPP solution. Then, ethanol was adjusted to final volume of 10 mL in 6.66 µL of stock *p*-NPP solution, resulting in 6.66 mM of *p*-NPP solution as substrate. The solution was kept at 20 ^{o}C.

2. Preparation of Tris-HCL buffer (pH 8.5)

4.4 g of Tris-HCL was dissolved in DI water. 1 M of HCL solution was added to adjust pH equal to 8.50. Then the soluble was adjusted to obtain final volume of 500 mL of 0.0726 M Tris-HCL buffer (pH 8.5) by DI water.

3. The lipase enzyme

5 mg of Porcine pancreatic lipase was dissolved in 1 mL of Tris-HCL buffer (pH 8.5) to a final concentration of 5 mg/mL.

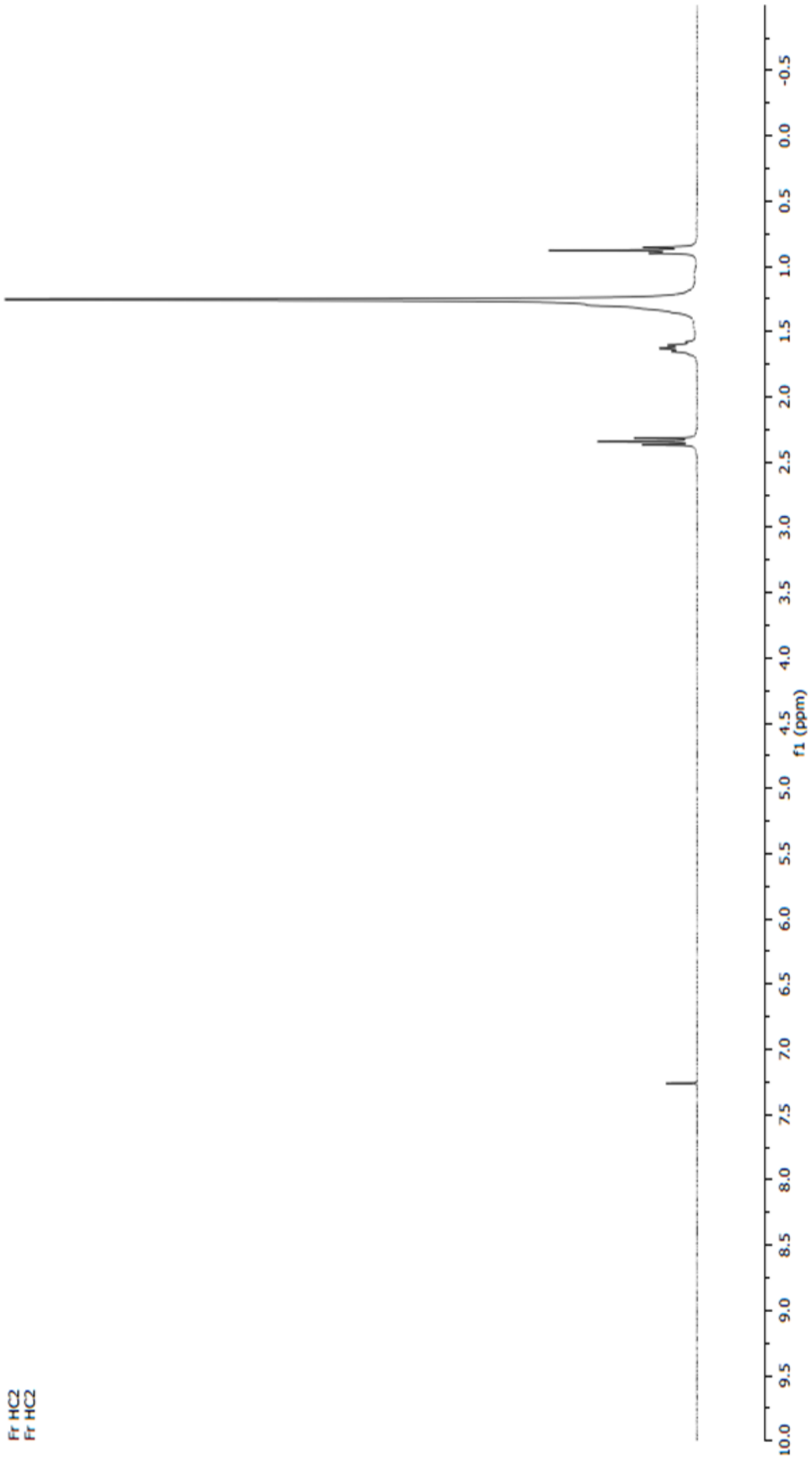

Figure 28 ^{1}H NMR spectrum ($CDCl_3$) of compound **209**

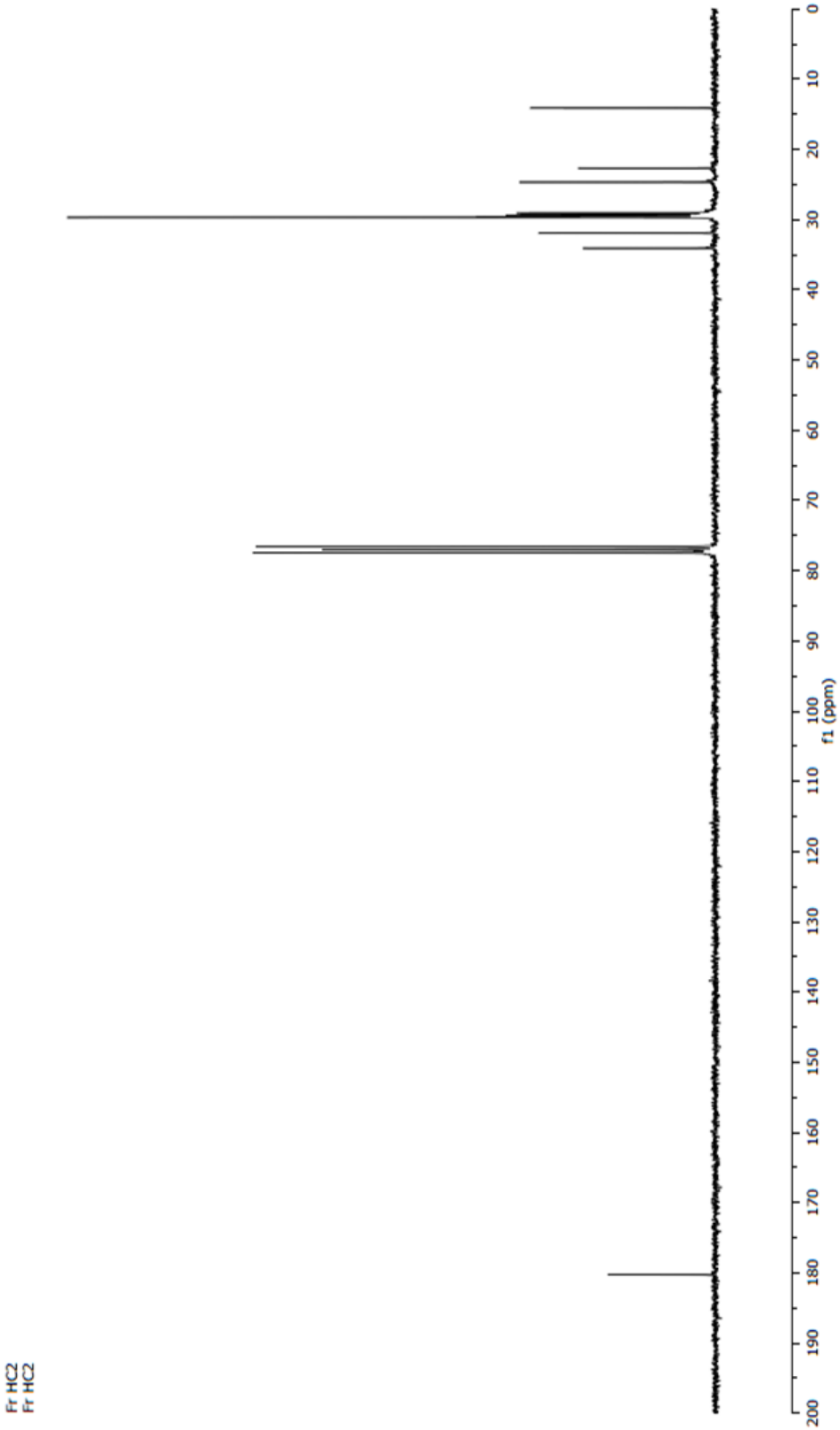

Figure 29 ^{13}C NMR spectrum ($CDCl_3$) of compound **209**

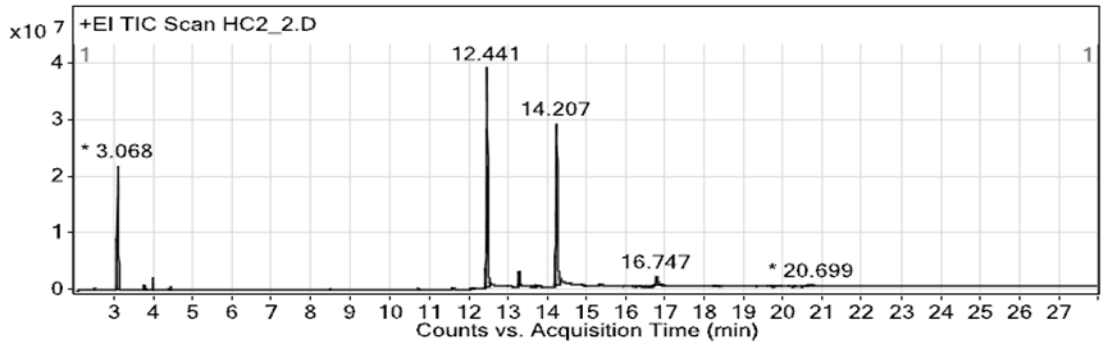

Figure 30 GC-chromatogram of compound **209**

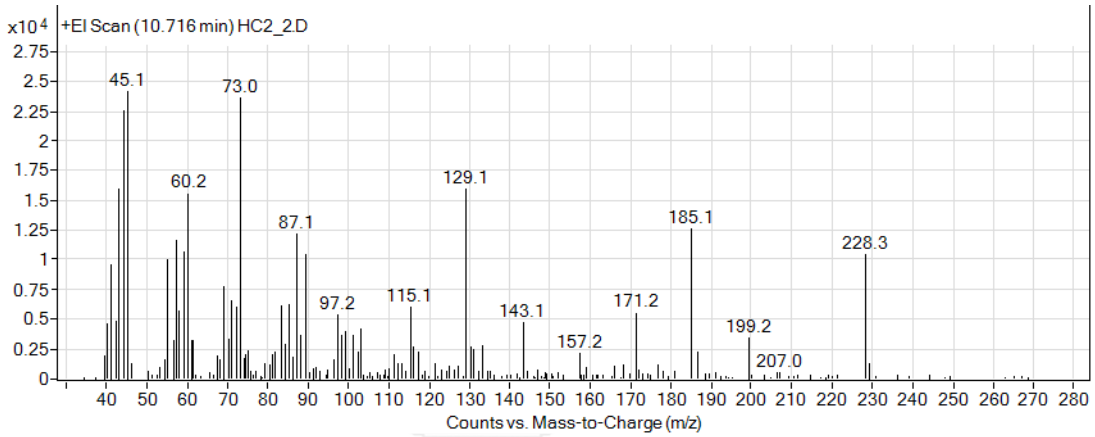

Figure 31 Mass spectrum of component at retention time 10.716 min of compound **209**

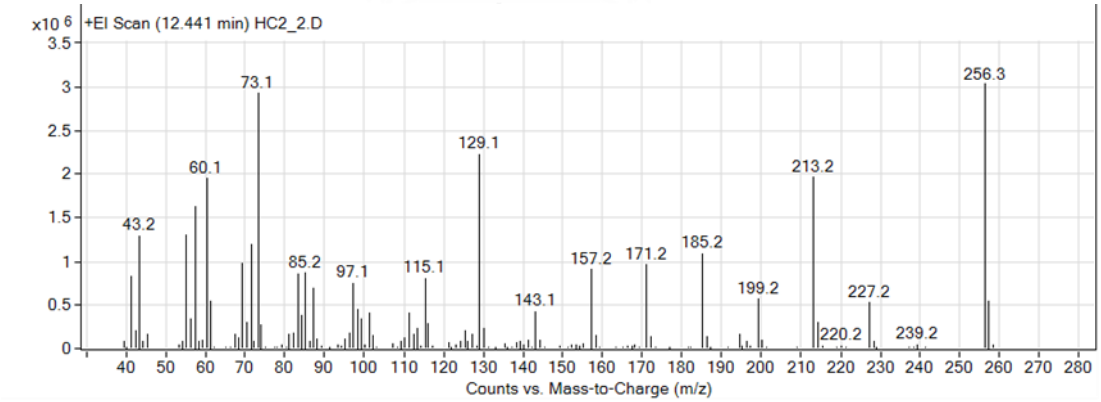

Figure 32 Mass spectrum of component at retention time 12.441 min of compound **209**

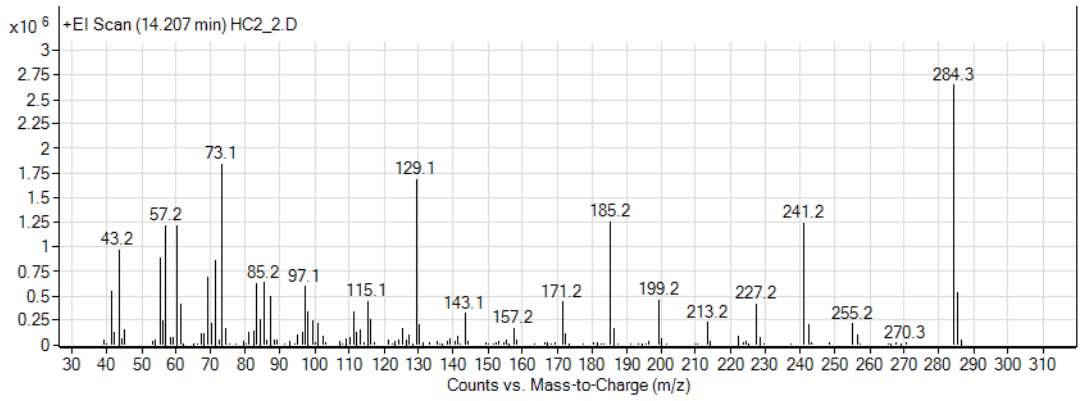

Figure 33 Mass spectrum of component at retention time 14.207 min of compound **209**

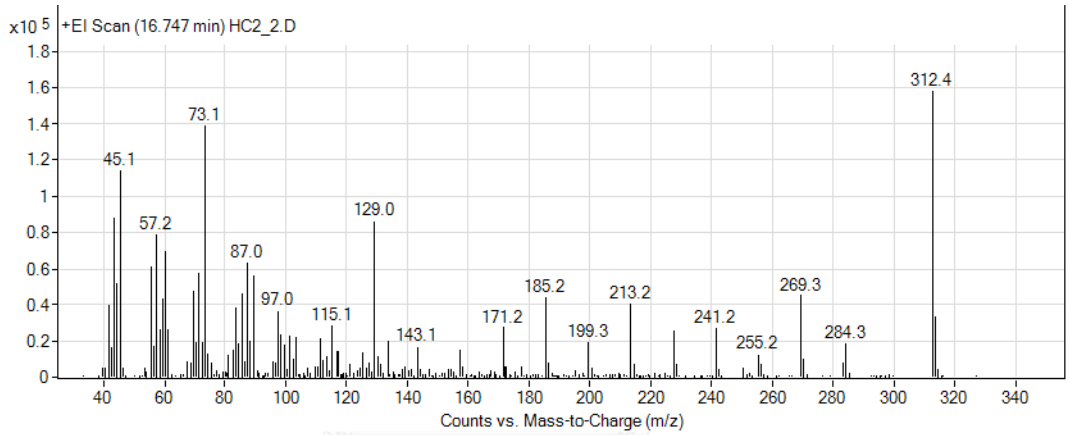

Figure 34 Mass spectrum of component at retention time 16.747 min of compound **209**

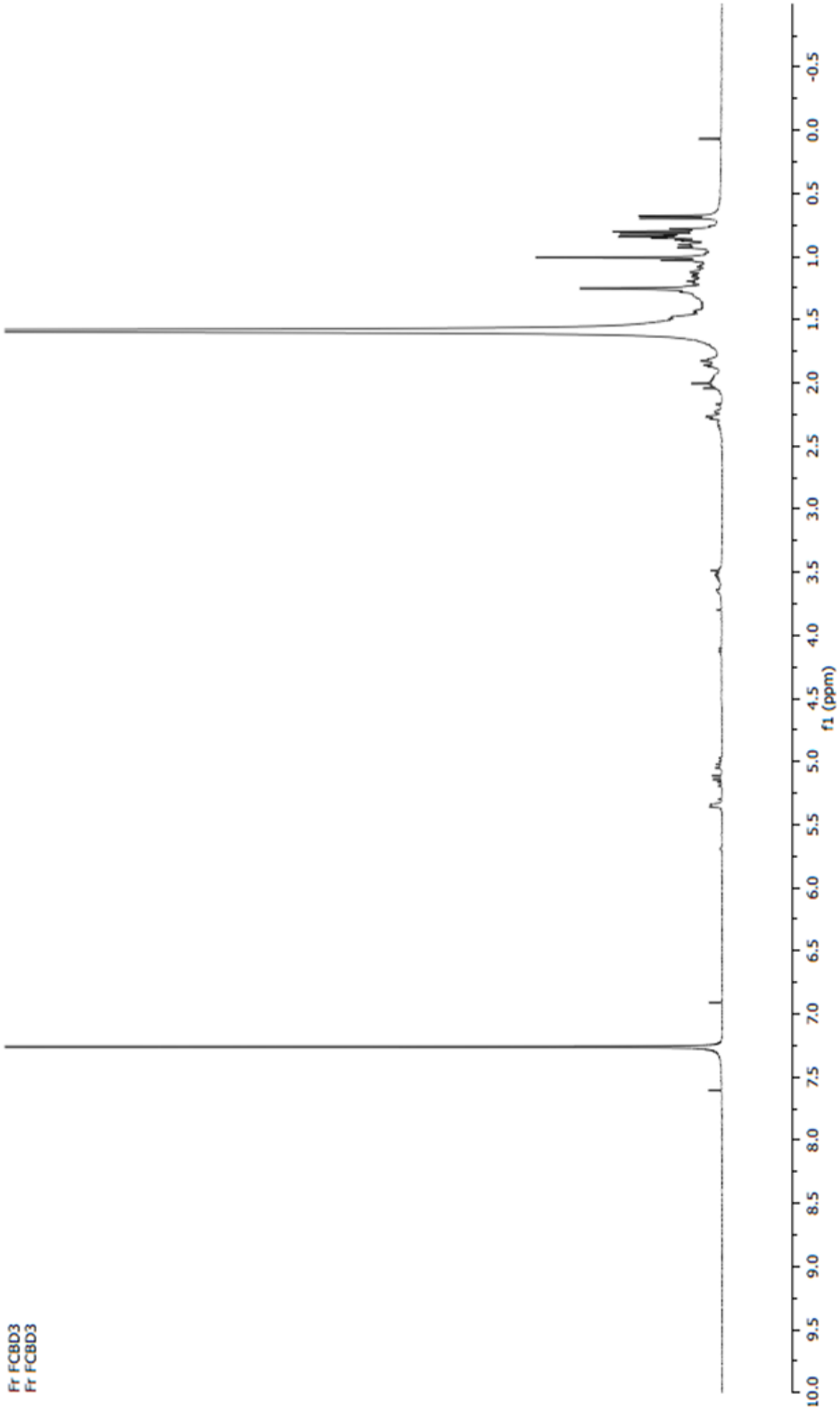

Figure 35 ^{1}H NMR spectrum ($CDCl_3$) of compound **210**

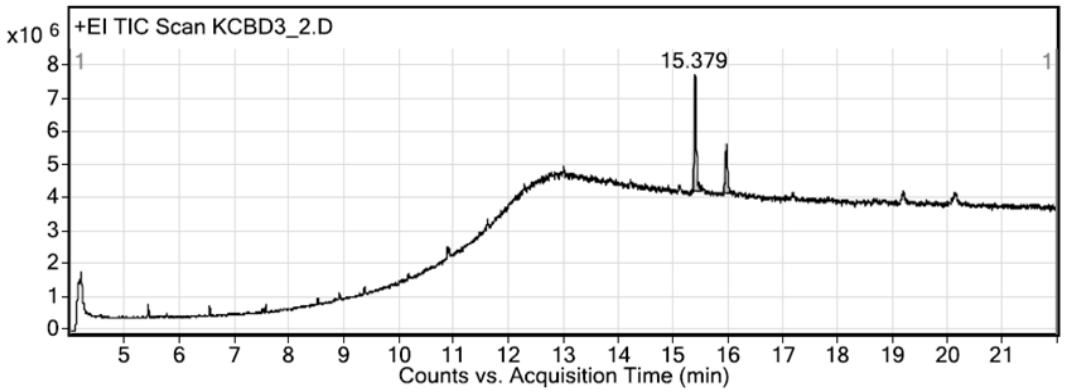

Figure 36 GC-chromatogram of compound **210**

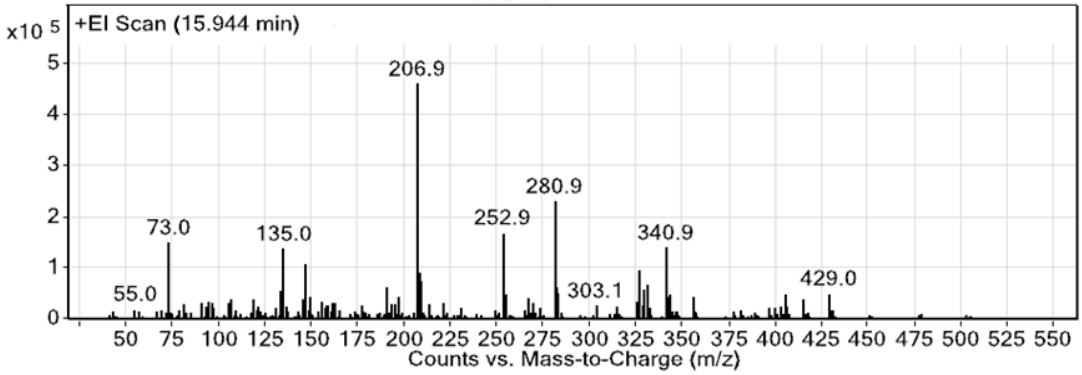

Figure 37 Mass spectrum of component at retention time 15.379 min of compound **210**

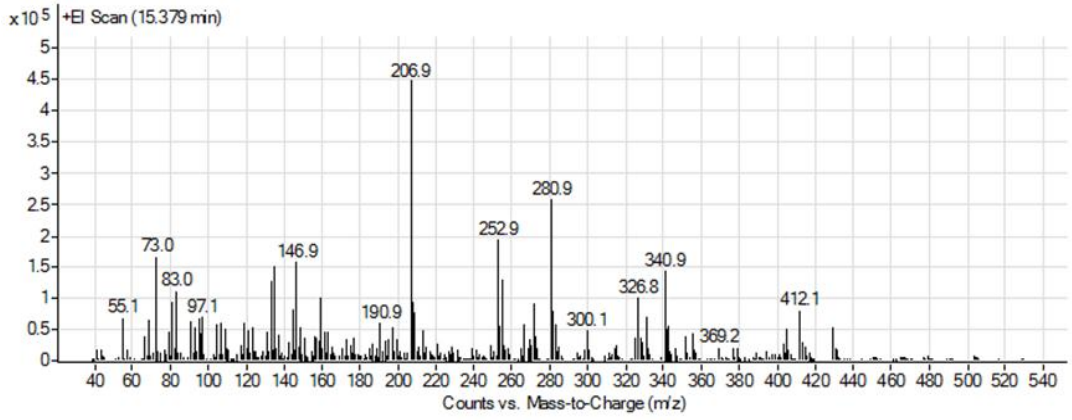

Figure 38 Mass spectrum of component at retention time 15.944 min of compound **210**

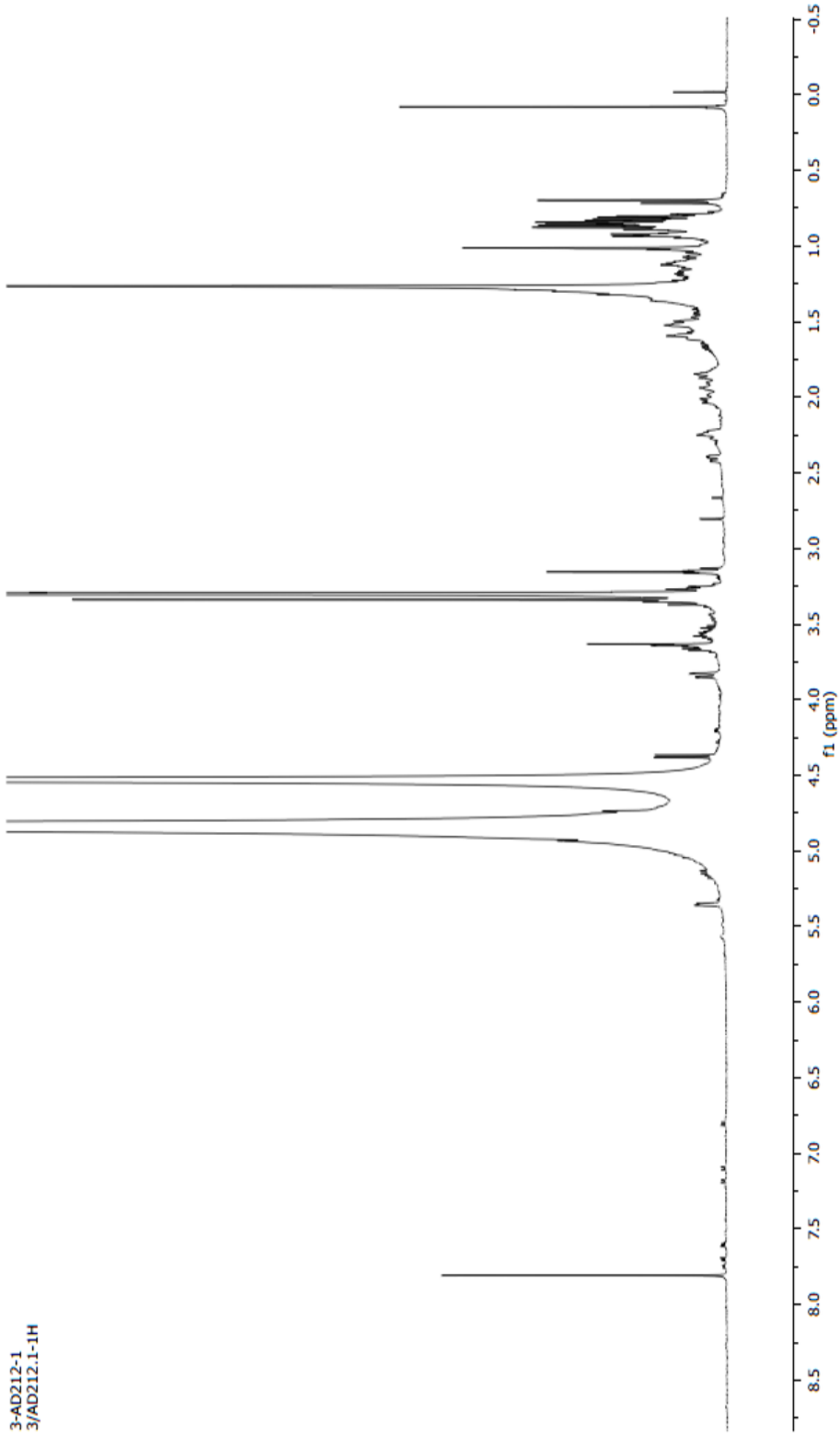

Figure 39 ^{1}H NMR spectrum (CD_3OD:$CDCl_3$) of compound **211**

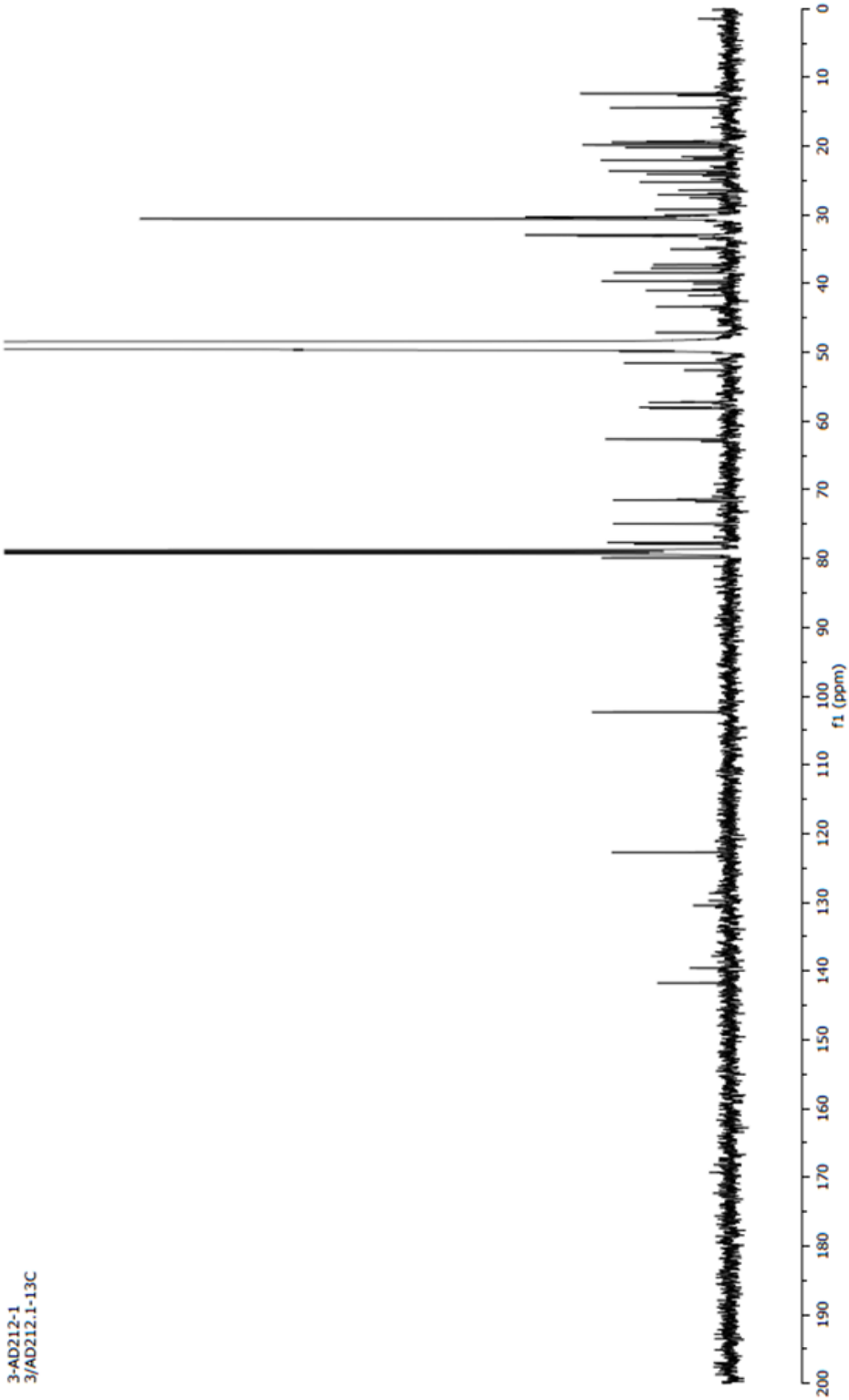

Figure 40 ^{13}C NMR spectrum (CD_3OD:$CDCl_3$) of compound **211**

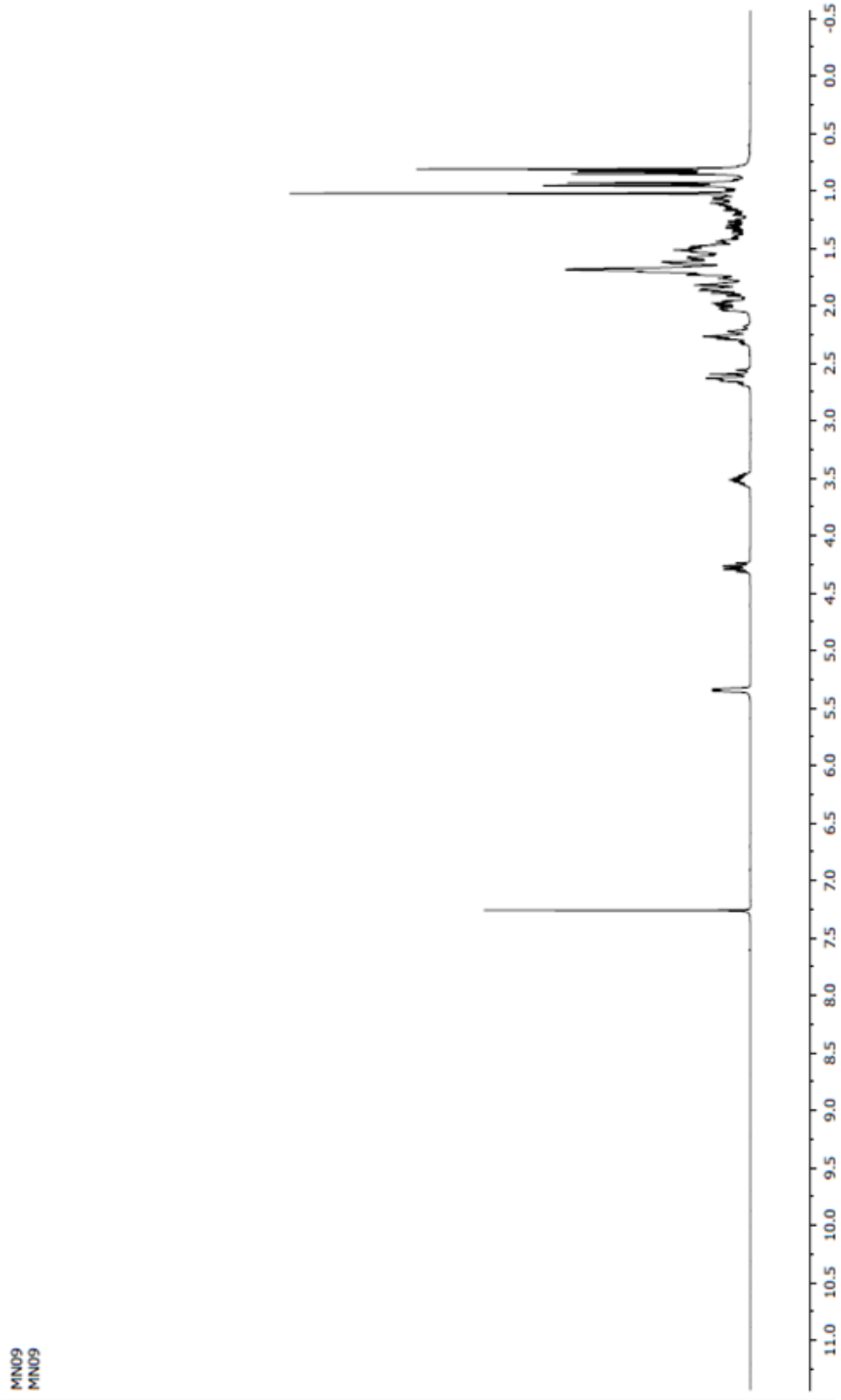

Figure 41 ^{1}H NMR spectrum ($CDCl_3$) of compound **212**

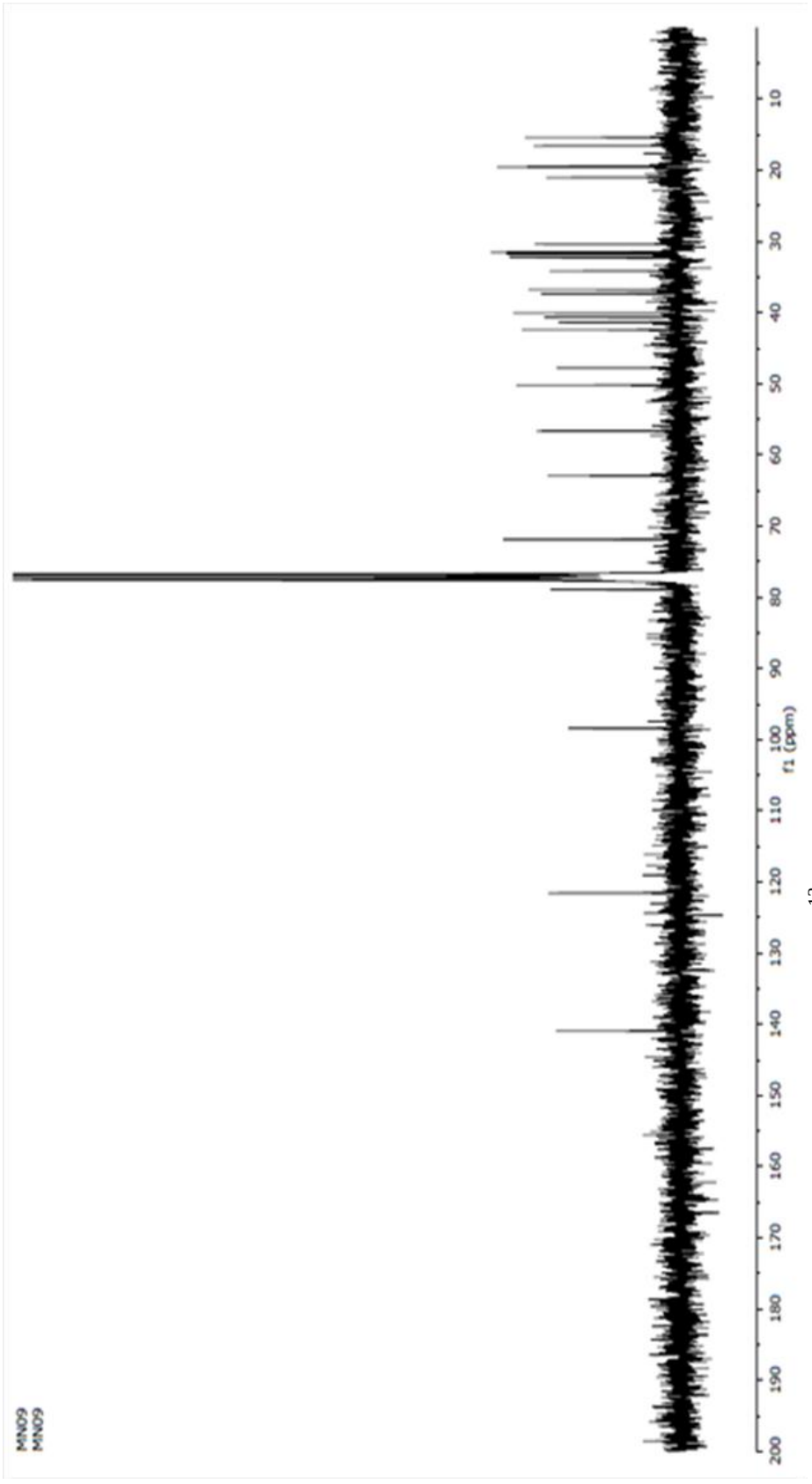

Figure 42 ^{13}C NMR spectrum ($CDCl_3$) of compound **212**

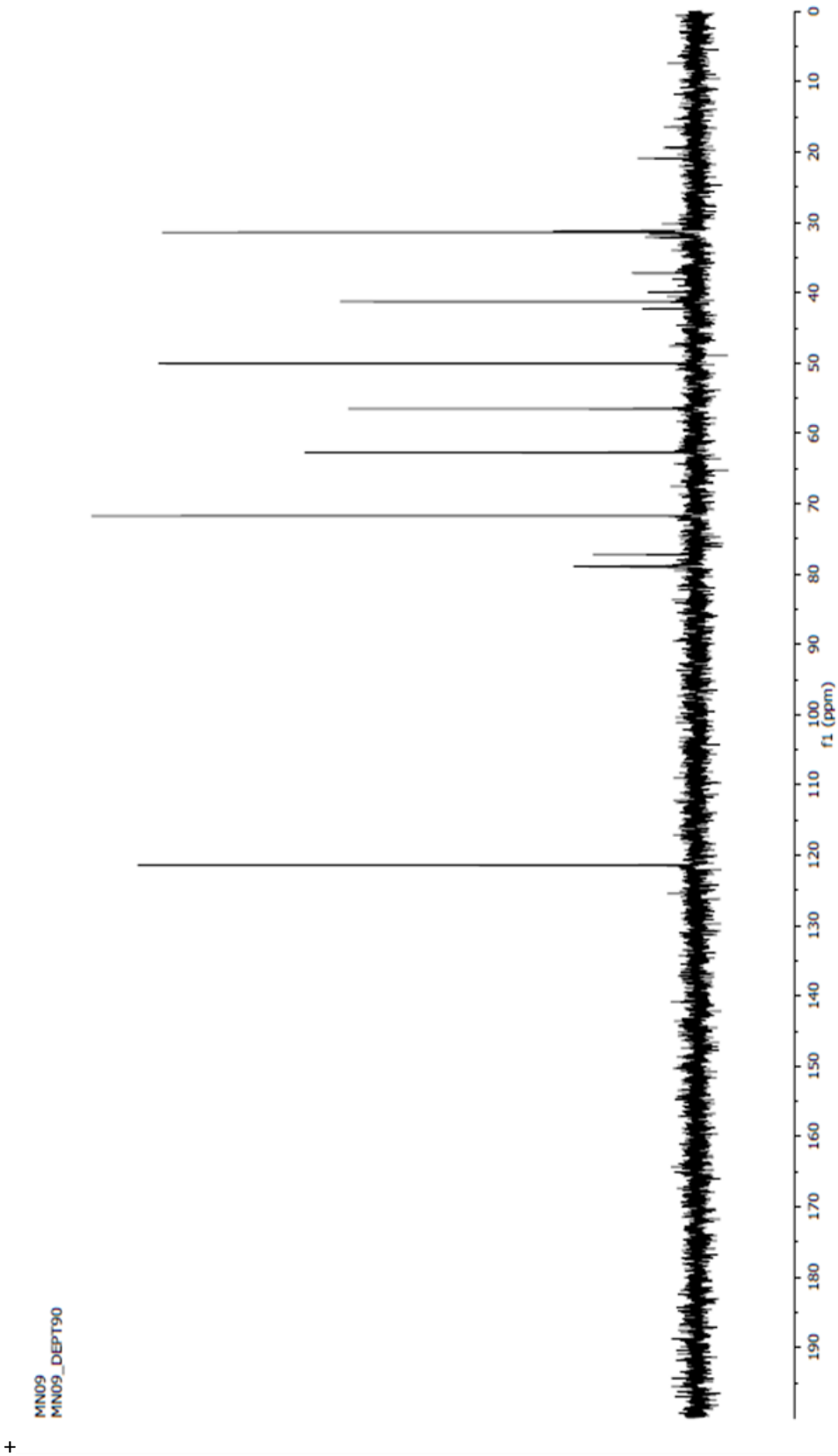

Figure 43 DEPT 90 spectrum ($CDCl_3$) of compound **212**

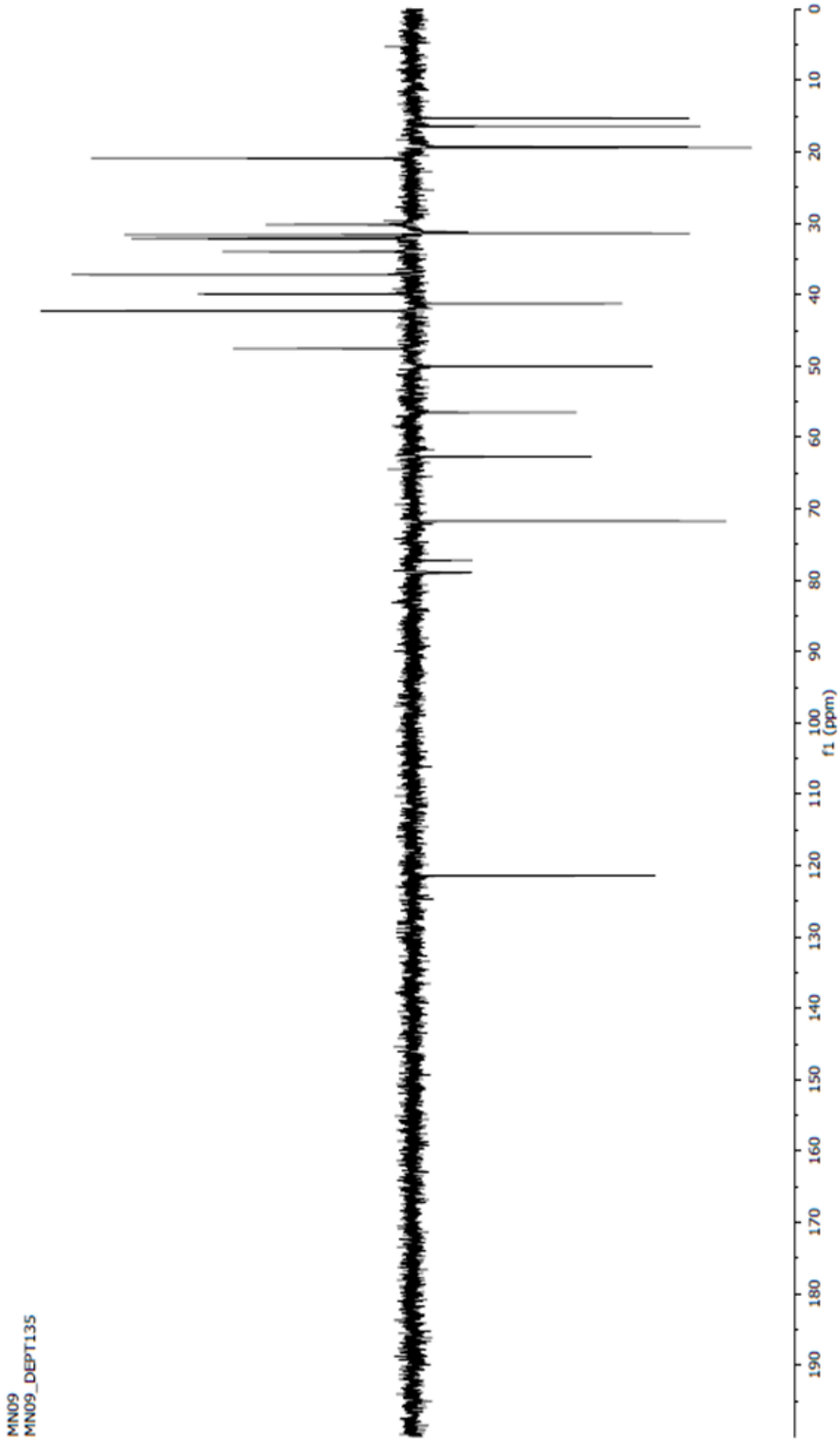

Figure 44 DEPT 135 spectrum ($CDCl_3$) of compound **212**

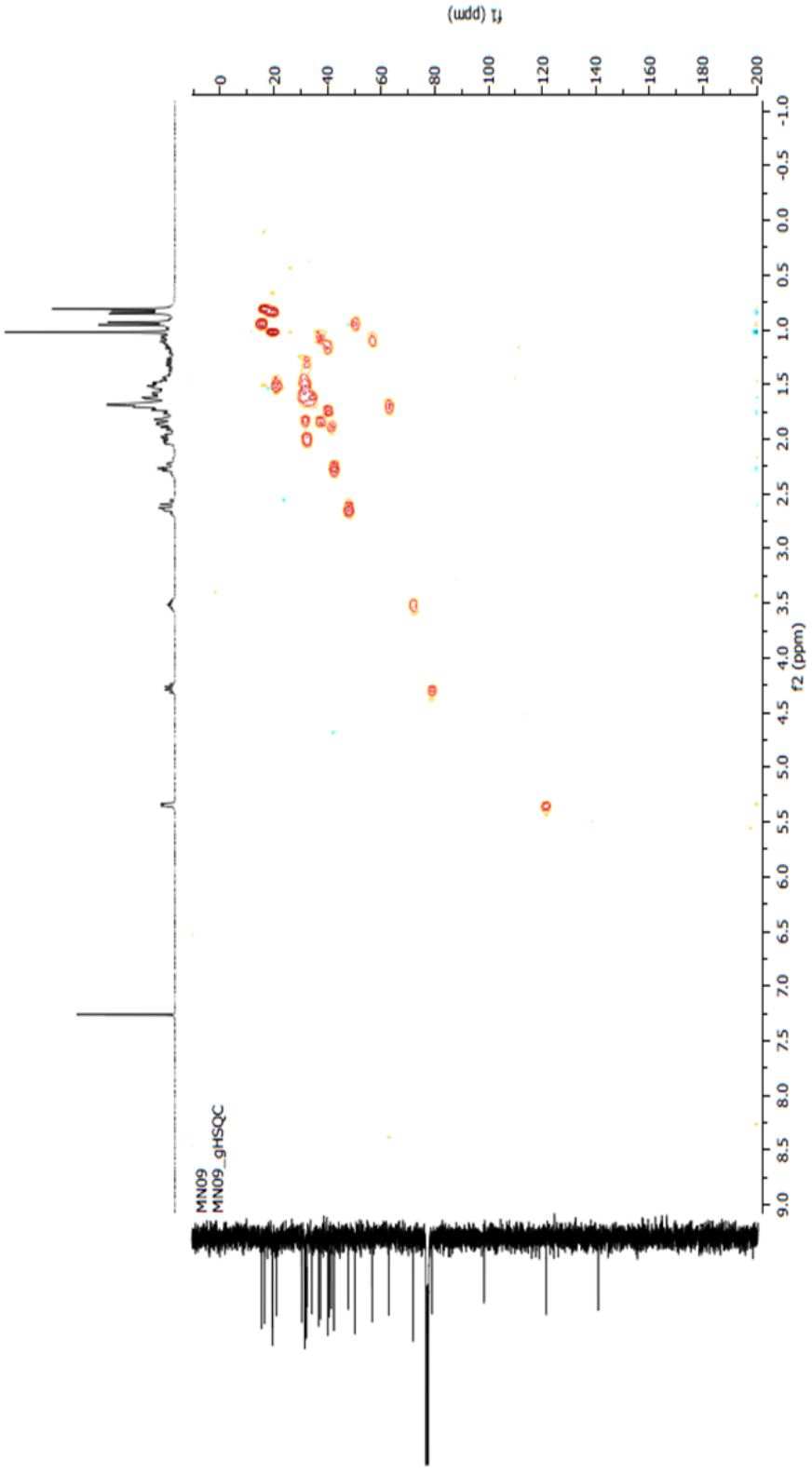

Figure 45 HSQC spectrum ($CDCl_3$) of compound **212**

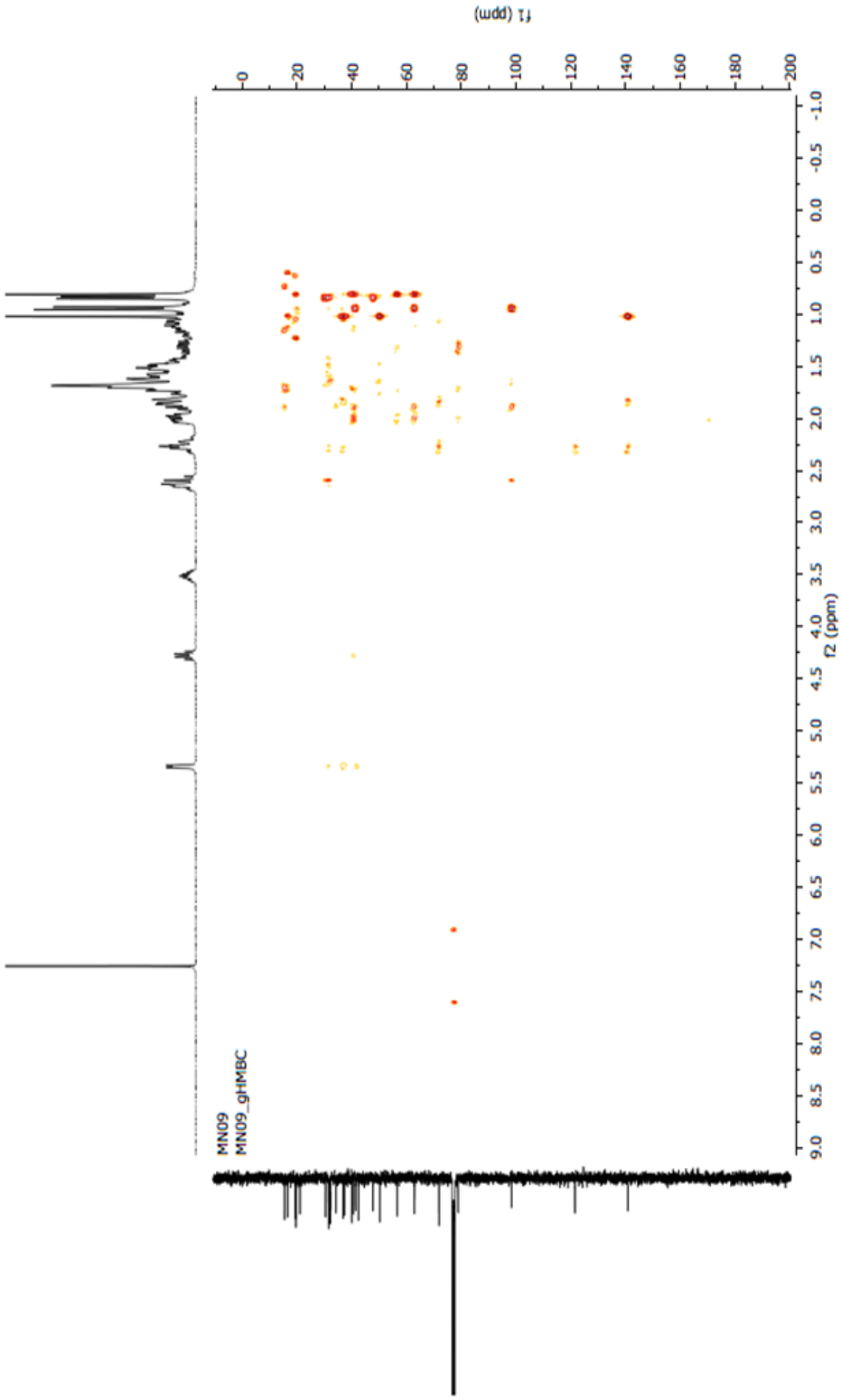

Figure 46 HMBC spectrum ($CDCl_3$) of compound **212**

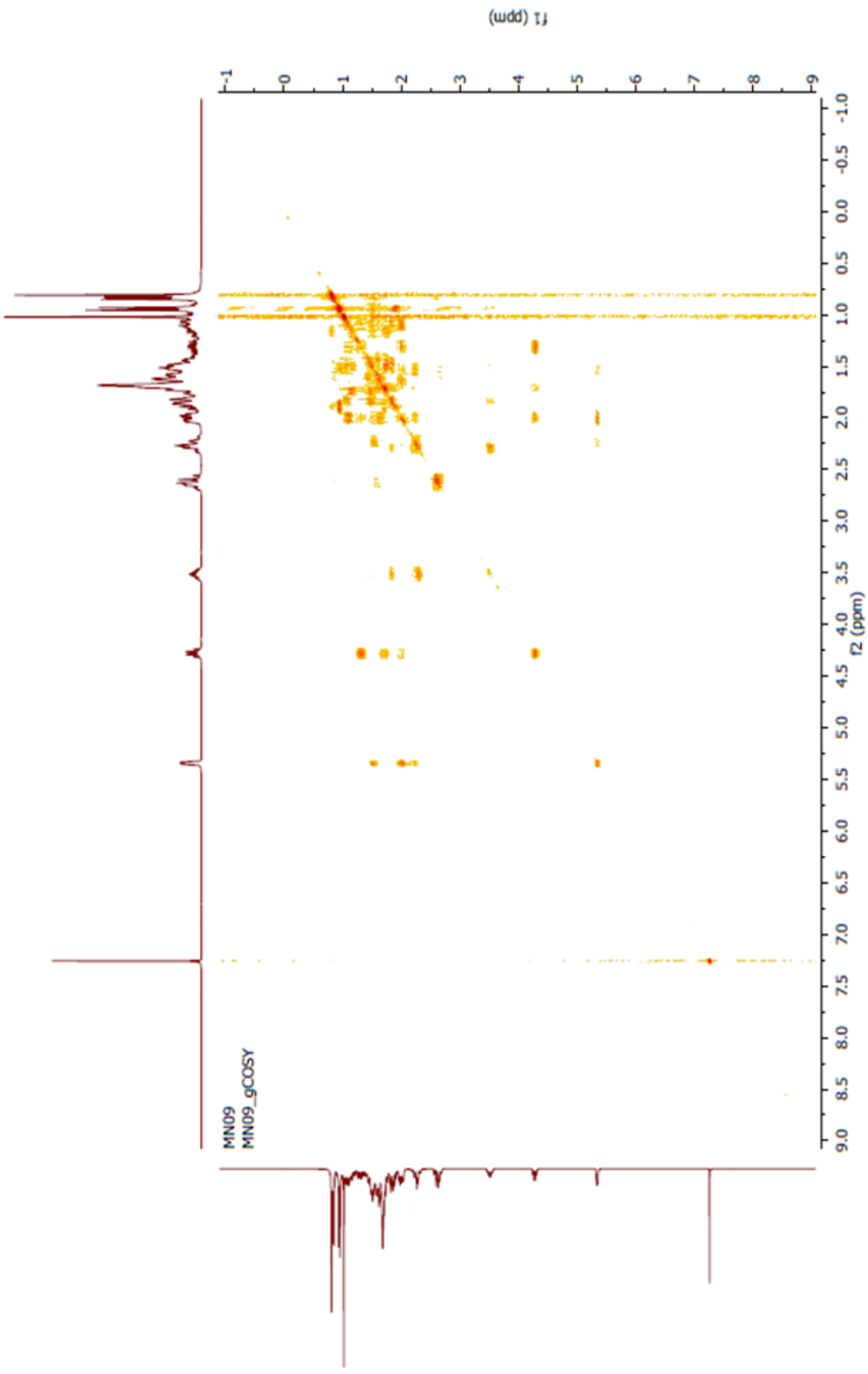

Figure 47 COSY spectrum ($CDCl_3$) of compound **212**

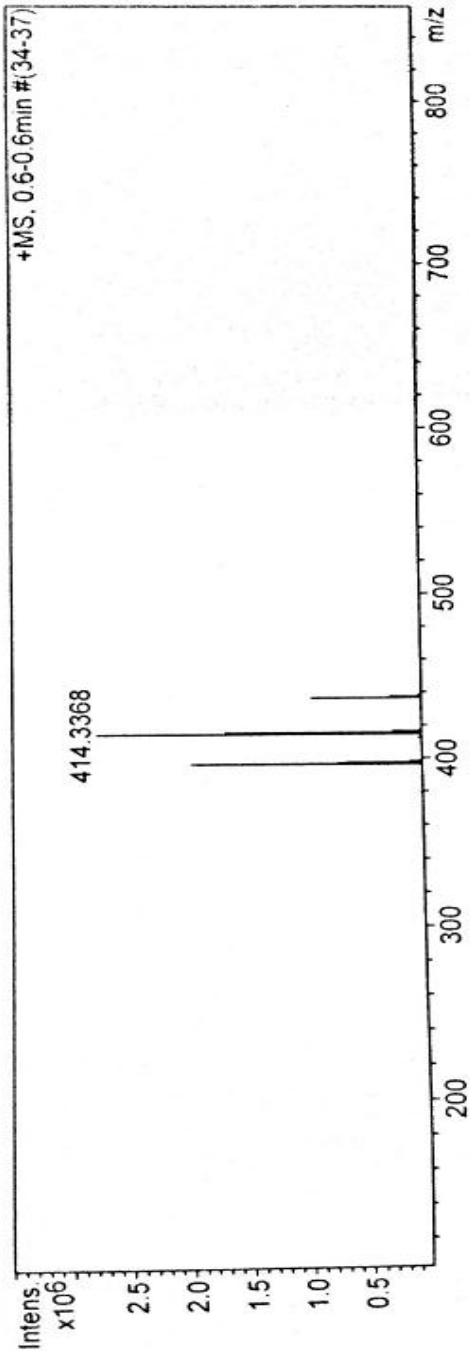

Figure 48 High resolution mass spectrum of compound **212**

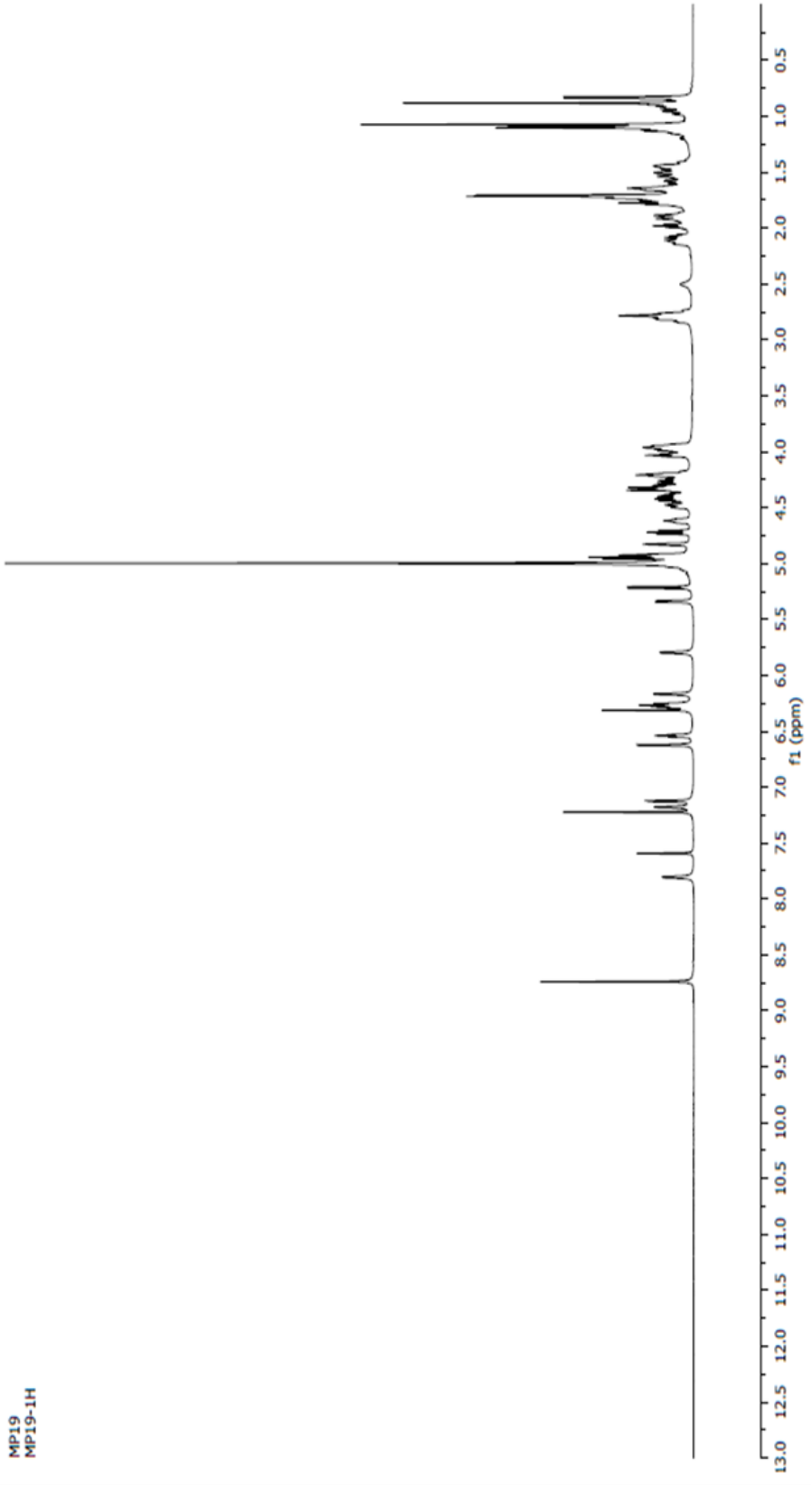

Figure 49 ^{1}H spectrum (pyridine-d_5) of compound **213**

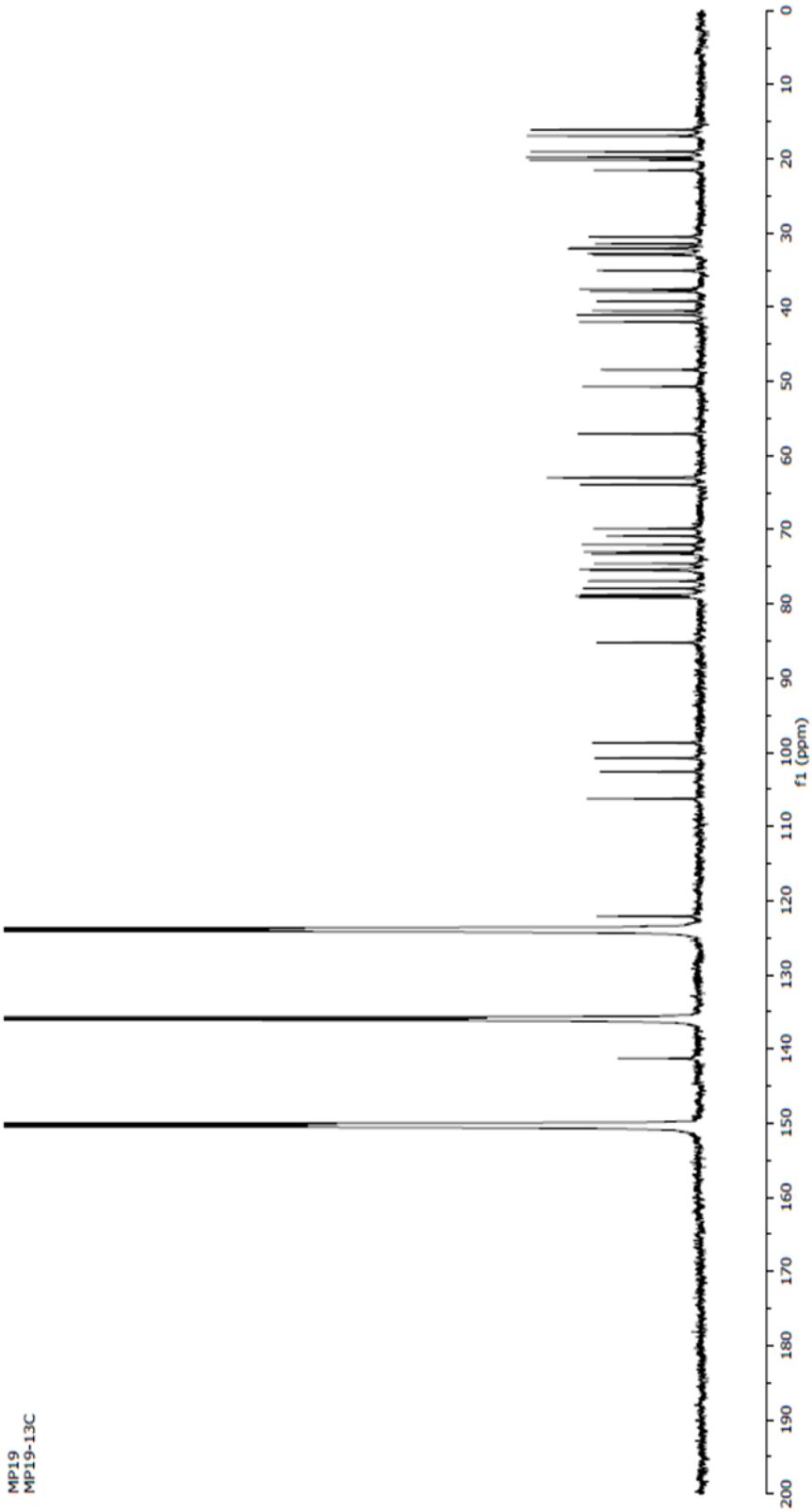

Figure 50 ^{13}C NMR spectrum (pyridine-d_5) of compound **213**

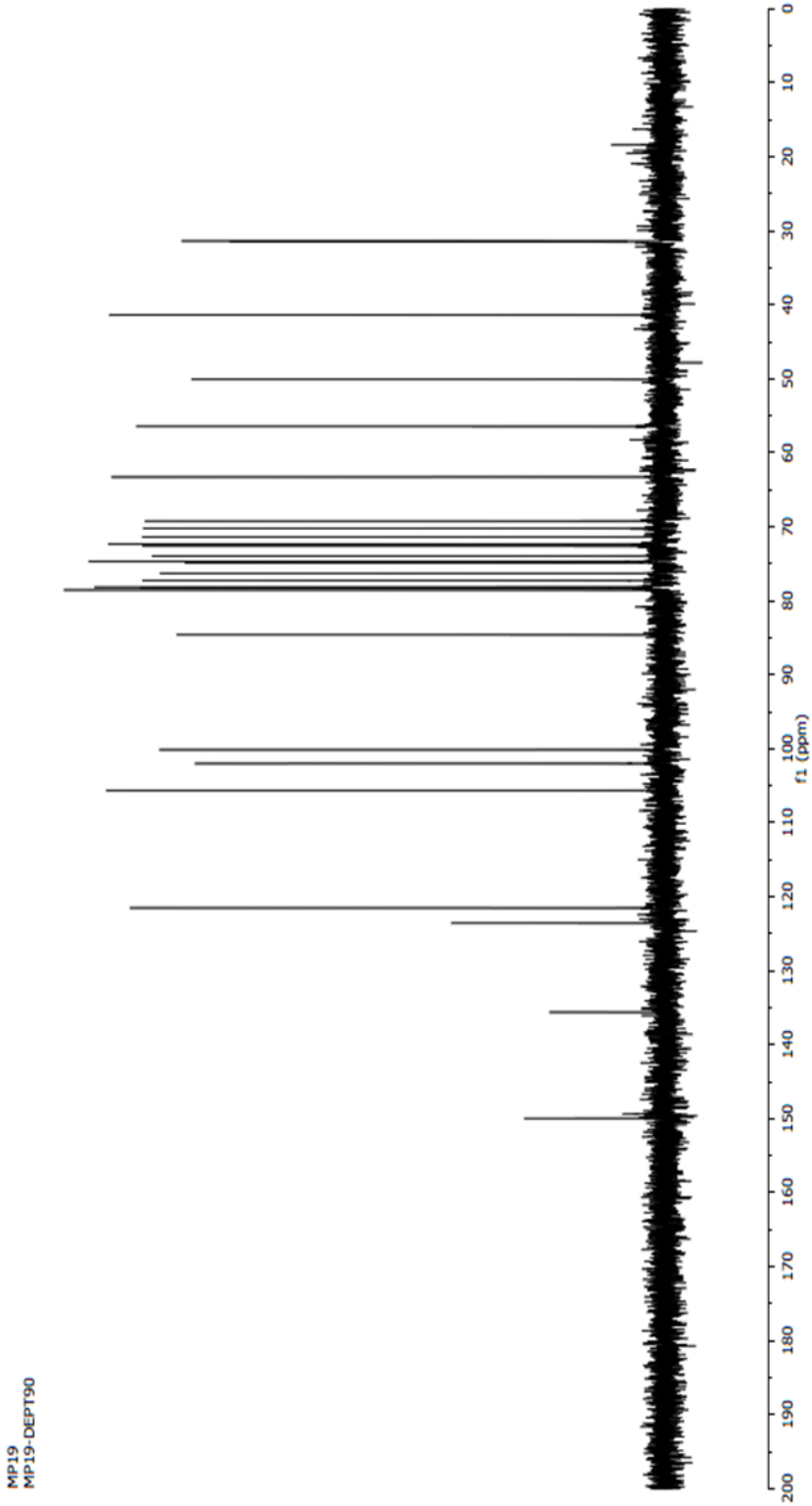

Figure 51 DEPT 90 spectrum (pyridine-d_5) of compound **213**

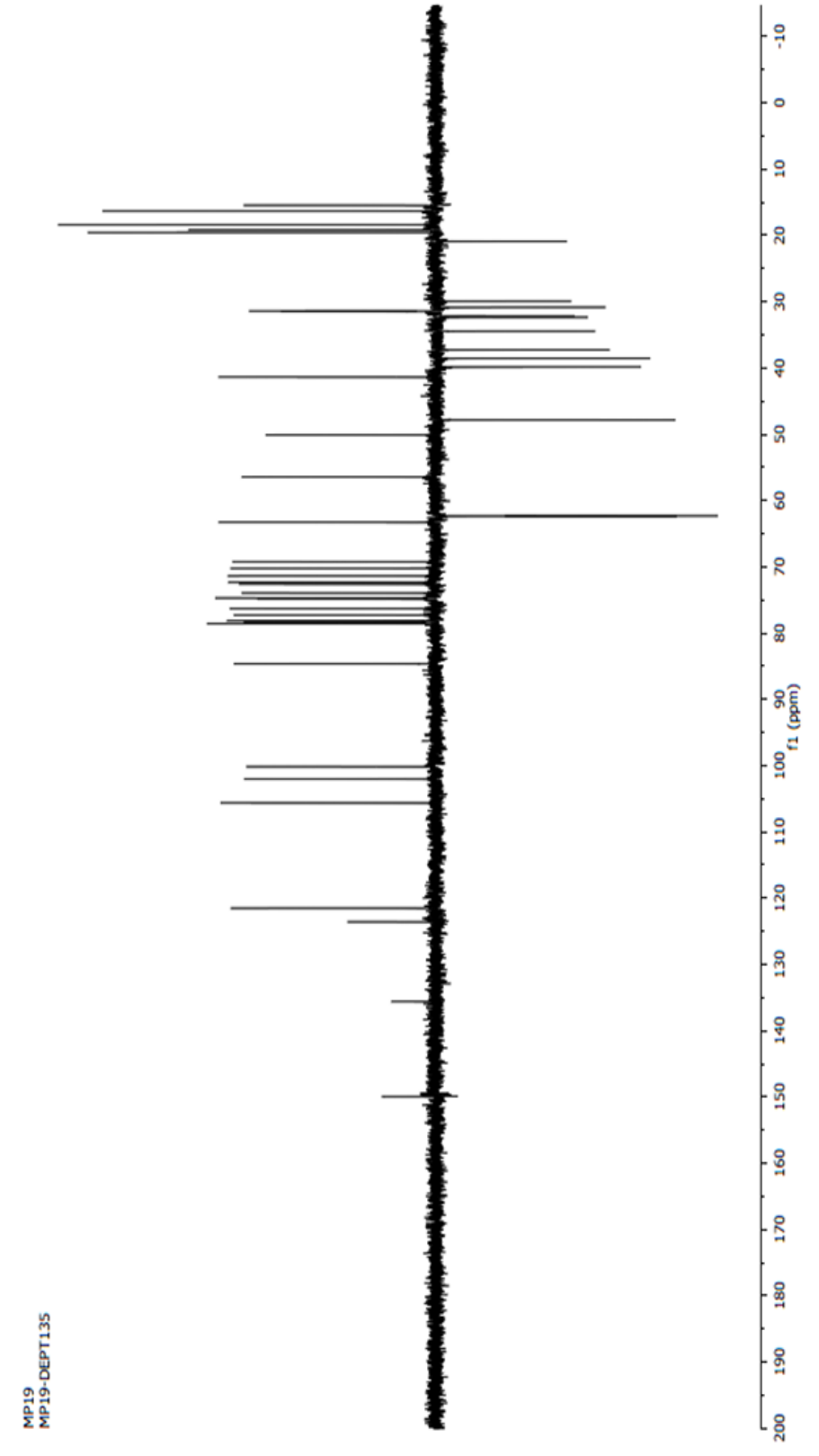

Figure 52 DEPT 135 spectrum (pyridine-d_5) of compound **213**

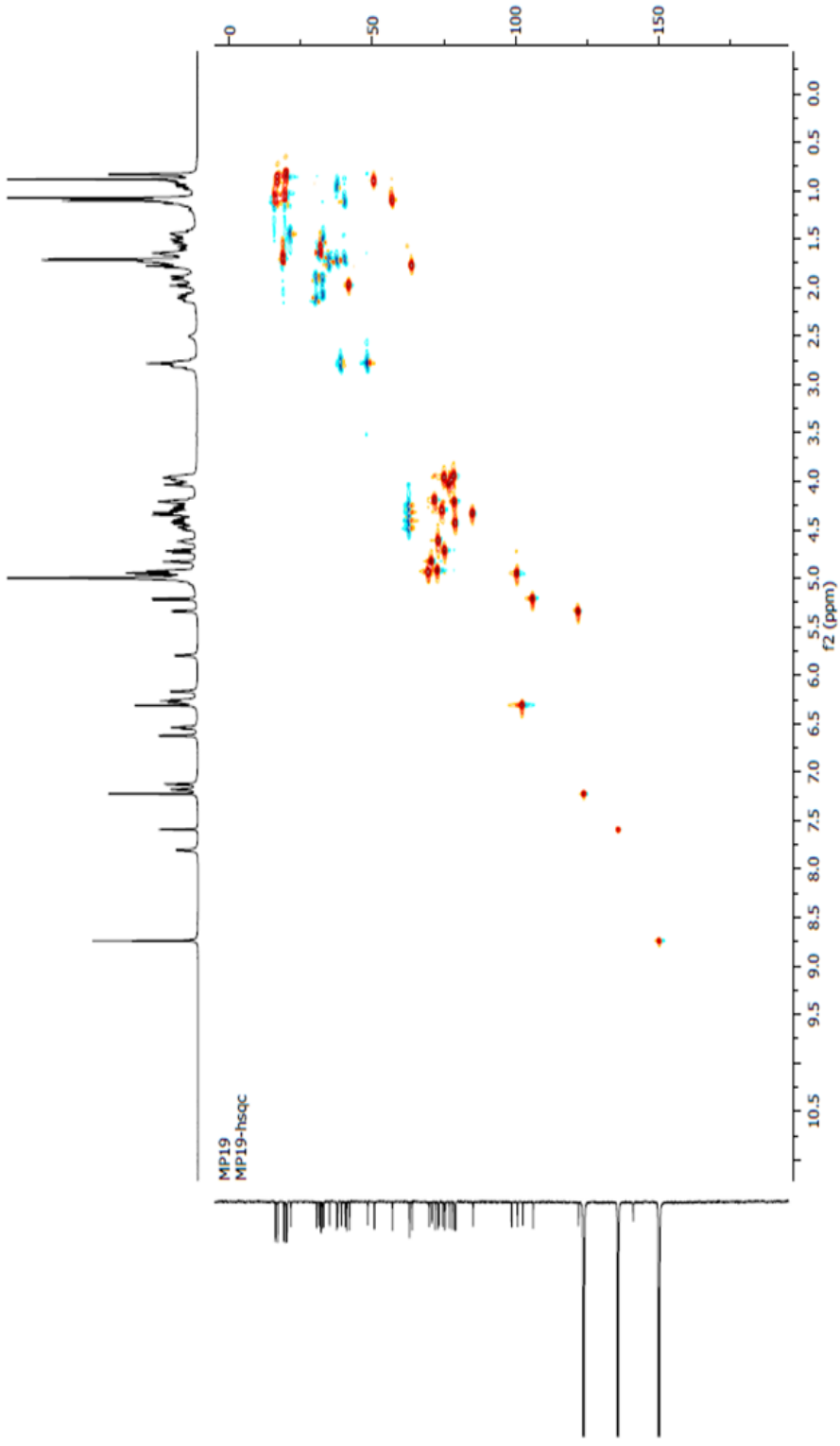

Figure 53 HSQC spectrum (pyridine-d_5) of compound **213**

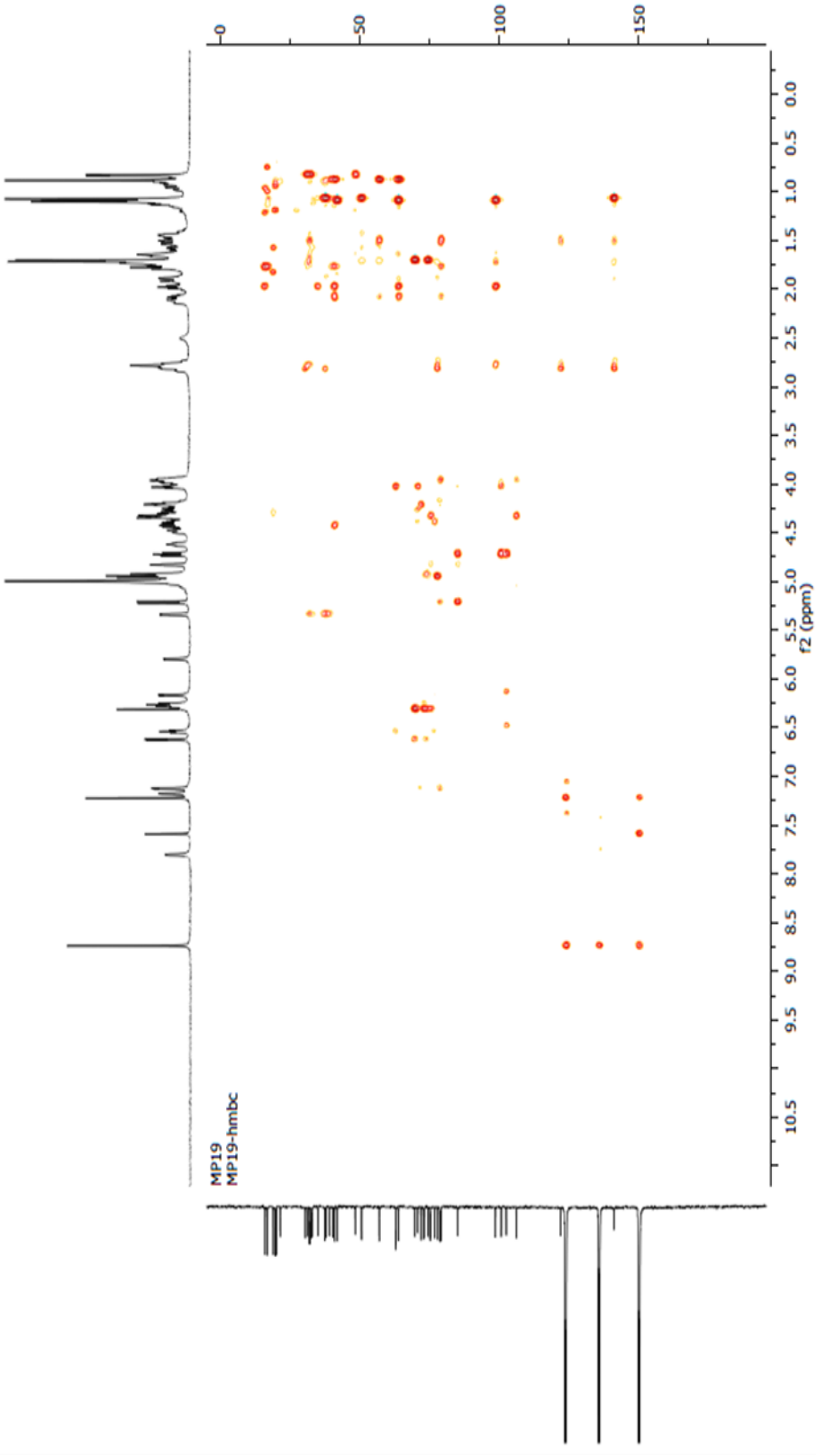

Figure 54 HMBC spectrum (pyridine-d_5) of compound **213**

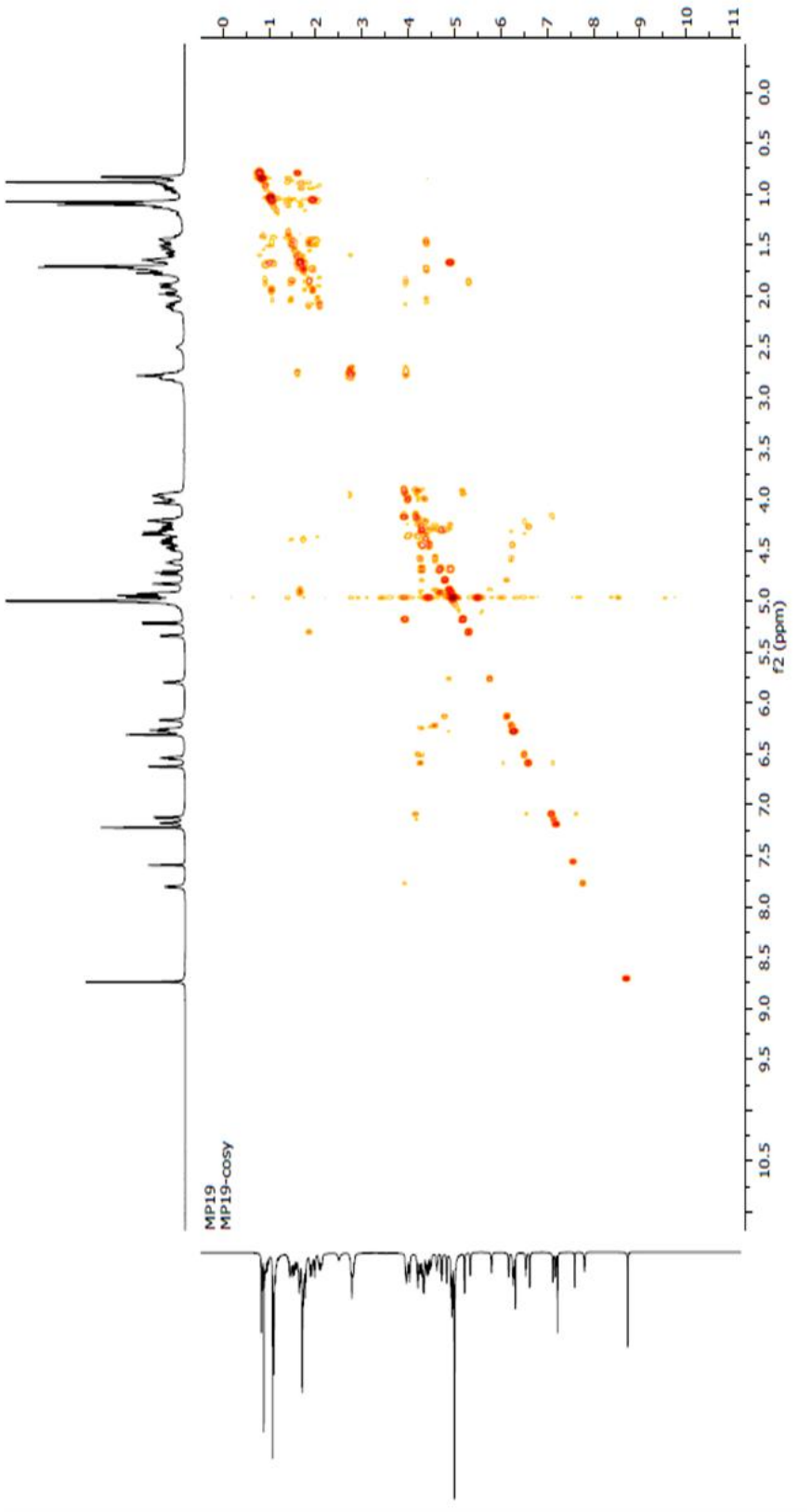

Figure 55 COSY spectrum (pyridine-d_5) of compound **213**

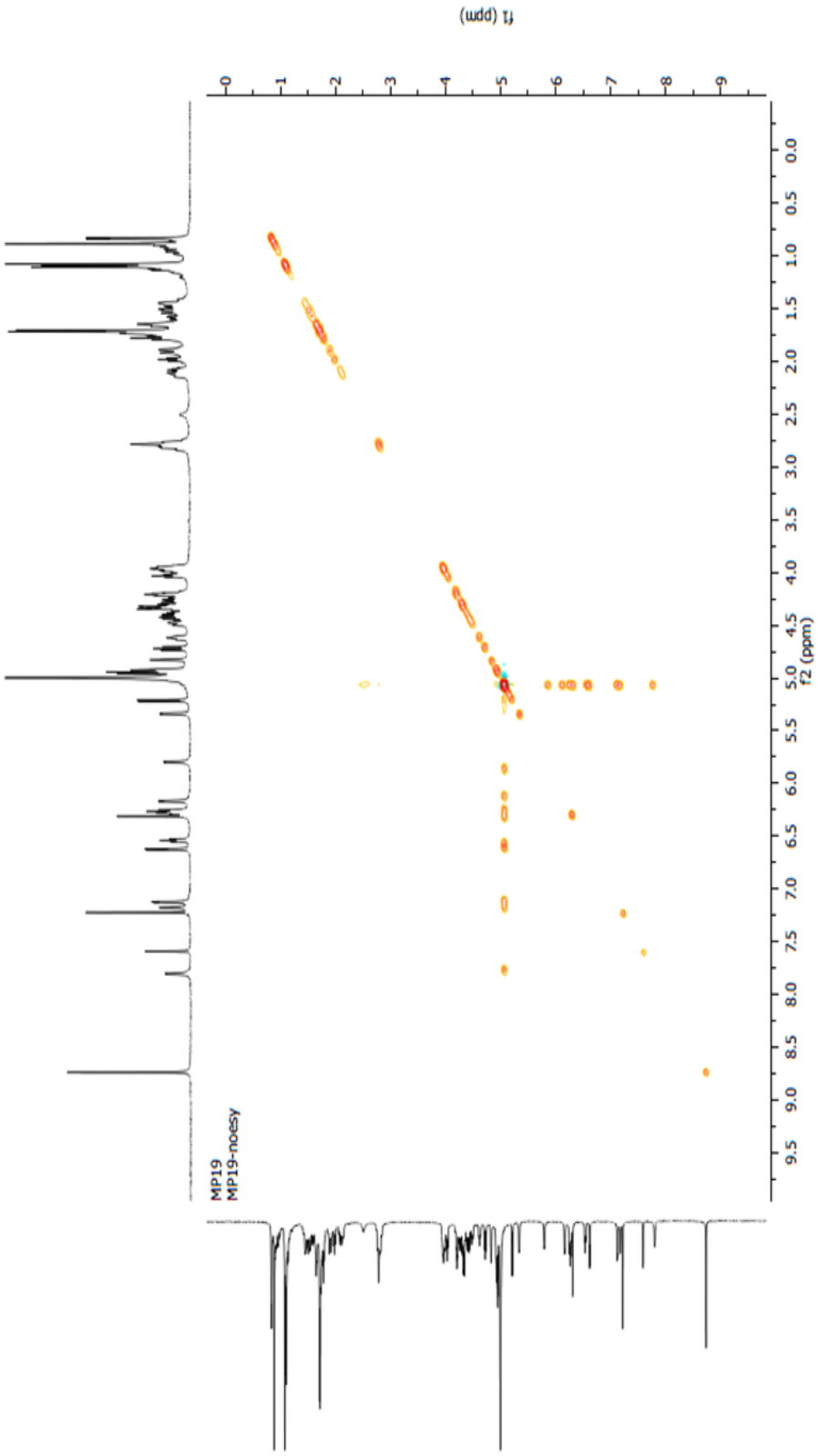

Figure 56 NOESY spectrum (pyridine-d_5) of compound **213**

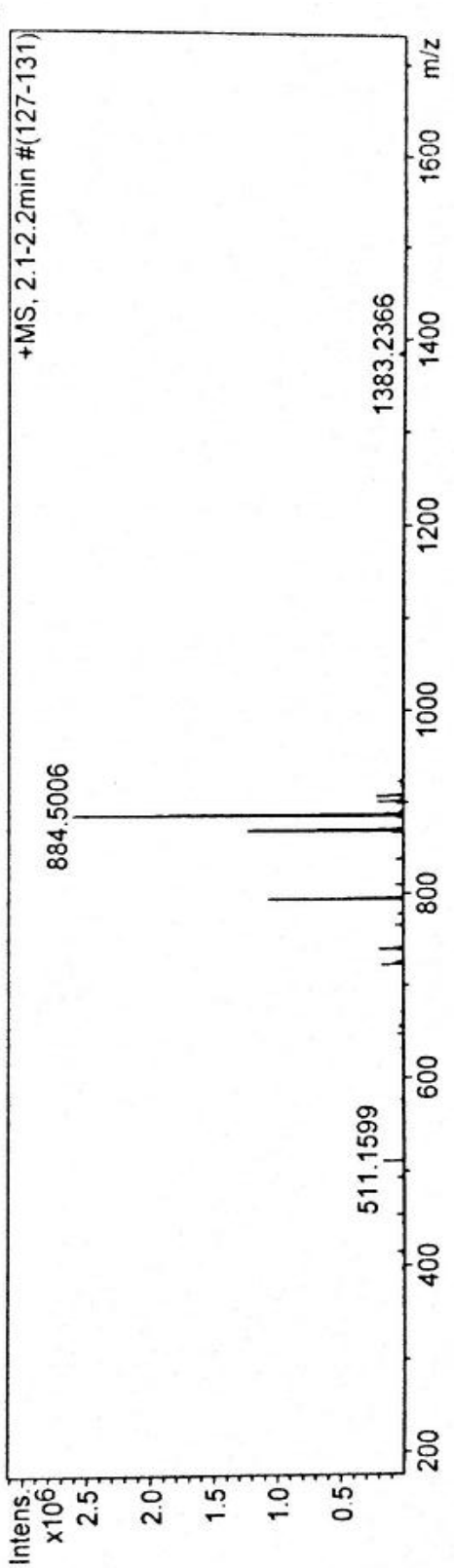

Figure 57 High resolution mass spectrum of compound **213**

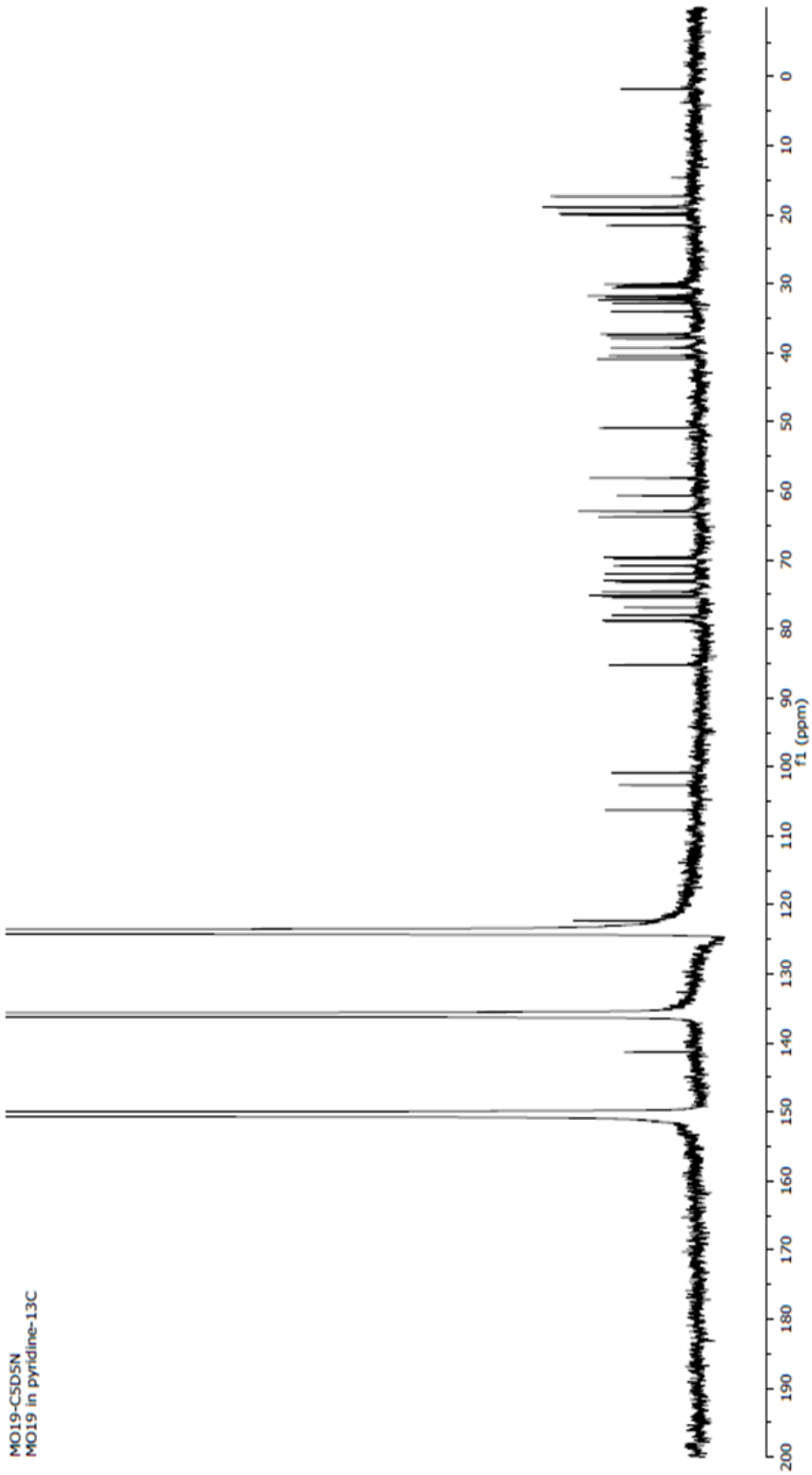

Figure 58 ^{13}C NMR spectrum (pyridine-d_5) of compound **214**

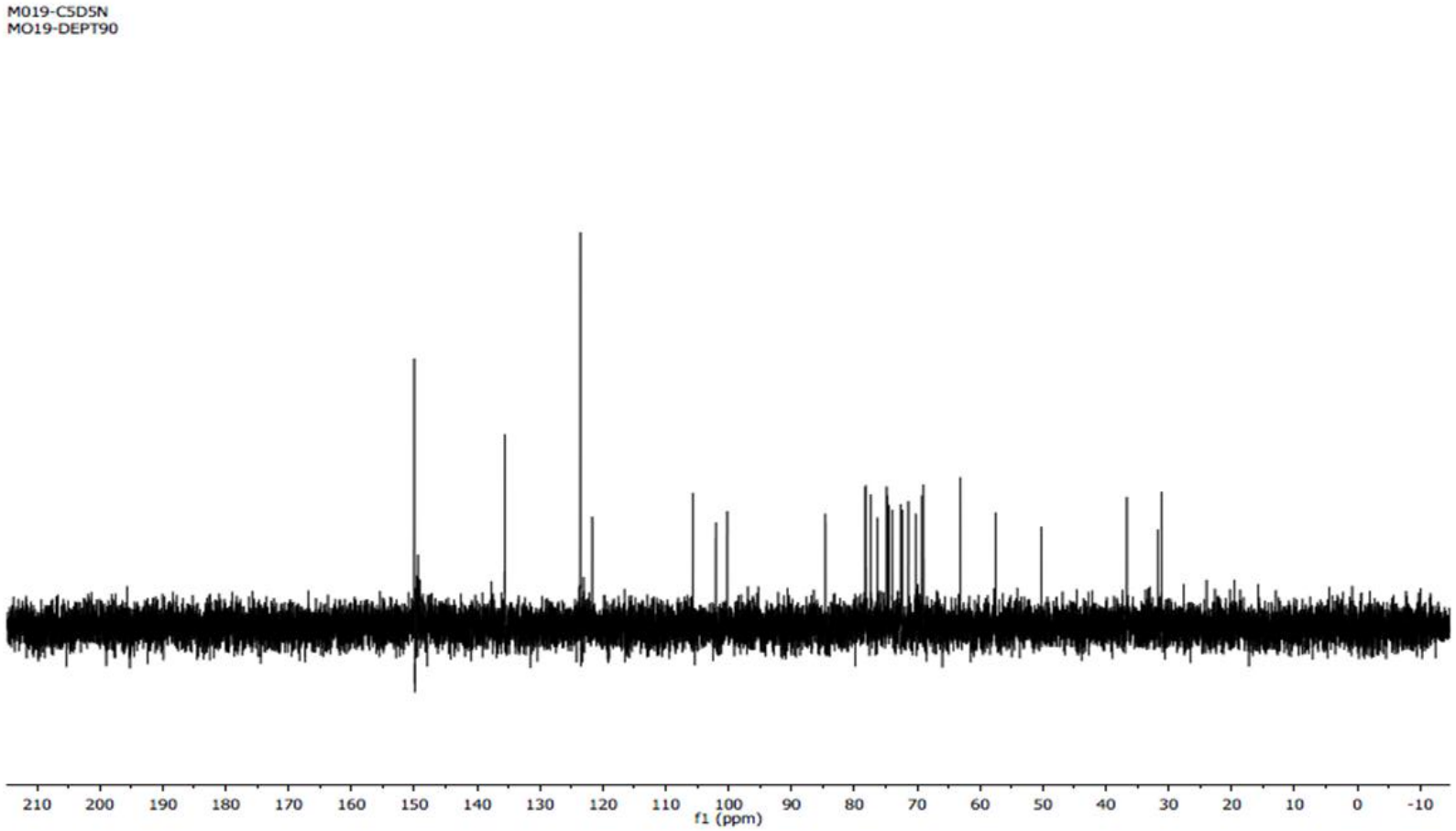

Figure 59 DEPT 90 spectrum (pyridine-d_5) of compound **214**

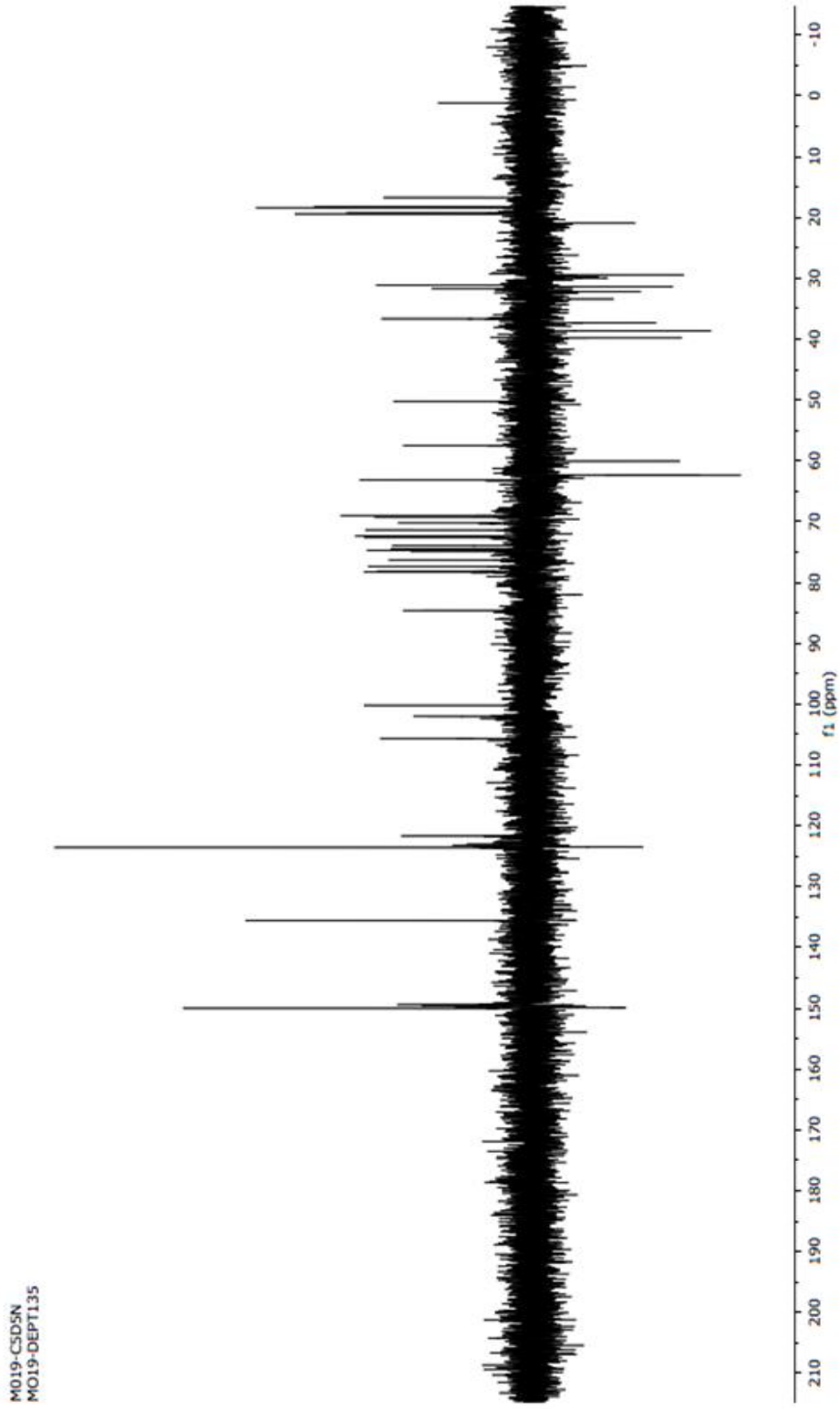

Figure 60 DEPT 135 spectrum (pyridine-d_5) of compound **214**

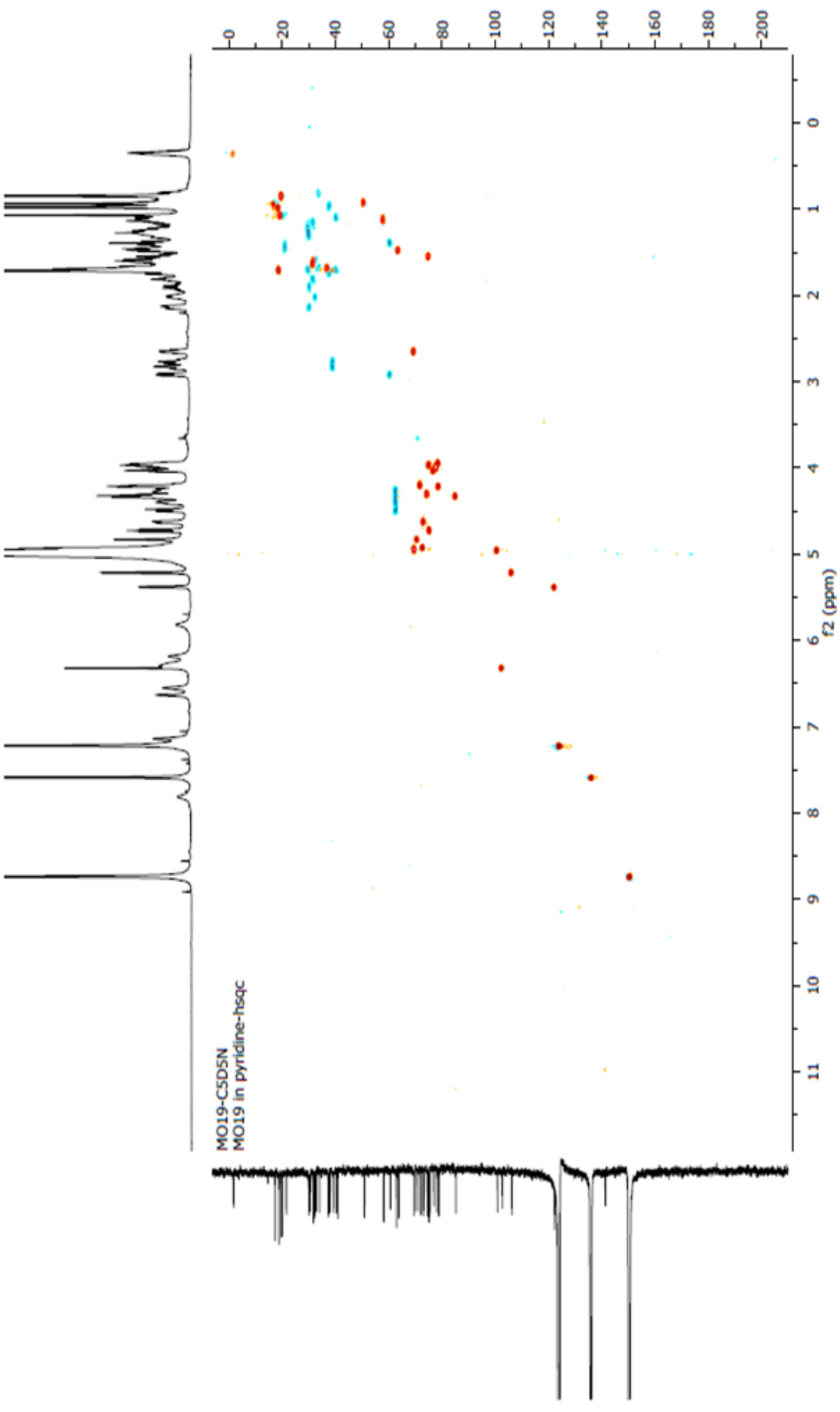

Figure 61 HSQC spectrum (pyridine-d_5) of compound **214**

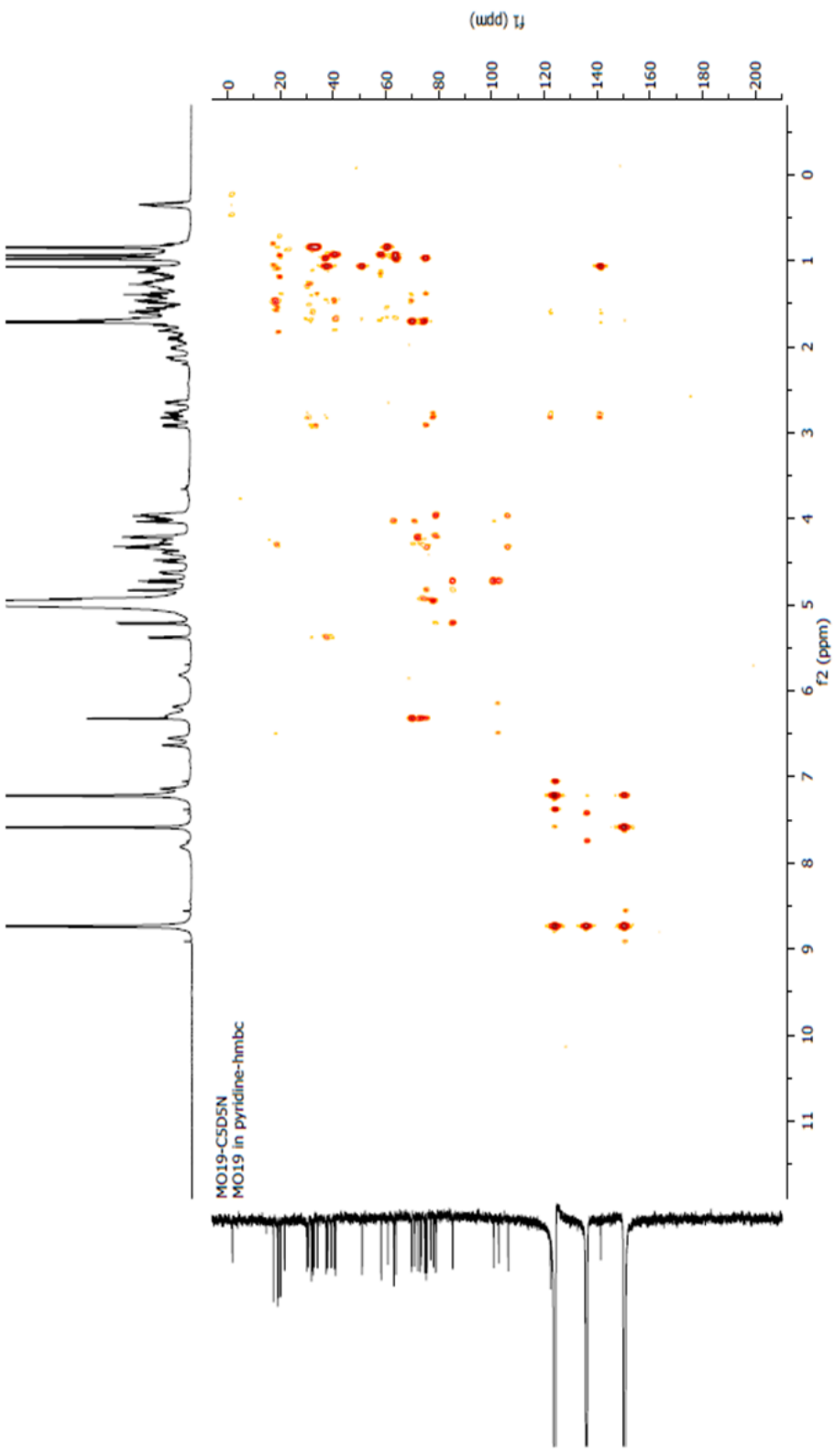

Figure 62 HMBC spectrum (pyridine-d_5) of compound **214**

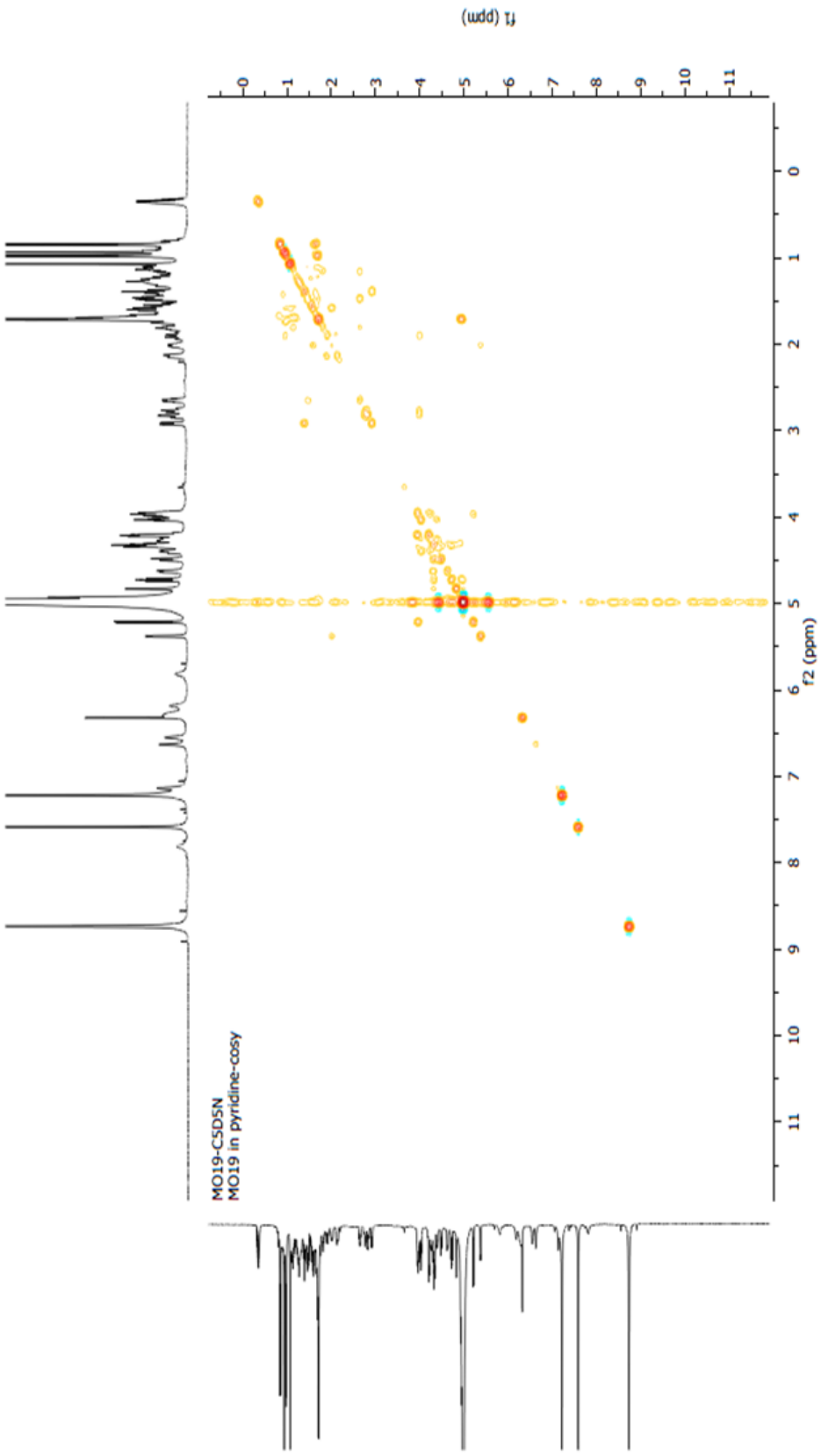

Figure 63 COSY spectrum (pyridine-d_5) of compound **214**

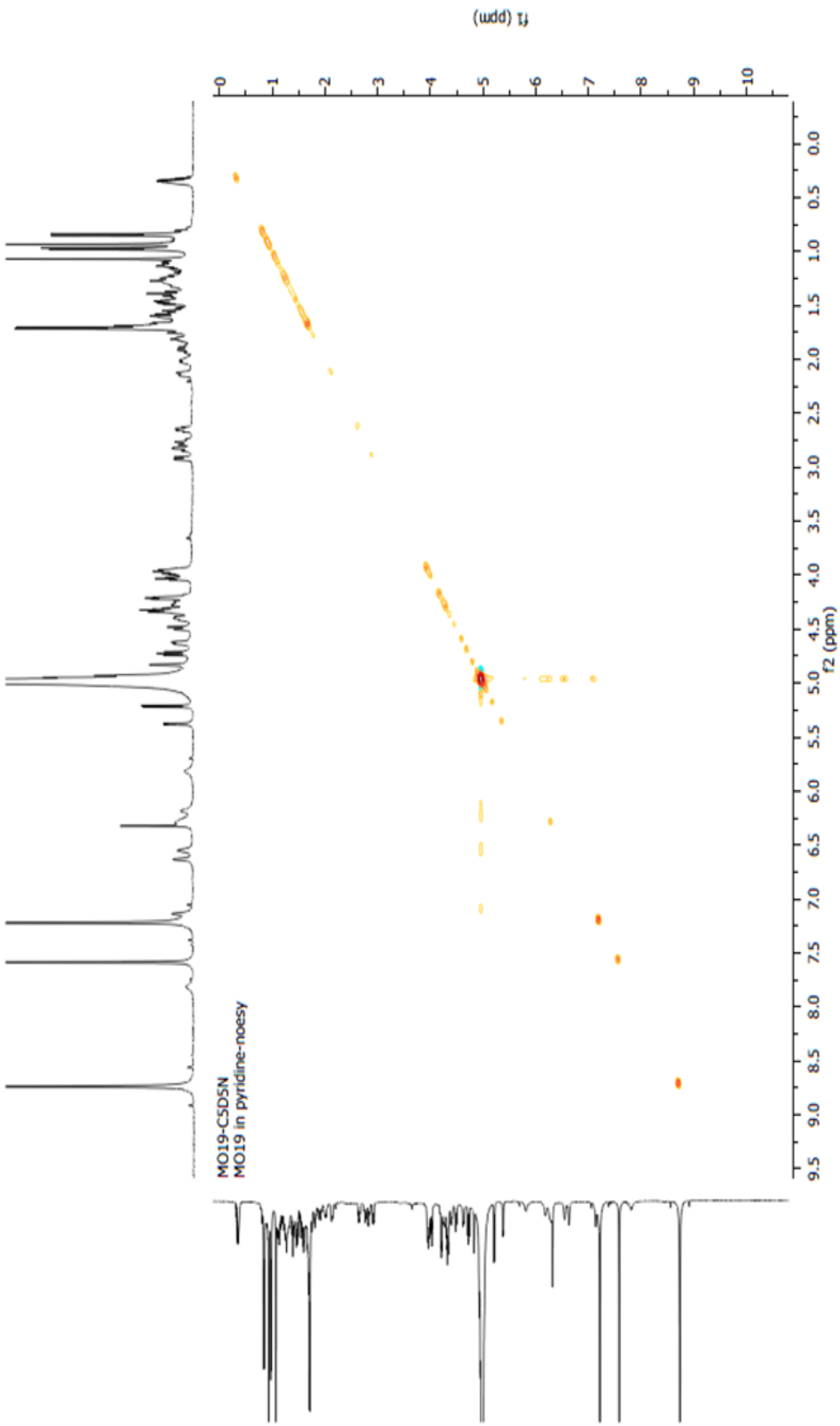

Figure 64 NOESY spectrum (pyridine-d_5) of compound **214**

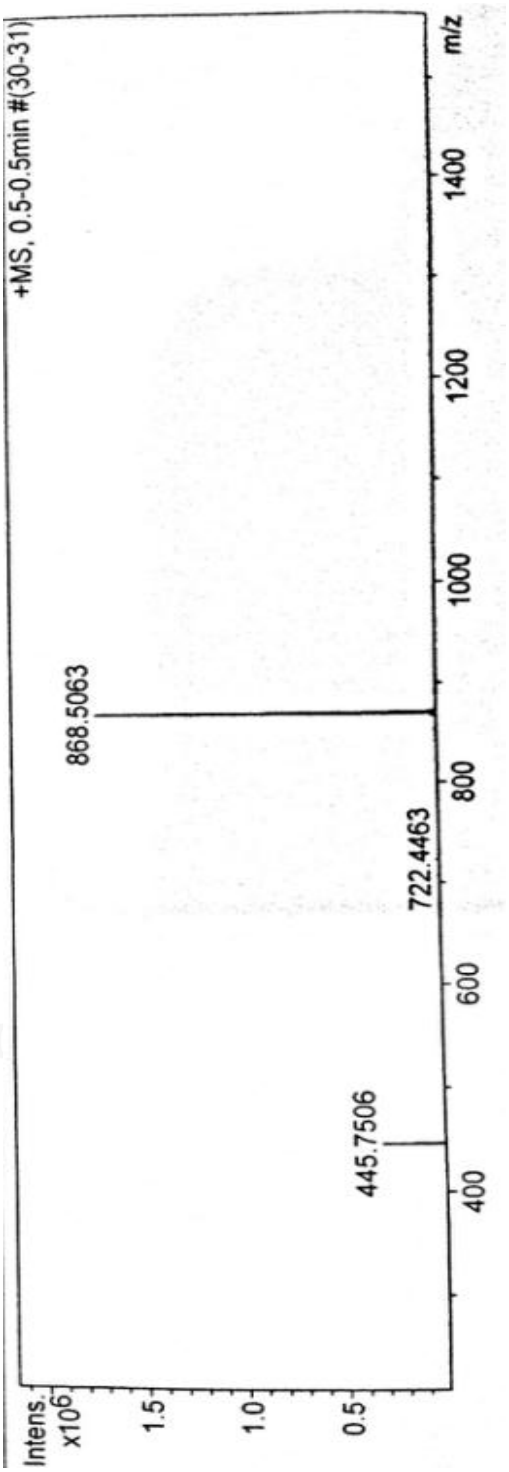

Figure 65 High resolution mass spectrum of compound **214**

VITA

Mr. Weerassak Megwee was born on December 25, 1988 in Yasothon Province, Thailand. He graduated high school in 2007 from Roi Et Wittayalai School in Roi Et Province. He received his Bachelor’s degree of Science, major in Cosmetic Science from Mae Fah Luang University in 2012. After that, he was admitted Master's degree of Program in Biotechnology, Faculty of Science, Chulalongkorn University in 2013.

Mr. Weerasak Megwee has attended the 36th National Graduate Research Conference (NGRC) scheduled on October 29-31, 2015 at Chiang Mai, Thailand for poster presentation.